USNDC-3
EANDC(US)-176"U"
INDC(USA)-56"U"

566

Reports to...

THE U.S. NUCLEAR DATA COMMITTEE

Meeting at

NATIONAL BUREAU OF STANDARDS

24-26 OCTOBER 1972

Compiled by...

H. E. Jackson, Secretary, USNDC
Physics Division

U of C-AUA-USAEC

Argonne National Laboratory

Printed in the United States of America
Available from
National Technical Information Service
U.S. Department of Commerce
5285 Port Royal Road
Springfield, Virginia 22151
Price: Printed Copy $3.00; Microfiche $0.95

USNDC-3
EANDC(US)-176"U"
INDC(USA)-54"U"

Physics

REPORTS TO
THE U.S. NUCLEAR DATA COMMITTEE

Meeting at

NATIONAL BUREAU OF STANDARDS

24-26 OCTOBER 1972

Compiled by

H. E. Jackson, Secretary
USNDC

ARGONNE NATIONAL LABORATORY
9700 South Cass Avenue
Argonne, Illinois 60439

PREFACE

The reports in this document were submitted to the United States Nuclear Data Committee (USNDC) at the meeting at the National Bureau of Standards, October 24-26, 1972. The reporting laboratories are those having a substantial effort in measuring neutron and nuclear cross sections of relevance to the U. S. applied nuclear energy program. The material contained in these reports is to be regarded as comprised of informal statements of recent developments and preliminary data. Appropriate subjects are listed as follows:

1. Microscopic neutron cross sections relevant to the nuclear energy program, including shielding. Inverse reactions where pertinent are included.

2. Charged particle cross sections, where they are relevant to 1) above, and where relevant to developing and testing nuclear models.

3. Gamma-ray production, radioactive decay, and theoretical developments in nuclear structure which are applicable to nuclear energy programs.

4. Proton and alpha-particle cross sections, at energies of up to 1 GeV, which are of interest to the space program.

These reports cannot be regarded as a complete summary of the nuclear research efforts of the AEC. A number of laboratories, whose research is less programmatically oriented do not submit reports; neither do the submitted reports reflect all the work related to nuclear cross sections in progress at the submitting laboratory. Budgetary limitations have made it mandatory to follow more strictly the subject guidelines described above and therefore to restrict the size of this document.

Persons wishing to make use of these data should contact the individual experimenter for further details. The data which appear in this document should be quoted only by permission of the contributor and should be referenced as private communication, and not by this document number.

This compilation has been produced almost completely from master copies prepared by the individual contributors listed in the Table of Contents. It is a pleasure to acknowledge their help in the preparation of these reports.

H. E. Jackson
Secretary, USNDC
Argonne National Laboratory
Argonne, Illinois 60439

TABLE OF CONTENTS

Recent Reports submitted to the USNDC or its predecessor, the AEC Nuclear Cross Sections Advisory Committee, include the following:

May 1972 Meeting at Los Alamos, New Mexico	USNDC- 1 EANDC(US)-168U INDC(USA) - 43U
November 1971 Meeting at Brookhaven National Laboratory	NCSAC- 42 EANDC(US)-165U INDC(USA) - 36U
May 1971 Meeting at Duke University	NCSAC- 38 EANDC(US)-156U INDC(USA) - 30U
December 1970 Meeting at Lawrence Radiation Laboratory	NCSAC- 33 EANDC(US)-150U INDC(US)- 25U
May 1970 Meeting at Argonne National Laboratory	NCSAC- 31 EANDC(US)-143U INDC(US) -- 22U
September 1969 Meeting at Rice University	WASH -1136 EANDC(US)-122U INDC(US) - 14U
April 1969 Meeting at Oak Ridge, Tennessee	WASH -1136 EANDC(US)-120U INDC(US) - 10U
October 1968 Meeting at Columbia University	WASH -1124 EANDC(US)-111U INDC(US)- 9U
April 1968 Meeting at Los Alamos, New Mexico	WASH -1093 EANDC(US)-105U INDC (US)- 2U
October 1967 Meeting at Idaho Falls, Idaho	WASH-1079 EANDC(US)-104U INDC (US)- 12U
April 1967 Meeting at Brookhaven, New York	WASH-1074 EANDC(US)- 99U INDC(US)- 9U

The CINDA-type index which follows was prepared by L. T. Whitehead, Nuclear Data Section, Science and Technology Branch, Oak Ridge National Laboratory, Oak Ridge, Tennessee.

ELEMENT S	A	QUANTITY	TYPE	ENERGY MIN	MAX	DOCUMENTATION REF VOL	PAGE	DATE	LAB	COMMENTS	SERIAL NO.
D	002	TOTAL XSECT	EXPT-PROG	0.0 0	1.0 3	USNDC-3	155	0/72	RPI	STOLER+. TRANS. CURVE	64429
HE	003	TOTAL XSECT	EXPT-PROG	NDG		USNDC-3	116	0/72	LAS	SEAGRAVE+. NO DATA GIVEN	64396
HE	003	TOTAL XSECT	EXPT-PROG	7.0 5	3.0 7	USNDC-3	161	0/72	RPI	GOULDING+. +-1PC. TRANS. NO DATA GVN	64425
HE	003	DIFF ELASTIC	EXPT-PROG	8.0 6	1.2 7	USNDC-3	177	0/72	DKE	LISOWSKI+. 2ES. POLARIZED BEAM. NDG	64369
HE	003	POLARIZATION	EXPT-PROG	8.0 6	1.2 7	USNDC-3	177	0/72	DKE	LISOWSKI+. 2ES. POLARIZED BEAM. NDG	64368
HE	004	TOTAL XSECT	EXPT-PROG	NDG		USNDC-3	116	0/72	LAS	SEAGRAVE+. NO DATA GIVEN	64397
HE	004	TOTAL XSECT	EXPT-PROG	5.0 5	3.0 7	USNDC-3	161	0/72	RPI	GOULDING+. TRANS. CURVE	64428
HE	004	DIFF ELASTIC	EXPT-PROG	1.4 7	1.7 7	USNDC-3	177	0/72	DKE	LISOWSKI+. 2ES. POLARIZED BEAM. NDG	64367
HE	004	POLARIZATION	EXPT-PROG	1.4 7	1.7 7	USNDC-3	177	0/72	DKE	LISOWSKI+. 2ES. POLARIZED BEAM. NDG	64366
LI	006	TOTAL XSECT	EXPT-PROG	5.0 5	3.0 7	USNDC-3	161	0/72	RPI	GOULDING+. TRANS. CURVE	64427
LI	006	N,ALPHA	EXPT-PROG	1.0 2	6.0 2	USNDC-3	8	0/72	ANL	POENITZ. LI-GLASS DET. TO BE COMPLTD	64204
LI	007	TOTAL XSECT	EXPT-PROG	5.0 5	3.0 7	USNDC-3	161	0/72	RPI	GOULDING+. TRANS. CURVE	64426
BE	009	DIFF ELASTIC	EXPT-PROG	7.5 6		USNDC-3	211	0/72	ABD	BUCHER+. 6ANGS 2.5-15DEG. NDG	64362
B	010	DIFF ELASTIC	EXPT-PROG	1.4 6	4.5 6	USNDC-3	154	0/72	OHO	HAUSLADEN+. SOME B11 LVL STRUCT GIVN	64430
B	010	N,ALPHA	EXPT-PROG	1.0 3	1.0 6	USNDC-3	84	0/72	GA	FRIESENHAHN+. CURVES. CFD OTHERS.	64386
B	011	DIFF ELASTIC	EXPT-PROG	NDG		USNDC-3	154	0/72	OHO	NELSON+.R-MATRIX ANAL TBC.B12 STATES	64431
C		TOTAL XSECT	EXPT-PROG	2.0 5	2.0 7	USNDC-3	142	0/72	ORL	PEREY+. TRANS. ABSTRACT OF ORNL-4823	64423
C		TOTAL XSECT	EXPT-PROG	1.5 6	4.0 6	USNDC-3	13	0/72	ANL	GUENTHER+. NO DATA GIVEN	64236
C		DIFF ELASTIC	EXPT-PROG	1.5 6	4.0 6	USNDC-3	13	0/72	ANL	GUENTHER+. NO DATA GIVEN	64223
C		DIFF ELASTIC	EXPT-PROG	7.5 6		USNDC-3	211	0/72	ABD	BUCHER+. 6ANGS 2.5-150EG. NDG	64361
C		DIFF ELASTIC	EXPT-PROG	1.0 7	1.4 7	USNDC-3	211	0/72	ABD	BUCHER+.THETA#2.5-15DEG.TO BE DONE	64365
C		NONEL GAMMAS	EXPT-PROG		2.0 7	USNDC-3	140	0/72	ORL	MORGAN+. GAM PROD SIGS. NO DATA GIVN	64321
C		DIFF INELAST	EXPT-PROG	1.5 6	4.0 6	USNDC-3	13	0/72	ANL	GUENTHER+. NO DATA GIVEN	64276
C	012	DIFF ELASTIC	EXPT-PROG	2.0 6	5.0 6	USNDC-3	213	0/72	YAL	FIRK+. ABSOL POL AND SIGS. CURVES	64196
C	012	POLARIZATION	EXPT-PROG	2.0 6	5.0 6	USNDC-3	213	0/72	YAL	FIRK+. ABSOL POL CURVES. 20-150DEG	64195
N		DIFF ELASTIC	EXPT-PROG	1.0 7	1.4 7	USNDC-3	211	0/72	ABD	BUCHER+.THETA#2.5-15DEG.TO BE DONE	64364
O		TOTAL XSECT	EXPT-PROG	2.0 5	2.0 7	USNDC-3	142	0/72	ORL	PEREY+. TRANS. ABSTRACT OF ORNL-4823	64422
O		DIFF ELASTIC	EXPT-PROG	1.0 7	1.4 7	USNDC-3	211	0/72	ABD	BUCHER+.THETA#2.5-15DEG.TO BE DONE	64363
F	019	TOTAL XSECT	EXPT-PROG	1.5 6	4.0 6	USNDC-3	13	0/72	ANL	GUENTHER+. NO DATA GIVEN	64235
F	019	RESON PARAMS	EXPT-PROG	2.7 4	1.5 6	USNDC-3	145	0/72	ORL	MACKLIN+. G*WN,WT,WG,J MEASD. DATA	64412
F	019	DIFF ELASTIC	EXPT-PROG	1.5 6	4.0 6	USNDC-3	13	0/72	ANL	GUENTHER+. NO DATA GIVEN	64222
F	019	DIFF INELAST	EXPT-PROG	1.5 6	4.0 6	USNDC-3	13	0/72	ANL	GUENTHER+. NO DATA GIVEN	64275
F	019	N,GAMMA	EXPT-PROG	3.0 3	5.0 5	USNDC-3	148	0/72	ORL	MACKLIN+. ANAL TBC.NO DATA GVN.ORELA	64356
NA	023	RESON PARAMS	EXPT-PROG	2.8 3	3.0 5	USNDC-3	66	0/72	COL	RAHN+. WT,L,J GIVN FOR 7 RESONANCES	64280
MG		EVALUATION	EXPT-PROG	NDG		USNDC-3	98	0/72	GA	DRAKE+. GAMMA AND NEUT PRODUCTN. NDG	64385
AL	027	TOTAL XSECT	EXPT-PROG	2.0 5	2.0 7	USNDC-3	142	0/72	ORL	PEREY+. TRANS. ABSTRACT OF ORNL-4823	64421
AL	027	DIFF ELASTIC	EXPT-PROG	7.5 6		USNDC-3	211	0/72	ABD	BUCHER+. 6ANGS 2.5-150EG. CURVE	64360
AL	027	N,GAMMA	EXPT-PROG	3.0 3	5.0 5	USNDC-3	148	0/72	ORL	MACKLIN+. ANAL TBC.NO DATA GVN.ORELA	64355
AL	027	N,PROTON	EXPT-PROG	2.5 6	5.9 6	USNDC-3	16	0/72	ANL	MEADOWS+. ACTIVATION. CURVE	64256
SI		TOTAL XSECT	EXPT-PROG	2.0 5	2.0 7	USNDC-3	142	0/72	ORL	PEREY+. TRANS. ABSTRACT OF ORNL-4823	64420
SI		TOTAL XSECT	EXTH-PROG	NDG		USNDC-3	174	0/72	DKE	CLEMENT+.THEORETICAL ANAL TBC. NDG	64372
SI		NONEL GAMMAS	EXPT-PROG		2.0 7	USNDC-3	140	0/72	ORL	MORGAN+. GAM PROD SIGS. NO DATA GIVN	64322
S		TOTAL XSECT	EXTH-PROG	NDG		USNDC-3	174	0/72	DKE	CLEMENT+.THEORETICAL ANAL TBC. NDG	64371
S	032	N,GAMMA	EXPT-PROG	3.0 3	5.0 5	USNDC-3	148	0/72	ORL	MACKLIN+. ANAL TBC.NO DATA GVN.ORELA	64354
CL		TOTAL XSECT	EXPT-PROG	1.0 1	1.5 4	USNDC-3	50	0/72	COL	SINGH+. CURVES. AVERAGE SIG VS. E	64285
CL	035	RESON PARAMS	EXPT-PROG	4.0 2	1.9 5	USNDC-3	50	0/72	COL	SINGH+. R-MATRIX PARAMS GIVEN	64284
CL	037	RESON PARAMS	EXPT-PROG	8.3 0	9.3 4	USNDC-3	50	0/72	COL	SINGH+. R-MATRIX PARAMS GIVEN	64283
CA		TOTAL XSECT	EXPT-PROG	2.0 5	2.0 7	USNDC-3	142	0/72	ORL	PEREY+. TRANS. ABSTRACT OF ORNL-4823	64419

ELEMENT S A	QUANTITY	TYPE	ENERGY MIN	MAX	DOCUMENTATION REF VOL PAGE DATE		LAB	COMMENTS	SERIAL NO.
CA 043	N,GAMMA	EXPT-PROG	3.0 3	5.0 5	USNDC-3 148	0/72	ORL	MACKLIN+. ANAL TBC.NO DATA GVN.ORELA	64353
CA 044	N,GAMMA	EXPT-PROG	3.0 3	5.0 5	USNDC-3 148	0/72	ORL	MACKLIN+. ANAL TBC.NO DATA GVN.ORELA	64352
CA 139	STRNTH FNCTN	EXPT-PROG	1.0 3	2.1 4	USNDC-3 50	0/72	COL	HACKEN+. SO GIVEN	64282
TI	TOTAL XSECT	EXPT-PROG	1.5 6	4.0 6	USNDC-3 13	0/72	ANL	GUENTHER+. NO DATA GIVEN	64234
TI	DIFF ELASTIC	EXPT-PROG	1.5 6	4.0 6	USNDC-3 13	0/72	ANL	GUENTHER+. NO DATA GIVEN	64221
TI	DIFF INELAST	EXPT-PROG	1.5 6	4.0 6	USNDC-3 13	0/72	ANL	GUENTHER+. NO DATA GIVEN	64264
TI 046	N,PROTON	EXPT-PROG	4.0 6	5.9 6	USNDC-3 16	0/72	ANL	MEADOWS+. ACTIVATION. CURVE	64255
TI 048	N,PROTON	EXPT-PROG	4.7 6	5.9 6	USNDC-3 16	0/72	ANL	MEADOWS+. ACTIVATION. CURVE	64254
V	TOTAL XSECT	EXPT-PROG	1.5 6	4.0 6	USNDC-3 13	0/72	ANL	GUENTHER+. NO DATA GIVEN	64233
V	DIFF ELASTIC	EXPT-PROG	1.5 6	4.0 6	USNDC-3 13	0/72	ANL	GUENTHER+. NO DATA GIVEN	64220
V	DIFF INELAST	EXPT-PROG	1.5 6	4.0 6	USNDC-3 13	0/72	ANL	GUENTHER+. NO DATA GIVEN	64265
V 051	N,GAMMA	EXPT-PROG	3.0 3	5.0 5	USNDC-3 148	0/72	ORL	MACKLIN+. ANAL TBC.NO DATA GVN.ORELA	64351
MN 055	N,GAMMA	EXPT-PROG	3.0 3	5.0 5	USNDC-3 148	0/72	ORL	MACKLIN+. ANAL TBC.NO DATA GVN.ORELA	64350
FE	TOTAL XSECT	EXPT-PROG	2.0 5	2.0 7	USNDC-3 142	0/72	ORL	PEREY+. TRANS. ABSTRACT OF ORNL-4823	64418
FE	TOTAL XSECT	EXPT-PROG	1.5 6	4.0 6	USNDC-3 13	0/72	ANL	GUENTHER+. NO DATA GIVEN	64232
FE	DIFF ELASTIC	EXPT-PROG	1.5 6	4.0 6	USNDC-3 13	0/72	ANL	GUENTHER+. NO DATA GIVEN	64219
FE	DIFF ELASTIC	EXPT-PROG	7.5 6		USNDC-3 211	0/72	ABD	BUCHER+. 6ANGS 2.5-15DEG. CURVE	64359
FE	DIFF ELASTIC	EXPT-PROG	3	5	USNDC-3 166	0/72	RPI	ZUHR+. ANAL TBC. NO DATA GIVEN.	64374
FE	NONEL GAMMAS	EXPT-PROG	8.0 5	2.0 7	USNDC-3 143	0/72	ORL	DICKENS+. ABSTRACT OF ORNL-4798	64415
FE	NONEL GAMMAS	EXPT-PROG	8.0 5	2.0 7	USNDC-3 142	0/72	ORL	DICKENS+. ABSTRACT OF ORNL-TM-3850	64416
FE	NONEL GAMMAS	EXPT-PROG		2.0 7	USNDC-3 140	0/72	ORL	MORGAN+. GAM PROD SIGS. NO DATA GIVN	64323
FE	DIFF INELAST	EXPT-PROG	1.5 6	4.0 6	USNDC-3 13	0/72	ANL	GUENTHER+. NO DATA GIVEN	64266
FE 054	TOTAL XSECT	EXPT-PROG	1.0 2	1.0 5	USNDC-3 155	0/72	RPI	HOCKENBURY+. TRANS. NO DATA GIVEN	64316
FE 054	RESON PARAMS	EXPT-PROG	3.1 3	3.9 4	USNDC-3 155	0/72	RPI	HOCKENBURY+. ES ONLY FOR 13 RESON	64308
FE 054	N,GAMMA	EXPT-PROG	1.0 2	1.0 5	USNDC-3 155	0/72	RPI	HOCKENBURY+. NO DATA GIVEN	64312
FE 054	N,PROTON	EXPT-PROG	1.5 6	5.8 6	USNDC-3 16	0/72	ANL	MEADOWS+. ACTIVATION. CURVE	64253
FE 056	N,PROTON	EXPT-PROG	4.0 6	5.9 6	USNDC-3 16	0/72	ANL	MEADOWS+. ACTIVATION. CURVE	64252
FE 058	TOTAL XSECT	EXPT-PROG	1.0 2	1.0 5	USNDC-3 155	0/72	RPI	HOCKENBURY+. TRANS. NO DATA GIVEN	64315
FE 058	RESON PARAMS	EXPT-PROG	2.3 2	1.9 4	USNDC-3 155	0/72	RPI	HOCKENBURY+. ES ONLY FOR 5 RESON	64307
FE 058	N,GAMMA	EXPT-PROG	1.0 2	1.0 5	USNDC-3 155	0/72	RPI	HOCKENBURY+. NO DATA GIVEN	64311
CO 059	TOTAL XSECT	EXPT-PROG	1.5 6	4.0 6	USNDC-3 13	0/72	ANL	GUENTHER+. NO DATA GIVEN	64231
CO 059	DIFF ELASTIC	EXPT-PROG	1.5 6	4.0 6	USNDC-3 13	0/72	ANL	GUENTHER+. NO DATA GIVEN	64218
CO 059	DIFF INELAST	EXPT-PROG	1.5 6	4.0 6	USNDC-3 13	0/72	ANL	GUENTHER+. NO DATA GIVEN	64267
CO 059	N,GAMMA	EXPT-PROG	3.0 3	5.0 5	USNDC-3 148	0/72	ORL	MACKLIN+. ANAL TBC.NO DATA GVN.ORELA	64349
NI	TOTAL XSECT	EXPT-PROG	1.5 6	4.0 6	USNDC-3 13	0/72	ANL	GUENTHER+. NO DATA GIVEN	64230
NI	DIFF ELASTIC	EXPT-PROG	1.5 6	4.0 6	USNDC-3 13	0/72	ANL	GUENTHER+. NO DATA GIVEN	64217
NI	DIFF ELASTIC	EXPT-PROG	3	5	USNDC-3 166	0/72	RPI	ZUHR+. ANAL TBC. NO DATA GIVEN.	64373
NI	DIFF INELAST	EXPT-PROG	1.5 6	4.0 6	USNDC-3 13	0/72	ANL	GUENTHER+. NO DATA GIVEN	64268
NI 058	N,PROTON	EXPT-PROG	4.0 5	5.9 6	USNDC-3 16	0/72	ANL	MEADOWS+. ACTIVATION. CURVE	64251
NI 060	RESON PARAMS	EXPT-PROG	1.3 1	5.0 4	USNDC-3 164	0/72	RPI	BROWN+. LINAC. CAPT MEAST. NO DATA	64376
NI 060	SPECT NGAMMA	EXPT-PROG	1.3 1	5.0 4	USNDC-3 164	0/72	RPI	BROWN+. LINAC. NO DATA GIVEN	64424
NI 061	TOTAL XSECT	EXPT-PROG	1.0 2	1.0 5	USNDC-3 155	0/72	RPI	HOCKENBURY+. TRANS CURVE ONLY	64314
NI 061	RESON PARAMS	EXPT-PROG	1.3 3	2.1 4	USNDC-3 155	0/72	RPI	HOCKENBURY+. ES ONLY FOR 28 RESON	64306
NI 061	N,GAMMA	EXPT-PROG	1.0 2	1.0 5	USNDC-3 155	0/72	RPI	HOCKENBURY+. PULSE-HEIGHT CURV ONLY	64310
NI 064	TOTAL XSECT	EXPT-PROG	1.0 2	1.0 5	USNDC-3 155	0/72	RPI	HOCKENBURY+. TRANS. NO DATA GIVEN	64313
NI 064	RESON PARAMS	EXPT-PROG	1.4 4	8.3 4	USNDC-3 155	0/72	RPI	HOCKENBURY+. ES ONLY FOR 9 RESON	64305
NI 064	N,GAMMA	EXPT-PROG	1.0 2	1.0 5	USNDC-3 155	0/72	RPI	HOCKENBURY+. NO DATA GIVEN	64309
CU	EVALUATION	EXPT-PROG	NDG		USNDC-3 98	0/72	GA	DRAKE+. GAMMA AND NEUT PRODCTN. NDG	64384

ELEMENT S	A	QUANTITY	TYPE	ENERGY MIN	ENERGY MAX	DOCUMENTATION REF VOL PAGE	DATE	LAB	COMMENTS	SERIAL NO.
CU		TOTAL XSECT	EXPT-PROG	1.5 6	4.0 6	USNDC-3 13	0/72	ANL	GUENTHER+. NO DATA GIVEN	64229
CU		DIFF ELASTIC	EXPT-PROG	1.5 6	4.0 6	USNDC-3 13	0/72	ANL	GUENTHER+. NO DATA GIVEN	64203
CU		DIFF ELASTIC	EXPT-PROG	7.5 6		USNDC-3 211	0/72	ABD	BUCHER+. 6ANGS 2.5-150DEG. NDG	64358
CU		DIFF INELAST	EXPT-PROG	1.5 6	4.0 6	USNDC-3 13	0/72	ANL	GUENTHER+. NO DATA GIVEN	64269
GE	073	RESON PARAMS	EXPT-PROG	1.0 2	4.1 2	USNDC-3 27	0/72	BNL	HOLM+. E0 ONLY FOR 7 RESONANCES	64241
GE	073	SPECT NGAMMA	EXPT-PROG	2		USNDC-3 27	0/72	BNL	HOLM+. CURVES. SEVERAL RESON SEEN	64242
SR	086	N,GAMMA	EXPT-PROG	3.0 3	6.0 5	USNDC-3 146	0/72	ORL	VANPRAET+. NO DATA GIVEN.	64409
SR	087	N,GAMMA	EXPT-PROG	3.0 3	6.0 5	USNDC-3 146	0/72	ORL	VANPRAET+. NO DATA GIVEN.	64408
SR	088	N,GAMMA	EXPT-PROG	3.0 3	6.0 5	USNDC-3 146	0/72	ORL	VANPRAET+. NO DATA GIVEN.	64407
Y	089	ELASTIC	EXPT-PROG	8.0 5	1.4 6	USNDC-3 16	0/72	ANL	ELWYN+. NO DATA GIVN. TBP IN NP	64250
Y	089	DIFF ELASTIC	EXPT-PROG	8.0 5	1.4 6	USNDC-3 16	0/72	ANL	ELWYN+. NO DATA GIVN. TBP IN NP	64249
Y	089	POLARIZATION	EXPT-PROG	8.0 5	1.4 6	USNDC-3 16	0/72	ANL	ELWYN+. NO DATA GIVN. TBP IN NP	64248
Y	089	N,GAMMA	EXPT-PROG	3.0 3	5.0 5	USNDC-3 148	0/72	ORL	MACKLIN+. ANAL TBC.NO DATA GVN.ORELA	64348
ZR		TOTAL XSECT	EXPT-PROG	1.5 6	4.0 6	USNDC-3 13	0/72	ANL	GUENTHER+. NO DATA GIVEN	64227
ZR		DIFF ELASTIC	EXPT-PROG	1.5 6	4.0 6	USNDC-3 13	0/72	ANL	GUENTHER+. NO DATA GIVEN	64201
ZR		DIFF INELAST	EXPT-PROG	1.5 6	4.0 6	USNDC-3 13	0/72	ANL	GUENTHER+. NO DATA GIVEN	64271
NB	093	TOTAL XSECT	EXPT-PROG	1.5 6	4.0 6	USNDC-3 13	0/72	ANL	GUENTHER+. NO DATA GIVEN	64228
NB	093	STRNTH FNCTN	EXPT-PROG	1.0 3	7.0 5	USNDC-3 129	0/72	NBS	CAMARDA. S1 VALUE GIVEN	64329
NB	093	DIFF ELASTIC	EXPT-PROG	1.5 6	4.0 6	USNDC-3 13	0/72	ANL	GUENTHER+. CURVES	64202
NB	093	DIFF INELAST	EXPT-PROG	1.5 6	4.0 6	USNDC-3 13	0/72	ANL	GUENTHER+. NO DATA GIVEN	64270
NB	093	N,GAMMA	EXPT-PROG	3.0 3	5.0 5	USNDC-3 148	0/72	ORL	MACKLIN+. ANAL TBC.NO DATA GVN.ORELA	64347
MO	092	RESON PARAMS	EXPT-PROG		2.5 4	USNDC-3 146	0/72	ORL	WASSON+. VALENCY NEUT. CAPTURE	64410
MO	092	RESON PARAMS	EXPT-PROG		3.2 4	USNDC-3 37	0/72	BNL	WASSON+. S- AND P-WAVE WG GIVEN	64258
MO	092	RESON PARAMS	EXPT-PROG		3.2 4	USNDC-3 148	0/72	ORL	WASSON+. AVG S,P WAVE WG GIVEN	64319
MO	092	STRNTH FNCTN	EXPT-PROG		3.2 4	USNDC-3 37	0/72	BNL	WASSON+. S- AND P-WAVE STF GIVEN	64257
MO	092	STRNTH FNCTN	EXPT-PROG		3.2 4	USNDC-3 148	0/72	ORL	WASSON+. S- AND P-WAVE STF GIVEN	64318
MO	092	SPECT NGAMMA	EXPT-PROG	NDG		USNDC-3 146	0/72	ORL	WASSON+. NO DATA GIVEN	64411
MO	092	SPECT NGAMMA	EXPT-PROG		1.0 5	USNDC-3 36	0/72	BNL	WASSON+. VALENCY NEUT CAPT.	64237
MO	098	TOTAL XSECT	EXPT-PROG	NDG		USNDC-3 34	0/72	BNL	CHRIEN+. NO DATA GIVEN. ANAL TBC	64239
MO	098	RESON PARAMS	EXPT-PROG	NDG		USNDC-3 34	0/72	BNL	CHRIEN+. NO DATA GIVEN. ANAL TBC	64238
AG		STRNTH FNCTN	EXPT-PROG	1.0 3	7.0 5	USNDC-3 129	0/72	NBS	CAMARDA. S1 VALUE GIVEN	64328
CD	106	N,GAMMA	EXPT-PROG	3.0 3	5.0 5	USNDC-3 148	0/72	ORL	MACKLIN+. ANAL TBC.NO DATA GVN.ORELA	64346
CD	108	N,GAMMA	EXPT-PROG	3.0 3	5.0 5	USNDC-3 148	0/72	ORL	MACKLIN+. ANAL TBC.NO DATA GVN.ORELA	64345
CD	110	TOTAL XSECT	EXPT-PROG	NDG		USNDC-3 50	0/72	COL	LIOU+. NO DATA GIVEN.TRANS+SELF-INDC	64290
CD	110	TOTAL XSECT	EXPT-PROG	NDG		USNDC-3 50	0/72	COL	LIOU+. NO DATA GIVEN.TRANS+SELF-INDC	64294
CD	111	RESON PARAMS	EXPT-PROG		2.3 3	USNDC-3 36	0/72	BNL	WASSON+. P-WAVE RESON. NDG	64260
CD	111	STRNTH FNCTN	EXPT-PROG		2.3 3	USNDC-3 147	0/72	ORL	WASSON+.S0 GVN.LOWER LIMIT S1	64405
CD	111	STRNTH FNCTN	EXPT-PROG		2.3 3	USNDC-3 36	0/72	BNL	WASSON+. S-WAVE GVN.P-WAVE LOWER LMT	64259
CD	111	SPECT NGAMMA	EXPT-PROG		2.3 3	USNDC-3 147	0/72	ORL	WASSON+. 162 RESON SEEN.STR FNC GVN	64406
CD	111	SPECT NGAMMA	EXPT-PROG		2.3 3	USNDC-3 36	0/72	BNL	WASSON+. P-WAVE RESON. NDG	64261
CD	112	TOTAL XSECT	EXPT-PROG	NDG		USNDC-3 50	0/72	COL	LIOU+. NO DATA GIVEN.TRANS+SELF-INDC	64289
CD	112	TOTAL XSECT	EXPT-PROG	NDG		USNDC-3 50	0/72	COL	LIOU+. NO DATA GIVEN.TRANS+SELF-INDC	64293
CD	112	N,GAMMA	EXPT-PROG	3.0 3	5.0 5	USNDC-3 148	0/72	ORL	MACKLIN+. ANAL TBC.NO DATA GVN.ORELA	64344
CD	113	N,GAMMA	EXPT-PROG	3.0 3	5.0 5	USNDC-3 148	0/72	ORL	MACKLIN+. ANAL TBC.NO DATA GVN.ORELA	64343
CD	113	SPECT NGAMMA	EXPT-PROG	THR		USNDC-3 24	0/72	ANL	SMITHER+. NO DATA. ANAL TO BE COMPLT	64246
CD	114	TOTAL XSECT	EXPT-PROG	NDG		USNDC-3 50	0/72	COL	LIOU+. NO DATA GIVEN.TRANS+SELF-INDC	64288
CD	114	TOTAL XSECT	EXPT-PROG	NDG		USNDC-3 50	0/72	COL	LIOU+. NO DATA GIVEN.TRANS+SELF-INDC	64292
CD	114	N,GAMMA	EXPT-PROG	3.0 3	5.0 5	USNDC-3 148	0/72	ORL	MACKLIN+. ANAL TBC.NO DATA GVN.ORELA	64342

ELEMENT S A	QUANTITY	TYPE	ENERGY MIN	ENERGY MAX	DOCUMENTATION REF VOL	PAGE	DATE	LAB	COMMENTS	SERIAL NO.
CD 116	TOTAL XSECT	EXPT-PROG	NDG		USNDC-3	50	0/72	COL	LIOU+. NO DATA GIVEN.TRANS+SELF-INDC	64287
CD 116	TOTAL XSECT	EXPT-PROG	NDG		USNDC-3	50	0/72	COL	LIOU+. NO DATA GIVEN.TRANS+SELF-INDC	64291
CD 116	N,GAMMA	EXPT-PROG	3.0 3	5.0 5	USNDC-3	148	0/72	ORL	MACKLIN+. ANAL TBC.NO DATA GVN.ORELA	64341
IN	STRNTH FNCTN	EXPT-PROG	1.0 3	7.0 5	USNDC-3	129	0/72	NBS	CAMARDA. S1 VALUE GIVEN	64327
SN	DIFF ELASTIC	EXPT-PROG	7.5 6		USNDC-3	211	0/72	ABD	BUCHER+. 6ANGS 2.5-15DEG. CURVE	64357
TE 128	RESON PARAMS	EXPT-PROG	5.0-1	7.0 3	USNDC-3	101	0/72	LRL	BROWNE+. NO DATA GIVN. ANAL TBC	64379
TE 128	N,GAMMA	EXPT-PROG	5.0-1	7.0 3	USNDC-3	101	0/72	LRL	BROWNE+. NO DATA GIVN. ANAL TBC	64381
TE 130	RESON PARAMS	EXPT-PROG	5.0-1	7.0 3	USNDC-3	101	0/72	LRL	BROWNE+. NO DATA GIVN. ANAL TBC	64378
TE 130	N,GAMMA	EXPT-PROG	5.0-1	7.0 3	USNDC-3	101	0/72	LRL	BROWNE+. NO DATA GIVN. ANAL TBC	64380
BA 135	SPECT NGAMMA	EXPT-PROG	2.4 1	1.1 2	USNDC-3	34	0/72	BNL	CHRIEN+. RESON CAPT SPEC. NDG. TBC	64240
LA 139	RESON PARAMS	EXPT-PROG	1.0 4	2.1 4	USNDC-3	50	0/72	COL	HACKEN+. G*WN GIVN FOR 29 RESONANCES	64281
ND 142	N,GAMMA	EXPT-PROG	3.0 3	5.0 5	USNDC-3	148	0/72	ORL	MACKLIN+. ANAL TBC.NO DATA GVN.ORELA	64340
ND 143	N,GAMMA	EXPT-PROG	3.0 3	5.0 5	USNDC-3	148	0/72	ORL	MACKLIN+. ANAL TBC.NO DATA GVN.ORELA	64339
ND 143	SPECT NGAMMA	EXPT-PROG	THR		USNDC-3	121	0/72	LAS	JURNEY+. SOME DATA.TBP APS MEETING	64389
ND 144	N,GAMMA	EXPT-PROG	3.0 3	5.0 5	USNDC-3	148	0/72	ORL	MACKLIN+. ANAL TBC.NO DATA GVN.ORELA	64338
ND 145	N,GAMMA	EXPT-PROG	3.0 3	5.0 5	USNDC-3	148	0/72	ORL	MACKLIN+. ANAL TBC.NO DATA GVN.ORELA	64337
ND 146	N,GAMMA	EXPT-PROG	3.0 3	5.0 5	USNDC-3	148	0/72	ORL	MACKLIN+. ANAL TBC.NO DATA GVN.ORELA	64443
ND 148	N,GAMMA	EXPT-PROG	3.0 3	5.0 5	USNDC-3	148	0/72	ORL	MACKLIN+. ANAL TBC.NO DATA GVN.ORELA	64442
ND 150	SPECT NGAMMA	EXPT-PROG	THR		USNDC-3	121	0/72	LAS	SMITH+. ND151 LEVELS GIVEN	64390
DY 162	RESON PARAMS	EXPT-PROG	5.4 0	2.7 2	USNDC-3	26	0/72	BNL	COLE+9WN AND WG FOR 3 RESON GIVEN	64243
DY 162	SPECT NGAMMA	EXPT-PROG	2.5-2	3.0 2	USNDC-3	26	0/72	BNL	COLE+.CURVS.SEARCH FOR DIRECT CAPT	64244
TM 169	RESON PARAMS	EXPT-PROG	8.3 1	4.0 2	USNDC-3	77	0/72	COL	ARBO+. CAPT RESON AREAS. 40 RESON.	64277
TM 169	RESON PARAMS	EXPT-PROG	3.9 0	3.0 3	USNDC-3	77	0/72	COL	ARBO+. RESON DIST+ENERGIES.MANY RES	64278
TM 169	THRMLSCATLAW	EXPT-PROG	NDG		USNDC-3	25	0/72	ANL	LANDER+. COHERENT SCAT LENGTH GIVEN	64245
TA 181	RESON PARAMS	EXPT-PROG	4.3 0	1.4 3	USNDC-3	50	0/72	COL	GARG+. G*WN,WT,WG GIVEN FOR MANY RES	64286
TA 181	NONEL GAMMAS	EXPT-PROG		2.0 7	USNDC-3	140	0/72	ORL	MORGAN+. GAM PROD SIGS. NO DATA GIVN	64324
TA 181	N,GAMMA	EXPT-PROG	2.4 4		USNDC-3	164	0/72	RPI	BLOCK+. SIG GIVEN. +-4 OR 5PC.	64300
W	DIFF ELASTIC	EXPT-PROG	7.5 6		USNDC-3	211	0/72	ABD	BUCHER+. 6ANGS 2.5-15DEG. NDG	64197
W 183	RESON PARAMS	EXPT-PROG	7.6 0	2.6 3	USNDC-3	72	0/72	COL	CAMARDA+. WT,G*WN,J FOR MANY RESON	64279
PT	SPECT NGAMMA	EXPT-PROG	2.4 4		USNDC-3	38	0/72	BNL	WASSON+. GE(LI) DET. CURVE	64295
AU 197	N,GAMMA	EXPT-PROG	2.4 4		USNDC-3	164	0/72	RPI	BLOCK+. SIG GIVEN. +-4 OR 5PC.	64302
AU 197	N,GAMMA	THEO-PROG	1.0 3	4.0 6	USNDC-3	103	0/72	LRL	GARDNER+. OPTMOD CALCULATN. CURVE	64377
HG 196	N,GAMMA	EXPT-PROG	3.0 3	5.0 5	USNDC-3	148	0/72	ORL	MACKLIN+. ANAL TBC.NO DATA GVN.ORELA	64441
PB 206	N,GAMMA	EXPT-PROG	NDG		USNDC-3	147	0/72	ORL	ALLEN+.ORELA.HI RESOL.NO DOORWAY ST	64320
BI 209	TOTAL XSECT	EXTH-PROG	NDG		USNDC-3	174	0/72	DKE	CLEMENT+.THEORETICAL ANAL TBC. NDG	64370
BI 209	N,GAMMA	EXPT-PROG	3.0 3	5.0 5	USNDC-3	148	0/72	ORL	MACKLIN+. ANAL TBC.NO DATA GVN.ORELA	64440
U 233	NU	EXPT-PROG	THR	1.0 2	USNDC-3	164	0/72	RPI	REED+. LINAC. ANALYSIS TBC. NDG	64299
U 233	DELAYD NEUTS	EXPT-PROG	1.0 5	1.5 7	USNDC-3	127	0/72	LAS	EVANS+. REVISED VALUES GIVEN.TBP NSE	64336
U 234	FISSION	EXPT-PROG	NDG		USNDC-3	115	0/72	LAS	SILBERT. NUCL SHOT. NO DATA GIVEN	64400
U 235	EVALUATION	EVAL-PROG	NDG		USNDC-3	1	0/72	AGN	SMITH. REICH-MOORE PARAMS. NO DATA	64215
U 235	TOTAL XSECT	EXPT-PROG	1.5 6	4.0 6	USNDC-3	13	0/72	ANL	GUENTHER+. NO DATA GIVEN	64226
U 235	TOTAL XSECT	EXPT-PROG	5.0 5	1.5 7	USNDC-3	129	0/72	NBS	SCHWARTZ+. 1 PC ACCURACY. CURVE	64332
U 235	RESON PARAMS	EVAL-PROG	NDG		USNDC-3	1	0/72	AGN	SMITH. REICH-MOORE PARAMS. NO DATA	64216
U 235	RESON PARAMS	EXPT-PROG	2.9-1	1.2 1	USNDC-3	43	0/72	BNL	REDDINGIUS+. TRANS. J FOR 11 RESON	64296
U 235	DIFF ELASTIC	EXPT-PROG	1.5 6	4.0 6	USNDC-3	13	0/72	ANL	GUENTHER+. NO DATA GIVEN	64200
U 235	NONEL GAMMAS	EXPT-PROG	1.0 6	8.0 6	USNDC-3	120	0/72	LAS	DRAKE. GAM PROD SIG. NDG. TBP LA RPT	64391
U 235	DIFF INELAST	EXPT-PROG	1.5 6	4.0 6	USNDC-3	13	0/72	ANL	GUENTHER+. NO DATA GIVEN	64272
U 235	FISSION	EXPT-PROG	1.0 2	2.0 5	USNDC-3	143	0/72	ORL	GWIN+.TABLE OF AVERAGE SIGS	64414

ELEMENT S A	QUANTITY	TYPE	ENERGY MIN	MAX	DOCUMENTATION REF VOL PAGE DATE		LAB	COMMENTS	SERIAL NO.
U 235	FISSION	EXPT-PROG	FISS		USNDC-3 134	0/72	NBS	GRUNDL+. ABSOL SIG GIVEN.CF252SOURCE	64326
U 235	FISSION	EXPT-PROG	1.0 6	6.0 6	USNDC-3 120	0/72	LAS	BARTON+. ABSOL MEAST. NO DATA GIVEN	64392
U 235	FISSION	EXPT-PROG	NDG		USNDC-3 150	0/72	ORL	PEELLE+. TBD. SEE ORNL-4800	64433
U 235	FISSION	EXPT-PROG	2.0-2	2.0 5	USNDC-3 149	0/72	ORL	GWIN+. NO DATA GIVEN. SEE ORNL-4800	64434
U 235	NU	EXPT-PROG	THR	4.0 1	USNDC-3 164	0/72	RPI	REED+. LINAC. ANALYSIS TBC. NDG	64298
U 235	NU	EXPT-PROG	5.0-1	5.0 1	USNDC-3 99	0/72	LRL	HOWE+.SOME STRUCT SEEN.TO BE COMPLET	64383
U 235	DELAYD NEUTS	EXPT-PROG	1.0 5	1.5 7	USNDC-3 127	0/72	LAS	EVANS+. REVISED VALUES GIVEN.TBP NSE	64335
U 235	SPECT FISS N	EXPT-PROG	1.8 6		USNDC-3 118	0/72	LAS	AUCHAMPAUGH+. VDG. CURVE	64395
U 235	N,ALPHA	THEO-PROG		5.8 6	USNDC-3 145	0/72	ORL	JOHNSON.R-MATRIX ANALYSIS.	64413
U 238	TOTAL XSECT	EXPT-PROG	1.5 6	4.0 6	USNDC-3 13	0/72	ANL	GUENTHER+. NO DATA GIVEN	64225
U 238	TOTAL XSECT	EXPT-PROG	5.0 5	1.5 7	USNDC-3 129	0/72	NBS	SCHWARTZ+. 1 PC ACCURACY. CURVE	64331
U 238	RESON PARAMS	EXPT-PROG		1.0 5	USNDC-3 166	0/72	RPI	BYOUN+. AVERAGE PARAMS GIVEN	64375
U 238	DIFF ELASTIC	EXPT-PROG	1.5 6	4.0 6	USNDC-3 13	0/72	ANL	GUENTHER+. NO DATA GIVEN	64199
U 238	DIFF INELAST	EXPT-PROG	1.5 6	4.0 6	USNDC-3 13	0/72	ANL	GUENTHER+. NO DATA GIVEN	64273
U 238	FISSION	EXPT-PROG	FISS		USNDC-3 134	0/72	NBS	GRUNDL+. ABSOL SIG GIVEN.CF252SOURCE	64325
U 238	DELAYD NEUTS	EXPT-PROG	NDG		USNDC-3 18	0/72	ANL	COX. NO DATA GIVN. TO BE COMPLETED	64247
U 238	DELAYD NEUTS	EXPT-PROG	3.1 6	1.5 7	USNDC-3 127	0/72	LAS	EVANS+. 2ES. REVISED VALUES GIVN TBP	64387
U 238	SPECT FISS N	EXPT-PROG	1.8 6		USNDC-3 118	0/72	LAS	AUCHAMPAUGH+. VDG. CURVE	64394
U 238	N,GAMMA	EXPT-PROG	2.4 4		USNDC-3 164	0/72	RPI	BLOCK+. SIG GIVEN. +-4 OR 5PC.	64301
U 238	N,GAMMA	EXPT-PROG	1.0 2	1.2 3	USNDC-3 150	0/72	ORL	SILVER+. AVGD OVER 100EV INTERVALS	64317
PU 238	STRNTH FNCTN	EXPT-PROG	1.8 1	2.0 5	USNDC-3 114	0/72	LAS	SILBERT+. SO GIVEN. TBP PR.	64404
PU 239	TOTAL XSECT	EXPT-PROG	1.5 6	4.0 6	USNDC-3 13	0/72	ANL	GUENTHER+. NO DATA GIVEN	64224
PU 239	TOTAL XSECT	EXPT-PROG	5.0 5	1.5 7	USNDC-3 129	0/72	NBS	SCHWARTZ+. 1 PC ACCURACY. CURVE	64330
PU 239	DIFF ELASTIC	EXPT-PROG	1.5 6	4.0 6	USNDC-3 13	0/72	ANL	GUENTHER+. NO DATA GIVEN	64198
PU 239	DIFF INELAST	EXPT-PROG	1.5 6	4.0 6	USNDC-3 13	0/72	ANL	GUENTHER+. NO DATA GIVEN	64274
PU 239	FISSION	EXPT-PROG	NDG		USNDC-3 150	0/72	ORL	PEELLE+. TBD. SEE ORNL-4800	64432
PU 239	FISSION	EXPT-PROG	2.0-2	2.0 5	USNDC-3 149	0/72	ORL	GWIN+. NO DATA GIVEN. SEE ORNL-4800	64435
PU 239	FISSION	EXPT-PROG	2.5-2	3.0 4	USNDC-3 149	0/72	ORL	WESTON+. RATIO NG/NF MEASD. NO DATA	64439
PU 239	NU	EXPT-PROG	NDG		USNDC-3 164	0/72	RPI	REED+. LINAC. TO BE COMPLETED. NDG	64297
PU 239	NU	EXPT-PROG	2.5-2	1.5 7	USNDC-3 99	0/72	LRL	HOWE+.TO BE DONE	64382
PU 239	DELAYD NEUTS	EXPT-PROG	1.0 5	1.5 7	USNDC-3 127	0/72	LAS	EVANS+. REVISED VALUES GIVEN.TBP NSE	64334
PU 239	SPECT FISS N	EXPT-PROG	1.8 6		USNDC-3 118	0/72	LAS	AUCHAMPAUGH+. VDG. CURVE	64393
PU 239	N,GAMMA	EXPT-PROG	2.5-2	3.0 4	USNDC-3 149	0/72	ORL	WESTON+. RATIO NG/NF MEASD. NO DATA	64438
PU 240	SPECT NGAMMA	EXPT-PROG	THR		USNDC-3 124	0/72	LAS	JURNEY. CURVES	64388
PU 241	FISSION	EXPT-PROG	2.5-2	3.0 4	USNDC-3 149	0/72	ORL	WESTON+. RATIO NG/NF MEASD. NO DATA	64437
PU 241	N,GAMMA	EXPT-PROG	2.5-2	3.0 4	USNDC-3 149	0/72	ORL	WESTON+. RATIO NG/NF MEASD. NO DATA	64436
PU 242	TOTAL XSECT	EXPT-PROG	1.5 1	3.0 4	USNDC-3 2	0/72	AGN	SIMPSON+.TRANS. NO DATA GIVEN. ORELA	64213
PU 242	RESON PARAMS	EXPT-PROG	2.3 1	4.9 2	USNDC-3 2	0/72	AGN	SIMPSON+.TRANS.WN AND WG FOR 34RESON	64214
PU 242	FISSION	EXPT-PROG	3.0 3	6.0 4	USNDC-3 155	0/72	RPI	HOCKENBURY+. TO BE COMPLETED. NDG	64303
PU 242	DELAYD NEUTS	EXPT-PROG	1.0 5	1.8 6	USNDC-3 127	0/72	LAS	EVANS+. REVISED VALUES GIVEN.TBP NSE	64333
PU 242	N,GAMMA	EXPT-PROG	3.0 3	6.0 4	USNDC-3 155	0/72	RPI	HOCKENBURY+. TO BE COMPLETED. NDG	64304
CM 244	TOTAL XSECT	EXPT-PROG	6.0 0	5.3 2	USNDC-3 4	0/72	AGN	SIMPSON+. TRANS. NO DATA GIVEN	64212
CM 244	RESON PARAMS	EVAL-PROG	-1. 0	5.2 2	USNDC-3 4	0/72	AGN	SIMPSON+.WN WF WG FOR 37 RESON	64208
CM 244	RESON PARAMS	EVAL-PROG	7.7 0		USNDC-3 4	0/72	AGN	SIMPSON+. WN WF WG (RECOMMENDED) GVN	64209
CM 244	FISSION	EXPT-PROG	6.0 0	5.3 2	USNDC-3 4	0/72	AGN	SIMPSON+. TRANS. NO DATA GIVEN	64210
CM 244	RES INT FISS	EVAL-PROG	-1. 0	5.2 2	USNDC-3 4	0/72	AGN	SIMPSON+.RECOMMENDED VALUE GIVEN	64206
CM 244	RES INT ABS	EVAL-PROG	-1. 0	5.2 2	USNDC-3 4	0/72	AGN	SIMPSON+.RECOMMENDED VALUE GIVEN	64207
CM 244	RES INT CAPT	EVAL-PROG	-1. 0	5.2 2	USNDC-3 4	0/72	AGN	SIMPSON+.RECOMMENDED VALUE GIVEN	64205

ELEMENT S A	QUANTITY	TYPE	ENERGY MIN	MAX	DOCUMENTATION REF VOL	PAGE DATE	LAB	COMMENTS	SERIAL NO.
CM 244	N,GAMMA	EXPT-PROG	6.0 0	5.3 2	USNDC-3 4	0/72	AGN	SIMPSON+. TRANS. NO DATA GIVEN	64211
CF 249	RESON PARAMS	EXPT-PROG	1.5 1	7.0 1	USNDC-3 114	0/72	LAS	SILBERT. AVG PARAMS GIVN. TBP PR	64402
CF 249	STRNTH FNCTN	EXPT-PROG	1.5 1	7.0 1	USNDC-3 114	0/72	LAS	SILBERT. SO GIVN. NUCL SHOT.TBP PR	64401
CF 249	FISSION	EXPT-PROG	1.3 1	3.0 6	USNDC-3 114	0/72	LAS	SILBERT. NUCL SHOT. NDG. TBP PR	64403
E 253	FISSION	EXPT-PROG	NDG		USNDC-3 115	0/72	LAS	SILBERT. NUCL SHOT. NO DATA GIVEN	64399
FM 257	NU	EXPT-PROG	SPON		USNDC-3 116	0/72	LAS	VEESER+. LIQ SCINT TANK.NU REL CF252	64398
MANY	DIFF ELASTIC	EXPT-PROG	2.0 6		USNDC-3 15	0/72	ANL	COX. NO DATA GIVEN. 25 ELEMENTS	64263
MANY	POLARIZATION	EXPT-PROG	2.0 6		USNDC-3 15	0072	ANL	COX. NO DATA GIVEN. 25 ELEMENTS	64262

AEROJET NUCLEAR COMPANY

A. MODIFICATIONS TO SCORE (J. R. Smith, N. H. Marshall)

The interactive graphics program SCORE, developed by Atomics International, includes resonance fitting procedures patterned after an early version of the Aerojet Nuclear program ACSAP. The utilization of this combination has been handicapped by an array of program bugs and operational problems, often encountered when programs from different laboratories are combined. Many of the problems have now been overcome.

In addition to the extensive debugging, several modifications to SCORE were made to increase its utility. Initial information, such as run identification, resolution and sample information, and resonance parameter input can now be read in from cards. This saves a large amount of console time, particularly when several similar runs are made in sequence. SCORE will read resonance parameters cards output by the batch-mode ACSAP program, and will punch out cards in the same format, thus bypassing the format conversion and resonance file preparation runs that were formerly necessary. The output listing of SCORE now includes a history of the selections and modifications made during the run, and notations when microfilm output was called for. This makes it much easier to identify the conditions under which the output plots were obtained.

Improvements in fitting techniques were also made. Some of the algorithms from the current batch-mode ACSAP were added to SCORE to speed its convergence. In addition, provision was made to change the relative angle of the fission vector for a resonance. The latter feature makes it possible to modify fission interference patterns slightly and quickly see the effect upon the predicted cross section. The most useful application of SCORE at present is in fitting fission cross sections in narrow energy regions where resonance spacing is small and interference is strong.

B. MULTILEVEL RESONANCE PARAMETERS FOR ^{235}U (J. R. Smith)

A set of Reich-Moore multilevel parameters has been generated for ^{235}U. The data fitted were deSaussure's fission and capture, Michaudon's total, and Blons' fission data. The same data normalizations and resolution assumptions were used that were used for the single level fits that went into ENDF/B, Version III. The objective was to obtain matched sets of single-level and multilevel parameters on which to base studies of multilevel effects. The fission widths appear to be closely comparable.

C. NEUTRON RESONANCE PARAMETERS OF ^{242}Pu BELOW 500 eV [F. B. Simpson, O. D. Simpson, H. G. Miller (ANC) J. A. Harvey, N. W. Hill (ORNL)]

The total neutron cross section and resonance parameters of ^{242}Pu are important in the evaluation of reactor parameters for the production of the transplutonium isotopes and the Fast Breeder Reactor Program. Total neutron cross section measurements on ^{242}Pu have been made from 15.0 to 30,000 eV using the Oak Ridge Electron Linear Accelerator (ORELA)[1]. However, because of funding limitations the data have not been analyzed above 500 eV.

Transmission data were taken on three different metal samples at liquid nitrogen temperature (77°K) having inverse thicknesses of 41.19, 175.5, and 763.9 barns/atom. The metal samples were made at Los Alamos and were originally prepared for thermal cross section measurements on the Materials Testing Reactor fast chopper[2].

The ORELA measurements were made using a 28 nsec accelerator burst width with a pulse rate of 600 bursts/sec. The neutrons produced by a (γ,n) reaction on tantalum were moderated in a 3 cm thick slab of water 15 cm in diameter around the target. Neutrons from the moderator were collimated and allowed to strike a 1.25 cm thick ^{6}Li glass scintillation neutron detector located at a flight path of 78.188 meters. The sample, open, and background data sets were normalized using a BF_3 beam monitor. The backgrounds were composed of static and time dependent interferences. These backgrounds were determined from calibrated $^{10}B_4C$ filters[3] and a "blacking-out" resonance technique.

The channel widths were varied from 4-128 nsec, with the shorter channel widths used for the high energy and the longer channel widths for the low energy. The neutron resonance parameter Eo (resonance energy), $\Gamma_n{}^o$ (reduced neutron width where $\Gamma_n{}^o = \Gamma_n E_o{}^{-1/2}$) and $\Gamma\gamma$ (capture width) are listed in Table C-1 from 20-500 eV.

---

[1] N. C. Pering and T. A. Lewis, "Performance of the 140 MeV High Current Short Pulse LINAC at ORNL", IEEE Trans. Nucl. Science NS-16 (3), 316 (1969).

[2] T. E. Young, F. B. Simpson, and R. E. Tate, "The Low-Energy Total Neutron Cross Section of ^{242}Pu", Nuc. Sci. Engr., 43, 343 (1971).

[3] O. D. Simpson, et al., "The Determination of Background for Neutron Sources", Nuc. Instr. and Methods, 30, 293 (1964).

TABLE C-1

^{242}Pu RESONANCE PARAMETERS

E_o (eV)	Γ_n^o 9meV)	$\Gamma\gamma$ (meV)
22.566	0.0550 ± 0.004	20.000 ± 5
40.950	0.0700 ± 0.006	29.000 ± 4
53.460	6.9300 ± 0.22	28.000 ± 3
67.620	0.6000 ± 0.05	22.000 ± 3
88.460	0.0700 ± 0.005	[29.000]
107.370	1.7200 ± 0.15	28.000 ± 7
131.430	0.5400 ± 0.02	34.000 ± 5
141.430	0.0100 ± 0.002	[29.000]
149.820	1.0700 ± 0.06	29.000
163.640	0.0450 ± 0.004	[29.000]
240.970	3.8000 ± 0.25	28.000 ± 6
210.100	0.280 ± 0.006	[29.000]
215.430	0.3650 ± 0.02	36.000 ± 3
219.580	0.0200 ± 0.002	[29.000]
232.870	0.3000 ± 0.03	28.000 ± 3
264.720	0.0240 ± 0.002	[29.000]
271.950	0.0100 ± 0.002	[29.000]
273.710	0.7560 ± 0.06	31.000 ± 4
274.950	0.0100 ± 0.002	[29.000]
281.050	0.0080 ± 0.003	[29.000]
298.760	0.4500 ± 0.04	[29.000]
303.650	1.0200 ± 0.08	[29.000]
319.980	13.1000 ± 0.4	34.000 ± 8
332.530	3.9000 ± 0.1	36.000 ± 3
374.390	0.3500 ± 0.02	[29.000]
379.630	0.0140 ± 0.002	[29.000]
382.420	2.5300 ± 0.13	28.000 ± 5
400.020	0.0800 ± 0.010	[29.000]
410.690	0.3400 ± 0.020	[29.000]
424.110	0.1850 ± 0.015	[29.000]
425.150	0.0134 ± 0.002	[29.000]
473.520	0.0400 ± 0.004	[29.000]
482.740	0.9100 ± 0.08	[29.000]
494.750	0.0120 ± 0.003	[29.000]

[ ] assumed $\overline{\Gamma}_\gamma$ = 29 meV.

D. AN ANALYSIS AND EVALUATION OF THE ^{244}Cm TOTAL, CAPTURE AND FISSION CROSS SECTIONS BELOW 530 eV (O. D. Simpson, F. B. Simpson, T. E. Young, Aerojet Nuclear Company, J. A. Harvey, N. Hill, Oak Ridge National Laboratory and R. W. Benjamin, Savannah River Laboratory)

Transmission measurements have been made on a sample of ^{244}Cm having an inverse thickness of 1212 b/a. Data were collected from 6-530 eV on the Oak Ridge Electron Linear Accelerator[1] using 40 nsec, 140 MeV electron bursts 16 nsec basic channel widths and a flight path of 17.77 meters. An evaluation was done incorporating these new data with the earlier total cross sections of Cote[2] and Berreth[3] and the capture and fission cross sections of Moore[4]. Breit-Wigner resonance parameters were obtained which best describe these sets of cross sections. Integral measurements of Schuman[5], Thompson[6] and Benjamin[7] were also used.

The neutron reduced scattering widths were determined from the transmission data using area analysis for the 7.667 and 15.785 eV levels by assuming absorption widths of 37.2[2] and 38.4 meV, respectively. The parameters for the 7.667 eV level were then combined with those of Cote[2] and Berreth[3] and an evaluation produced the recommended parameters (see Table D-1). The fission width of 1.00 was determined so that the resonance fission integral as calculated from the parameters of Table D-2 yielded a value of 18 b-eV[7]. The resonance parameters above 20 eV, Table D-2, were obtained from area analyses of the total data of Simpson (this report) and the capture and fission data of Moore[4]. These sets of data were the only ones used above 20 eV because of their superior resolution. An average level spacing of 14.1 eV was observed.

The resonance integrals for the absorption, capture and fission cross sections are listed in Table III. The absorption integrals of Cote', Berreth, and Simpson were calculated from resonance parameters as determined by each experimentor. The data of Schuman, Thompson, and Benjamin were determined by direct integral measurements. The recommended integrals are compared with the ENDF/B Version II and III values.

TABLE D-1

^{244}Cm Resonance Parameters for the 7.667 eV Level

	Cote'	Berreth	Simpson	Recommended
Γ_n^o	3.7 ± 0.2	3.4 ± 0.2	3.2 ± 0.2	3.44 ± 0.20
Γ_a	37.2 ± 3.3	35 ± 2	37.2 (a)	37.1 ± 3.3
Γ_f	--	--	--	1.00 ± 0.06(b)
Γ_γ	--	--	--	36.1 ± 3.3(c)

(a) Assumed
(b) Adjusted so the resonance fission integral as calculated from the resibabce oaraneters if Table II was 18 b-eV.
(c) Obtained by subtracting the fission width from the absorption width.

TABLE D-2

^{244}Cm Resonance Parameters

E_o (eV)	Γ_n^o (meV)	Γ_γ (meV)	Γ_f (meV)
-1.48 (a)	0.0685	37	2.1
7.667 (b) ± 0.004	3.44 ± 0.2	36.1 ± 3.3	1.00 ± 0.06
16.785 ± 0.008	0.46 ± 0.03	37 ± 2	1.4 ± 0.1
22.825 ± 0.01	0.179 ± 0.01	35 ± 2	3.5 ± 0.2
35.00 ± 0.02	0.64 ± 0.04	23 ± 3	1.57 ± 0.20
52.80 ± 0.02	0.084 ± 0.08	35 ± 2	1.60 ± 0.09
70.05 ± 0.03	0.078 ± 0.016	20 ± 3	1.70 ± 0.26
86.05 ± 0.04	2.76 ± 0.14	30 ± 3	0.52 ± 0.05
96.30 ± 0.05	0.69 ± 0.07	51 ± 7	2.33 ± 0.34
132.90 ± 0.06	1.10 ± 0.06	46 ± 5	1.62 ± 0.18
139.20 ± 0.07	0.20 ± 0.04	30 ± 6	2.70 ± 0.54
171.30 ± 0.08	0.23 ± 0.05	34. ± 6	1.17 ± 0.21
181.6 ± 0.09	0.65 ± 0.07	34 ± 5	1.84 ± 0.27
197.0 ± 0.10	2.30 ± 0.12	50 ± 5	1.34 ± 0.13
209.8 ± 0.11	3.12 ± 0.16	34 ± 5	0.48 ± 0.07
222.1 ± 0.11	2.78 ± 0.14	52 ± 8	1.80 ± 0.28
230.7 ± 0.11	0.99 ± 0.10	50 ±12	0.50 ± 0.12
234.5 ± 0.12	0.26 ± 0.08	41 ±15	0.85 ± 0.31
264.8 ± 0.13	0.70 ± 0.09	40 ±10	0.92 ± 0.24
274.2 ± 0.14	1.30 ± 0.13	35 ± 5	0.39 ± 0.06
317.4 ± 0.15	0.34 ± 0.08	35 ±15	0.28 ± 0.09
329.5 ± 0.16	2.33 ± 0.15	45 ± 8	0.41 ± 0.07
343.6 ± 0.17	2.54 ± 0.16	30 ± 5	0.80 ± 0.13
353.1 ± 0.18	6.25 ± 0.34	35 ± 5	1.22 ± 0.17
361.8 ± 0.18	1.20 ± 0.10	42 ± 7	1.38 ± 0.23
364.6 ± 0.18	0.32 ± 0.12	39 ±10	2.20 ± 0.56
386.3 ± 0.19	1.33 ± 0.11	30 ± 5	0.90 ± 0.15
397.6 ± 0.20	0.90 ± 0.10	39 ± 5	0.70 ± 0.09
414.0 ± 0.21	1.05 ± 0.10	35 ± 5	0.21 ± 0.03
420.6 ± 0.21	6.00 ± 0.30	33 ± 5	0.85 ± 0.13
426.9 ± 0.21	1.00 ± 0.15	19 ± 5	0.18 ± 0.05
443.7 ± 0.22	3.20 ± 0.26	41 ± 6	1.00 ± 0.15
471.1 ± 0.24	2.04 ± 0.16	46 ± 9	2.80 ± 0.55
489.2 ± 0.25	1.00 ± 0.20	20 ± 5	0.27 ± 0.07
492.1 ± 0.25	2.77 ± 0.25	33 ± 5	0.42 ± 0.08
511.1 ± 0.26	5.44 ± 0.28	41 ± 5	0.22 ± 0.03
520.6 ± 0.26	1.76 ± 0.16	28 ± 4	1.61 ± 0.23

(a) Value obtained by Berreth (see ENDF/B III).

(b) See Table D-1

Note: These parameters were obtained by doing a complete analysis of the total data of Simpson et al., and the fission and capture data of Moore et al. The Automated Cross Section Analysis Program (ACSAP) was used in obtaining the above parameters.

TABLE D-3

^{244}Cm Resonance Integrals

	$\int_{0.625}^{\infty} \sigma_{nx} \frac{dE}{E}$	$\int_{0.625}^{\infty} \sigma_{n\gamma} \frac{dE}{E}$	$\int_{0.625}^{\infty} \sigma_{nf} \frac{dE}{E}$
Cote' (1964)	648 ± 32	--	--
Schuman (1969)	[667 ± 70] (a)	650 ± 50	--
Berreth (1971)	605 ± 36	--	--
Thompson (1971)	[662 ± 70] (b)	650 ± 50	12.5 ± 2.5
Benjamin (1972)	--	--	18 ± 1
Simpson (1972)	594 ± 30	--	--
Recommended	624 ± 23 (c)	606 ± 23 (d)	18 ± 1
ENDF/B II	654 ± 35	637 ± 37	17 ± 11
ENDF/B III	631 ± 38	595 ± 43	36 ± 21

(a) Obtained by substracting 1 b-eV (the estimated integral between Cd cutoff and 0.625 eV) and adding 18 b-eV due to fission. The error was arbitrarily increased to ± 70 by the authors of this report.

(b) Summation of fission plus capture minus the 1 b-eV described above.

(c) Obtained by weighting the individual values inversely as the square of the error.

(d) Obtained by subtracting the recommended fission and absorption integrals.

Note: The resonance parameters of Table II predict the recommended resonance integrals as listed above.

References

1. N. C. Pering and T. A. Lewis, "Performance of the 140 MeV High Current Short Pulse LINAC at ORNL", IEEE Trans. Nucl. Science NS-16 (3), 316 (1969).

2. R. E. Cote', R. F. Barnes and H. Diamond, "Total Neutron Cross Section of ^{244}Cm", Phys. Rev., 134, B1281 (1964).

3. J. R. Berreth, F. B. Simpson and B. C. Rusche, "The Total Neutron Cross Section of the Cm Isotopes from 0.01 to 30 eV", accepted for publication by Nuc. Science and Engr. (1972).

4. M. S. Moore and G. A. Keyworth, "Analysis of the Fission and Capture Cross Sections of the Curium Isotopes", Phys. Rev. C, 3, 1656 (1971).

5. R. P. Schuman, "Resonance Integrals from the Cadmium Shielded Irradiation of ^{244}Cm", Nuclear Technology Branch Annual Report for Period Ending June 30, 1969, 59 (1970).

6. M. C. Thompson, M. L. Hyder, and R. J. Rueland, "Thermal Neutron Cross Sections and Resonance Integrals for ^{244}Cm through ^{248}Cm", J. Inorg. Nucl. Chem., 33, 1553 (1971).

7. R. W. Benjamin, K. W. MacMurdo, and J. D. Spencer, "Fission Cross Sections for Five Isotopes of Curium and Californium 249", Nuclear Science and Engr., 47, 203 (1972).

E. INTEGRAL CROSS SECTION MEASUREMENTS IN THE CFRMF (Y. D. Harker)

Capture cross section measurements for different materials have and are being measured in the Coupled Fast Reactivity Measurement Facility. Recent efforts in this program have been directed toward establishing different techniques for cross section measurements associated with samples prepared in the recently acquired isotope separator. Samples of xenon isotopes have been prepared, measured and analyses of the data are currently in progress. Along with our cross section measurement program, we have been involved with the Interlaboratory LMFBR Reaction Rate Program, and phase I of this program was completed. Results of this phase have established the reaction rates of the non-fission dosimetry detectors to uncertainties of less than ten percent at the 95% confidence level.

ARGONNE NATIONAL LABORATORY

A. FAST NEUTRON PHYSICS

1. Thick Target Neutron Yields from Proton and Deuteron Bombardment of ^{9}Be for Neutron Radiation-Therapy (F. T. Kuchnir,* L. S. Skaggs,* A. J. Elwyn, and F. P. Mooring)

As mentioned in a previous report,[1] a time-of-flight technique in conjunction with the pulsed beam from the ANL tandem accelerator has been used to measure the energy spectra and angular distributions of neutrons produced in the bombardment of a thick ^{9}Be target with deuterons of 8 and 16 MeV and protons of about 15 MeV. Some of the results, which are now more complete than those mentioned in ref. 1, are shown in Figures A-1, A-2, A-3, and A-4. The total neutron yields integrated over 4π are (10.7, 2.7, and 7.1) $\times 10^{10}$ neutrons/μc for the deuteron-induced reactions at 16.0 and 8.3 MeV and the proton-induced reaction at 14.8 MeV, respectively. The experimentally observed neutron-energy spectra and angular distributions will be used to optimize the collimator and shielding design for a neutron radiation-therapy facility in conjunction with a medical cyclotron at the Argonne Cancer Research Hospital.

---

*Cancer Research Hospital, Chicago, Illinois.

[1] USNDC-1 (EANDC(US)-168"U"), 23 May 1972.

2. Measurements of the $^{6}Li(n,\alpha)$ Cross Section in the 100-600 keV Range (W. P. Poenitz)

A Lithium-glass detector is an increasingly important neutron flux monitor in the keV energy region. However, discrepancies exceeding 10 percent exist even between more recent measurements of the $^{6}Li(n,\alpha)$ cross section. Thus, measurements were carried out in the 100-600 keV energy range to obtain additional information about this cross section.

One of the problems related to the discrepancies in the existing data is the large correction needed for scattering in the glass. A one-millimeter thick Li-glass was used in the present experiment and the correction for scattering effects was evaluated with a detailed Monte Carlo code. The Li-glass was mounted virtually mass-free in a detector used previously for fission ratio measurements.[1] This assures that there are no additional effects due to scattered neutrons from multipliers,

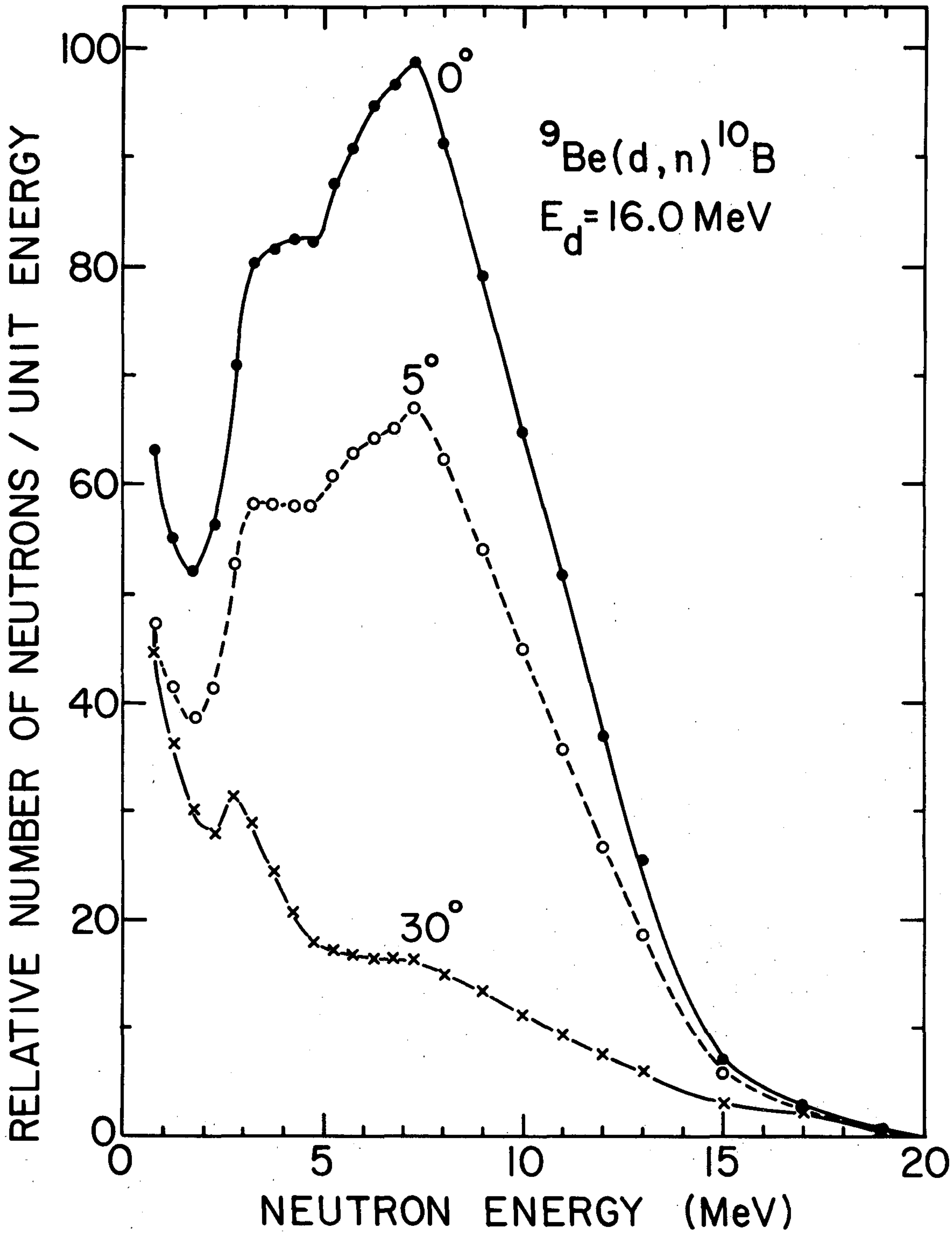

RELATIVE NUMBER OF NEUTRONS / UNIT ENERGY
NEUTRON ENERGY (MeV)
0°
5°
30°
9Be(d,n)10B
Ed=16.0 MeV
0
20
40
60
80
100
0
5
10
15
20

Fig. A-1

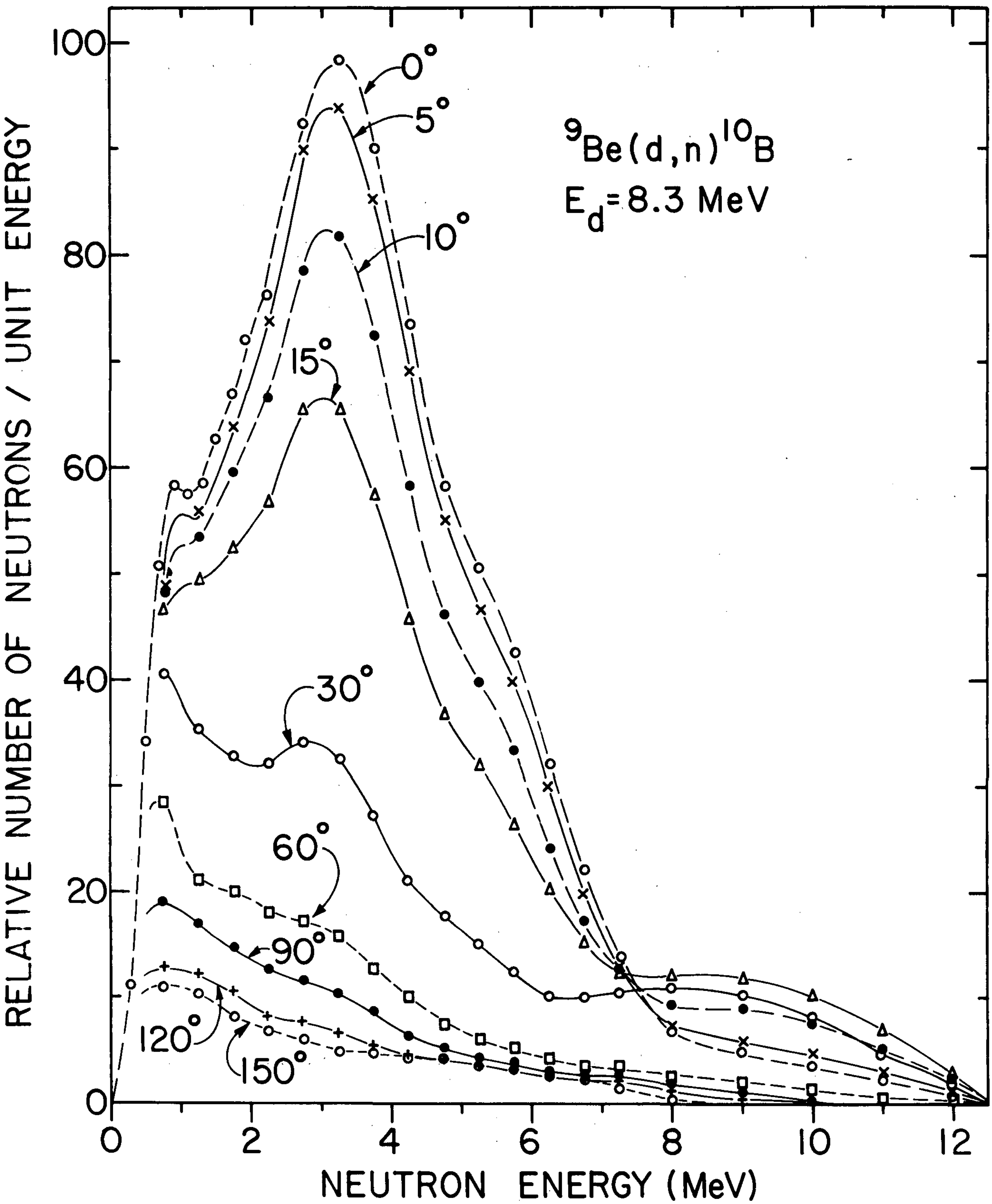

$^9Be(d,n)^{10}B$
$E_d = 8.3$ MeV
0°
5°
10°
15°
30°
60°
90°
120°
150°
RELATIVE NUMBER OF NEUTRONS / UNIT ENERGY
NEUTRON ENERGY (MeV)
0
2
4
6
8
10
12
20
40
60
80
100

Fig. A-2

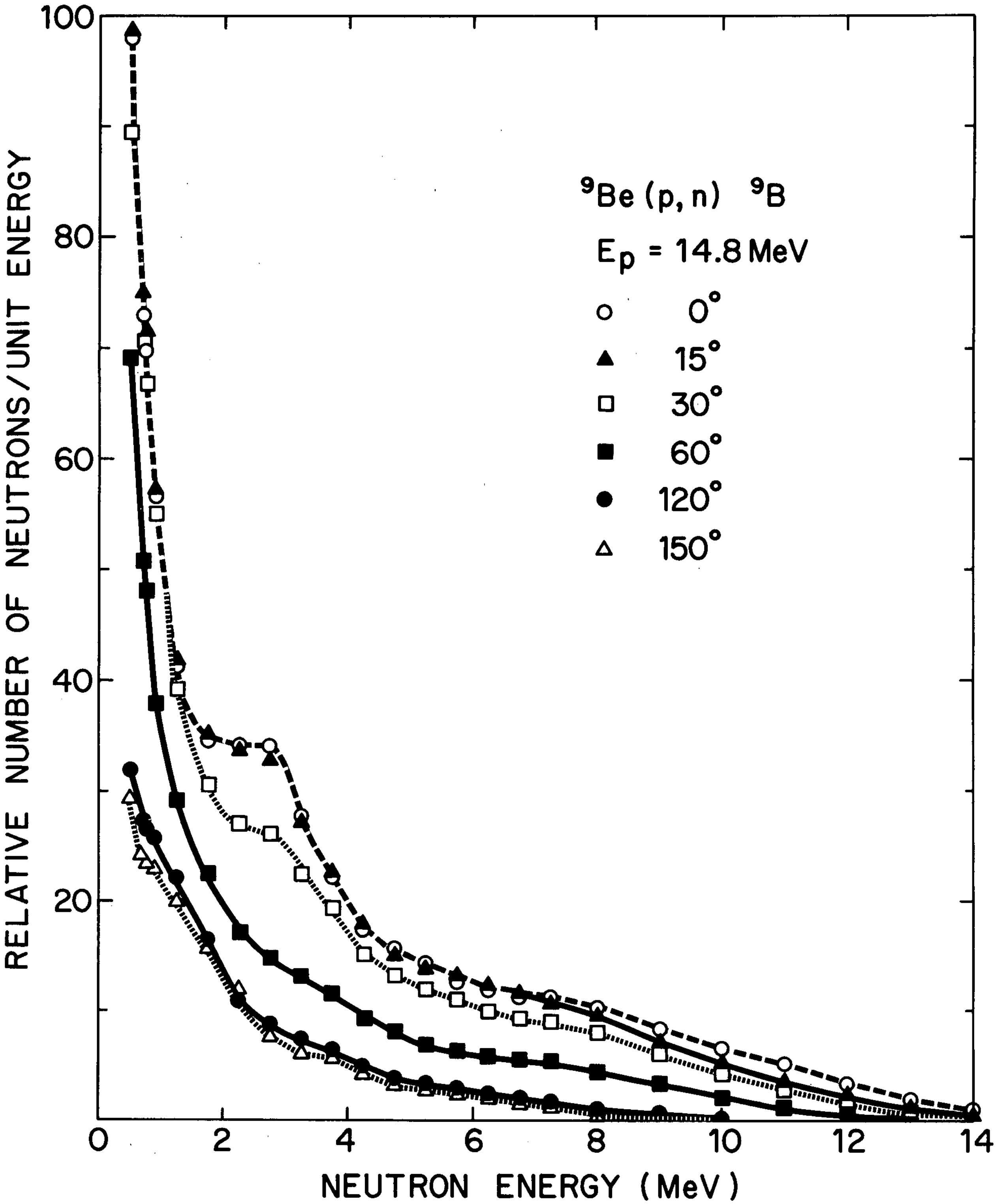

RELATIVE NUMBER OF NEUTRONS/UNIT ENERGY
NEUTRON ENERGY (MeV)
^{9}Be (p, n) ^{9}B
E_p = 14.8 MeV
0°
15°
30°
60°
120°
150°
0
20
40
60
80
100
2
4
6
8
10
12
14

Fig. A-3

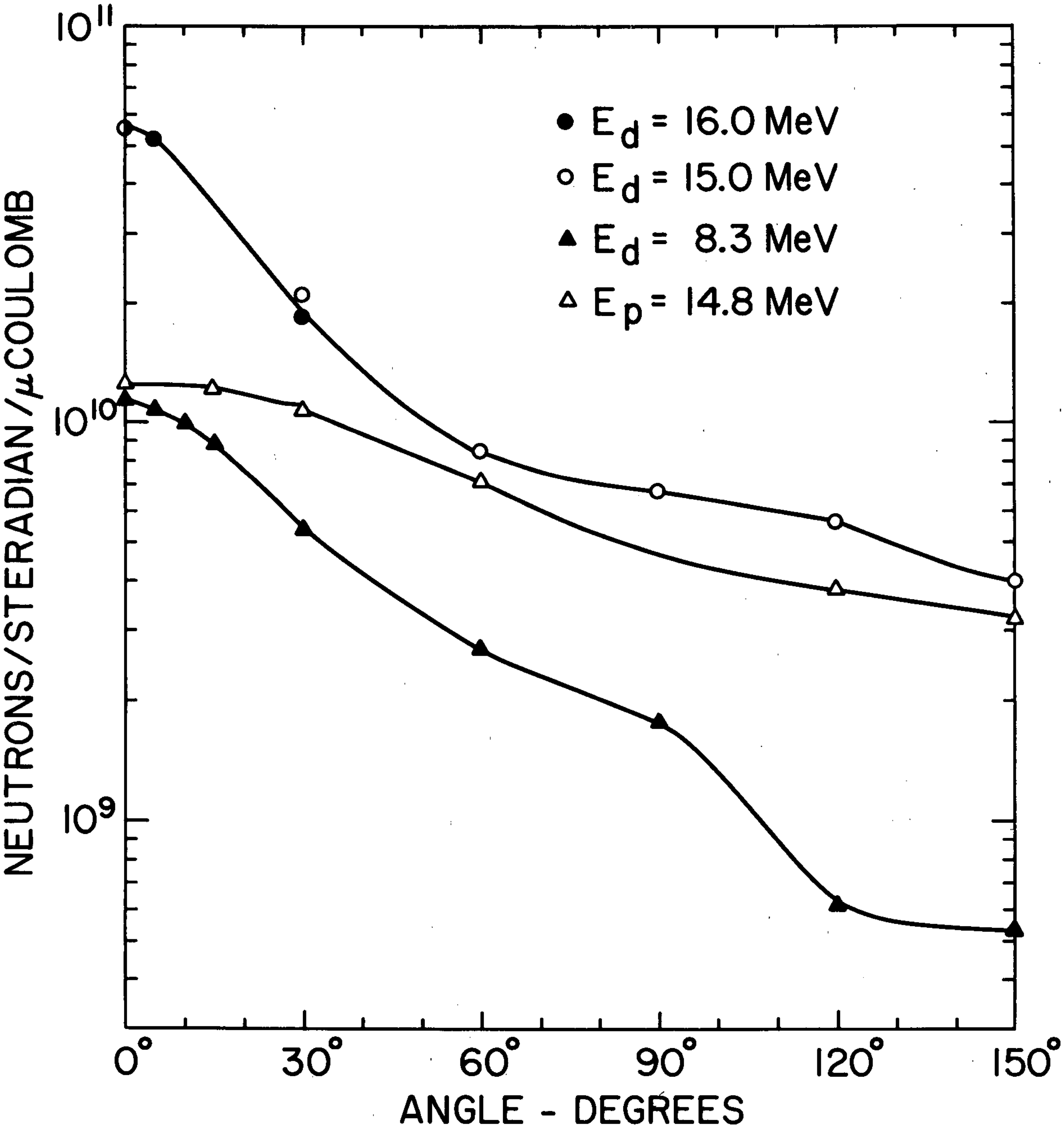

NEUTRONS/STERADIAN/μCOULOMB
10^{11}
10^{10}
10^{9}
● E_d = 16.0 MeV
○ E_d = 15.0 MeV
▲ E_d = 8.3 MeV
△ E_p = 14.8 MeV
0°
30°
60°
90°
120°
150°
ANGLE - DEGREES

Fig. A-4

counter walls, etc. The neutron flux was measured with a "Grey Neutron Detector" which has a flat and smooth efficiency in this energy range. The resulting values give the shape of the cross section while the absolute values will be obtained in a later step of the experiment. Normalizing our results at 100 keV to 0.65 barns (a value well supported by several absolute measurements) yields agreement with the recent measurements by Fort[2] over the present energy range. Normalizing to the 0.7 barn at 100 keV deduced by Meadows[3] from a fit of the measured total cross section results in agreement with Meadows results too. Thus, the present work appears to agree with the shape of the $^{6}Li(n,\alpha)$-cross section obtained by Fort[2] and by Meadows[3], but not with those obtained by Uttley _et al._[4] and Coates _et al._[5] Additional measurements are planned to establish more accurately the resonance at 250 keV and the absolute cross section values.

---

[1] W. P. Poenitz, Nucl. Sci. & Eng. 40, 383 (1970).

[2] E. Fort, Proc., Nucl. Data for Reactors, CN 26/72, Helsinki 1970.

[3] J. F. Meadows, to be published (1972).

[4] C. A. Uttley et al. Proc., Neutron Standards and Flux Normalization, pp. 80, Argonne 1971.

[5] M. S. Coates et al., Proc., Neutron Standards and Flux Normalization, pp. 121, Argonne 1971.

3. Fast Neutron Total and Scattering Cross Sections (P. Guenther, P. Moldauer, A. Smith and J. Whalen)

This program continues to concentrate on the incident energy range 1.5-4.0 MeV and includes the elements/isotopes; carbon, flourine, titanium, vanadium, iron, cobalt, nickel, copper, niobium, zirconium (92-90), U-235, U-238 and Pu-239. During the period, a number of total cross section measurements were made using mono-energetic and self-normalizing techniques. The emphasis was on accurate cross section magnitudes. There were some measurements of elastic and inelastic neutron scattering cross sections in the vicinity of 3.0 MeV. Some indication of the current status is given by the elastic scattering cross section of niobium shown in Fig. A-5. Curves indicate least-square fits of a legendre series to the measured data. Results to 1.5 MeV are previous values[1]

---

[1] Nucl. Phys. 48, 593 (1963).

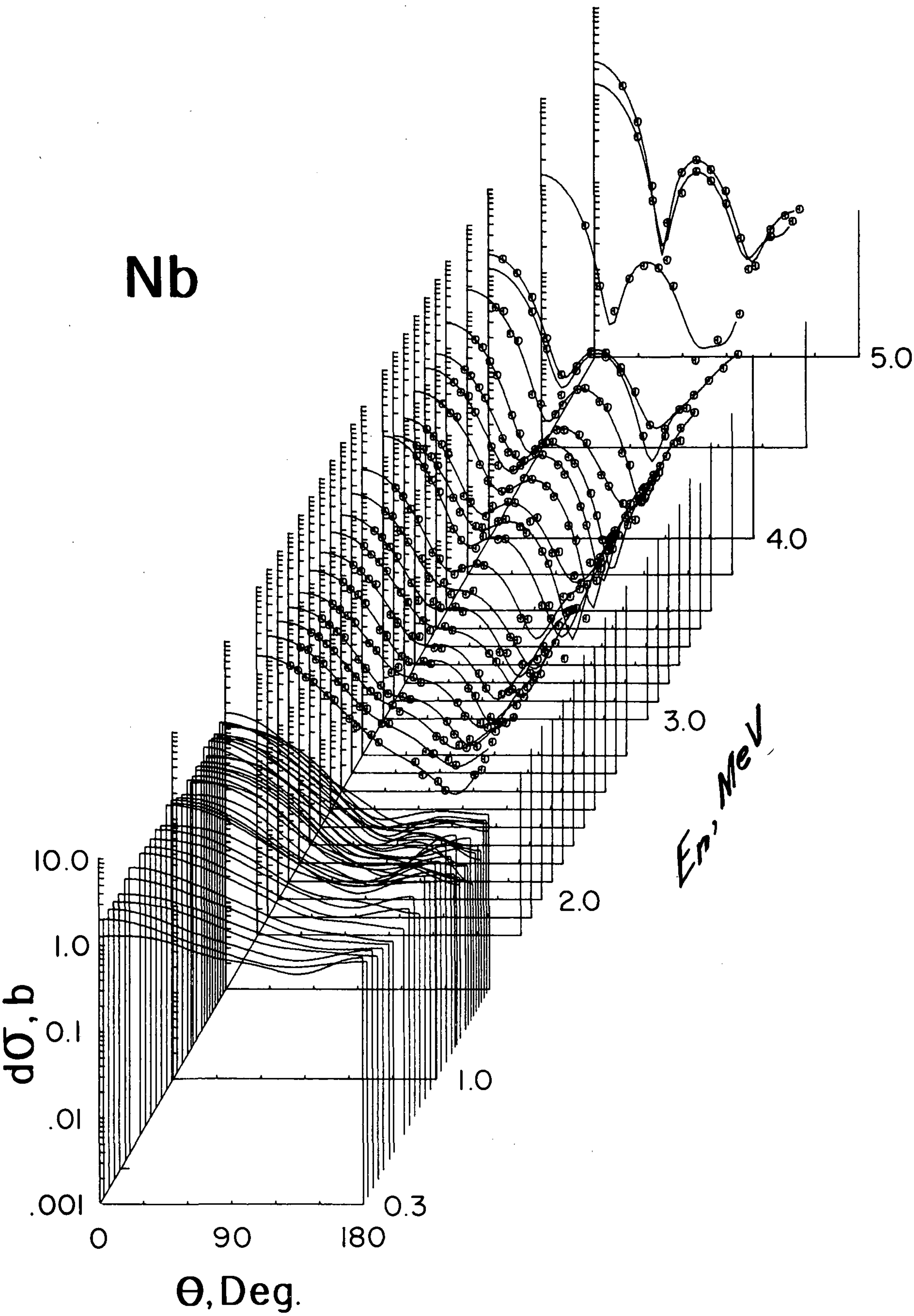

Fig. A-5

from this laboratory. Values from 1.5-4.0 MeV are the result of recent work here. Distributions at 4.0, 4.5, and 5.0 MeV are taken from the work of R. Coles.[2]

Major attention was given to the analysis and interpretation of already completed measurements. Detailed Monte-Carlo procedures for multiple scattering corrections were carefully checked and applied to the data. The codes are in FORTRAN-IV and system independent. The measured values were examined in the context of optical and statistical models with particular attention to the statistical "synthetic" cross section and its relation to the measured quantities.[3] A particularly good statistical correlation between measured and calculated total and scattering cross sections of titanium was achieved using a deformed optical potential. The nautre of the synthetic cross section is sensitive to the choice of optical potential in a fluctuating region where good optical potentials are not easily obtained from the energy-averaged cross sections. Further, synthetic cross sections appear to have promise in applied usage where strong fluctuations are important but not easily obtained from direct experiment (e.g. shielding).

4. Polarization in the Elastic Neutron Scattering from Medium and Heavy Weight Elements (S. A. Cox)

A systematic survey of the differential elastic scattering cross section and differential polarization in elastic neutron scattering at 2 MeV neutron energy has been carried out for 25 elements distributed from aluminum to uranium. Data were collected at 16 angles from 20 deg. to 160 deg. The data have been corrected for multiple scattering, hardening and angular resolution effects. Comparison with predictions of the optical model—Hauser Feshbach theory are in progress. In general, the polarization effects are much more pronounced at 2 MeV incident neutron energy than for the previously reported data at 1 MeV. The objective is to obtain a consistent nuclear model which can be used for reliable interpolation and extrapolation to include nuclides which are either very difficult to study or are so unstable as to make measurement not feasible (e.g. fission products).

---

[2] R. Coles, AWRE-0-66/71.

[3] P. A. Moldauer, Statistical Properties of Nuclei, Plenum Pub. Co. Ed. S. Garg, New York, 1972.

5. Measurement of (n, p) Cross Sections by Activation Methods
(J. W. Meadows and D. L. Smith)

Cross sections for the $Al^{27}(n,p)Mg^{27}$, $Ti^{46}(n,p)Sc^{46}$, $Ti^{48}(n,p)Sc^{48}$, $Fe^{54}(n,p)Mn^{54}$, $Fe^{56}(n,p)Mn^{56}$, and $Ni^{58}(n,p)Co^{58}$ reactions were measured for neutron energies up to ~5.9 MeV. The results are shown in Fig. A-6. The vertical error bars indicate the standard deviation relative to the fission cross section. The horizontal bars show the energy resolution. Additional measurements were made between 2.85 and 4.02 MeV with ~0.04 MeV energy resolution to search for structure in the excitation function. All measurements are relative to the ENDF/B-III ^{235}U fission cross section.

6. Neutron Decay from the ^{49}Ca Ground-State Analog in ^{49}Sc
(Elwyn, Kuchnir,* Monahan, Mooring, Lemming,** and Stoppenhagen***)

A paper with the above title has been accepted for publication in the Physical Review. The abstract follows: Relative angular distributions of neutrons from the $^{48}Ca(p,n)^{48}Sc$ reaction to four positive-parity states in ^{48}Sc have been measured at 11 proton energies between 1.955 and 1.995 MeV. This energy interval encompasses a number of the components of the $\frac{3}{2}^-$ isobaric analog of the ^{49}Ca ground state in ^{49}Sc. The neutron decay of ^{49}Sc in the region of the two largest components is discussed in terms of a model of the (p, n) reaction in which the isospin-violating forces are assumed to manifest themselves through boundary-condition mixing only. The gross features of most of the data throughout this energy interval can be described in terms of two $T_< \frac{3}{2}^-$ states and a number of $\frac{3}{2}^+$ and $\frac{5}{2}^+$ levels. The branching ratio for neutron decay to the various levels in ^{48}Sc suggest that the two major $\frac{3}{2}^-$ components have fairly simple but somewhat different shell-model configurations.

7. Possible Resonance Structure in the Elastic Scattering of Neutrons by Y near 1 MeV (Elwyn, Monahan, Cox, Adams,† and Chen†)

A paper with the above title has been submitted for publication to Nuclear Physics. The abstract follows: The total cross section as well

---

*Now at Argonne Cancer Research Hospital, Chicago, Illinois.

**Now at Ohio University, Athens, Ohio.

***Ohio University, Lancaster, Ohio.

†Ohio University, Athens, Ohio.

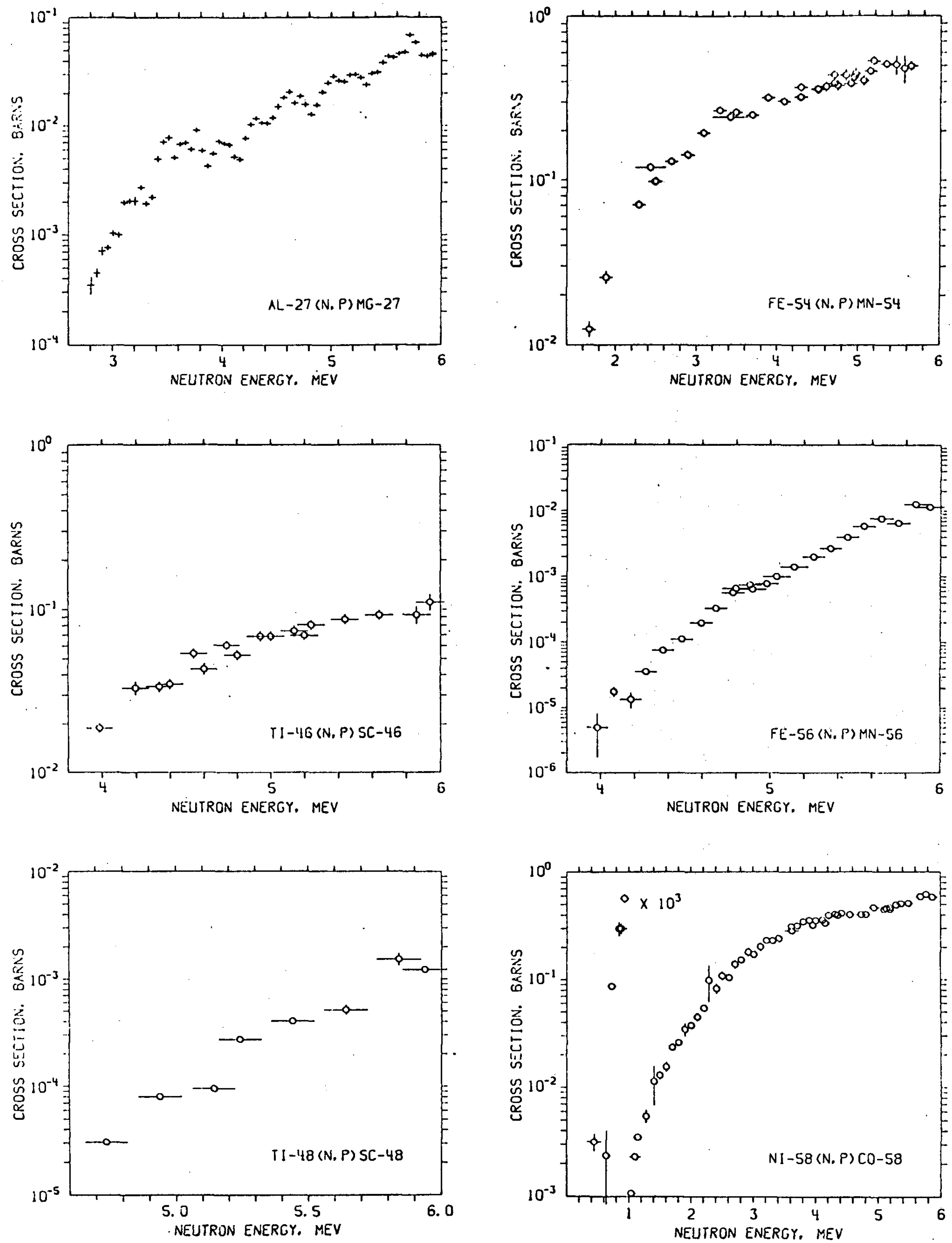
AL-27 (N, P) MG-27
FE-54 (N, P) MN-54
TI-46 (N, P) SC-46
FE-56 (N, P) MN-56
TI-48 (N, P) SC-48
NI-58 (N, P) CO-58
X 10^3
CROSS SECTION, BARNS
NEUTRON ENERGY, MEV

Fig. A-6

as the differential cross section and polarization in the elastic scattering of 0.8—1.4-MeV neutrons by Y have been measured with neutron beams of energy spread less than 20 keV. Rather weak structure with widths ~50 keV was observed at a few energies within this range. The data were analyzed by use of a model in which the scattering process is described in terms of resonance amplitudes superimposed on an optical-potential background. Although not completely definitive, this analysis indicates the existence of three intermediate-width resonances (two 1^- and one 1^+) at neutron energies between ~1.0 and 1.2 MeV. The properties of the 1^- resonances suggest that these are the parent states of the proposed $T_>$ components of the E1 giant resonance observed near 21 MeV excitation energy in ^{90}Zr produced in the $^{89}Y(p, \gamma_0)$ reaction. The resolved resonance structure in this energy region is in reasonable agreement with a recent calculation of the energies and widths of negative-parity states in ^{90}Y.

8. Facilities

a. Fast Neutron Generator (FNG)[a] Facility

Since the past report, this facility has operated ~3000 hours with no significant failures. Most operation is in the nsec pulsed mode. In addition, a capability for very slow pulses for delayed neutron studies has been added. A small portion of the operating time was used in neutronic studies of large fast-critical systems. A new beam-switching system has been put in service providing for seven target stations. One of these is employed in a new facility for $(n, n'\gamma)$ studies using GeLi detectors.

b. Total Delayed Neutron Yields from Fissile and Fissionable Nuclides (S. A. Cox)

The experimental facility for the measurement of the total delayed neutron yield from neutron induced fission has been completed. Of prime importance for the successful measurement of the absolute delayed neutron yield are the quality of the large slab detector for measuring the delayed neutron yield, the quality of the beam pulsing system and the quality of the fission counter. The slab detector consists of three layers of BF_3 counters in a polyethylene moderator. Extensive tests have shown that an essentially flat efficiency can be achieved over the neutron energy range of interest (i.e. $\lesssim$ 2 MeV). The absolute efficiency response will be

[a]Basic accelerator a 8 MeV Tandem Dynamitron.

measured at three neutron energy regions using Sb-Be, Ra-Be, and Cf^{252} sources calibrated at the National Bureau of Standards. A pulsed beam is used during data collection. One cycle consists of four time periods. The beam is pulsed on for sample irradiation (T1) then pulsed off. After a moderater decay time (T2) the counting circuitry is gated on for a time T3≅T1. Then after a short time T4 to ensure that the counting circuitry is gated off the beam is pulsed on. The pulse train is generated under computer control. The computer program sets the time T1, T2, T3, T4. Since all four times are determined by the one computer clock, the identity of times T1 and T3 is assured. Preliminary measurements were made using a ^{238}U target. The ^{238}U disk (1" dia. by .2" thick) was placed at 0^o relative to the proton beam incident on a lithium target (100 keV thick to ~2 MeV proton) at a distance of 1 inch. The slab detector was positioned at 90^o relative to the incident proton beam at a distance of 3 feet from the target. Delayed neutron counting rates in excess of 1000 cts/min were achieved with a background of ~1%. The low background was possible because the beam was pulsed at the negative ion source of the Tandem Dynamitron rather than after the beam has been accelerated in full energy.

B. CHARGED PARTICLE PHYSICS

1. Reaction-Spectroscopy Studies of the Actinide Elements. III. Levels in ^{241}Pu and ^{243}Pu (T. H. Braid, R. R. Chasman, J. R. Erskine, and A. M. Friedman)

As part of a continuing study of the actinide elements by means of reaction-spectroscopy measurements has been completed on ^{241}Pu and ^{243}Pu. A paper describing the results to be published in the Physical Review is abstracted as follows: Properties of levels in ^{241}Pu and ^{243}Pu were determined by (d, p) and (d, t) reactions on targets of ^{240}Pu and ^{242}Pu. The reactions $^{240}Pu(d, d')^{241}Pu$ were also studied. On the basis of these data, single-particle assignments are made for levels in ^{241}Pu and ^{243}Pu. Single-particle spectra, extracted from the data by means of a pairing-force calculation, are compared both with those of the isotonic nuclides and with the single-particle spectra calculated from a deformed Woods-Saxon potential.

2. A Study of ^{248}Bk, ^{241}Am, and ^{231}Pa with Proton-Transfer Reactions (J. R. Erskine, G. Kyle,* A. Friedman, and R. Chasman)

*University of Minnesota.

The (α, t) and (^{3}He, d) reactions at a bombarding energy of 29 MeV have been used to investigate the single-proton excitations in ^{249}Bk, while ^{241}Am and ^{231}Pa were studied with the (α, t) only. An Enge split-pole spectrograph was used to record the data. Several orbital assignments previously made on the basis of studies of radioactive decay were confirmed by the signatures seen in the transfer spectra. Many new levels were observed, and some of them could be given orbital assignments. In ^{249}Bk the level structure appears quite complex between 500 and 800 keV. Four orbitals—the $\frac{5}{2}^-[523]$, $\frac{1}{2}^-[530]$, $\frac{1}{2}^-[521]$, and $\frac{7}{2}^-[514]$—are present, and there is strong Coriolis mixing between some of them. The observed signatures of the ^{231}Pa levels near the ground state are seriously changed by strong Coriolis mixing.

C. PHOTONUCLEAR PHYSICS

1. Threshold Photoneutron Resonances from ^{207}Pb(γ, n)^{206}Pb (L. R. Medsker, H. E. Jackson, and R. E. Toohey)

The threshold photoneutron facility has been used in a high-precision study of photoneutron spectra from an enriched target of ^{207}Pb. The target was irradiated by a pulsed bremsstrahlung beam with end-point energy of 7.8 MeV so that the nuclear states excited by photon absorption cannot decay by neutron emission except to the ground-state of ^{206}Pb. By performing another measurement at an end-point energy of 8.4 MeV, states with energies up to 1400 keV could be studied.

Neutron resonance groups corresponding to each of the states excited were observed by time-of-flight measurements. A typical photoneutron time-of-flight spectrum is shown in Fig. C-1. Resonance energies are indicated in keV. The detection system was set to observe neutrons emitted at 90° and 135° to the photon beam, and spin assignments of 1/2 and 3/2 were based on angular distributions inferred from the observed spectra at those two angles. The values of the ground-state radiation widths for most resonances were determined from the observed yields. Parity assignments for the spin 1/2 states were based on a comparison of the data with the total neutron cross sections of ^{206}Pb. The $3/2^+$ states are not expected to be observed in this measurement because they decay by d-wave neutron emission.

An interesting result derived from the present analysis is the intense p-wave component whose integrated strength is much greater than expected. These resonances are excited by absorption of magnetic dipole radiation, and their intensity suggests the existence of a giant M1 resonance in ^{207}Pb. Another feature of the present results is that the

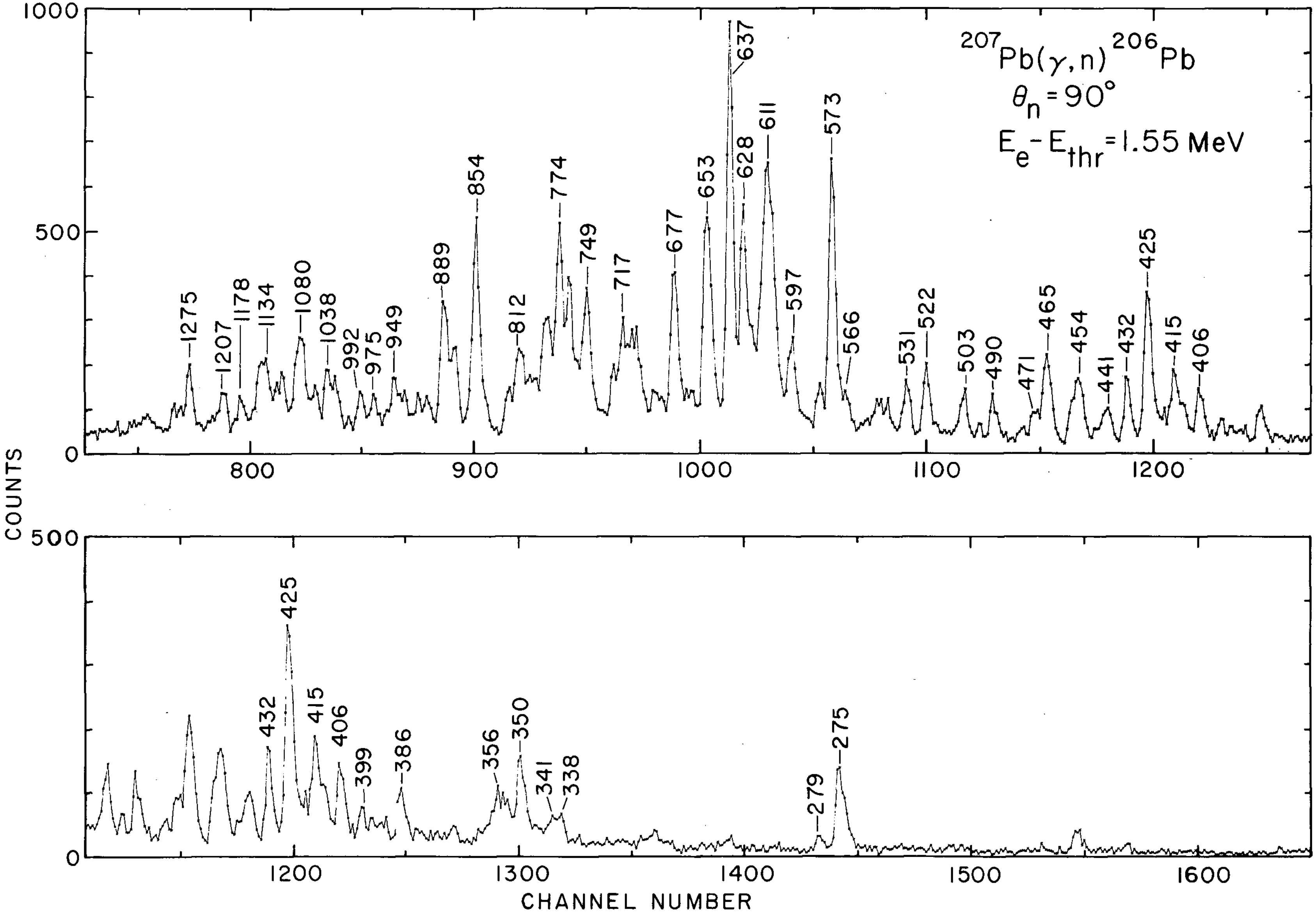

$^{207}Pb(\gamma,n)^{206}Pb$
$\theta_n = 90°$
$E_e - E_{thr} = 1.55$ MeV
COUNTS
CHANNEL NUMBER
1275
1207
1178
1134
1080
1038
992
975
949
889
854
812
774
749
717
677
653
637
628
611
597
573
566
531
522
503
490
471
465
454
441
432
425
415
406
399
386
356
350
341
338
279
275

Fig. C-1

correlation between reduced neutron widths for s-wave resonances and for corresponding ground-state radiation widths was found to be consistent with zero. A value of +0.09 was derived, as compared to the value +0.44 reported in the literature. From the present results, no evidence can be found for the previously proposed doorway state in the $^{207}Pb(\gamma, n)$ reaction.

The final analysis of these $^{207}Pb(\gamma, n)$ measurements is being completed, and theoretical interpretations of the results will be investigated.

2. $^{91}Zr(\gamma, n)^{90}Zr$ and the Valency Model (R. E. Toohey and H. E. Jackson)

^{91}Zr is an appropriate nucleus with which to test the predictions of the valency model. It can be described in terms of a single $d\frac{5}{2}$ neutron outside a closed ^{90}Zr core. The $3p\frac{3}{2}$ single-particle state is predicted at about 1 MeV above the neutron threshold. Consequently one expects the photoneutron resonance spectrum to be dominated by $p\frac{3}{2}$ states excited by E1 photons absorbed by the ground state. Conversely, neutron capture in ^{90}Zr can proceed from $p\frac{3}{2}$ resonances by E1 decay to the ground state, and such transitions should be well described by the valency model.

Ground state radiation widths ($\Gamma_{\gamma 0}$) for 40 $p\frac{3}{2}$ resonances in ^{91}Zr have been measured in the energy range 5—200 keV above threshold using the threshold photoneutron technique. The average value is 135 meV, yielding an E1 strength function of 2.55×10^{-5}. The individual widths follow a chi-squared distribution with $\nu = 1.8$.

Reduced neutron widths (γ_n^2) for these same resonances were obtained from total cross-section measurements on ^{90}Zr performed at ORELA in collaboration with Good, Harvey, et al. The average value of γ_n^2 is 1.89 keV and these widths follow a chi-squared with $\nu = 1.4$ consistent with a Porter-Thomas distribution.

The correlation coefficient between $\Gamma_{\gamma 0}$ and γ_n^2 is $\rho \doteq +0.6$, confirming the strong positive correlation predicted by the model. The valency model also predicts quantitatively correct values of $\Gamma_{\gamma 0}$ for those resonances with larger (> 2 keV) values of γ_n^2. The average of the calculated widths is 125 meV. Both the measured and calculated numbers have an error range of ±20%.

3. Intense Electron "Picopulse" (G. Mavrogenes)

A fine structure pulse of 7 nC charge less than 50 picosec duration and ≈ 200 A amplitude is now available at ANL for photoneutron experiments and radiation chemical experiments investigating the very short-time reaction region. The pulse shape is shown in Fig. C-2. The energy of the pulse can vary from ≈ 4 MeV to 20 MeV with energy spread

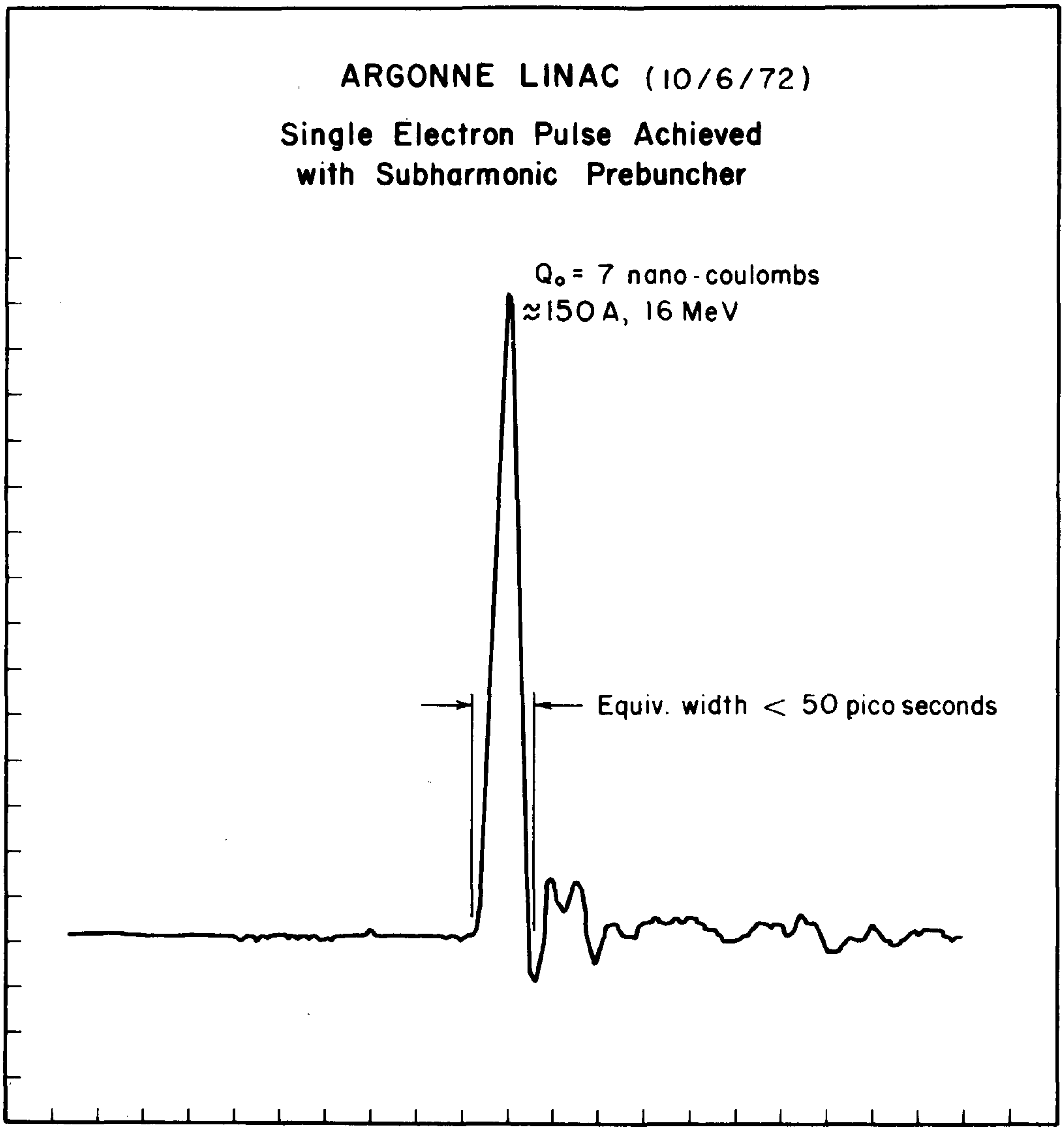
ARGONNE LINAC (10/6/72)
Single Electron Pulse Achieved
with Subharmonic Prebuncher
Q_o = 7 nano-coulombs
≈150 A, 16 MeV
Equiv. width < 50 pico seconds

Fig. C-2

(ΔE) less than 300 keV. The repetition rate covers the span of 1 pps to 800 pps. The pulse can be delivered for experiments to any of the more than 10 parts of the transport system. The resolution of the fine structure pulse was accomplished by inserting between the electron gun and the fundamental frequency prebuncher a 6th subharmonic (217 MHz) prebuncher powered by a separate RF power supply with independent phase shift. With the correct parameters of power, phase and drift distance in the S. H. prebuncher determined by a computer program that includes the space charge effects and the image forces—a ≈ 2.5 nsec pulse of 100 keV energy injected from the electron gun is compressed in time to ≈ 400 psec at the entrance of the fundamental frequency (1300 MHz) prebuncher to be further compressed there and injected into the accelerator proper resulting in an accelerated pulse of one fine structure with no satellites. If two small satellite pulses containing less than 10% of the charge can be accepted by the experimenter, a pulse of 11 nC is available. Efforts are being made to devise a method that will enable us to measure accurately the pulse width and studies are continuing for the enhancement of the pulses charge.

D. REACTOR NEUTRON PHYSICS

1. Thermal Neutron Capture in ^{113}Cd (R. K. Smither and G. E. Thomas)

The absolute intensities of the high energy portion of the ^{113}Cd $(n, \gamma)^{114}$Cd gamma ray spectrum were measured using special multielement samples in the Argonne (n, γ) facility at the CP-5 research reactor. The analysis of the data has not been completed, but preliminary results give absolute intensities that are 50% higher than those previously reported.[1]

2. Argonne 7.7m Bent-Crystal Spectrometer (R. K. Smither and D. L. Bushnell)

The Bragg angle measurement system used in the Argonne bent crystal spectrometer to measure low energy gamma-ray energies for (n, γ) spectra has been completely recalibrated. An improvement of a factor of four in the energy precision of the instrument is expected as a result of this work. A recalibration of the absolute efficiency of the bent-crystal spectrometer as a function of gamma energy is presently under way. It is hoped that this recalibration will lead to the measurement of absolute intensities with errors of ±1%.

---

[1] Nuclear Data Tables 5, No. 1-2, Nov. 1968, Editor K. Way, Academic Press.

3. <u>The Coherent Scattering Length of ^{169}Tm</u> (G. H. Lander and T. O. Brun)

From a study of magnetization density of the induced moment in the compound TmSb, the coherent scattering length of ^{169}Tm was determined to be $(0.705 \pm 0.005) \times 10^{-12}$ cm (G. H. Lander, T. O. Brun, and Oscar Vogt, Phys. Rev., to be published) using a scattering length for antimony of $(0.564 \pm 0.001) \times 10^{-12}$ cm (C. G. Shull, private communication). The scattering length for thulium was obtained from a large number of unpolarized as well as polarized neutron measurements for a neutron wavelength of 1.05 Å. Previously published results for the coherent scattering length of ^{169}Tm are $(0.69 \pm 0.02) \times 10^{-12}$ cm (W. C. Koehler, *et al.*, Phys. Rev. **126**, 1672 (1962) and $(0.720 \pm 0.006) \times 10^{-12}$ cm (A. Atoji, J. Chem. Phys. **52**, (1970).

BROOKHAVEN NATIONAL LABORATORY

A. NEUTRON PHYSICS

1. Fast Chopper

a) Instrumental Developments (G. W. Cole, R. E. Chrien and O. A. Wasson)

A 100 MHz, 8192 channel analog-to-digital converter[1] with dual parameter hardware stabilization system has been obtained for use with the 25 keV iron filter facility described below. An identical pulse-height analysis system has been used for 12 months in the fast chopper capture γ-ray measurements, and has shown excellent performance. The SDS-910 computer system is now equipped to record 4096 channel γ-ray spectra from the filtered beam, as well as two-parameter data from two independent detectors in the fast chopper experiment.

b) Experimental

1. Search for direct capture in Dy-162 (n,γ) Dy-163 (G.W. Cole, S.F. Mughabghab* and R.E. Chrien)

The existence of a significant direct reaction amplitude in neutron capture is a topic of considerable interest in the study of departures from the extreme statistical model of resonance reactions. Direct neutron capture is likely to be important near the 4S giant resonance in the S-wave neutron strength function, since single particle admixtures in the capturing wave function are larger there. Dy-162 is expected to be a favorable case for several reasons: 1) unusually large total radiation widths have been reported;[2] 2) a band having its head at 351 keV is strongly populated in (d,p) stripping;[3] and 3) the thermal capture cross section is accounted for by known resonance parameters.

A 115 gram sample of 96.26% $(Dy\text{-}162)_2O_3$ was studied from thermal to 300 eV at the fast chopper, and the intensity variation of six primary E1 transitions determined. Particular care was taken to eliminate time-of-flight dependent effects by the use of pileup rejection

---

* Department of Applied Science, BNL.

[1] Northern Scientific Model 623; dual pulser designed by V. Radeka of BNL Instrumentation Division.

[2] S. F. Mughabghab and R. E. Chrien, Phys. Rev. C-1, 1850 (1970).

[3] O. W. B. Schult et al., Phys. Rev. 154, 1146 (1967).

techniques, and by the use of a free-running pulser stored in the pulse height spectrum. Additional runs using a Cd envelope around the target showed that there is no spurious contribution between resonances due to capture of thermalized room return neutrons.

Table A-I lists the reduced neutron widths and total and partial radiation widths used in an interference analysis. The partial radiation widths were determined in the present work. A non-linear least squares procedure was used to find the direct capture amplitude giving the best fit to the intensity variation for each transition. Figure A-1 shows the results for the 5449 keV transition, populating a state which does not have a strong single particle character. The solid curve is computed with zero direct amplitude, while the dashed curve is the best-fit result. A direct component of $\sim$ 1.4 mb at 1 eV produces this fit. By contrast, Figures A-2 and A-3 show the results for the 5919 and 5880 keV transitions, populating the $1/2^-$ and $3/2^-$ members of the [521↓] band. This band is strongly single particle in nature.[3] In Figure A-2, the best fit dashed curve requires a 13.6 mb direct cross section at 1 eV, while in Figure A-3, the best fit requires a 22.9 mb direct cross section at 1 eV. Analysis of other transitions in addition to these E1 γ-rays is in progress.

Table A-I

Widths for Dy-162 (n,γ) Interfence Analysis

			$\Gamma_{\gamma f}$(meV)					
E_{Res}(eV)	Γ_n^o(meV)	Γ_γ(meV)	5919	5880	5848	5448	5213	5219 keV
5.43	9.1	155	1.28	1.31	1.31	3.34	2.14	2.00
70.7	47.1	150	5.70	2.78	3.86	0.73	3.47	0.24
267.	35.5	150	8.52	0.83	0.49	0.80	1.08	1.07

c) Capture γ-rays from Ge-73 (J. L. Holm, D. I. Garber* and R. E. Chrien)

An analysis of measurements of epithermal neutron capture in natural germanium is presently being carried out. The measurements were

* Department of Applied Science, BNL.

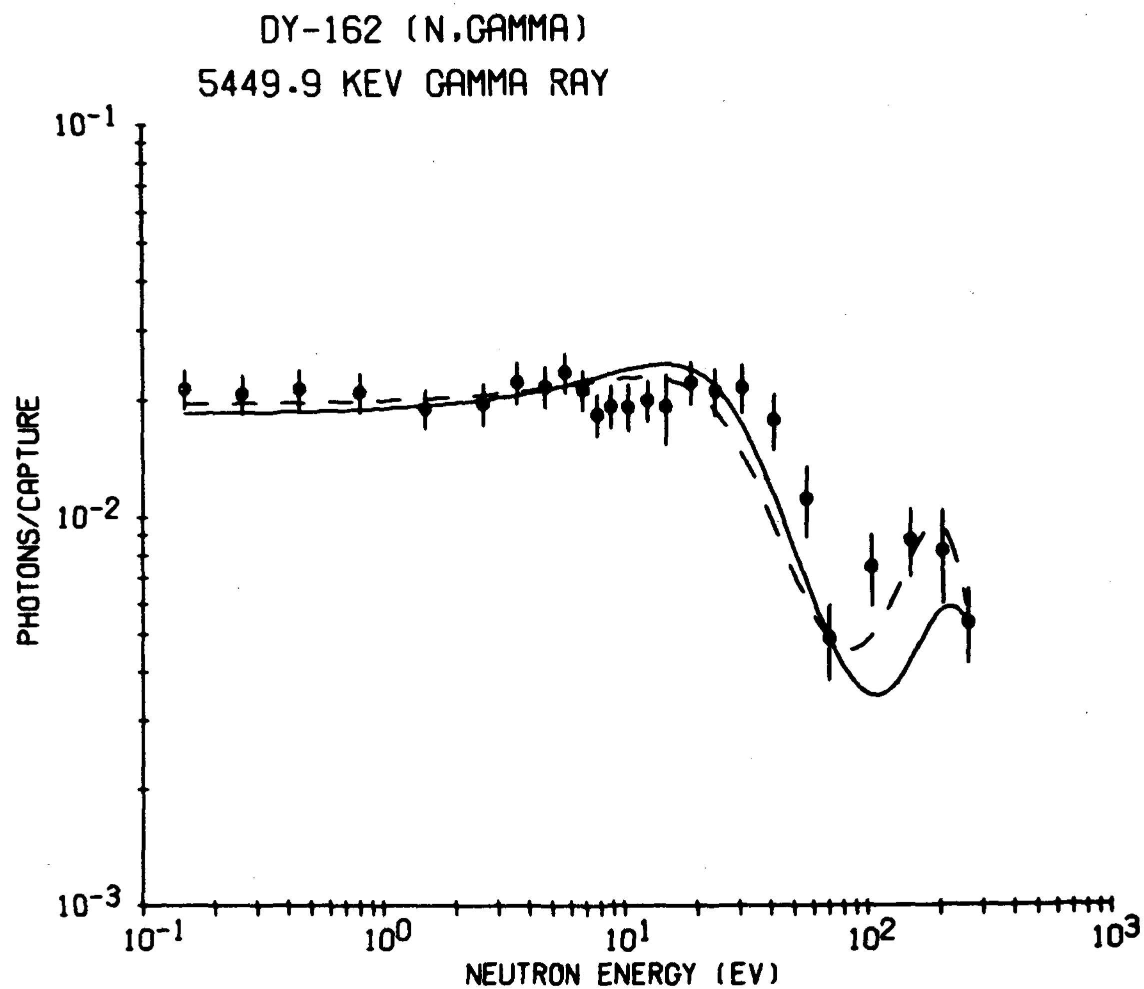

Fig. A-1: Intensity variation of the 5449.9 keV transition in Dy-162(n,γ). The solid line was obtained with the parameters of Table A-I, and zero direct capture amplitude. The dashed line is a least-squares best fit, giving 1.4 mb direct cross section at 1 eV.

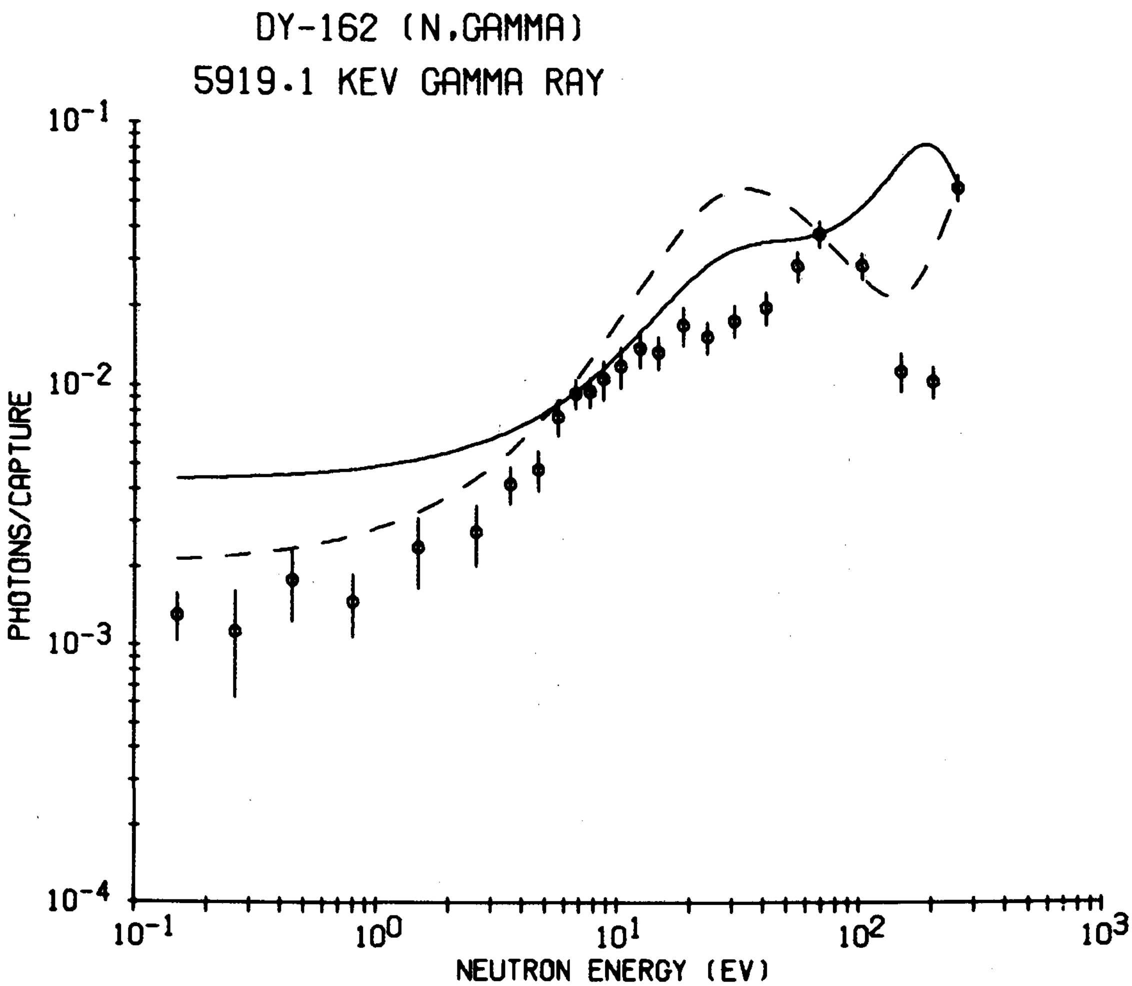

Fig. A-2: See Fig. A-1. The best fit value is 13.6 mb direct cross section at 1 eV.

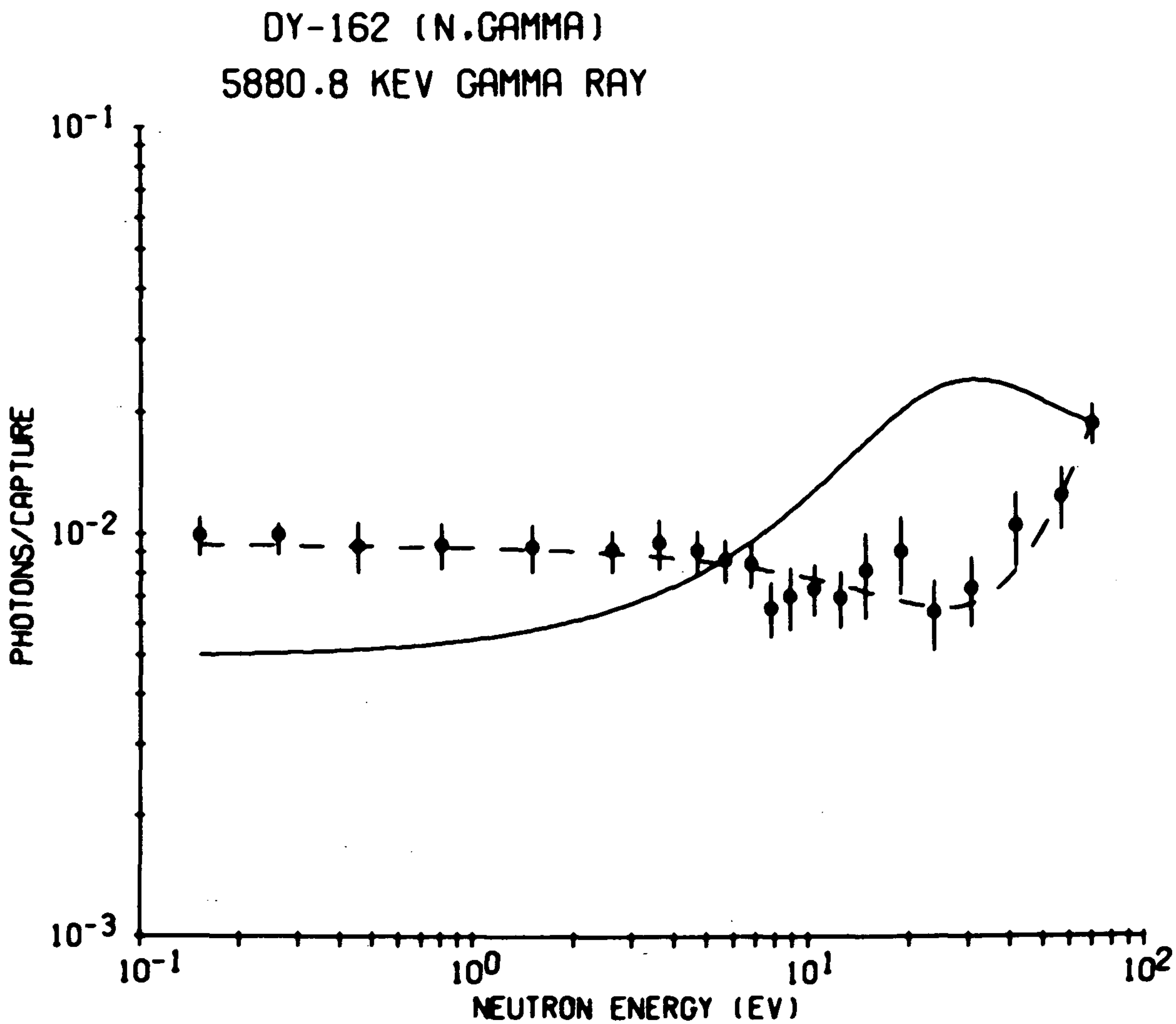

Fig. A-3: See Fig. A-1. The best fit value is 22 mb direct cross section at 1 eV.

performed at the fast chopper facility of the Brookhaven High Flux Beam Reactor. The target germanium was formed into an annular collar and mounted around the outside of the detector cryostat to maximize solid angle efficiency. The detector was shielded from the neutron beam by a cylindrical lead shadow core placed upstream in the neutron flight path from the detector.

The germanium isotopes have low neutron capture cross sections relative to other materials present in the experimental apparatus, most noticeably copper (from the cryostat cold finger), iron and aluminum. Thus these experimental contaminents contribute gamma rays of significant intensity to the raw data. Further, the background alone cannot be measured since after removing the germanium target, germanium is still present in the Ge(Li) detector. However, an attempt was made to evaluate the relative contributions from the germanium and from the contaminants by replacing the germanium target with an annular lead target whose mass was determined to give the same neutron scattering as the germanium target. The time-of-flight spectra fromthe germanium and lead targets are shown in Figure A-4.

From these spectra we are able to identify neutron resonances in ^{73}Ge(n,γ) at 102 eV, 204 and 224 eV, and a peak which is from unresolved resonances, 320, 332, 367, and 408 eV. The first resonance in any germanium isotope other than A = 73 is the 550 eV resonance in ^{76}Ge; we are not able to resolve the resonances in this energy region.

Again referring to Figure A-4, we have located several resonances due to the experimental contaminents. The most important of these are 577 and 650 eV resonances in copper, a weaker resonance in copper at 229 eV, and a weak resonance at 132 eV in cobalt, a component of stainless steel. After removing all gamma rays due to contaminants, the remaining gamma ray energies and intensities may be tabulated for the neutron resonances. Over 250 distinct gamma lines were observed between 5 and 10 meV in the raw data, and 150 to 200 of these lines are well-defined as transitions in germanium. These results for the first three resonances are presented as a bar graph in Figure A-5, along with the results of thermal capture[4] for comparison.

Emphasis is placed on accounting for all gamma lines due to contaminants as we intend to produce a comprehensive tabulation of gamma lines of germanium seen in neutron resonances or in certain neutron energy ranges where we are unable to resolve neutron resonances. This tabulation should of itself be of use to any experimenters using Ge(Li) detectors near epithermal neutrons.

[4] C. Weitkamp, W. Michaelis, H. Schmidt, and U. Fanger, J. Physik 192, (1966) p. 423-438.

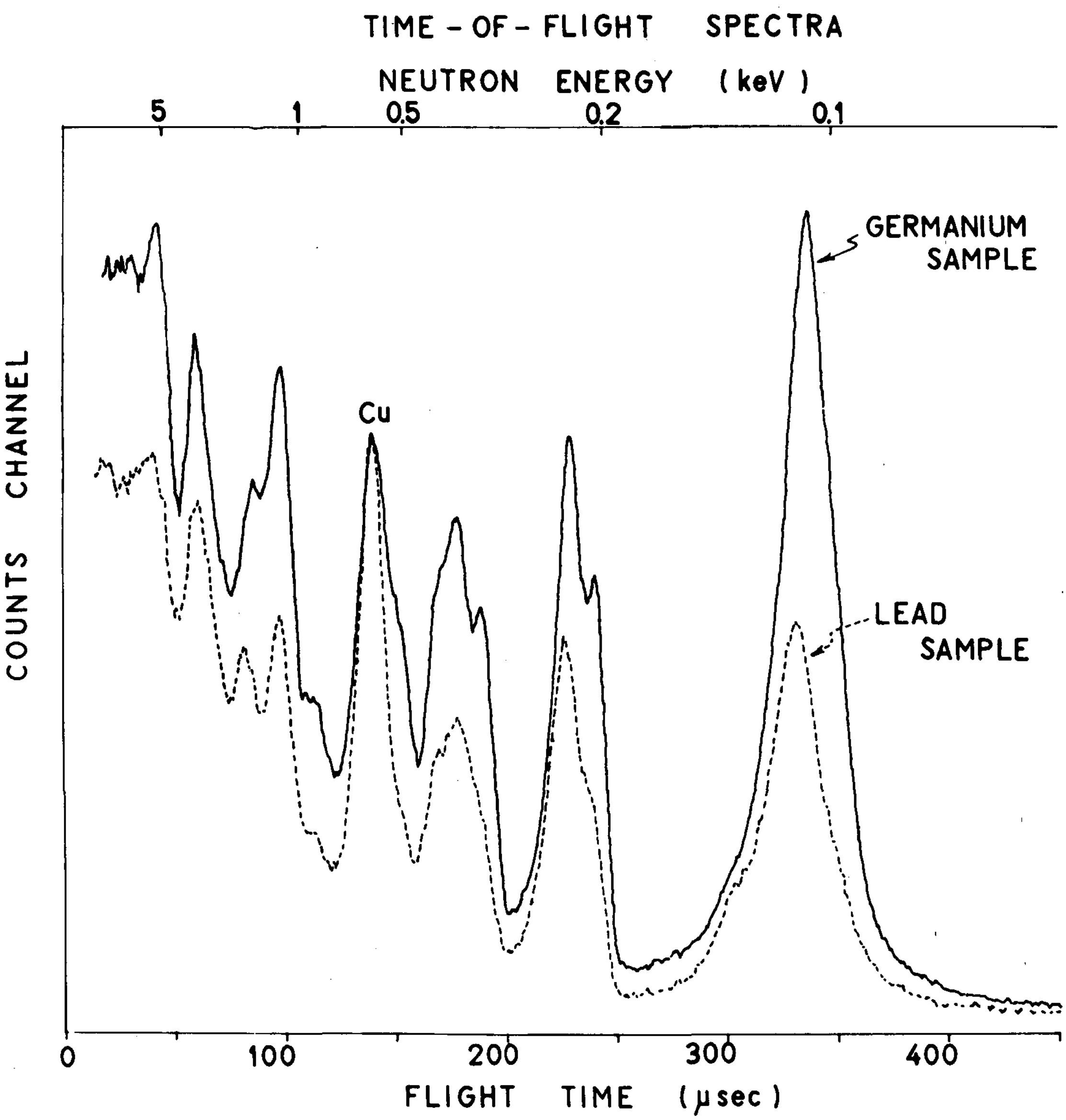

Fig. A-4: Time-of-flight spectra for the germanium sample and for a lead scatterer. Relative normalization between the curves is arbitrary.

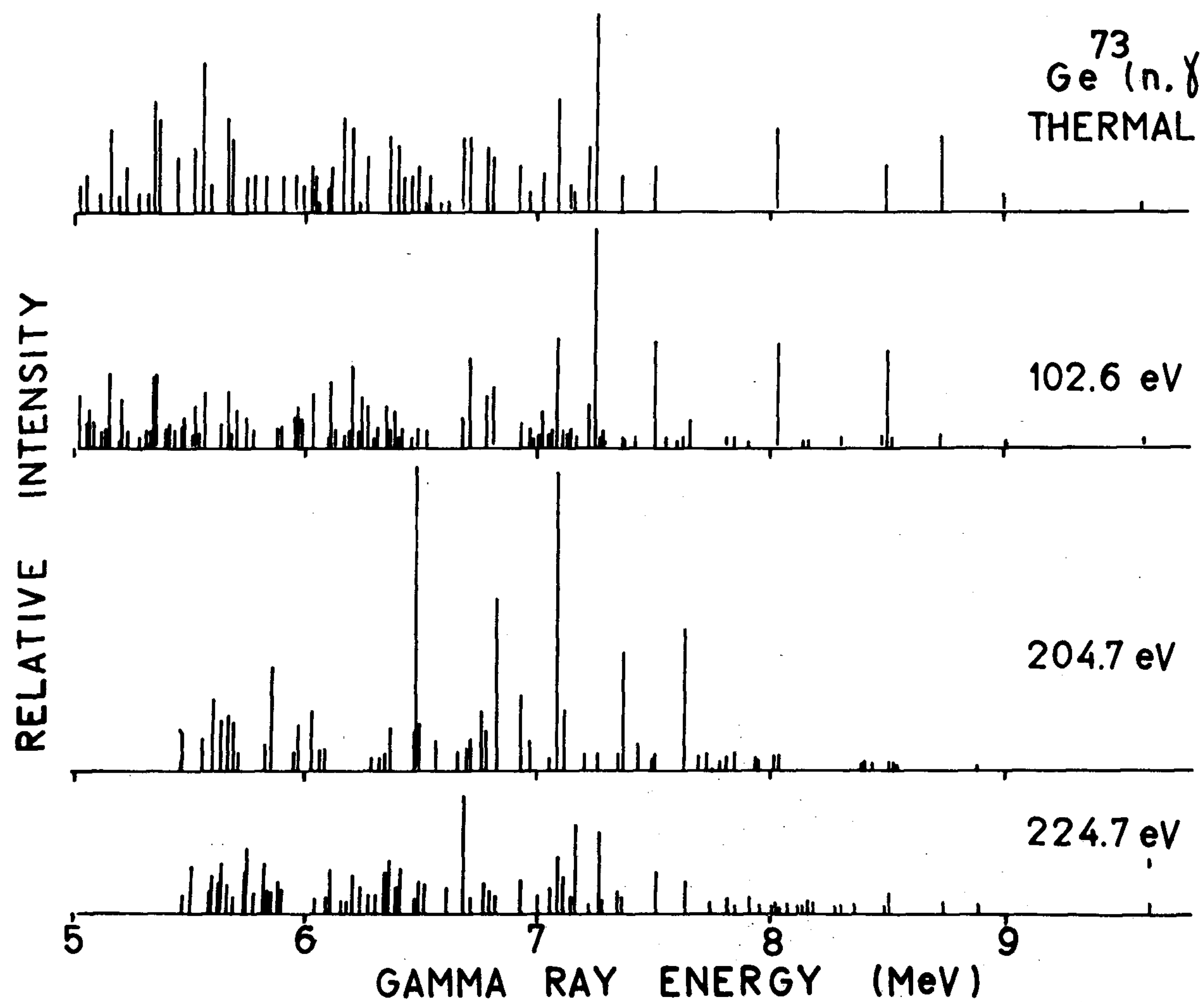

Fig. A-5: Relative intensities of transitions observed in $Ge^{73}(n,\gamma)$.

d) Ba-135 (n,γ) Ba-136 (R. E. Chrien and G. W. Cole)

Previous workers[5] have reported an apparent case of anomalously strong M-1 decay of resonant capturing states in the Ba-135(n,γ) reaction. In the hope of clarifying this situation, studies of the resonances at 24.5, 82, 88 and 106 eV have been undertaken at the fast chopper. Both high energy and low energy γ-ray spectra have been measured, and angular correlation measurements have also been carried out. The combination of these results should yield a unique determination of resonance spins and parities, which will in turn clarify the nature of the primary γ-ray transitions in question. In addition, the intensity variation of the primary transitions will be determined between resonances and down to thermal energies, which may shed further light on the reaction mechanism involved.

Initial runs were made using a target of natural $BaCO_3$; more recently, an enriched target containing $\sim$ 50 grams of Ba-135 has been used.

e) Total neutron cross section measurements in Mo-98 (R. E. Chrien, J. A. Harvey* and R. C. Byrd**)

The success of the valence neutron capture model of Lynn[6] in the first few resonances of Mo-98[7] has led naturally to the investigation of this model at higher neutron energies.[8] An essential ingredient of such an analysis is knowledge of the neutron resonance parameters. Therefore, a total cross section measurement has been performed on Mo-98 at ORELA. A target 98% enriched in Mo-98 and having a thickness of 0.0434 atoms/barn was used. The flight path length was 78.2 m and the nominal resolution was 0.064 nsec m^{-1}.

The Atta-Harvey area analysis program has been modified to accommodate the large data arrays (50,000 time-of-flight channels) obtained. Resonances up to 100 keV are being studied. The analysis is nearing completion.

---

* Oak Ridge National Laboratory, Oak Ridge, Tennessee.

** BNL Neutron Physics Summer Student.

5 F. Becvar et al., Czech. J. Phys. B19, 899 (1969).

6 E. Lynn, "Theory of Neutron Resonance Reactions," Clarendon Press, Oxford (1968).

7 Mughabghab, Chrien, Wasson, Cole and Bhat, Phys. Rev. Lett. 26, 1118 (1971).

8 Cole, Mughabghab, Bhat, Wasson, Chrien and Slaughter, contributed to the International Conf. on Statistical Properties of Nuclei, Albany, NY, (1971).

f) Boron density profiles by $B^{10}(n,\alpha)$
(G. W. Cole and J. F. Ziegler*)

The use of the $B^{10}(n,\alpha)$ reaction to determine the concentration of boron as a function of depth in various substrates[9] has been applied to various problems in the physics of semiconductor devices in experiments at the H-1 beam port of HFBR. The effects of annealing cycles on ion-implanted boron distributions in silicon, and the effects of pre-existing impurities on the diffusion of boron in silicon were among the early investigations.[10,11]

More recent runs have expanded the original studies, and have explored some new questions. In ref. 10, the diffusion constant of boron in silicon was deduced from measurements on annealled and un-annealed ion-implantation profiles. This quantity depends on the concentration of the boron, which has a Gaussian distribution and therefore a concentration gradient. Another quantity of interest is the concentration-independent diffusion constant, which normally can be measured only with great difficulty. However, in the boron case, advantage was taken of the fact that the (n,α) reaction is sensitive only to B^{10}. By a series of implants of B^{11}, a uniform boron distribution having a dip in the center was created in a silicon wafer. This dip was then filled by a B^{10} implant, so that the total profile of B^{10} plus B^{11} was flat. Examination of annealed and un-annealed samples then allows the determination of the boron diffusion constant in the absence of any boron concentration gradient.

Studies of the diffusion of boron in silicon which has been pre-doped with arsenic revealed[11] the probable existence of an anomaly in the expected boron distribution of the base region of NPN transistors. In an extension of this work, a silicon wafer 3 cm in diameter was prepared by all the steps used in fabrication of an NPN transistor. The boron base region has been profiled at HFBR. Following profiling of the arsenic collector and emitter layers by α-particle backscattering, the same sample will be etched for the attachment of electrodes. The behavior of the resulting transistor will be compared with electrical characteristics predicted using the measured dopant distributions in a test of semiconductor device theory.

---

[9] J. F. Ziegler, G. W. Cole and J. E. E. Baglin, J. Appl. Phys. 43, 3809 (1972).

[10] Ziegler, Crowder, Cole, Baglin and Masters, Appl. Phys. Lett. 21, 16 (1972).

[11] J. F. Ziegler, G. W. Cole and J. E. E. Baglin, Appl. Phys. Lett. 21, 177 (1972).

* Thomas J. Watson Research Center, IBM, Yorktown Heights, N.Y.

Finally, extensive tests have been made of the behavior of boron doping in silicon when oxide layers are grown on the crystal surface. Preliminary results indicate considerably larger entry of boron into the oxide layer than was expected.

The following three abstracts are of work done by O. A. Wasson in collaboration with the group at the Oak Ridge Electron Accelerator.

g) Valency neutron capture in $^{92}Mo(n,\gamma)^{93}Mo$
(O. A. Wasson and G. G. Slaughter*)

Capture γ ray spectra from the $^{92}Mo(n,\gamma)^{93}Mo$ reaction were measured for neutron energies below 100 keV using the 10 m flight path at the Oak Ridge Electron Linear Accelerator. For neutron energies less than 25 keV a total of 23 different s- and p-wave resonances were resolved. The neutron binding energy is 8067.4 $\pm$ 1.5 keV. The partial radiation widths for the 12 highest energy γ rays which populate positive parity states below 2.5 MeV excitation were deduced and compared to the valency model predictions of Lane and Lynn. For γ-ray energies less than 6.5 MeV, the average M1 partial radiation width is approximately equal to the average E1 partial radiation width. The reduced transition strengths as defined by Bartholomew for these transitions are $\bar{k}(E1) = (1.2 \pm 0.2) \times 10^{-3}$ and $\bar{k}(M1) = (11.5 \pm 2.3) \times 10^{-3}$. For the 7129 keV transition to the s1/2 first excited state the average reduced strength is enhanced by a factor of 5 and 2 for the E1 and M1 transitions respectively. Nearly 30% of this enhancement for the E1 multipoles is attributed to the valency model contribution while the remainder is assigned to other processes such as the giant dipole resonance and doorway state components. The average E2 width for the 8067 keV ground state γ rays is approximately 10% of the average E1 ground state width.

h) P-wave resonances in $^{111}Cd(n,\gamma)^{112}Cd$
(O. A. Wasson and B. J. Allen**)

Gamma-ray spectra and total capture yields were measured for resonant neutron capture in an enriched ^{111}Cd sample for neutron energies less than 2.3 keV. The experiment utilized the 40 m flight path of the Oak Ridge Electron Linear Accelerator and a non-hydrogenous liquid scintillator γ-ray detector. A total of 162 resonances were observed in this interval, and the resonance energies and neutron widths deduced. Approximately 14% of the resonances are assigned to p-wave capture on the basis of the γ-ray spectral measurements while an

* Oak Ridge National Laboratory.

** Lucas Heights, Australia.

additional 23% are assigned to s-wave capture on the basis of their large neutron widths. The parity of the remainder is undetermined. A lower limit of 0.9×10^{-4} is observed for the p-wave neutron strength function $[\Sigma g\Gamma_n^1/(2\ell+1)\Delta E]$ while the s-wave neutron strength function $[\Sigma g\Gamma_n^o/\Delta E]$ is 0.15×10^{-4}.

i) Neutron resonance parameters of ^{92}Mo (Wasson, Allen, Winters,* Macklin** and Harvey†)

Neutron transmission and total neutron capture yields were measured using the time-of-flight technique at the Oak Ridge Electron Linear Accelerator facility using enriched samples of ^{92}Mo. A total of 42 resonances were observed for neutron energies less than 32 keV. Twelve are assigned to s-wave interactions while 23 are assigned to p-wave interactions. The resonant energies, neutron widths, radiation widths and spins are deduced. The average s- and p-wave radiation widths are equal to 0.178 ± 0.015 eV and 0.24 ± 0.03 eV, respectively. The s-wave neutron strength function is $(0.65 \pm 0.26) \times 10^{-4}$ while the p-wave strength function is $(3.3 \pm 1.1) \times 10^{-4}$.

---

* Denison University.

** Oak Ridge National Laboratory.

2. <u>The 24.5 keV neutron Beam Facility at the HFBR reactor</u>
(O. A. Wasson, R. E. Chrien and R. G. Greenwood*)

A 24.5 keV neutron beam has been installed at the H1B beam port of the Brookhaven High Flux Beam Reactor. This quasi-monoenergetic beam is obtained by inserting a neutron filter consisting of iron, aluminum, and sulfur. The beam is rectangular in cross section with dimensions 1.25" X 1.5". By using an external geometry, the relative filter components are easily modified to optimize the spectrum for a specific experiment. The filter design was based on that previously used at the MTR Reactor by Howes et al.[12] Fe-56 in the filter selectively transmits neutrons with energies in the various minima in the Fe-56 total cross section. Thus, in addition to the 24.5 keV neutron group, higher energy groups are also transmitted. The function of the aluminum and sulfur is to reduce the higher energy neutron components.

The integrated neutron fluxes for the various filter combinations are listed in Table A-II. Shown are the integrated fluxes for the 24.5 keV, 75 keV, 137 keV and higher energy windows in units of 10^4 neutrons per cm^2 per sec. The percentage of the flux contained in each window is enclosed in parenthesis. The relative flux measurements were obtained in collaboration with R. G. Greenwood, of Aerojet Nuclear Corporation, by measuring proton recoils in a hydrogen-filled proportional counter. The energy resolution of the counter is sufficient to resolve the various neutron groups as is apparent in Fig. A-6, which shows the spectrum for the filter consisting of 12 in. Fe, 14 in. Al., and 2 in. S. The absolute flux was obtained from the activation of a cadmium-clad gold foil using a gold capture cross section of 600 mb at 24.5 keV.

By suitable filter choices a factor of 10 variation in neutron flux is obtainable. As is shown in Table A-II, the purity of the neutron beam is excellent, even for the thinnest filters where nearly 97% of the beam is in the 24.5 keV window. The width of the 24.5 keV beam is estimated to vary between 1 and 2 keV (FWHM) for the range of filters listed, based on the iron transmission measurements of J. A. Harvey[13] at Oak Ridge. The well-collimated beam size is 1.25 in. X 1.5 in. The

---

* Aerojet Nuclear Corporation, Idaho Falls, Idaho.

12 Howes, Bruggen, Rogers, Schuman, F.B. Simpson and O.D. Simpson, "The MTR 25-keV Neutron Beam," IN-1308, July 1969 (Unpublished).

13 J. A. Harvey (Private Communication).

γ-ray component in the neutron beam is 15 mr/hr for the thinnest filter. It is estimated that it is possible to increase the neutron flux by a factor of 10 by decreasing the collimation in the beam hole.

A program to measure 25 keV neutron capture γ-ray spectra with a Ge(Li) detector is in progress. Figure A-7 shows preliminary results obtained for a five hour run on a Pt sample using the 9 in. Fe, 14 in. Al, and 2 in. S filter. This spectrum results from capture into many resonances. As a result the intensities of the three highest energy γ-rays are nearly equal. Since no shielding was placed around the detector in this test, the building background iron γ-rays from thermal neutron capture are observed. The amount of thermal neutron capture, as well as capture from higher energy neutrons, is determined from the shift in the γ-ray peak energies. From the fact that no thermal peaks are visible in this spectrum, we conclude that the thermal capture rate is no more than 5% of the epithermal rate in this sample.

A modification of the internal reactor collimation at H-1 beam port will result in an order-of-magnitude increase in the available flux. This facility will be available for other types of measurements such as neutron activation, cross section and hot-atom chemistry studies.

Table A-II

H1B Neutron Fluxes. Relative Measurement from Proportional Counter. Absolute Measurement for 21 in. Fe from Au Activation.

Filter	$\varphi(E)dE$, 10^4 n/cm^2 sec 24 keV	75 keV	137 keV	>284 keV
9"Fe, 8"Al, 2½"S	45.7 (96.9)	0.49 (1.1)	0.42 (0.9)	0.56 (1.2)
12"Fe, 8"Al, 2½"S	30.0 (97.9)	0.18 (0.6)	0.22 (0.7)	0.29 (1.0)
15"Fe, 8"Al, 2½"S	19.8 (98.3)	0.051(.25)	0.13 (.7)	0.16 (.8)
21"Fe, 8"Al, 2½"S	8.8 (98.6)	0.012(.14)	0.05 (.5)	0.058(.7)
27"Fe, 8"Al, 2½"S	5.09(98.6)	0.007(.14)	0.020(.4)	0.035(.7)
6"Fe, 14"Al, 2½"S	51.6 (98.0)	0.58 (1.10)	0.24 (0.45)	0.23 (0.42)
9"Fe, 14"Al, 2½"S	31.1 (98.8)	0.15 (0.5)	0.13 (0.4)	0.10 (.33)
12"Fe, 14"Al, 2½"S	19.9 (99.1)	0.05 (0.2)	0.07 (0.4)	0.05 (0.2)
15"Fe, 14"Al, 2½"S	12.9 (99.3)	0.018(0.13)	0.035(0.28)	0.035(0.28)

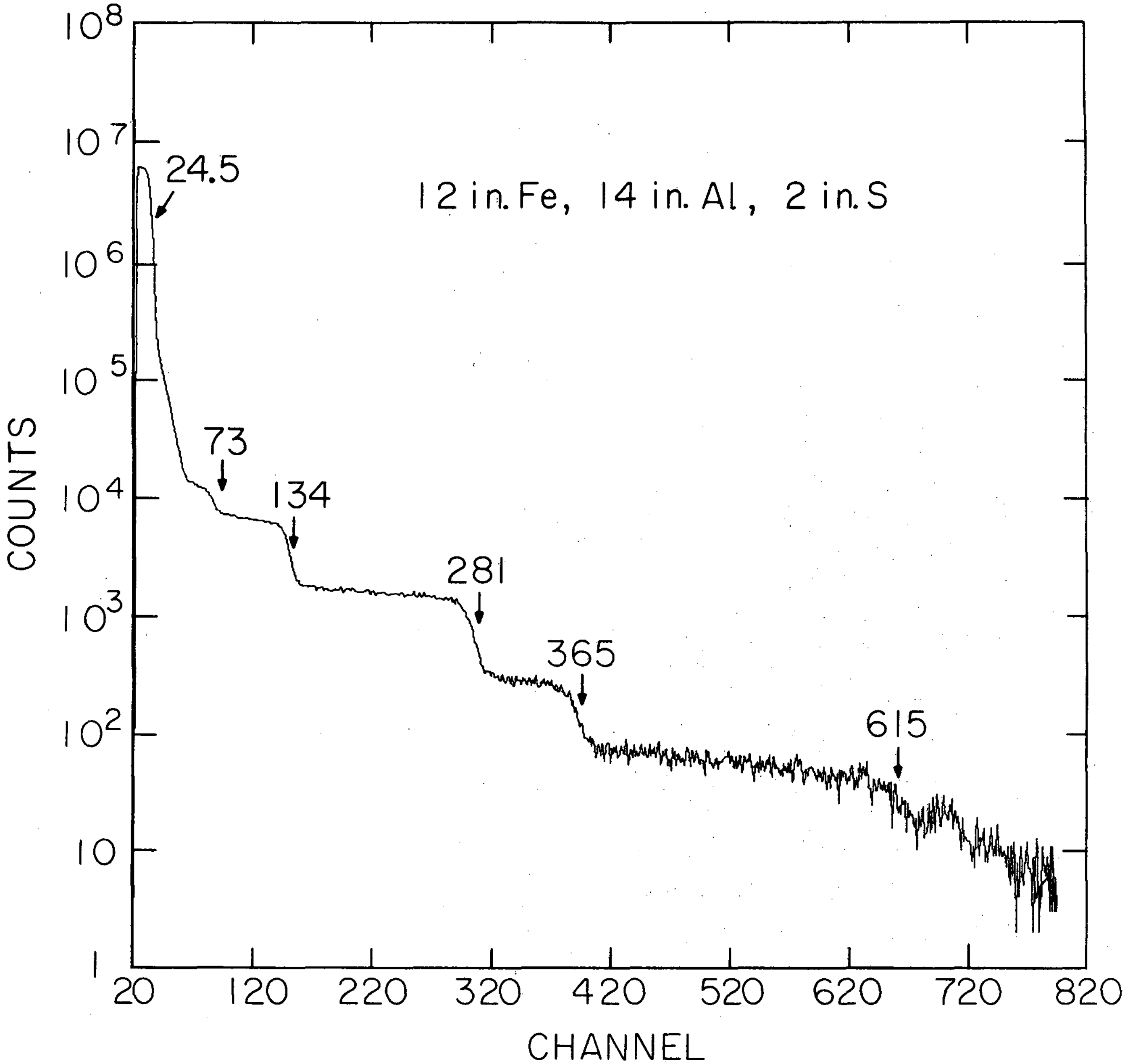

Fig. A-6 Proton-recoil pulse distribution for reactor neutrons transmitted through 12 in. Fe, 14 in. Al, and 2 in. S.

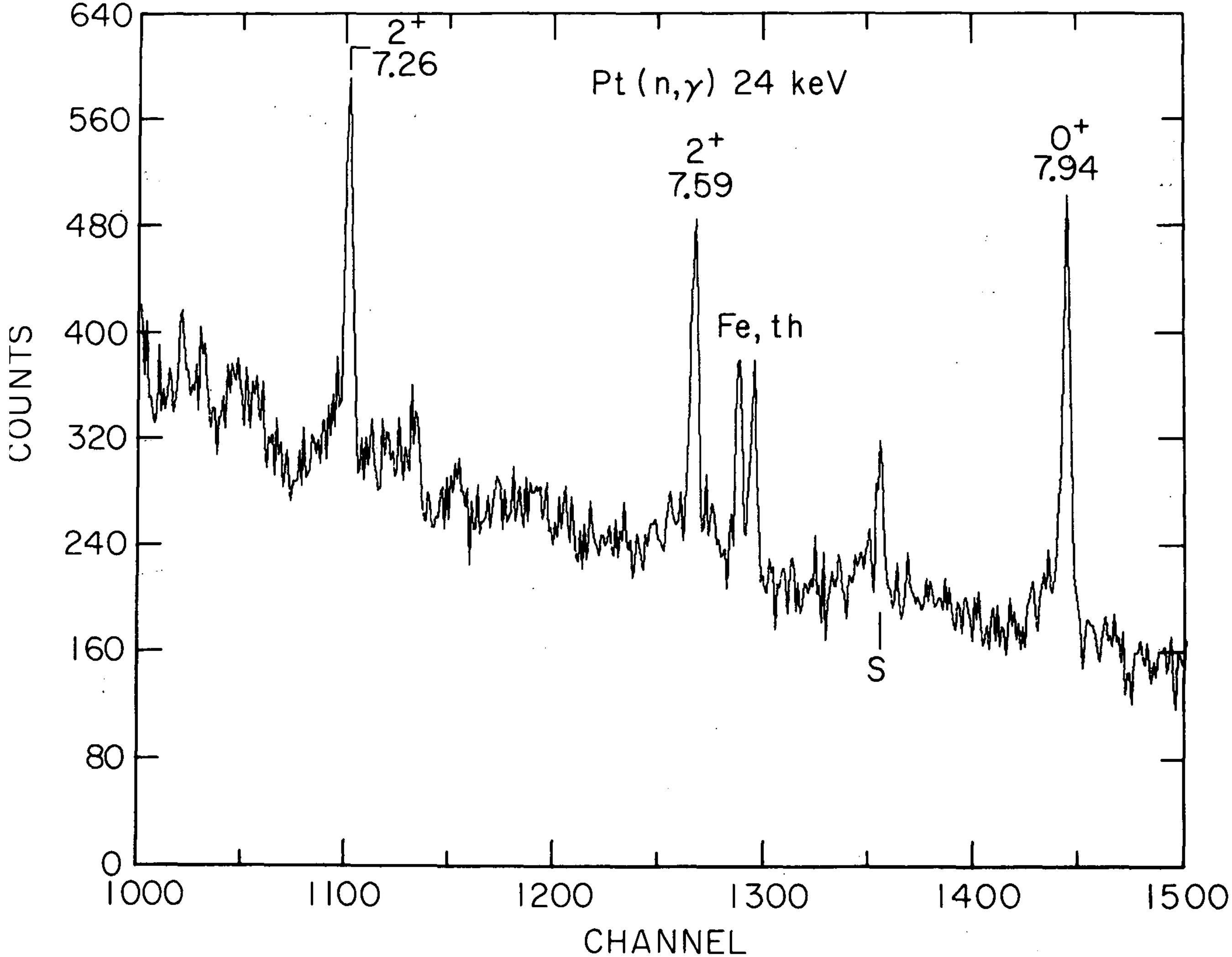

Fig. A-7 Gamma-ray spectrum from capture of 24.5 keV neutrons in platinum. The three highest energy γ-rays are indicated. No shielding was used on the 20 cc Ge(Li) detector.

B. NUCLEAR CRYOGENICS

1. Spins of low energy neutron resonances of ^{235}U (Reddingius,* Postma,** Olsen,*** Rorer‡ and Sailor)

Spins of neutron resonances in ^{235}U have been assigned by several authors.[1-5] The results are not completely consistent, which is probably due to difficulties involved in the various experimental techniques and to various assumptions that must be made. Methods using gamma ray intensities or multiplicities are applicable only to resonances with relatively large radiative capture partial widths and the gamma rays from fission products often interfere. Spin assignments determined from resonance scattering measurements are marginal for most resonances due to the fact that the resonance scattering is extremely small compared with potential scattering and the difference in the two possible g-values is small for a I = 7/2 target nucleus.

A more direct determination of spins of neutron resonances is provided by measuring the transmission of polarized neutrons through a sample of polarized ^{235}U nuclei. In an early experiment of this kind,[6] carried out at BGRR only the first three resonances could be studied, because of limitations on the neutron beam intensity.

Recently new polarization measurements were begun at HFBR using the more intense polarized neutron beam provided by the H-1A crystal spectrometer.

The sample consisted of uranium monosulfide† pressed in a lead matrix; the enrichment in ^{235}U is 99.91%. Nuclear orientation of the uranium nuclei was achieved by cooling the sample in an external magnetic field of 27 kOe. The degree of neutron polarization at the position of the sample was determined by measuring the transmission effect of an indium sample attached to the sample holder. The lowest

---

* Guest at BNL, permanent address Reactor Centrum Nederland Petten (N.H.), The Netherlands.

** Permanent address Rijks Universiteit Groningen, The Netherlands.

*** Permanent address Los Alamos Scientific Laboratory, New Mexico.

1 M. Asgar et al., Phys. Rev. Lett. 26, (1968) 664.

2 H. Weigmann et al., Nucl. Phys. 134, (1969) 535.

3 F. Poortmans et al., Nuclear Data for Reactors, IAEA Vienna, 1970, I. 449.

4 W. R. Kane, Phys. Rev. Lett. 25, (1970) 953.

5 F. Corvi et al., European Conference on Nuclear Phys. 1972, Aix-en-Provence.

6 R. I. Schermer et al., Phys. Rev. 167, (1968) 1121.

† The uranium monosulfide was prepared by C. E. Olsen.

‡ Long Island Lighting Company, New York.

temperatures, reached by adiabatic demagnetization of an iron alum cooling salt, was about 0.05 K. The transmission effects were of the order of 1-2% for the most prominent resonances and have opposite signs for resonances with spin I $-\frac{1}{2}$ and I $+\frac{1}{2}$. Assuming that the nuclear magnetic moment of ^{235}U is negative the data yield the following spin assignments (J = spin of compound state).

E_0 (eV)	J
0.29	3
1.14	4
2.04	3
3.14	3
3.61	4
4.85	4
6.39	4
7.08	4
8.79	4
11.67	4
12.39	3

C. NUCLEAR STRUCTURE

1. Study of ^{241,243}Pu with the (n,γ) Reaction. (W. R. Kane, R. F. Casten)

These nuclei have been studied with the (n,γ) reaction using resonant energy neutrons. Especially helpful in assigning quasiparticle states has been a comparison with published and unpublished (d,p) and (d,t) studies. Together with the present high and low energy γ-ray data the ½+[631], ½+[620], 3/2+[622], ½-[501], and 3/2+[631] orbitals have been firmly or tentatively identified. The location of the ½-[501] orbital, in particular, is important in view of the crucial role it plays in the recent explanations of apparently anomalous (p,t) and (t,p) reaction cross sections to 0^+ states in the mass region.

2. High Excited States in ^{179}Hf, ^{183,184}W. (R. F. Casten, W. R. Kane)

A study of the fractionation and distribution of single particle strength in Hf and W led to the observation of considerable fragmentation in the odd nuclei ^{179}Hf and ^{183}W, with significantly more in the latter. A study of ^{184}W has now been completed to extend the investigation of this topic. Using information from a number of recent experiments leading to ^{184}W in conjunction with (n,γ) data taken at the resonant neutron energy of 7.6 eV the level structure (J^π assignments) up to ~ 2.3 MeV has been elucidated. A comparison of measured (d,p) strengths to states assigned on $J^\pi = 1^+, 2^+$ with recent theoretical calculations in the random phase approximation by I. Hamamoto indicate that the present theory is still unable to account for the fragmentation observed. In particular, the calculations predict no (d,p) strength to 2^+ states between the levels dominated by the lowest two-quasiparticle configuration (~ 1400 keV) and the next two-quasiparticle states at ~ 3 MeV. The data, however, show at least five intrinsic excitations between 1800 and 2300 keV alone, none of which contains more than ~ 30% of the strength predicted for the calculated levels at 3 MeV. A similar situation occurs for the 1^+ levels. Finally, from the energies of the states which receive the largest (d,p) strength in ^{183}W and ^{184}W, it is apparent that there is a significantly larger energy region of mixing in the latter than in the former, and that some of the intrinsic states in ^{184}W above 1500 keV may be distributed over as much as 2 MeV of energy.

3. Study of ^{174}Yb with the (n,γ) Reaction. (R. F. Casten, S. Mughabghab, D. Breitig, W. R. Kane)

A study is being made of the features of the nucleus ^{174}Yb. First there is a 0^+ level at ~ 1500 keV with a rotational band built upon it. The (p,t) reaction cross section to the bandhead is two orders of magnitude larger than for any other excited 0^+ state in the

Yb isotopes. Consequently, the 0^+ level has been interpreted as a pairing vibrational state due to a partial gap in the Nilsson diagram. If true this implies that its structure is fundamentally different than that of other 0^+ levels in ^{174}Yb and than those observed in ^{172}Yb. This difference would be expected to show up in the γ decay of the rotational members of this band. We have used the (n,γ) reaction to study this and have indeed found the branching ratios for decay of the 2^+ and 4^+ levels to be significantly different from those known in ^{172}Yb. It may be possible to understand these in terms of the presumed structure of the pairing vibrational band.

The second purpose centers on a study of several levels in the energy region from 2.5 to 3.0 MeV that are populated very strongly in the primary radiation in the 17 volt neutron resonance. It is felt that these may be of relatively simple structure and we are studying their decay properties to investigate this point. It has been suggested, for example, that these levels may constitute a group of well behaved rotational bands with low K value. While not at all established as of now, it would be very interesting, if true, to observe well behaved bands at such an energy.

4. Study of ^{152}Eu. (D. Breitig, R. F. Casten, W. R. Kane (B.N.L.) in collaboration with T. v. Egidy et al.)

The B.N.L. group is contributing a resonance capture study of the final nucleus ^{152}Eu to a large collaborative effort to understand the first 350 keV of excitation in this odd-odd nucleus. About 40 levels below 400 keV have been identified in the other neutron and charged particle induced reactions. A number of spin assignments or limitations were feasible. The present study, comprising data taken at several resonances with spins of 2^+ and 3^+, has contributed new information on the J^π assignments for about half of these levels and has observed a few levels not previously seen in the neutron capture work. In one case in particular the apparent identity of a level observed in the present study with one of the strongest states populated in the (d,t) reaction has led to the possible identification of a specific two quasiparticle configuration.

D. NATIONAL NEUTRON CROSS SECTION CENTER (S. Pearlstein, R. A. Dannels, M. R. Bhat, H. R. Connell, D. I. Garber, M. D. Goldberg, P. Hlavac, R. E. Kinsey, T. J. Krieger, B. A. Magurno, V. M. May, S. F. Mughabghab, O. Ozer, A. Prince, J. R. Stehn, H. Takahashi)

The scope, format, and manner of publication of the new BNL-325 are now well defined. It will be a completely new Third Edition, compressed to two volumes for ready usefulness. Volume I (tables) will contain only recommended values of thermal cross sections, resonance parameters, and associated quantities such as resonance integrals and strength functions. Volume II (curves) will contain graphical representations of the energy dependence of the cross sections, together with some of the experimental data points. In both volumes, references to all the experimental measurements will be listed, even when the values themselves do not appear explicitly. The data pages of both volumes will be computer prepared; and the curves of Volume II will be developed by automatic fitting routines applied under interactive graphics control. Completeness of data input is being verified by checking against CINDA. Volume I will appear first, in 1973.

Programs have been developed to add to the usefulness of the Evaluated Nuclear Data File, ENDF/B. One, RESEND, uses the resonance parameters given in the ENDF/B file to produce the corresponding microscopic cross sections in the ENDF/B format. This program has been sent to the Argonne Code Center. A second, DOPEND, computes from the microscopic cross sections the Doppler-broadened microscopic cross sections at any specified temperature. A third, INTEND, integrates microscopic cross sections, weighted with an arbitrary weight function, over specified energy ranges. INTEND can be used to produce group constants or spectrum-averaged cross sections.

Evaluations have been completed on Si, Kr, and Xe. They have been put into ENDF/B format.

The ENDF/B-III files for six materials used as cross section standards have been sent to the Nuclear Data Section of the IAEA for world-wide use: H, ^{3}He, ^{6}Li, ^{10}B, ^{197}Au, ^{235}U. The bases for these evaluations were assembled in BNL-17188 (ENDF-179), "ENDF/B-III Cross Section Measurement Standards," by M. K. Drake, in July, 1972.

E. BROOKHAVEN LINAC ISOTOPE PRODUCER

The following publications from BNL contain information on charged particle cross sections and isotope production capabilities:

The production of radioisotopes by spallation. BNL 50195(T-547). L. G. Stang, Jr., M. Hillman and E. Lebowitz. Isotopes & Rad. Tech. 8, No. 1, 1-12, Fall 1970.

Production of ^{52}Fe for medical use. M. W. Greene, E. Lebowitz, P. Richards and M. Hillman. Presented at the 17th Ann. Mtg. of the Soc. of Nucl. Med., Washington, D. C., July 1970. Int. J. Appl. Radiat. Isotopes 21, 719-723 (1970).

An auxiliary cyclotron beam monitor. E. Lebowitz and M. W. Greene. Int. J. Appl. Radiat. Isotopes 21, 625-627 (1970).

Proton reactions with copper for auxiliary cyclotron beam monitoring. M. W. Greene and E. Lebowitz. Tech. Note Int. J. Appl. Radiat. Isotopes 23, 342-343 (1972).

On the production of ^{123}I for medical use. E. Lebowitz, M. W. Greene, and P. Richards. Int. J. Appl. Radiat. Isotopes 22, 789-793 (1971).

COLUMBIA UNIVERSITY

I. NEUTRON SPECTROSCOPY

A. Neutron Resonance Cross Section Measurements, (J. Rainwater, F. Rahn, H. Liou, G. Hacken, W.W. Havens, Jr., W. Makofske, M. Slagowitz, and U. Singh)

Since the last report, the emphasis has been on analyzing and publishing the results of our 1970 run.

Many major research papers reporting the results have been submitted for publication and a number have been published. The published paper on the Er isotopes, confirming Dyson's theories concerning level spacings systematics, has led to extensive Monte-Carlo theoretical studies by our group, partly on the basis of interactions with Professor Freeman Dyson. These studies have extended the understanding of the implications of the statistical orthogonal ensemble theory and have permitted a detailed comparison with our results for many even-even nuclei, $150 < A < 190$, which supports this theory well for the first time. We now have extensive results for the resonance parameters and systematics for a large number of nuclei for which papers have been submitted for publication (and/or published) or are being prepared for publication. These include the Er isotopes, the Yb isotopes, ^{232}Th and ^{238}U, ^{152,154}Sm and ^{151,153}Eu, Fe at the cross section interference minima, La and the In isotopes, the W isotopes, Ta, the even A Gd isotopes, F, Mg, Al, S, Cl, K, and Ca.

Necessary preparations are being carried out for use of the modified synchrocyclotron which will have $\sim$ 10 to 100 times greater intensity and allow for the simultaneous use of many different flight paths. The modified Nevis synchrocyclotron, is expected to be in operation in early 1973. The NVS operation will have many flight paths available. Our preparations have included: (a) a necessary re-aim and other improvements for our 200 m flight path, (b) preparation for the simultaneous use of our 40 m self indication detector, (c) modification of the computer interface and programming for the new operation, (d) seeing through the design construction and de-bugging of new NVS deflector system hardware and (e) for a neutron production target-moderator system to go inside the modified cyclotron chamber, (f) preparation of a new hydrogen thyratron deflector pulsing system and its associated circuits, (g) preparation of new collimator systems through the (new) main cyclotron shields and along the various new flight paths, (h) moving the computer from the old lab building attic to the position which it will occupy near the cyclotron control console in the extended cyclotron building balcony, (i) checking that all of our old and new detectors are operating properly, with a re-wiring of signal cables to the cyclotron balcony instead of to the old lab attic, and (j) obtaining and preparing samples for the first run when the new and greatly improved cyclotron operation begins during 1973.

B. Preliminary Results for Even A Isotopes of Cd (H. Liou, J. Rainwater)

The cross sections of the even-even separated Cd isotopes (110, 112, 114, 116) and various thickness Cd natural samples for 1970 data have been obtained by Dr. H.I. Liou through investigation of both transmission and self-indication data, 530 Cd levels to $\sim$ 10 keV were identified and assigned to different isotopes where possible. Table B-1 lists their energy positions in units of eV. The extraction of level parameters ($\Gamma_n{}^o$, $\Gamma\gamma$, and J) is underway. The preliminary results will be reported in the near future. The "between level" cross section from our thick natural sample results is about 5 barns.

C. The Resonance Parameters of Ta^{181} (J. Garg, G. Hacken, H. Liou, J. Rainwater, F. Rahn)

Our 1964 data for Ta^{181} have been analyzed by Dr. Garg in Albany. His results were recently checked at Nevis. Many level identifications were corrected by using our higher resolution data of 1970. The level spacing distribution up to 200 eV was tested by comparison to the Wigner distribution. The Dyson-Mehta Δ statistic and the correlation coefficient for adjacent level spacings for various energy ranges were also tested for 1964 data. The results (shown in Table C-2) indicate that many levels were missed above 80 eV. In the meantime, we are processing the cross section of our 1970 data.

D. Results for Cl. (U. Singh, J. Garg, F. Rahn, J. Rainwater)

The 1970 data for Cl has been carefully reviewed to assure best accuracy, in preparation for publication of these results in the Physical Review. The work involving the R-matrix analysis of resonance and between resonance cross sections versus energy is finished. Table D-1 is a listing of our R-matrix resonance parameters. The many channel average non-resonant total cross section to 15 keV is shown in Fig. D-1 from the measured σ vs E in the region of the levels at 398 eV, 4.247 keV, 8.3 keV, and 14.8 keV. The wing and between resonance σ values are from the thickest sample. The values near σ_{max} are from the data using the appropriate thinner sample.

E. Extension of Results of ^{139}La (G. Hacken, J. Rainwater)

Our previous results to 10 keV on ^{139}La from our 1968 data have been extended to 20 keV. Table E-1 gives the resonance parameters obtained in

TABLE B1

Energy Levels in Cadmium

$Cd^{111,\ 113,\ 106,\ 108}$ (275)

4.58 ± 0.03		196.02 ± 0.39		456.55 ± 0.43	
6.98 ± 0.03		203.52 ± 0.16		465.37 ± 0.56	
18.40 ± 0.03	(113)	208.57 ± 0.17		478.01 ± 0.45	
27.53 ± 0.03	(111)	215.16 ± 0.28	(113)	484.01 ± 0.47	
54.17 ± 0.06		225.05 ± 0.15	(111)	489.66 ± 0.48	
56.33 ± 0.07	(113)	233.41 ± 0.16	(111)	494.64 ± 0.62	
59.65 ± 0.08		237.59 ± 0.21		500.89 ± 0.25	
62.41 ± 0.09		245.95 ± 0.22		517.90 ± 0.33	
63.68 ± 0.09	(113)	261.03 ± 0.19	(113)	524.66 ± 0.26	
69.43 ± 0.10	(111)	269.26 ± 0.20	(113)	540.27 ± 0.28	
84.82 ± 0.07	(113)	275.56 ± 0.21	(111)	548.20 ± 0.28	
86.11 ± 0.07	(111)	281.57 ± 0.26		551.59 ± 0.29	
99.41 ± 0.09	(111)	286.47 ± 0.27		575.92 ± 0.30	
102.93 ± 0.09	(111)	291.56 ± 0.22	(113)	592.37 ± 0.81	
108.30 ± 0.10	(113)	311.38 ± 0.24	(111)	598.67 ± 0.32	
110.77 ± 0.11		331.97 ± 0.27	(111)	603.52 ± 0.33	
114.75 ± 0.11		336.66 ± 0.27		622.63 ± 0.34	
115.84 ± 0.11		355.99 ± 0.29	(111)	634.89 ± 0.35	
125.34 ± 0.13		361.65 ± 0.30		661.27 ± 0.74	
138.11 ± 0.14	(111)	376.56 ± 0.32		688.53 ± 0.79	
140.78 ± 0.15		389.02 ± 0.33	(111)	706.28 ± 0.82	
143.08 ± 0.15	(113)	410.01 ± 0.36		717.94 ± 0.42	
145.89 ± 0.16		414.03 ± 0.37	(113)	723.45 ± 0.43	
158.72 ± 0.17	(113)	422.66 ± 0.38		764.32 ± 0.47	
164.11 ± 0.18	(111)	431.94 ± 0.39	(113)	782.69 ± 0.47	
167.10 ± 0.30		438.31 ± 0.40	(111)	790.43 ± 0.49	
192.82 ± 0.14	(113)	446.67 ± 0.41		809.26 ± 0.51	
841.45 ± 0.54		1289.4 ± 0.5		1820.5 ± 0.4	
851.43 ± 0.55	(113)	1307.6 ± 0.5		1825.6 ± 0.9	
860.48 ± 0.55		1310.2 ± 0.5		1866.9 ± 0.5	
878.17 ± 0.57		1333.7 ± 0.5		1883.6 ± 0.5	
901.28 ± 0.30		1356.1 ± 0.5		1908.2 ± 0.5	
903.65 ± 0.30		1364.0 ± 0.6		1928.5 ± 0.9	
924.69 ± 0.31		1371.2 ± 0.6		1934.1 ± 0.5	
939.18 ± 0.32		1399.1 ± 0.3		1937.1 ± 0.9	
955.14 ± 0.65		1403.2 ± 0.3		1963.3 ± 1.0	
965.24 ± 0.33		1448.6 ± 0.6		2007.5 ± 0.5	
975.51 ± 0.34		1467.7 ± 0.6		2018.7 ± 0.5	
1003.1 ± 0.4		1522.3 ± 0.3		2022.7 ± 0.5	
1018.2 ± 0.7		1581.7 ± 0.4		2053.2 ± 0.5	
1042.0 ± 0.4		1596.9 ± 0.4		2082.8 ± 1.1	
1056.9 ± 0.8		1617.4 ± 0.4		2114.6 ± 0.6	
1067.7 ± 0.4		1628.0 ± 0.4		2138.3 ± 1.1	

TABLE B1 (cont.)

$Cd^{111, 113, 106, 108}$

1088.6 ± 0.4	1630.9 ± 0.4	2144.0 ± 1.1
1120.0 ± 0.4	1645.6 ± 0.4	2200.0 ± 0.6
1148.8 ± 0.4	1654.2 ± 0.4	2236.6 ± 0.6
1169.1 ± 0.5	1659.7 ± 0.4	2241.2 ± 0.6
1174.4 ± 0.5	1710.5 ± 0.8	2290.5 ± 0.6
1202.2 ± 0.5	1734.0 ± 0.4	2294.4 ± 1.2
1216.8 ± 0.5	1742.3 ± 0.4	2303.5 ± 1.2
1237.2 ± 0.5	1752.3 ± 0.8	2330.4 ± 0.6
1252.1 ± 0.5	1753.9 ± 0.8	2345.2 ± 0.6
1261.6 ± 0.5	1766.5 ± 0.8	2388.1 ± 1.3
1267.3 ± 0.5	1787.0 ± 0.4	2430.8 ± 0.7
2450.0 ± 0.7	3141.1 ± 1.0	4221.0 ± 3.0
2465.3 ± 1.4	3197.7 ± 2.0	4340.6 ± 1.6
2489.0 ± 0.7	3213.6 ± 1.0	4368.1 ± 1.6
2497.1 ± 0.7	3240.8 ± 1.0	4414.3 ± 1.6
2526.1 ± 0.7	3256.5 ± 1.0	4436.1 ± 1.6
2534.1 ± 0.7	3274.4 ± 1.0	4468.6 ± 1.6
2560.5 ± 0.7	3391.3 ± 1.1	4513.1 ± 1.7
2603.6 ± 0.7	3430.0 ± 1.1	4624.8 ± 1.7
2650.1 ± 0.8	3456.6 ± 1.1	4657.7 ± 1.8
2745.7 ± 0.8	3478.4 ± 1.1	4773.8 ± 1.8
2752.3 ± 0.8	3528.3 ± 2.3	4807.4 ± 1.8
2771.8 ± 0.8	3535.2 ± 2.4	4842.3 ± 1.9
2777.4 ± 0.8	3549.1 ± 1.2	4889.7 ± 1.9
2791.9 ± 0.8	3579.4 ± 1.2	4952.0 ± 1.9
2827.4 ± 1.6	3605.3 ± 1.2	5011.8 ± 2.0
2867.3 ± 0.9	3616.0 ± 1.2	5043.0 ± 2.0
2899.9 ± 0.9	3676.3 ± 1.2	5170.9 ± 2.1
2927.9 ± 0.9	3683.7 ± 1.2	5273.2 ± 2.1
2943.6 ± 0.9	3804.1 ± 1.3	5328.1 ± 2.1
2965.6 ± 0.9	3829.9 ± 1.3	5394.8 ± 2.2
2993.6 ± 0.9	3914.3 ± 1.4	5479.3 ± 2.2
3020.3 ± 0.9	3926.4 ± 1.4	5500.5 ± 2.2
3054.2 ± 0.9	3992.6 ± 1.4	5602.4 ± 2.3
3073.3 ± 0.9	4054.1 ± 1.4	5623.1 ± 2.3
3082.1 ± 1.0	4127.9 ± 2.9	5764.3 ± 2.4
3089.7 ± 1.0	4141.7 ± 1.5	5776.3 ± 2.4
3120.4 ± 1.0	4192.6 ± 1.5	5802.8 ± 2.4
5724.7 ± 2.5	9443.1 ± 5.0	
5930.8 ± 2.5	9496.1 ± 5.1	
6014.2 ± 5.2	9603.5 ± 5.2	
6221.2 ± 2.7	9720.5 ± 5.3	
6556.6 ± 5.8	9773.2 ± 5.3	
6683.5 ± 3.0		

TABLE B_1 (cont.)

$Cd^{111, 113, 106, 108}$

6719.5 ± 3.0
6795.6 ± 3.1
6804.8 ± 3.1
6827.9 ± 3.1
6863.6 ± 3.1
7018.7 ± 3.2
7051.1 ± 3.3
7129.5 ± 3.3
7232.8 ± 3.4
7481.6 ± 3.6
7513.6 ± 3.6
7574.6 ± 3.6
7698.9 ± 3.7
7910.3 ± 3.7
8048.9 ± 4.0
8122.6 ± 4.0
8461.6 ± 4.3
8745.6 ± 4.5
8861.0 ± 4.6
8913.7 ± 4.6
9328.6 ± 4.9

Cd^{110} (79)

89.27 ± 0.15	2723.3 ± 1.6	5291.0 ± 2.1
230.93 ± 0.16	2739.7 ± 1.6	5369.9 ± 2.2
339.66 ± 0.28	3042.2 ± 0.9	5694.2 ± 2.4
369.61 ± 0.20	3105.7 ± 1.0	5802.8 ± 2.4
505.34 ± 0.25	3153.1 ± 1.0	5983.7 ± 2.6
652.05 ± 0.37	3183.7 ± 5.0	6089.0 ± 2.6
761.78 ± 0.46	3375.1 ± 1.1	6259.0 ± 2.7
799.76 ± 0.50	3496.4 ± 1.1	6343.9 ± 2.8
824.08 ± 0.52	3636.4 ± 1.2	6468.9 ± 2.9
916.89 ± 0.31	3667.8 ± 2.4	6487.4 ± 2.9
920.85 ± 0.31	3702.1 ± 1.2	6601.9 ± 3.0
1115.9 ± 0.4	3744.4 ± 1.3	6913.7 ± 3.2
1135.3 ± 0.4	3804.4 ± 6.6	6937.3 ± 3.2
1241.5 ± 0.5	3953.5 ± 1.4	7083.6 ± 3.3
1318.1 ± 0.3	3981.0 ± 7.0	7276.8 ± 3.4
1346.7 ± 0.3	4099.0 ± 1.4	7669.4 ± 3.7
1685.8 ± 0.4	4161.5 ± 1.5	8718.8 ± 4.5
1809.5 ± 0.4	4180.7 ± 1.5	8822.2 ± 4.6
1828.2 ± 0.4	4242.8 ± 1.5	8934.5 ± 4.7

TABLE B1 (cont.)

Cd^{110} (79)

1982.9 ± 0.5	4304.8 ± 1.6	9025.4 ± 4.7
2065.7 ± 0.5	4402.3 ± 1.6	9146.3 ± 4.7
2099.5 ± 0.6	4483.4 ± 1.7^{T}	9221.0 ± 4.8
2353.0 ± 0.6	4661.1 ± 1.8^{T}	9250.2 ± 4.8
2376.0 ± 0.6	4675.1 ± 1.8^{T}	9269.7 ± 4.9
2410.6 ± 0.7	4747.7 ± 1.8	9896.0 ± 5.0
2476.8 ± 0.7	4864.5 ± 1.9^{T}	
2492.0 ± 0.7	5121.4 ± 2.0	

Cd^{112} (99)

66.77 ± 0.09	2684.8 ± 0.8	5001.1 ± 2.0
82 57 ± 0.09	2813.4 ± 0.8	5136.5 ± 2.0
83.24 ± 0.07	2817.5 ± 0.8	5236.6 ± 2.1
226.46 ± 0.15	2951.5 ± 0.9	5285.8 ± 2.1
442.97 ± 0.41	3006.7 ± 1.8	5552.2 ± 2.3
452.68 ± 0.27	3103.8 ± 1.0	5574.9 ± 2.3
565.76 ± 0.30	3153.6 ± 1.0	5686.0 ± 2.4
737.28 ± 0.44	3224.7 ± 1.0	5734.4 ± 2.4
810.61 ± 0.64	3289.8 ± 1.0	5948.3 ± 2.5
884.47 ± 0.57	3306.9 ± 1.0	6085.1 ± 2.6
894.50 ± 0.30	3320.5 ± 1.1	6112.4 ± 2.6
908.73 ± 0.30	3404.3 ± 1.1	6359.1 ± 2.8
1052.5 ± 0.4	3491.9 ± 1.2	6433.4 ± 2.8
1101.5 ± 0.4	3710.1 ± 1.2	6529.1 ± 2.9
1115.4 ± 0.4	3776.3 ± 1.3	6577.0 ± 2.9
1207.3 ± 0.5	3861.9 ± 1.3	6874.5 ± 3.1
1337.3 ± 0.5	3885.7 ± 1.3	6920.0 ± 3.2
1423.3 ± 0.6	4106.9 ± 1.4	6937.3 ± 3.2
1640.1 ± 0.4	4152.7 ± 1.5	6975.5 ± 3.3
1706.0 ± 0.4	4200.0 ± 1.5	7167.6 ± 3.3
1814.4 ± 0.4	4263.3 ± 1.5	7640.0 ± 3.7
1942.5 ± 0.5	4392.7 ± 1.6	8007.5 ± 3.8
2035.5 ± 0.5	4486.7 ± 1.7	8029.2 ± 3.8
2226.2 ± 0.6	4558.3 ± 1.7	8248.3 ± 4.0
2336.5 ± 0.6	4798.3 ± 1.8	8377.0 ± 4.0
2456.6 ± 0.7	4854.3 ± 1.9	8519.4 ± 4.0
2573.7 ± 0.7	4907.5 ± 1.9	8536.7 ± 4.1

Cd^{112}

8665.5 ± 4.4

TABLE B1 (cont.)

Cd^{112}

8876.9 ± 4.5
9041.9 ± 4.7
9153.5 ± 4.8
9225.9 ± 4.9
9570.1 ± 5.1
9738.9 ± 5.3
10043 ± 6
10262 ± 6
10464 ± 6
10582 ± 6
10678 ± 6
10899 ± 6
11018 ± 7
11153 ± 7
11280 ± 7
11322 ± 7
11455 ± 7

Cd^{114} (55)

56.40 ± 0.05	2849.3 ± 0.9	10088 ± 6
120.10 ± 0.15	2955.9 ± 0.9	
227.07 ± 0.15	3027.1 ± 0.9	
392.24 ± 0.34	3178.0 ± 1.0	
567.78 ± 0.38	3305.4 ± 2.1	
670.68 ± 0.38	3333.6 ± 1.1	
752.19 ± 0.45	3698.4 ± 6.3	
962.13 ± 0.33	3819.5 ± 1.3	
1037.9 ± 0.9	4258.0 ± 1.5	
1099.7 ± 0.4	4346.9 ± 3.2	
1326.5 ± 0.3	4418.4 ± 3.2	
1425.7 ± 0.6	4582.8 ± 1.7	
1475.3 ± 0.3	4645.5 ± 1.7	
1485.3 ± 0.6	4691.8 ± 1.8	
1604.3 ± 0.4	5357.0 ± 2.2	
1638.6 ± 0.7	5515.0 ± 2.3	
1690.0 ± 0.7	6042.4 ± 2.6	
1921.1 ± 0.5	6406.6 ± 2.8	
1964.9 ± 0.5	7202.6 ± 3.4	
2132.6 ± 0.6	7393.8 ± 3.5	
2267.3 ± 0.6	7495.8 ± 3.6	
2284.2 ± 0.6	7662.0 ± 3.7	
2512.9 ± 0.7	7837.6 ± 3.8	
2589.5 ± 0.7	8368.6 ± 4.2	
2635.9 ± 0.8	8946.0 ± 4.6	

TABLE B1 (cont.)

Cd^{114}	(55)	
2804.0 ± 0.8		9958.3 ± 5.5
Cd^{116}	(21)	
28.97 ± 0.05		
676.41 ± 0.39		
888.96 ± 0.29		
1048.3 ± 0.4		
1122.4 ± 0.4		
1384.1 ± 0.3		
1566.5 ± 0.4		
1857.7 ± 0.5		
1968.5 ± 0.5		
2361.5 ± 0.6		
2541.2 ± 0.8		
2651.6 ± 0.8		
3358.0 ± 1.1		
3652.6 ± 1.2		
4206.7 ± 1.5		
4615.3 ± 1.7		
4873.8 ± 1.9		
5072.5 ± 2.0		
5300.5 ± 2.2		
7347.1 ± 3.5		
8822.2 ± 4.6		

TABLE C1

Resonance Parameters of ^{181}Ta

Total 52 levels seem likely to be spurious

E_o (ev)	ΔE_o (ev)	$g\Gamma n^o$ (meV)	$\Delta g\Gamma n^o$ (meV)	$\Gamma+\Delta\Gamma$ (meV)	$\Gamma\gamma+\Delta\Gamma\gamma$ (meV)
4.28*	.01	0.99	0.028		56±6
0.34*	.05	0.63	0.017		61±6
8.60*	.10	0.15	0.005		52±3
10.40*	.20	0.09	0.01		85±20
22.80*	.10	0.12	0.005		64±5
24.10*	.10	0.025	0.002		51±14
30.00	.10	0.65	0.02		61±4
34.20*	.05	.020	.002	55±15	55±15
35.16	.05	.98	.05	90±15	78±15
35.90	.05	1.50	.10	75±10	57±10
39.13	.06	3.90	.50	110±25	61±25
49.15	.08	.09	.01	65±15	64±15
55.80 x	.08	.0017			
57.54	.08	.018	.002		
59.05	.08	.008	.002		
63.12	.08	.33	.02	65±15	60±15
76.85	.08	.70	.03	60±15	46±15
77.64	.10	.35	.05	60±15	54±15
78.92	.10	.085	.01		
82.94	.05	.75	.05	60±10	46±10
85.11	.05	.22	.02	65±10	61±10
85.90	.05	.01	.005		
89.60	.05	.17	.02		
91.42	.05	.13	.01		
97.00	.06	.15	.02		
99.32	.06	5.75	.50	145±15	40±15
103.52	.06	0.05	.02		
105.54	.07	1.40	.20	80±10	52±10
115.08	.07	1.80	.20	95±10	59±10
118.32	.08	.12	.02		
126.46	.08	1.80	.20	95±10	55±10
136.48	.09	.95	.05	60±10	38±10

TABLE C1 (Cont.)

E_0 (eV)	ΔE_0 (eV)	$g\Gamma_n^0$ (meV)	$\Delta g\Gamma_n^0$ (meV)	E_0 (eV)	ΔE_0 (eV)	$g\Gamma_n^0$ (meV)	$\Delta g\Gamma_n^0$ (meV)
138.33	.09	.55	.05	264.65	.24	.32	.04
144.21	.09	0.065	.005	271.75	.24	.30	.05
148.31	.09	.18	.02	273.85	.24	2.00	.20
149.82	.10	.22	.02	277.22	.26	1.00	.20
157.38	.10	0.005	.001	280.28	.26	.55	.05
159.75	.10	0.005	.001	287.70	.26	.55	.05
166.39	.12	.33	.03	290.40	.28	.40	.10
174.90	.12	3.8	.5	291.05	.28	.28	.05
175.80	.12	2.5	.5	304.04	.28	.11	.01
178.60	.12	.05	.02	306.22	.30	.60	.05
182.58	.14	.035	.005	311.72	.30	.50	.05
185.52	.14	.022	.005	313.23	.30	3.10	.60
189.30	.14	.025	.005	322.80	.30	.20	.02
191.30*	.14	.001	.001	327.60*	.30	.05	.05
191.61				329.40	.16	1.80	.20
192.00*	.14	.001	.001	341.57	.16	.13	.01
194.80	.14	4.50	.50	344.53	.16	.55	.05
200.00	.16	1.4	.20	346.82	.18	.40	.05
204.66	.16	.085	.01	349.20	.18	.65	.05
208.40	.16	.35	.03	354.30	.18	.85	.08
214.96	.16	2.00	.500	357.30	.18	.10	.01
216.52	.16	.60	.06	370.21	.20	.98	.10
219.68	.16	.55	.05	378.55	.20	.40	.10
222.30	.16	.10	.02	379.80*	.20	.10	.005
225.26	.18	.70	.10	382.10	.20	.009	.003
230.53	.18	.55	.05	388.90	.20	.65	.05
232.26	.18	1.50	.50	396.50	.20	.30	.20
237.28	.18	.04	.01	397.50	.20	.90	.20
242.60	.20	.30	.04	403.7	.25	.005	.003
247.24	.20	.19	.02	409.9	.25	2.00	.20
248.36	.20	.07	.01	415.7	.25	1.60	.40
252.60	.22	.005	.005	417.1	.25	1.60	.40
259.00	.22	.33	.03	419.6	.25	.05	.05
259.90*	.22	.05	.03	421.8	.25	.07	.01
263.25	.22	1.40	.30	428.9	.25	.16	.02

TABLE C1 (Cont.)

E_0 (eV)	ΔE_0 (eV)	$g\Gamma_n^0$ (meV)	$\Delta g\Gamma_n^0$ (meV)	E_0 (eV)	ΔE_0 (eV)	$g\Gamma_n^0$ (meV)	$\Delta g\Gamma_n^0$ (meV)
434.2	.25	.58	.05	591.6	.4	1.00	.10
439.2	.30	1.50	.20	596.5	.4	6.00	2.00
443.8	.30	1.70	.20	600.5	.4	.025	.015
446.1	.30	1.50	.20	604.0*	.4	.01	.01
449.7	.30	.30	.03	606.0	.4	.15	.05
461.4	.30	.92	.10	608.8	.4	.9	.3
465.2	.30	.10	.02	613.2*	.4	.03	.01
467.7	.35	2.00	.20	617.4	.4	1.60	.3
471.5	.35	.90	.08	624.1	.2	.75	.05
473.6*	.35	.04	.02	626.4	.2	2.20	.20
477.3	.35	.02	.01	631.5*	.2	.01	.01
482.2	.35	.35	.03	636.0	.2	.10	.01
483.6	.35	.30	.03	644.7	.2	.12	.02
490.2	.35	.82	.08	647.4	.2	1.50	.20
493.8	.35	.30	.03	651.1	.2	1.70	.20
495.3	.35	.27	.03	654.6*	.2	.01	.005
497.5	.35	.01	.01	658.1	.2	.18	.02
500.0	.4	.05	.02	660.0*	.25	.01	.01
502.0	.4	1.20	.20	666.5	.25	.11	.04
519.4	.4	.33	.03	668.4	.25	.06	.02
522.8	.4	2.00	.40	674.0*	.25	.01	.01
524.3	.4	.10	.05	675.1	.25	.03	.01
527.1	.4	2.00	.30	677.9	.25	.15	.02
533.9	.4	1.70	.30	680.7	.25	1.0	.15
536.3	.4	.30	.03	692.3*	.25	.01	.01
542.5	.4	.90	.10	695.9	.25	1.0	.10
548.9	.4	.35	.05	699.8	.25	.015	.005
554.3	.4	.06	.01	702.5	.3	.40	.04
557.0	.4	.95	.10	706.5	.3	2.10	.40
561.3	.4	.025	.005	710.3	.3	.15	.05
567.2	.4	.05	.01	716.0	.3	2.10	.40
569.5	.4	1.10	.10	719.7	.3	.01	.01
576.3	.4	.09	.01	723.5*	.3	.01	.01
581.5	.4	.005	.005	729.2	.3	.28	.08
589.0	.4	.008	.005	731.9	.3	3.0	.5

TABLE C1 (Cont.)

E_0 (eV)	ΔE_0 (eV)	$g\Gamma_n^0$ (meV)	$\Delta g\Gamma_n^0$ (meV)	E_0 (eV)	ΔE_0 (eV)	$g\Gamma_n^0$ (meV)	$\Delta g\Gamma_n^0$ (meV)
735.5	.3	.65	.05	878.9	.35	.95	.05
739.4	.3	2.2	.4	880.7	.35	.25	.15
747.2	.3	1.1	.1	886.8*	.35	.05	.02
752.7*	.3	.01	.01	883.3	.35	.15	.05
757.3	.3	1.2	.1	894.6	.35	1.1	.2
760.3	.3	.4	.1	896.9	.35	.7	.2
763.6*	.3	.01	.01	908.4	.4	1.2	.2
766.5*	.3	.01	.01	912.8	.4	1.0	.3
769.2	.3	.10	.02	915.3	.4	.8	.2
773.7*	.3	.01	.01	919.2	.4	.8	.1
776.8	.3	1.25	.25	925.6	.4	.7	.1
780.0*	.3	.010	.005	929.8	.4	2.5	.5
782.7	.3	.022	.005	931.8	.4	2.0	.5
786.6*	.3	.01	.01	936.4	.4	.1	.02
789.1	.3	.9	.1	942.8	.4	3.0	.5
797.6	.3	.7	.1	945.3	.4	4.5	1.0
801.2*	.35	.01	.01	947.5	.4	4.0	1.
802.4*	.35	.01	.01	952.4	.4	.6	.1
805.2	.35	.035	.015	956.0	.4	.06	.01
808.2	.35	.95	.15	961.6*	.4	.01	.01
813.1	.35	2.3	.4	966.0	.4	1.2	.5
820.8	.35	2.5	.4	966.8*	.4	.8	.5
825.5	.35	.5	.1	968.2	.4	.65	.1
829.2	.35	.01	.01	973.6	.4	1.20	.2
833.3	.35	1.2	.2	977.4*	.4	.01	.01
836.6*	.35	.01	.01	982.9	.4	1.10	.2
839.0*	.35	.01	.01	988.3	.4	.06	.02
841.0*	.35	.02	.01	989.4*	.4	.04	.02
841.6*	.35	.02	.01	993.4	.4	.45	.15
846.3	.35	.7	.1	996.0	.4	1.30	.30
847.3*	.35	.15	.05	1001.6	.45	1.	.10
852.5	.35	.9	.1	1006.2	.45	.22	.02
862.7	.35	.01	.01	1008.2*	.45	.02	.02
870.02	.35	.35	.05	1015.6	.45	.60	.10
873.9	.35	.90	.10	1018.6	.45	.80	.10

TABLE C1 (Cont.)

E_0 (eV)	ΔE_0 (eV)	$g\Gamma_n^0$ (meV)	$\Delta g\Gamma_n^0$ (meV)	E_0 (eV)	ΔE_0 (eV)	$g\Gamma_n^0$ (meV)	$\Delta g\Gamma_n^0$ (meV)
1025.5	.45	.15	.03	1208.1	.6	.35	.15
1031.0	.45	.10	.03	1211.8	.6	.25	.1
1033.4*	.45	.50	.20	1216.0			
1035.4	.45	6.0	1.0	1218.5	.6	.5	.1
1043.0	.45	2.5	.5	1226.6	.6	1.7	.4
1047.0*	.45	.02	.01	1230.2*	.6	.05	.01
1050.1*	.45	.01	.01	1233.0	.6	.10	.02
1052.1	.45	.01	.01	1236.1*	.6	.02	.01
1055.8	.45	.60	.10	1239.7	.6	.35	.07
1063.3	.45	.85	.10	1246.6	.6	3.5	.70
1071.2	.45	4.0	1.0	1251.1			
1073.1*	.45	.01	.01	1252.9*	.6	.02	.01
1080.2	.45	2.5	.5	1259.0	.6	3.0	.6
1081.9	.45	1.0	.50	1263.0	.6	.7	.2
1085.5*	.45	.02	.01	1268.0	.6	.1	.05
1090.4	.45	2.5	.5	1270.7*	.6	.02	.01
1093.4	.45		.1	1275.7	.6	1.6	.3
1096.8	.45	2.0	.5	1280.0	.6	.05	.02
1103.3	.45	.15	.05	1283.2	.6	.4	.1
1106.1				1286.7	.6	.2	.05
1109.5*	.5	.01	.01	1293.0	.6	2.0	.5
1112.9	.5	.70	.05	1299.7	.6	2.6	.6
1116.3*	.5	.01	.01	1307.0	.7	.2	.05
1119.1	.5	.12	.03	1312.6	.7	1.5	.4
1124.5*	.5	.05	.02	1316.9	.7	1.2	.3
1130.9	.5	3.0	.5	1323.5	.7	.2	.05
1136.1*	.5	.01	.01	1328.4	.7	3.5	.8
1138.5	.5	.2	.05	1332.0	.7	3.5	.8
1141.4*	.5	.01	.01	1335.0	.7	2.5	.5
1145.1	.5	1.0	.2	1342.8	.7	.1	.05
1151.0	.5	2.5	.5	1346.5*	.7	.02	.01
1156.9	.5	.75	.15	1348.7			
1165.0	.5	1.50	.3	1352.0	.7	.15	.05
1169.9	.5	.01	.01	1356.1			
1174.8	.5	3.7	.8	1361.0	.7	5.0	1.0
1177.9	.5	6.0	1.0	1363.0	.7	2.0	.5
1185.4*	.5	.01	.01	1366.6*	.7	.1	.05
1191.6	.5	10.0	2.0	1371.8	.7	.5	.10
1198.3*	.5	.05	.02	1376.7	.7	1.8	.5
1203.5	.6	.3	.1	1388.0	.7	.8	.2
				1391.5	.7	1.5	.3
				1397.9	.7	3.0	1.0

Weak levels with * after energies are probably spurious on the basis of the 1970 data.

TABLE C.2

Results of Statistical
Orthogonal Ensemble
Statistics for Tantalum

Ta^{181} 1964 Data Results

ΔE	N	P(Sj, Sj+1)*	Δexp	Δtheory
0 — 80 ev	19	—0.051 ± 0.189	0.64	0.94 ± 0.2
0 — 100 ev	26	—0.043 ± 0.166	0.76	0.50 ± 0.2
0 — 120 ev	30	—0.095 ± 0.151	0.77	0.53 ± 0.2
0 — 140 ev	33	—0.053 ± 0.156	0.94	0.55 ± 0.2
0 — 160 ev	38	—0.105 ± 0.148	1.05	0.58 ± 0.2
0 — 180 ev	42	—0.104 ± 1.142	1.15	0.60 ± 0.2
0 — 200 ev	49	—0.068 ± 0.136	1.13	0.63 ± 0.2
0 — 300 ev	74	—0.111 ± 0.115	1.44	0.72 ± 0.2
0 — 500 ev	119	—0.137 ± 0.089	2.82	0.81 ± 0.2
0 — 1000 ev	236	—0.123 ± 061	2.56	0.95 ± 0.2

* Monte Carlo results for P(sj, Sj+1) for two merged populations with density ratio = 9/7 is (—0 - 2.55)

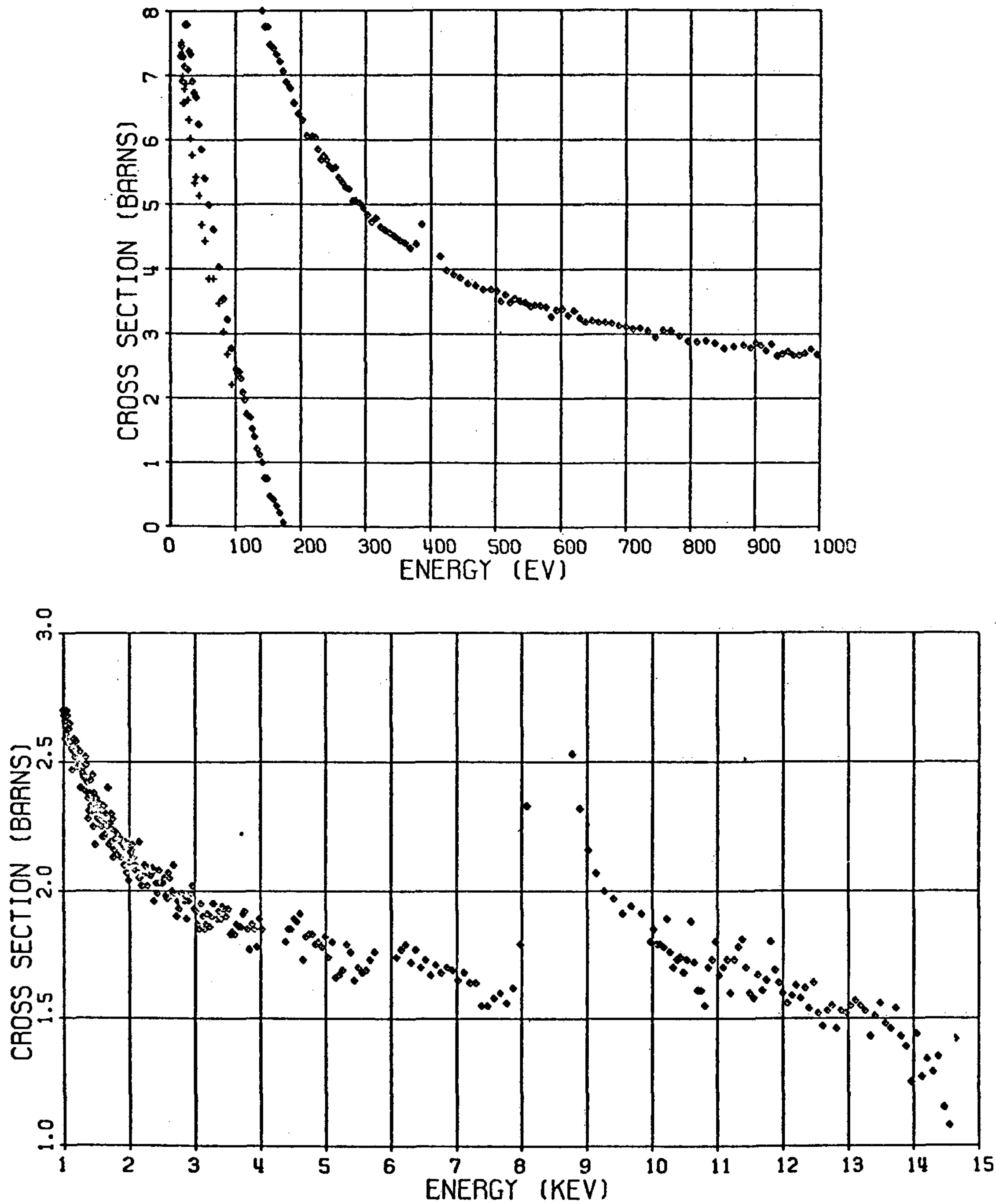

Fig. D1

σ_{av} vs E for Cl to 15 keV (many channel averages)

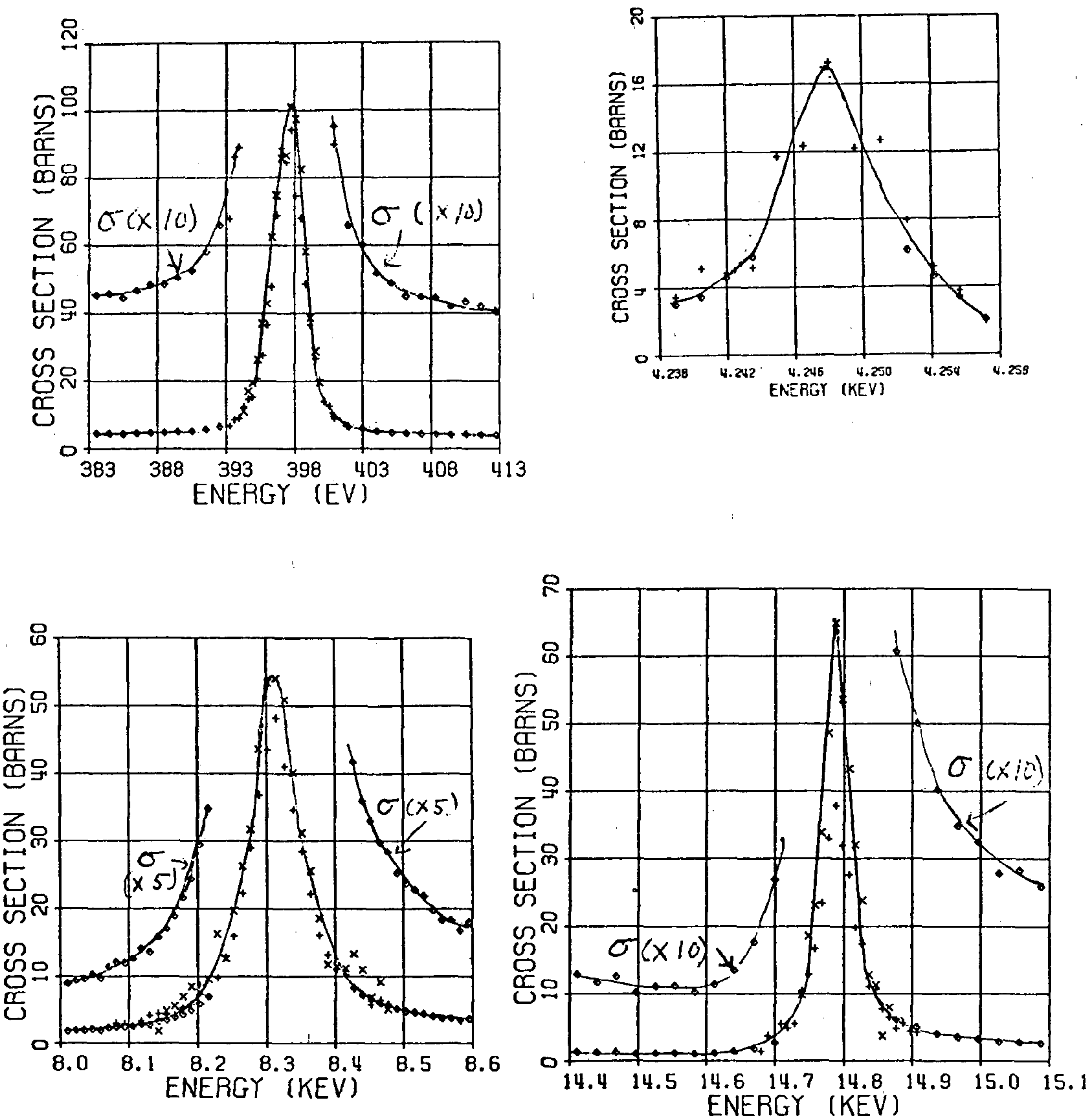

Fig. D2

Measured σ vs E near the four Cl resonances to 14.8 keV

Cl^{35}: $I^{\pi}=3/2^{+}$ Cl^{37}: $I^{\pi}=3/2^{+}$

TABLE D1

Cl^{35}: 75.77% Cl^{37}: 24.23%

Chlorine Resonance Parameters (July 1972)

E_o (keV)	Isotope	$ag\Gamma_n$ (eV)	ℓ	J
0.398 ± 0.0005	35	0.040±0.006	1	
4.248 ± 0.002	35	0.135±0.020	1	
8.314 ± 0.007	37	11.5 ±1.0	0	2
14.788 ± 0.015	35	14.0 ±2.0	0	2
16.338 ± 0.017		2.65 ±0.30	1	
17.120 ± 0.018	35	6.0 ±1.0		2
25.586 ± 0.031		60 ±10		
26.601 ± 0.033	35	65 ±10	0	2
27.328 ± 0.034	37	1.65 ±0.2	1	0
27.804 ± 0.035		0.64 ±0.06		
44.146 ± 0.066		(4.1 ±1.0	1	
46.579 ± 0.071	37	(60 ±5	0	2
51.509 ± 0.082		(1.2 ±0.2	1	
54.936 ± 0.089		16.4 ±3.5		2
55.361 ± 0.090		18 ±4	1	
57.717 ± 0.096	35	46 ±5	1	2
62.644 ± 0.106		35 ±5	1	
66.788 ± 0.117		8 ±2	1	
68.132 ± 0.121	37	55 ±5	0	2
90.328 ± 0.180		6 ±2		
93.065 ± 0.188	37	98 ±8	0	2
103.327 ± 0.218	35	120 ±20	1	
113.268 ± 0.248	35	240 ±30	1	2,3
127.661 ± 0.294		60 ±6		
133.607 ± 0.314		250 ±30		
136.322 ± 0.323		210 ±30		
140.553 ± 0.333		90 ±15		
142.890 ± 0.346	35	420 ±50	1	
149.627 ± 0.370		55 ±10		
165.347 ± 0.427		55 ±15		
182.822 ± 0.493	35	850 ±150	1	
188.070 ± 0.513	35	440 ±40		2
190.323 ± 0.522	35	280 ±45		1

this region. A plot of the cumulative sum of the reduced neutron widths versus energy is shown in fig. E-1, for the entire range to 20 keV. The slope of the straight line to the experimental data gives the s strength function. Our best choice is $S_o = (0.67 \pm 0.11) \times 10^{-4}$. Fig. E-2 shows the distributioln of our reduced neutron widths for La^{139} compared with the theoretical Porter-Thomas distribution. An examination of this figure reveals an excess of levels with small Γ_n^o which are interpreted to be p wave levels. The analysis gives ≈ 78 s wave levels (in the first 21 keV) with an average $<\Gamma_n^o> = 18$ meV. The early stages of analysis yield σ versus E curves, which do not provide a good picture of the true behavior of σ at resonance. At and near resonance, σ is best reconstructed from the tabulated Breit-Wigner parameters. A thick La^{139} sample did, however, give reliable information on σ versus E between (and not too close to) levels. Fig. E-3 shows our cross section result. Many channel averaging was used in this figure.

F. R-Matrix Fitting of Natural Sodium (F. Rahn, M. Slagowitz, W.W. Havens, Jr., J. Rainwater, U. Singh)

We have completed the analysis of our 1968 and 1970 sodium data in the energy region 0 to 300 keV.

The results of our R-matrix analysis are given in table F-1. In this table we give the multilevel parameters E_i, Γ_i, J_i and ℓ_i which best fit our experimental data to 300 keV.

2.850 keV level Our analysis indicates a spin assignment of J=1 with ℓ = o for this level. This spin assignment is consistent with the observed peak cross section of $\sigma \simeq 390$ barns. The data indicates that the width of this resonance is Γ = 388 eV, wider than the earlier measurements of Garg and in better agreement with the measurements of Moxon and Lynn.

53.15 keV level Because of the peak cross section σ_o = 37 barns and symmetry of shape this resonance is assigned J = 2 with ℓ = 1. We find the total width to be Γ = 1.23 keV. These parameters are in general agreement with those previously reported by Moxon et. al. (ℓ=1, $g\Gamma_n$=750, J=2).

198.8 keV level This cross section for this level agrees well with Γ = 3.6 keV, J = 1 and ℓ = o obtained previously. The lack of a pronounced interference dip is caused by the wide p wave level at 212 keV. The evidence for the s wave character of this level is due mainly to the behavior of the cross section on the high energy side of the resonance.

212 keV level The best R-matrix fit ocurred for $E_o = 212 \pm 1$ keV. The

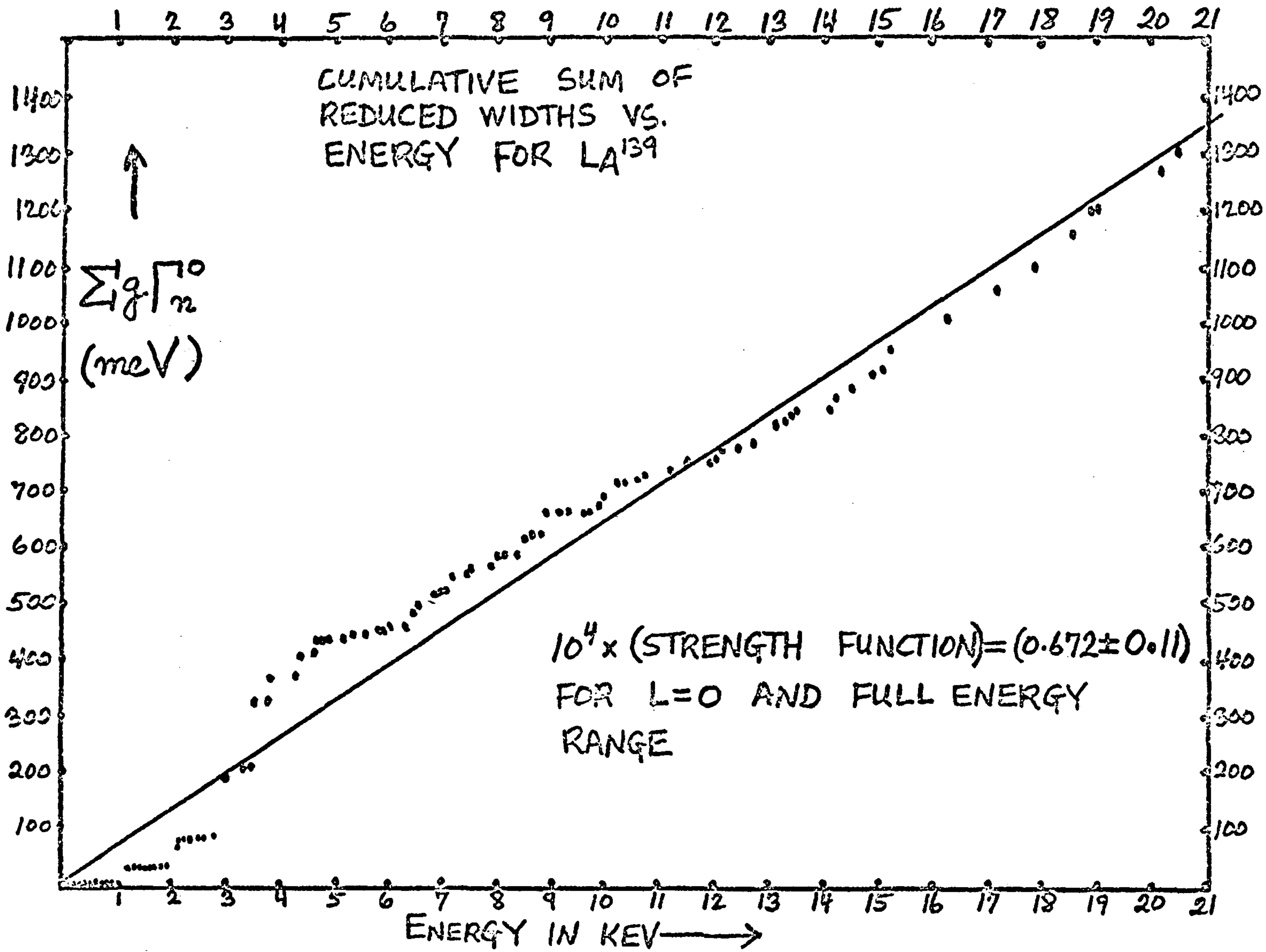
CUMULATIVE SUM OF
REDUCED WIDTHS VS.
ENERGY FOR LA139
$\Sigma g\Gamma_n^0$
(meV)
10^4 x (STRENGTH FUNCTION) = (0.672±0.11)
FOR L=0 AND FULL ENERGY
RANGE
ENERGY IN KEV

Fig. E1

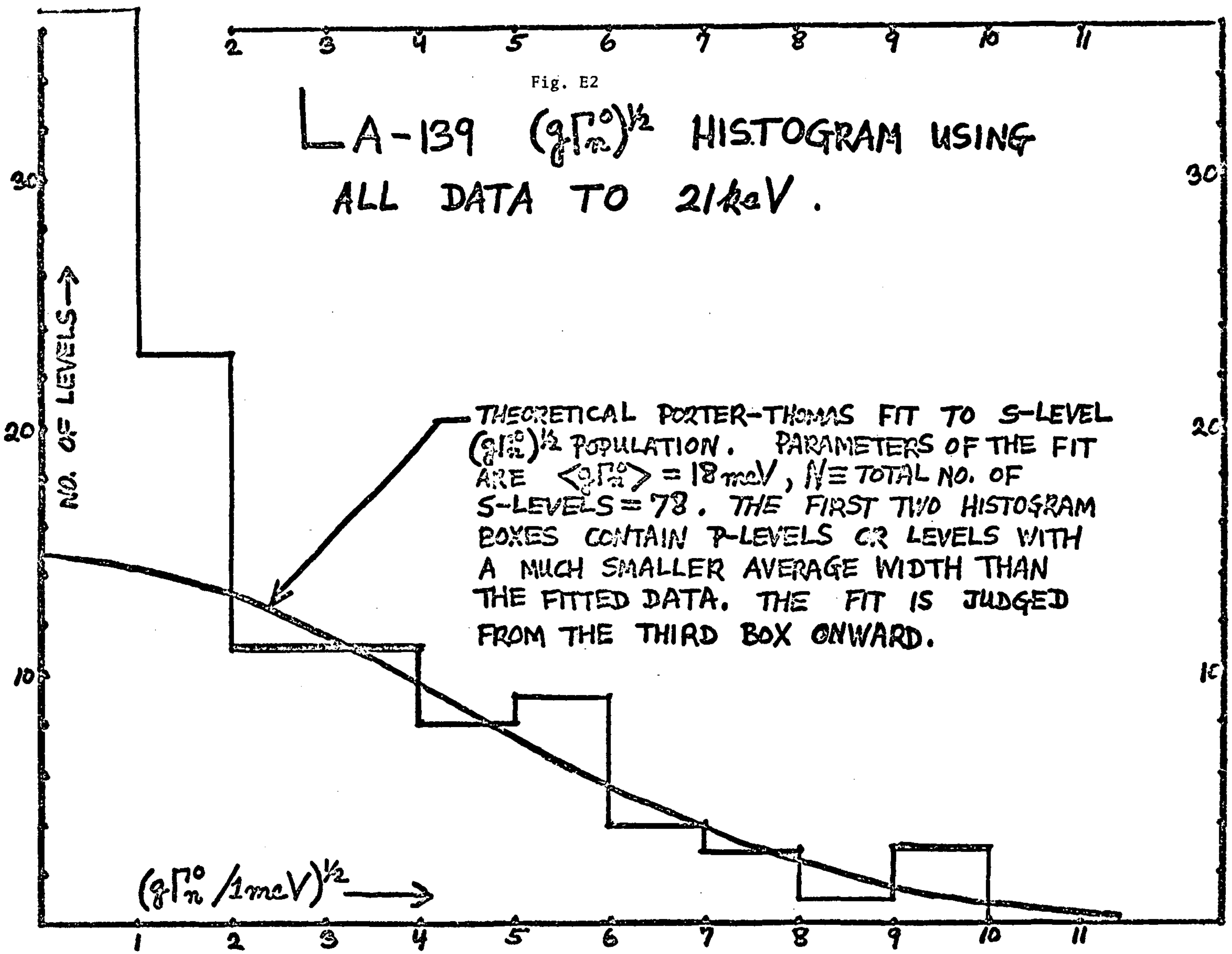
LA-139 $(g\Gamma_n^0)^{1/2}$ HISTOGRAM USING ALL DATA TO 21keV.
NO. OF LEVELS →
$(g\Gamma_n^0 / 1meV)^{1/2}$ →
THEORETICAL PORTER-THOMAS FIT TO S-LEVEL $(g\Gamma_n^0)^{1/2}$ POPULATION. PARAMETERS OF THE FIT ARE $\langle g\Gamma_n^0 \rangle = 18$ meV, $N \equiv$ TOTAL NO. OF S-LEVELS = 78. THE FIRST TWO HISTOGRAM BOXES CONTAIN P-LEVELS OR LEVELS WITH A MUCH SMALLER AVERAGE WIDTH THAN THE FITTED DATA. THE FIT IS JUDGED FROM THE THIRD BOX ONWARD.
1
2
3
4
5
6
7
8
9
10
11
10
20
30

Fig. E2

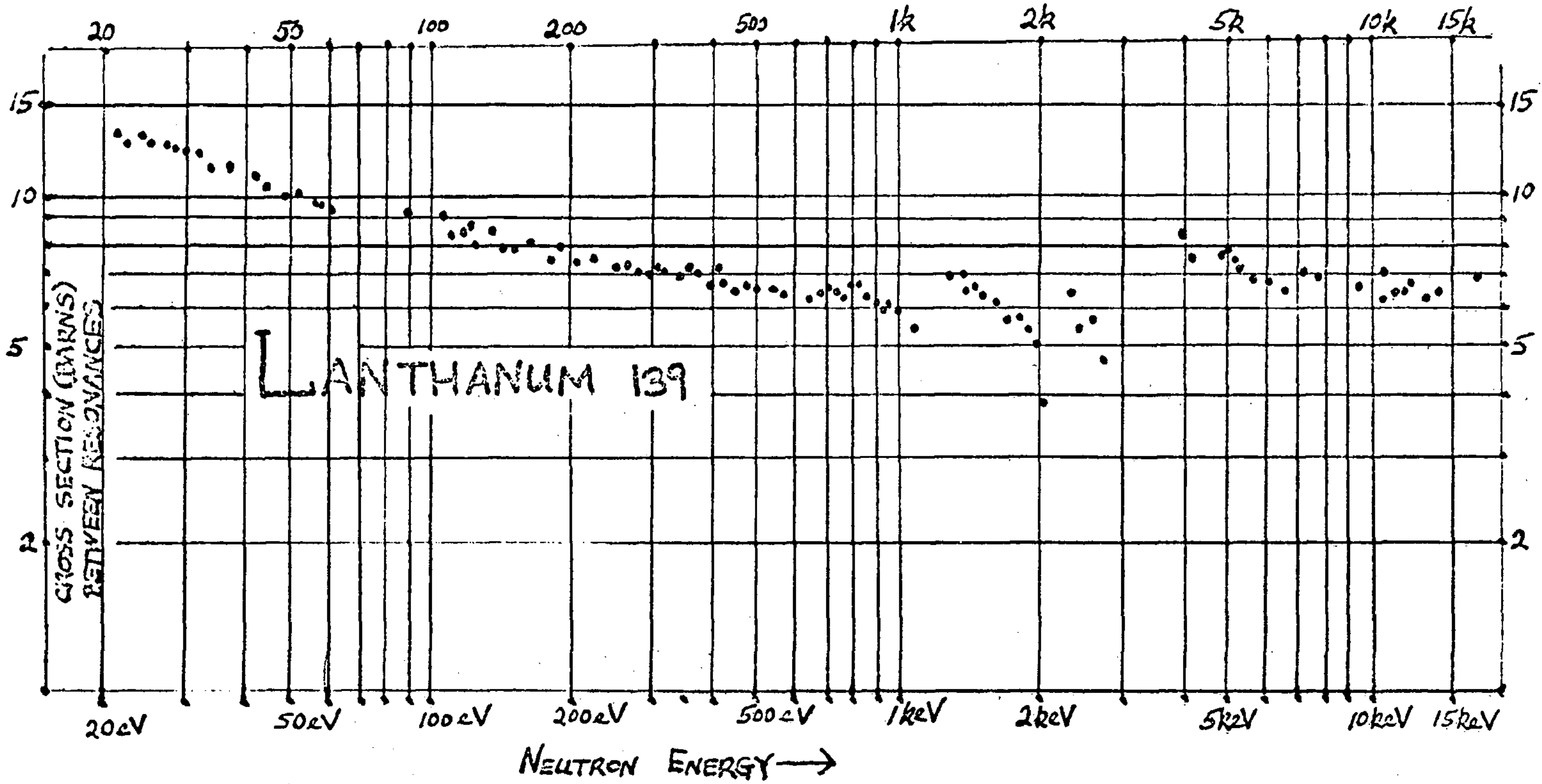

20
50
100
200
500
1k
2k
5k
10k
15k
15
10
5
2
CROSS SECTION (BARNS) BETWEEN RESONANCES
LANTHANUM 139
20eV
50eV
100eV
200eV
500eV
1keV
2keV
5keV
10keV
15keV
NEUTRON ENERGY ⟶

Fig. E3

TABLE E1

Extension of Results for ^{139}La (10 keV to 21 keV) (July 1972)

E_o	$g\Gamma_n^o$	$\Sigma g\Gamma_n^o$
10375	5.3	715.3
10580	4.0	719.3
10731	2.1	721.4
11170	14.2	735.6
11518	15	750.6
11908	1.8	752.4
11989	5.5	757.9
12134	11.8	769.7
12404	3.9	773.6
12673	10.6	784.2
13124	30.6	814.8
13280	6.6	821.4
13396	11.2	832.6
13492	7.1	839.7
14125	3.8	843.5
14217	17.2	860.7
14584	22.3	883.0
14890	24.6	907.6
15142	6.6	914.2
15206	35	949.2
16273	62.5	1011.7
17207	49.5	1061.2
17891	37	1098.2
18565	59	1157.2
18880	29	1186.2
19023	18	1204.2
20227	70	1274.2
20465	35	1309.2
21017	103	1412.2

S_o to 21 keV: $= 0.672 \times 10^{-4}$

TABLE F1

R - Matrix Parameters of Na

E_o (keV)	Γ (keV)	J	ℓ
2.850	0.388	1	0
53.15	1.23	2	1
198.8	3.6	1	0
212	15.5	0	1
(236.9)	4.4	1	1
(238.9)	3.3	1	0
298.1	∿168	2	0

peak cross section which is partly superimposed on the tail of the 198.8 level requires an assignment of J = 0, with ℓ = 1, the only allowed orbital value. The total width is $\Gamma \simeq$ 15.5 keV, and we choose ℓ=1 to be consistent with this large width.

238 keV levels The peak cross section of 8.3 barns is too small for a J = 2 or J = 3 assignment (even with resolution effects considered) and too large for a J = 1 spin state. The shape of the resonance suggests a doublet. A reasonable if not completely satisfying fit has been achieved with the following choice of level parameters:

E_o=236.9 keV, $\Gamma \simeq$ 4.4 keV, J=1, ℓ=o and E_o=238.9 keV, $\Gamma \simeq$3.3, J=1, and ℓ=0. Choosing one of the levels to have J=o gives a decidedly poorer fit to the observed data. Most likely the structure at 238 keV contains two levels with J=1 and different parity.

298.1 keV level This level is difficult to analyze because of resolution problems. The strong interference dip indicates a ℓ=0 level, while the observed σ_0 of 5.36 (which is lower that the true σ_0 because of resolution effects) indicates an assignment of J=2. The total width Γ is about 1.8 keV, in agreement with the results of Nebe and Kirouac for this level.

G. Neutron Resonance Parameters of W^{183} (H.Camarda, H. Liou, W. Makofske)

Natural tungsten samples, useful in the analysis of $W^{182, 184, 186}$ (previously reported), provided additional information on the resonances of W^{183}, after the even A resonances were subtracted.

A significant portion of the energy interval was unavailable for ^{183}W level analysis due to strong even A isotope levels.

The ^{183}W level analysis in certain cases gave a significantly superior fit using either J = 0, or J = 1 rather than the opposite choice. We favor J = 0 for the levels at 47.85, 154.4, 258.9*, 695.1 and 1313 eV, and J = 1 for the levels at 27.05, 46.24, 101.1*, 279.6, 321.8, 347.3, 646.6, 1241, and 1313 eV. The levels with asterisks above have the opposite J favored in the BNL 325 listings which extend to ∿ 420 eV, or by the RPI results to 760 eV.

The ^{183}W levels are those which are observed in the natural W sample, but are not identified as belonging to the even isotopes. Most

TABLE G1

^{183}W Resonance Parameters

E(eV)	$g\Gamma_n$(meV)	$g\Gamma_n^0$(meV)	Γ(meV)	J
7.63±.03	1.1±.3	.40±.11		
27.05±.03	31.±5.	6.0±1.		1
40.68±.03	1.3±.3	.20±.05		
46.24±.07	96.±15.	14.1±2.2		1
47.85±.04	26.5±3.	3.83±.43		0
65.34±.03	1.45±.2	.18±.03		
101.1±.1	65.±10.	6.5±1.		1
103.9±.1	1.9±.3	.19±.03		
138.0±.1	2.1±.4	.18±.03		
144.2±.1	24.±2.5	2.0±.2	131. 20.	
154.4±.1	108.±15.	8.69±1.21		0
157.0±.1	40.±8.	3.2±.6		
173.8±.2	39.±6.	3.0±.5		
192.1±.2	29.±5.	2.1±.36		
[a]203.2±.2	.8±.3	.056±.02		
[a]229.2±.3	.5±.3	.033±.02		
235.1±.2	4.1±.6	.27±.04		
240.3±.2	7.2±1.5	.46±.09		
258.9±.1	52.±7.	3.23±.44		0
279.6±.2	100.±10.	5.98±.6	210. 25.	1
[a]288.1±.3	.3±.2	.018±.012		
296.3±.2	17.±2.	.99±.11		
321.8±.2	57.±8.	3.18±.45		1
337.0±.2	3.9±.6	.21±.03		
347.3±.2	98.±.9	5.26±.48		1
[a]352.8±.2	.5±.3	.027±.016		
360.4±.2	24.±3.	1.26±.16		
377.6±.4	70.±30.	3.62±1.55		
390.9±.2	21.±4.	1.1±.2		
417.8±.3	25.±6.	1.2±.3		
425.4±.3	15.±5.	.73±.24		
430.7±.3	40.±15.	1.93±.72		
459.7±.3	8.5±1.5	.40±.07		
[a]468.3±.7	2.0±.5	.092±.023		
[a]492.7±.4	1.0±.5	.045±.022		

TABLE 61 (Cont.)

^{183}W Resonance Parameters

E(eV)	$g\Gamma_n$(meV)	$g\Gamma_n^0$(meV)	Γ(meV)	J
[a]495.1±.4	.8±.4	.036±.018		
[a]512.5±.4	1.2±.5	.053±.022		
534.6±.4	12.4±3.5	.54±.15		
550.7±.4	46.±8.	1.96±.34		
558.2±.4	50.±10.	2.12±.42		
567.7±.4	18.±5.	.76±.21		
571.1±.4	36.±7.	1.51±.29		
587.9±.4	20.±3.	.83±.12		
603.0±.4	48.±10.	1.96±.41		
608.3±.4	11.±4.	.45±.16		
646.6±.4	123.±15.	4.84±.59		1
675.9±.5	41.±8.	1.58±.31		
690.1±.5	22.±5.	.84±.19		
695.1±.5	150.±30.	5.69±1.14		0
700.6±.5	15.5±3.5	.59±.13		
752.0±.6	120.±20.	4.38±.73		
807.7±.6	20.±5.	.70±.18		
852.1±.3	10.±3.	.34±.1		
862.5±.3	40.±10.	1.36±.34		
867.3±.3	15.±8.	.51±.3		
869.4±.3	90.±40.	3.1±1.4		
894.0±.3	44.±8.	1.5±.3		
940.9±.4	40.±10.	1.3±.3		
1059.±1.	13.±5.	.40±.15		
1062.±1.	37.±10.	1.14±.31		
1114.±1.	21.±5.	.63±.15		
1141.±1.	340.±40.	10.1±1.2		
1151.±1.	27.±8.	.80±.24		
1176.±1.	27.±4.	.79±.12		
1241.±1.	265.±35.	7.52±.99		1
1313.±1.	115.±20.	3.17±.55		1
1370.±1.	130.±30.	3.51±.81		
1451.±1.	26.±5.	.68±.13		
1521.±1.	41.±8.	1.0±.2		
1567.±1.	30.±6.	.76±.15		

TABLE G1 (Cont.)

^{183}W Resonance Parameters

E(eV)	$g\Gamma_n$(meV)	$g\Gamma_n^0$(meV)	Γ(meV)	J
1626.±1.	83.±8.	2.1±.2		
1663.±1.	80.±30.	2.0±.7		
1685.±1.	23.±7.	.56±.17		
1710.±1.	200.±60.	4.84±1.45		0
1738.±1.	66.±15.	1.6±.4		
1754.±1.	47.±15.	1.1±.4		
1820.±1.	110.±25.	2.58±.59		
1836.±1.	220.±35.	5.13±.82		
1857.±1.	265.±30.	6.15±.70		
1866.±1.	150.±50.	3.47±1.16		
1870.±1.	170.±60.	3.93±1.39		
1955.±1.	84.±20.	1.9±.5		
1993.±1.	175.±35.	3.92±.78		
2144.±1.	200.±40.	4.32±.86		
2158.±1.	220.±40.	4.74±.86		
2167.±1.	230.±40.	4.94±.86		
2219.±1.	360.±70.	7.6±1.5		
2237.±1.	100.±50.	2.1±1.		
2260.±1.	59.±25.	1.24±.53		
2281.±1.	120.±30.	2.51±.63		
2316.±1.	330.±70.	6.86±1.45		
2444.±1.	650.±100.	13.1±2.0		
2640.±1.	220.±40.	4.28±.78		

have $g\Gamma_n$ values large enough to have been seen in the separated even isotope samples if they had belonged to the even isotopes. There are also some levels in the natural W which would not have been seen in the even A isotope samples even if they had been even A isotope levels. Those levels having "a" before the energy of this class which had been identified as ^{183}W levels by the RPI group[6] are believed by us to be ^{183}W levels. Many of the weaker levels reported by the RPI group for ^{183}W were not seen in our data and are not included in our list.

Some weak levels which were observed but not identified as belonging to any particular W isotope have not been included in the main tables These unidentified levels might be ^{180}W resonances. The following listing gives each resonance energy followed by the corresponding $ag\Gamma_n$ value (in meV) in parentheses: (74.85 ± 0.03) eV (0.041), (107.6 ± 0.1) eV (0.025 ± 0.01), (168.9 ± 0.1) eV (0.13 ± 0.11), (356.5 ± 0.2) eV (0.12 ± 0.06), (373.9 ± 0.2) eV (0.21 ± 0.10), (613.7 ± 0.4) eV (0.22 ± 0.10).

The resonance parameters for the levels identified as W^{183} levels are given in table G-1. Our tungsten results are presently being prepared for publication in the Physical Review.

H. Capture Resonance Parameters of Thulium-169 (J. Arbo, J. Felvinci, E. Melkonian, F. Rahn, C. Ho, and W.W. Havens, Jr.)

The values of capture resonance areas, $\sigma_0\Gamma\gamma$, and total widths, Γ, for thulium-169 will be reported at the American Nuclear Society meeting in November, 1972. The thulium capture cross sections were measured relative to the capture cross section of gold-197. Our measurements, with a best resolution of 0.6 nanoseconds/meter, used an array of 8 Moxon-Rae type detectors[1] and a 34 meter helium flight path. The detectors were built following the design of S. F. Eccles, et al.[2] A one-half inch thick slab of epoxy-bonded lithium orthosilicate (Li_4SiO_4) covered the face of the upper and lower detector boxes, serving as both the first-stage photon-electron converter and as a shield against neutrons scattered from the sample. The volume between detector units in the detector boxes was filled with lithium orthosilicate powder to provide further neutron shielding. Calibration of the relative gamma detection efficiency per MeV for the detector array was carried out using radioisotopic and capture gamma sources. The intrinsic detection efficiency was found to be about 1.5%/MeV and was essentially constant from 0.3 MeV to 8 MeV. This efficiency calibration, discussed in NCSAC-33, is shown in Figure H-1.

Thulium samples were 3 x 8 inch rolled metal sheet, cast from a tungsten crucible. The effective thicknesses of the samples were 400, 1500, and 6000 barns/atom. Rare earth impurities were less than 0.09%. The 4 gold samples used were also rolled metal sheet, 99.99+% pure, with effective thicknesses of 83, 320, 2100, and 6700 barns/atom.

Pulses from each of the 8 Moxon-Rae detectors were combined in a linear adder having individually adjustable input gains, and passed to a 262,000 channel, 20 nanosecond/channel time-of-flight buffer.[3] From the buffer, data was periodically dumped to a PDP-8 computer which formed a time-collapsed 14,000 channel histogram on a fixed-head magnetic disk. The histogram contents were displayable for monitoring during data accumulation, and were transferred to magnetic tape at the end of each sample run.

The data on tape were analyzed on a SEL 810-B computer. A total of 255 resonances were identified in the neutron energy range up to 3000 eV. In the energy range reported by Julien[4] three new resonances were identified at 185.3, 254.8, and 509.0 eV, while doublets were resolved for the resonances reported at 213., 584.8, and 671.8 eV. Figure H2 shows the distribution of observed resonances up to 3000 eV. The value of the observed level spacing, based on a least squares fit to the first 40 levels (up to 300 eV.) was found to be $< D > = 7.7 \pm 0.5$ eV, which is larger than the value of 6.0 ± 1.5 eV reported by Singh.[5] A list of observed resonance energies is given in Table H1. The energies are preliminary and should be considered to include an error of ±0.5%. Table H2 reports measured values of $\sigma_o\Gamma_\gamma$ for resonances from 83.4 to 400.2 eV. These measured values are preliminary. The relative internal accuracy, resonance to resonance, is about 10% for the larger resonances to 40% for resonances with $\sigma_o\Gamma_\gamma$ smaller than 10 barns-eV. The absolute

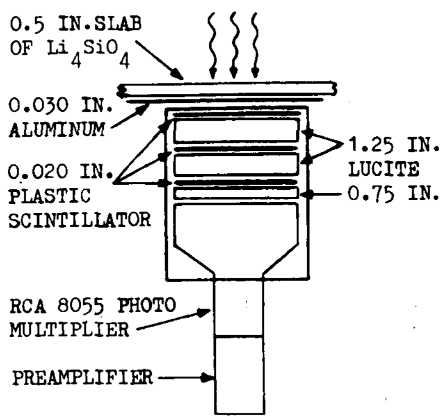

INDIVIDUAL MOXON-RAE DETECTOR

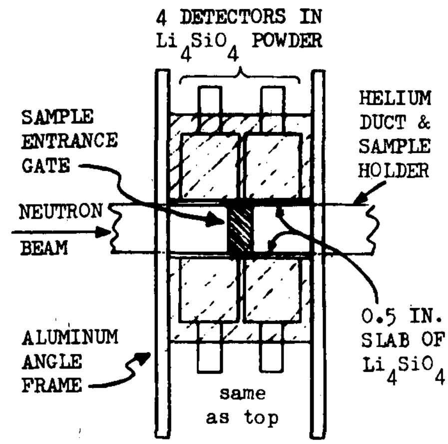

SIDE VIEW OF DETECTOR ARRAY

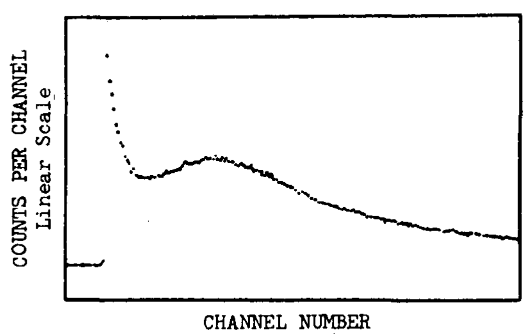

PULSE HEIGHT SPECTRUM FROM MOXON-RAE DETECTOR WITH Co^{60} SOURCE

RELATIVE EFFICIENCY PER MEV OF MOXON-RAE DETECTOR AS A FUNCTION OF GAMMA ENERGY

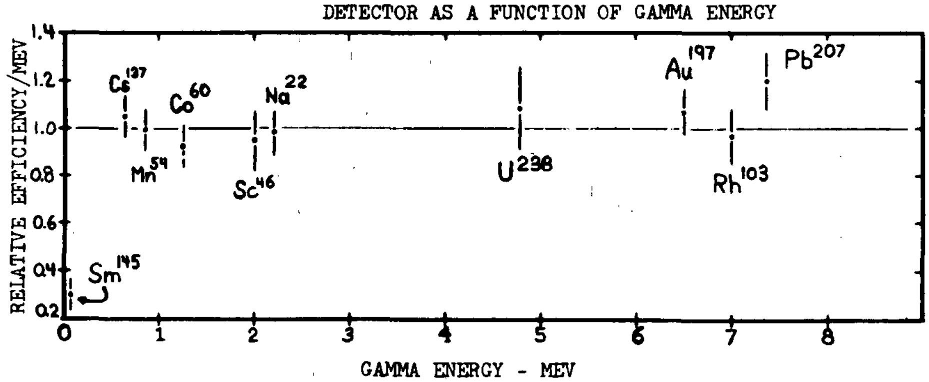

Figure H1. Moxon-Rae Detectors: Detail and Calibration.

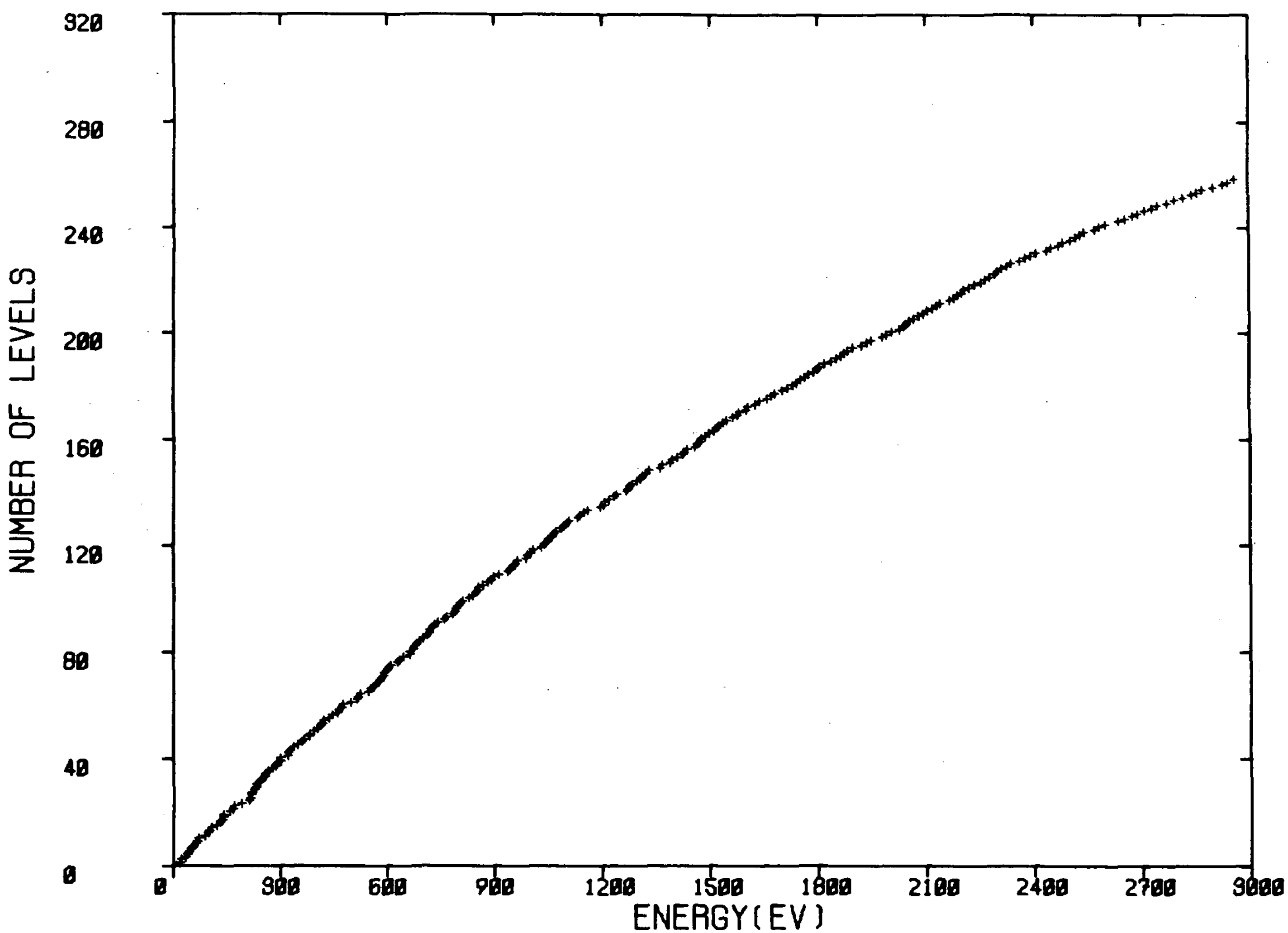

Figure H2. Distribution of Observed Neutron Resonances of Thulium-169.

Table H1. Observed Resonance Energies of Thulium-169. (Ev)

3.92	416.2	888.3	1465.6	2136.
14.4		895.2	1471.1	2162.
17.46	440.8	909.5	1482.2	2175.
28.75	455.5	932.1	1493.5	2185.
34.86	459.7	939.	1504.8	2195.
37.61	467.7	947.2	1514.4	2201.
44.86	471.6	953.8	1522.1	2218.
50.68	492.6	960.6	1531.8	2232.
59.23	509.0	984.3	1541.6	2249.
63.2	512.2	988.4	1559.5	2263.
65.8	519.1	996.6	1571.6	2274.
83.4	542.7	1005.8	1577.8	2288.
93.9	549.4	1024.8	1596.3	2295.
95.6	556.5	1035.6	1602.6	2306.
101.8	565.0	1042.1	1621.6	2321.
115.5	573.1	1047.6	1634.4	2335.
125.1	578.2	1055.4	1656.2	2357.
132.2	584.6	1062.1	1667.2	2372.
135.9	586.0	1066.7	1678.3	2388.
153.5	592.1	1082.7	1698.7	2403.
160.6	599.0	1088.6	1712.5	2434.
164.3	607.1	1098.0	1727.7	2446.
185.3	624.7	1105.1	1738.2	2465.
207.6	631.0	1127.0	1750.0	2477.
209.6	642.5	1134.4	1762.0	2500.
211.9	658.5	1147.0	1769.3	2514.
213.9	669.3	1155.9	1783.9	2526.
224.2	673.2	1191.3	1793.8	2539.
228.1	677.3	1199.4	1801.2	2568.
238.4	686.2	1202.1	1816.3	2581.
243.6	694.9	1215.8	1831.5	2598.
251.0	707.2	1231.1	1846.9	2633.
254.8	713.1	1235.4	1859.9	2652.
260.2	714.4	1262.7	1867.8	2673.
273.8	723.	1267.1	1878.4	2687.
283.4	730.	1273.0	1894.4	2705.
288.6	737.	1278.9	1916.1	2728.
296.0	757.3	1292.5	1932.6	2742.
297.0	762.7	1303.1	1943.7	2770.
318.5	779.5	1309.3	1974.8	2789.
319.3	786.	1315.5	1986.3	2814.
324.7	787.7	1324.9	2000.8	2838.
333.1	793.	1355.3	2021.4	2853.
346.3	801.5	1363.4	2033.3	2868.
357.5	807.0	1383.3	2039.3	2899.
364.0	825.	1390.1	2048.3	2924.
376.8	833.	1405.4	2060.4	2939.
378.6	842.	1419.2	2076.	2957.
390.5	848.3	1421.0	2088.	
400.2	850.7	1431.5	2101.	
408.3	864.7	1452.9	2116.	
414.4	878.0	1458.4	2126.	

Table H2. Capture Resonance Areas of Thulium-169...

Energy (ev)	$\sigma_o\Gamma_\gamma$ (barns-ev)	Energy (ev)	$\sigma_o\Gamma_\gamma$ (barns-ev)
83.4	151.	243.6	46.
93.0	20.	251.0	453.
93.9	497.	254.8	2.
95.6	25.	260.2	73.
101.8	7.	273.8	103.
115.5	236.	283.4	224.
121.1	113.	288.6	168.
132.2	10.	296.0	30.
135.9	252.	297.0	75.
153.5	221.	318.5	310.
160.8	17.8	319.5	
164.3	63.	324.7	45.
185.3	0.9	333.1	180.
207.6	130.	346.3	89.
209.6	32.	357.5	71.
211.9	9.	364.0	9.
213.9	224.	376.8	47.
224.2	51.	378.6	52.
228.1	31.	390.5	150.
238.4	114.	400.2	18.

error is larger because the normalization of these data to the Au-197 standard is not complete. Our measurements support the assignment of J = 1 to the 153.5 and 283.4 eV. resonances, and indicate J = 0 for the 125.1 eV resonance. The total width for the 153.5 eV resonance is estimated as 300 ± 50 meV, compared to 166 ± 7 meV as given in BNL-325.

References

1. M.C. Moxon, Nucl. Instr. Methods, 24, 445, (1963)

2. S.F. Eccles, et al, UCRL-50126, (1966)

3. Pegram Nuclear Phys. Labs., NYO-73-243, UC-34 Physics, 171, (1969)

4. J. Julien, et al, BNL-325, 2nd Ed., 69-0-1, (1966)

5. The Theory of Neutron Resonance Reactions, Clarendon Press, Oxford, 115, (1966)

I. Possible Background in Nevis Time-of-Flight Measurements Arising From Delayed Neutrons From Induced Fission in the Lead Target
(E. Melkonian and J. Felvinci)

At Nevis, neutrons have been obtained by evaporation from highly excited nuclei produced by high energy protons striking a lead target. A small fraction of fissioning nuclides are also produced in this process, giving rise to some delayed neutrons. A very crude estimate indicates that about 0.1% of all neutrons is delayed. However, the effectiveness of the delayed neutrons is increased by an order of magnitude because they have energies about 1/10 of the energies of the boil-off neutrons. This increased effectiveness results from two causes: a) the hydrogen cross section of the water moderator drops rapidly with increasing neutron energy and therefore the moderator is more transparent to the higher energy neutrons, and traps less of them, and b) in slowing down from the higher energies, a larger fraction of the neutrons which enter the moderator is lost through leakage. Furthermore, the effect is considerably magnified at these neutron energies, where the fission cross section to be measured is low, since the delayed neutrons would average the larger cross sections over all energies. In the case of transmission measurements, this implies that the background at any one energy is a function of sample thickness and cannot be treated as a constant.

We plan to install a tungsten target for the next run to reduce the contribution of delayed neutrons.

GULF RADIATION TECHNOLOGY
A Division of Gulf Energy and Environmental Systems
San Diego, California

A. NEUTRON CROSS SECTIONS

1. Measurements of the $^{10}B(n,\alpha)$ Cross Sections for Neutron Energies From 1 to 1000 keV (S. J. Friesenhahn, A. D. Carlson, V. J. Orphan and M. P. Fricke)

The $^{10}B(n,\alpha)$ and $^{10}B(n,\alpha_1\gamma)$ cross sections have been measured[1] relative to the H(n, n) cross section from $\sim$1-1000 keV. These measurements were made with a Linac pulsed neutron source and time-of-flight techniques using a 230-meter flight path. The $^{10}B(n,\alpha)$ data were obtained with BF_3 gas proportional counters and also with a large ion chamber constructed with thin ^{10}B-loaded self-supporting films. The $^{10}B(n,\alpha_1\gamma)$ data were obtained with a Ge(Li) detector. The incident neutron flux spectrum was measured with a hydrogen gas proportional counter from $\sim$ 1-50 keV and with a methane gas proportional counter from 13-1000 keV. Presently, the measurements have been analyzed for neutron energies from 4 to 750 keV for the $^{10}B(n,\alpha)$ reaction and from 4 to 1000 keV for the $^{10}B(n,\alpha_1\gamma)$ reaction. Analysis is continuing, and it is expected that final results for both of these cross sections will be obtained from $\sim$1 - 1000 keV with an overall uncertainty varying from $\sim$ 1% at 1 keV to $\sim$3% at 1000 keV.

The incident neutron flux measurements obtained in the present work are of much higher accuracy than those used in earlier determinations of the $^{10}B(n,\alpha)$ cross sections. The total systematic uncertainty is $\sim$ 1% from 10 keV to 1 MeV. It is anticipated that the data will be improved below 10 keV, and extended below 4 keV, when recently completed neutron spectrum measurements are analyzed.

The present cross sections determined from the flux data and the ionization-chamber, BF_3 and Ge(Li) data have been normalized in the interval from 10-20 keV to the $^{10}B(n,\alpha)$ and $^{10}B(n,\alpha_1\gamma)$ cross sections obtained from ENDF/B Version III and the branching ratio of

---

[1] S. J. Friesenhahn et al., "Measurements of the $^{10}B(n,\alpha_1\gamma)$ and $^{10}B(n,\alpha)$ Cross Sections," Gulf Radiation Technology Report Gulf-RT-A12210 (Oct., 1972).

Irving.[2] With further improvements in the quality of the flux data below 10 keV, these normalizations can be performed at lower energies where the cross section is even closer to 1/v.

The $^{10}B(n,\alpha_1\gamma)$ measurements obtained with the Ge(Li) spectrometer yield a significant improvement in the precision of this cross section. This is largely a result of the excellent signal-to-background ratio provided by the high-resolution Ge(Li) detector combined with the high-efficiency ring-geometry configuration. These advantages also minimize the statistical uncertainties. Although they are small, the backgrounds, such as those due to scattered neutrons, have been carefully assessed.

The present $^{10}B(n,\alpha_1\gamma)$ measurements are shown in Fig. A-1 together with previous data. The error bars shown on the present measurements are a result of a detailed error analysis combining both systematic and statistical uncertainties. The present results introduce direct measurements below 100 keV and high-accuracy data in the 100- to 1000-keV energy range. The present data are seen to disagree significantly with the earlier measurements shown in Fig. A-1; however, they are in very good agreement with preliminary measurements of Coates[3] which extend up to ~250-keV neutron energy. A comparison of the present data with those of Coates is shown in Fig. A-2, and the agreement between 10 and 250 keV is seen to be within ~ 1-2%.

The cross sections determined from the ion chamber and the BF_3 detectors are shown in Fig. A-3. The $^{10}B(n,\alpha)$ cross section presently adopted is a composite of the BF_3 data below 60 keV (which have superior counting statistics) and the ion-chamber data at higher energies. A comparison is shown in Fig. A-3 between the BF_3 results and the ion-chamber data for the structure near 450-keV neutron energy. The time-response function of the BF_3 data was folded into the ion-chamber data so a more meaningful comparison could be made between the two sets of measurements. The agreement between the two data sets is excellent, thus confirming that the structure observed in the higher-resolution ion-chamber data is consistent with that seen in the BF_3 results. Also shown in Fig. A-3 are absolute BF_3 cross-section results, which were

---

[2] D. C. Irving, "Evaluation of Neutron Cross Sections for Boron 10," ORNL-TM-1872 (1967).

[3] M. Coates, private communication (1971).

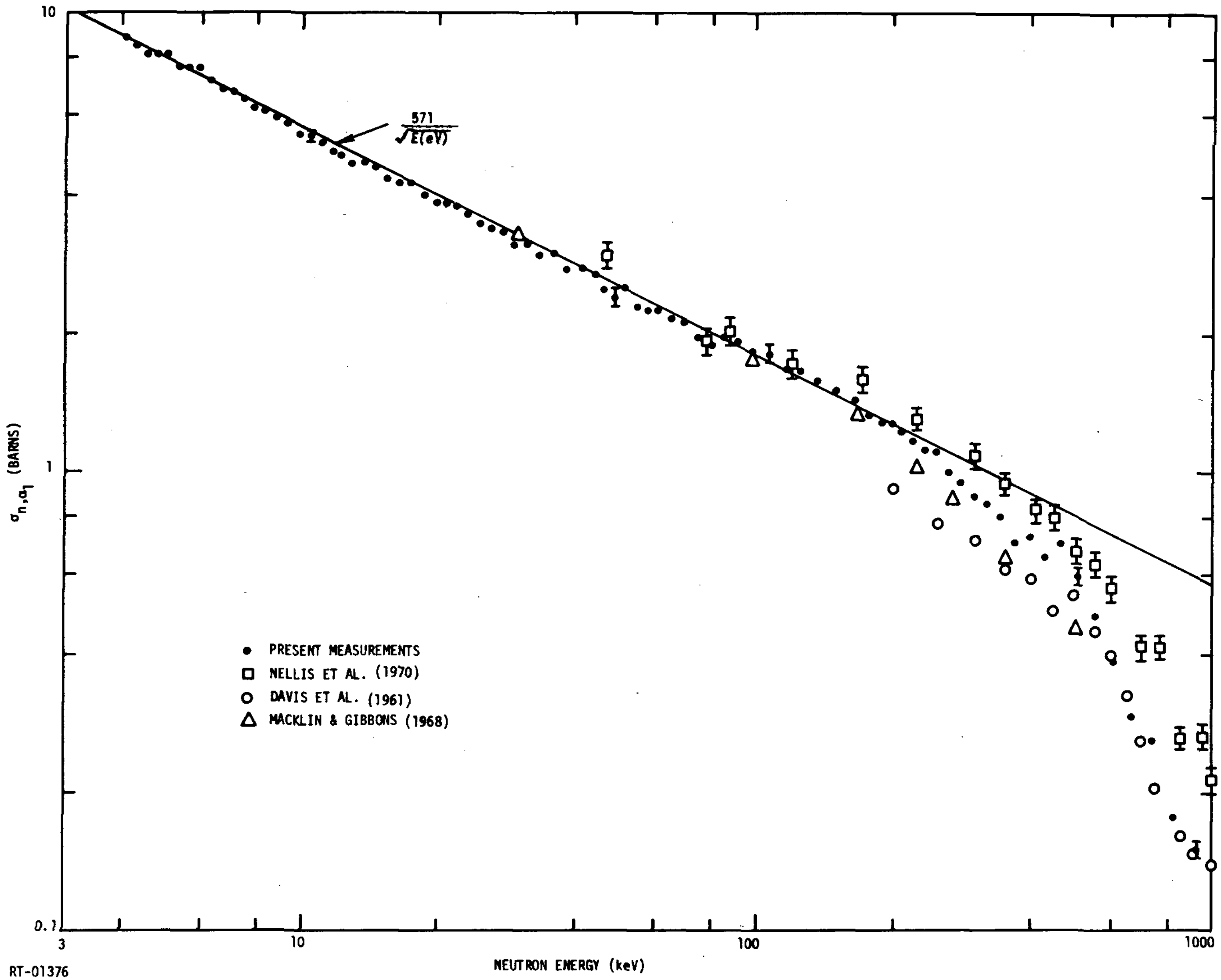

Fig. A-1. $^{10}B(n,\alpha_1\gamma)$ cross sections. The present measurements are normalized between 10 and 20 keV using ENDF/B, Version III, values and the branching ratio as evaluated by Irving.[2]

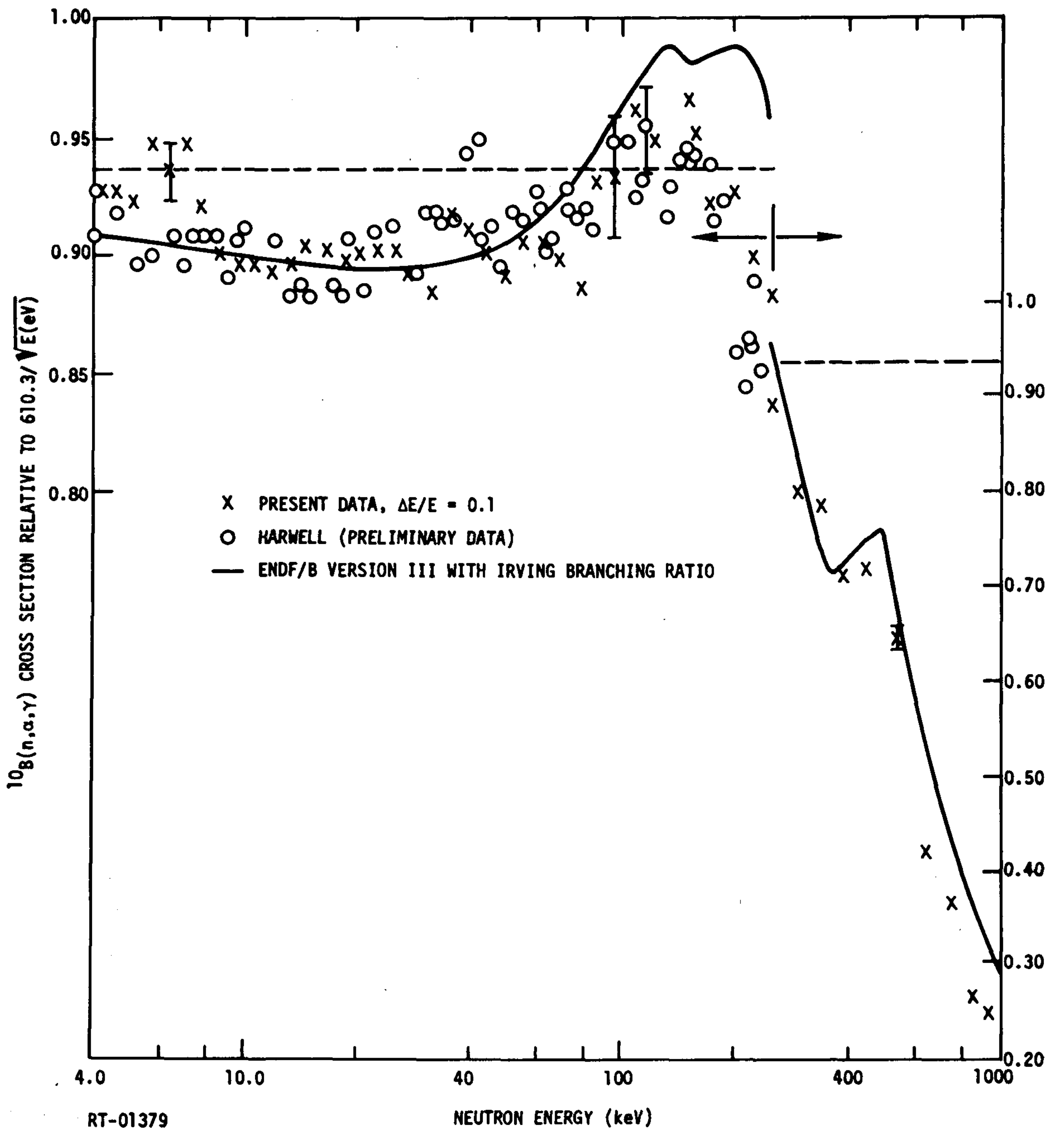

Fig. A-2. Comparison of the present $^{10}B(n,\alpha_1\gamma)^7Li$ cross section with preliminary Harwell data and the ENDF/B Version III evaluation using the branching ratio as evaluated by Irving.

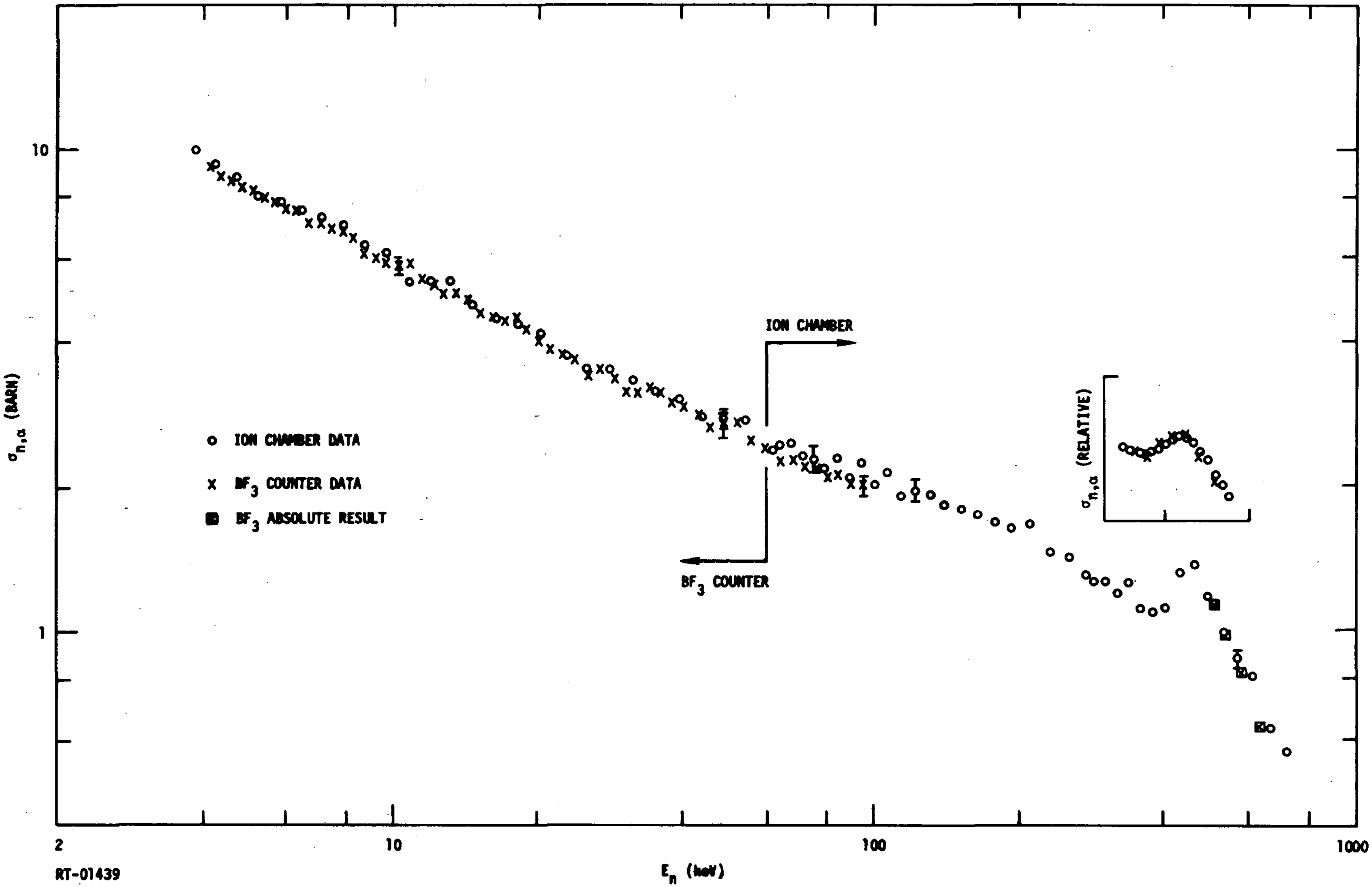

Fig. A-3. BF_3 plus ion-chamber data. The absolute results above 500 keV are described in the text. The insert illustrates the result of broadening the ion-chamber cross section data with the BF_3 time resolution function. The broadened results are compared with the BF_3 data in the region near 450-keV neutron energy.

obtained from a mass spectrographic analysis of the BF_3 + CH_4 gas together with a direct comparison of the proton and alpha-particle pulse-height distributions from the proportional counter. Agreement of this determination with the ion-chamber measurements above 500 keV is excellent.

The composite $^{10}B(n,\alpha)$ cross section is shown in Fig. A-4, along with earlier measurements and the ENDF/B Version III data. Again, the error bars shown for the present results are the total uncertainties. The present $^{10}B(n,\alpha)$ data which are now considered completely final are those below 100 keV, where, in general, they agree well with earlier results and provide an improvement in the uncertainties in this energy region.

The present $^{10}B(n,\alpha)$ cross-section results above 100 keV, which were obtained with the ion chamber, are substantially higher than the ENDF/B-III data. Our data are in best agreement with the direct measurements of Bogart and Nichols.[4] Also, structure in the cross section near 450 keV, which is not well resolved in previous measurements, is clearly defined in the ion-chamber data. This structure is qualitatively similar to that predicted in the (n,α_0) channel by Lane et al.[5] from an R-matrix analysis of elastic scattering, polarization and other reactions proceeding through the compound nucleus ^{11}B.

The ratio of the cross sections $\sigma(n,\alpha_1\gamma)/\sigma(n,\alpha)$ found in the present work is compared in Fig. A-5 to that determined from the branching ratio measurements of Macklin and Gibbons[6] and Sowerby[7] and the evaluation of Irving.[2] The present cross-section ratio is substantially lower than the previous results at energies above 100 keV. In their paper, Macklin and Gibbons state: "The $^{10}B(n,\alpha_0)/^{10}B(n,\alpha_1\gamma)$ ratio measurements in the 100- to 300-keV range are the most difficult part of the present approach. Neutron source strength is low; thermalized neutron effects are important and difficult to measure." We note

---

4 Donald Bogart and Lowell L. Nichols, Nucl. Phys. A125 (1969) 463.

5 R. O. Lane et al., Phys. Rev. C4 (1971) 380.

6 R. L. Macklin and J. H. Gibbons, Phys. Rev. 165 (1968) 1147-1153.

7 M. G. Sowerby, J. Nucl. Energy A/B 20, 135 (1966).

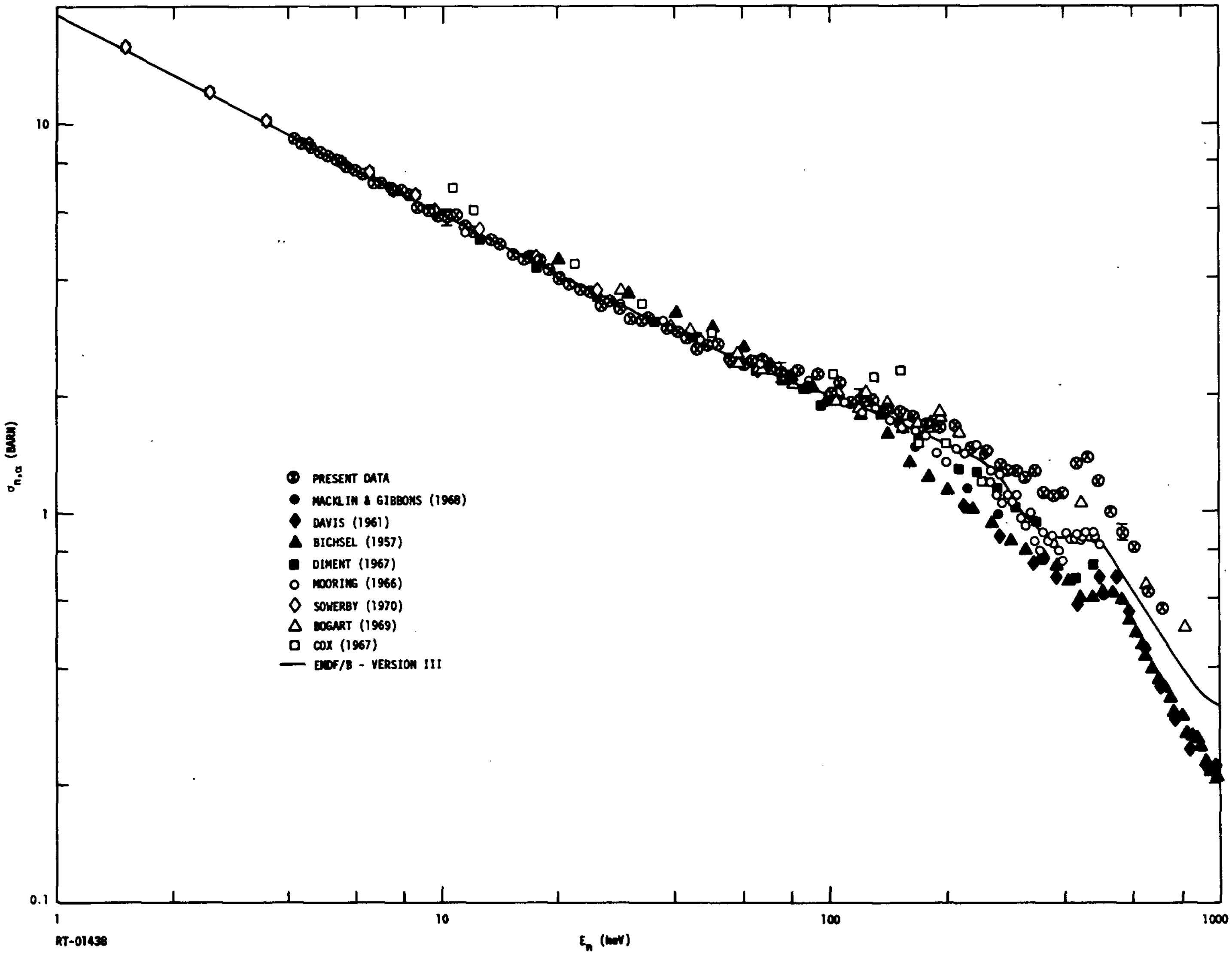

Fig. A-4. Comparison of the present measurement of the $^{10}B(n,\alpha)$ cross section with previous measurements.

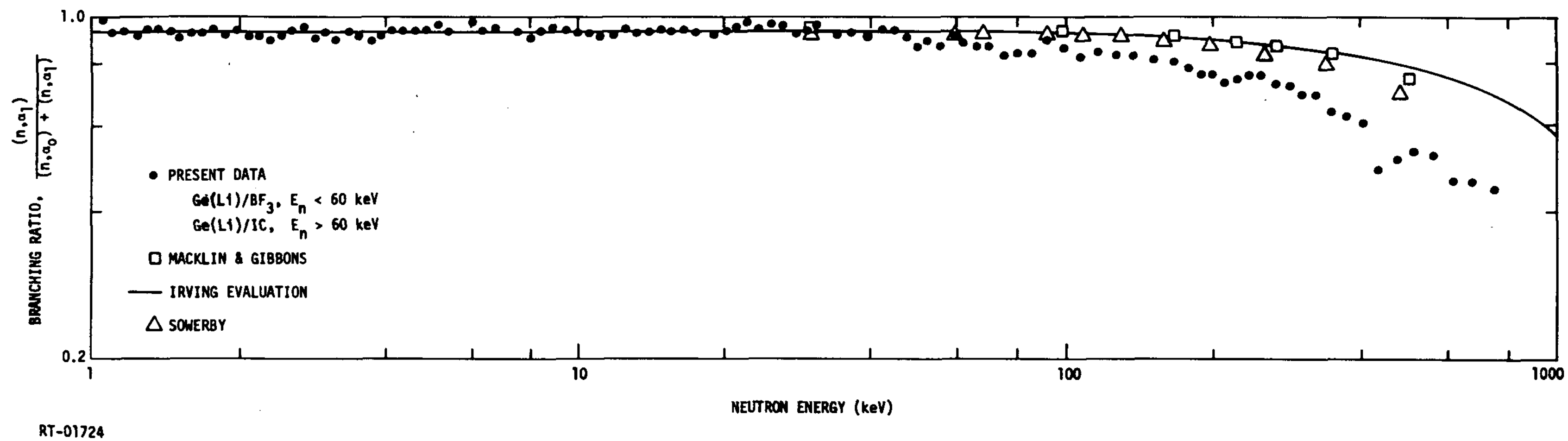

Fig. A-5. Branching ratio calculated from present data compared to other determinations.

that, due to the large difference in the $^{10}B(n,\alpha)$ cross section between thermal and a few-hundred-keV neutron energy, a thermal neutron contamination of only $\sim$0.1% in the data of Macklin and Gibbons would be sufficient to account for their discrepancies with the present results [a thermal contamination increases the ratio $\sigma(n,\alpha_1\gamma)/\sigma(n,\alpha)$]. While Sowerby believes that any serious thermal contamination in his experiment could be detected via kinematics, he feels his proportional counter data above 100 keV may not be reliable due to wall effects that have not been treated in detail.[8] Corrections for this should tend to reduce the discrepancies between Sowerby's data and the present results, although one cannot presently say to what extent.

As work progresses in the continuing standard cross-section program at this laboratory, it is expected that the present $^{10}B(n,\alpha)$ results above 100 keV will rapidly be finalized and thereby establish this cross section to an overall uncertainty of $\sim$3% up to 750 keV. In this continuing program, ion-chamber measurements of the $^6Li(n,\alpha)T$ reaction will be made, and a number of measurements are planned for this work which should also help to reduce some of the systematic uncertainties in the present $^{10}B(n,\alpha)$ data. (This work pertinent to request numbers 28 and 29 in NCSAC-35.)

2. Gamma-Ray Production Cross Sections for Carbon and Nitrogen (C. G. Hoot, V. J. Orphan, G. D. Trimble and V. V. Verbinski)

Preparations are in progress for the measurement of gamma-ray production cross sections for $(n,x\gamma)$ reactions on nitrogen and carbon from the threshold for inelastic scattering to $\sim$20 MeV. A linac pulsed neutron source and a 14% efficient (relative to NaI at 1.33 MeV) Ge(Li) gamma-ray detector will be used. The corresponding neutron energy will be determined by the time-of-flight technique. The experimental apparatus and computerized two-parameter data acquisition system have been described previously.[9] Analysis of the spectral data by unfolding will give a measure of the "continuum" gamma-ray contribution to the total gamma-ray production cross section in addition to the

[8] M. G. Sowerby, private communication (1972).

[9] V. J. Orphan et al., Nucl. Inst. and Methods 73 (1969) 1.

line data obtained previously for nitrogen.[10] Plans are being formulated for a careful study of the background associated with neutrons scattered from the sample into the Ge(Li) detector in order to minimize its contribution to the uncertainty in the measured (n, xγ) cross sections. It is expected that the relatively simple (n, xγ) spectra from carbon will provide a sensitive test of the procedures for unfolding and for subtracting scattered-neutron backgrounds. (This work pertinent to request numbers 35 and 42 in NCSAC-35.)

B. INTEGRAL TESTS OF CROSS SECTION DATA

1. Integral Experiments to Test Gamma-Ray Production and Neutron Scattering Cross Sections of Carbon and Nitrogen

(L. Harris, J. C. Young and G. D. Trimble)

The white-source, pulsed-neutron, time-of-flight integral experiment method reported in 1969 by Harris and Kendrick[1,2] has been used for a new type of integral experiment. This experiment was designed to provide high-sensitivity tests for gamma-ray production and neutron scattering cross sections in the MeV energy range. Measurements for carbon and nitrogen were completed recently, and measurements for oxygen and iron will be performed next.

The experimental geometry is shown in Fig. B-1. A new high-power Ta/Aℓ/Be Linac target was used to produce intense 50-nsec (FWHM) photoneutron pulses. Small samples, a graphite sphere and a liquid nitrogen sphere, both with diameters on the order of a neutron mean-free-path, were located at the end of a 50-meter neutron flight path. The liquid nitrogen was held in a 15-cm-ID and 20-cm-OD spherical styrofoam container with an overhead reservoir. A single 5 by 5-cm cylindrical NE-213 detector, positioned at 30, 55, 90 and 125° relative

---

[10] V. J. Orphan et al., "Measurement of Gamma-Ray Production Cross Sections for Nitrogen and Oxygen," Report GA-8006 (January 31, 1969).

[1] L. Harris, Jr. and H. Kendrick, "Fast-Neutron and Secondary Gamma-Ray Transport in Concrete," Trans. Am. Nucl. Soc., 12, 959 (1969).

[2] L. Harris, Jr. et al., "Time-Dependent Fast Neutron and Secondary Gamma-Ray Spectrum Measurements in Concrete," DASA 2401-1 and DASA 2401-2, Gulf General Atomic, Inc. (1969).

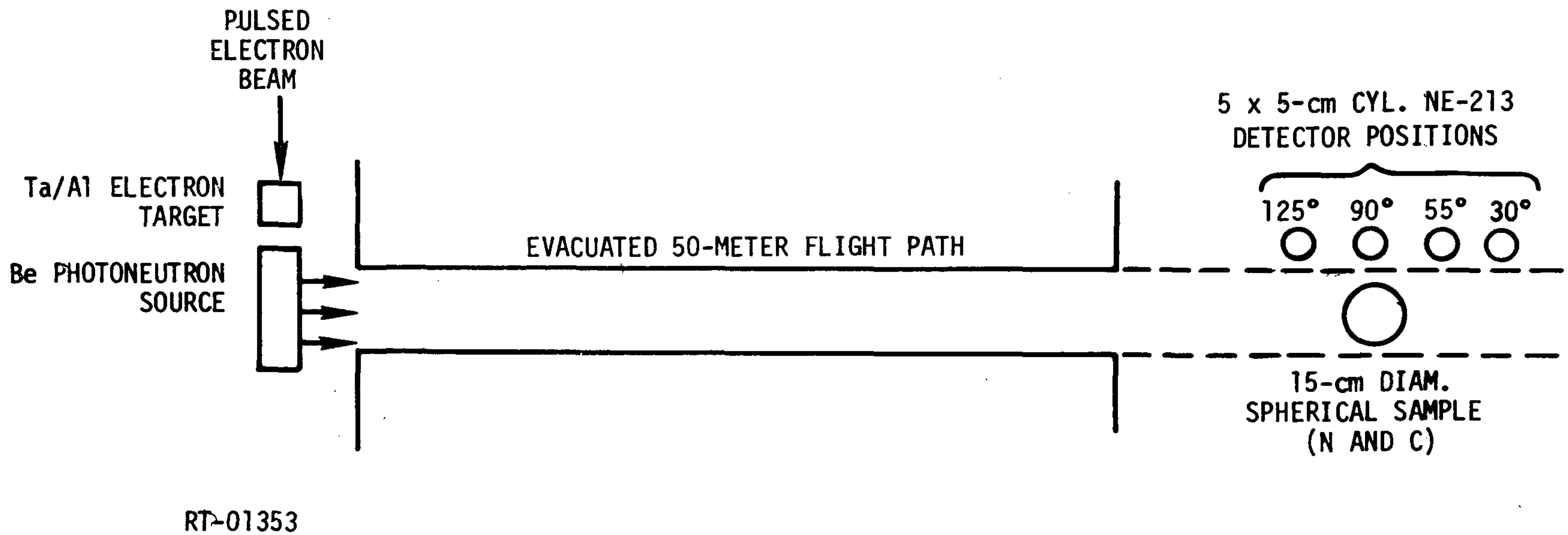

Fig. B-1. Experimental geometry for integral experiment to test gamma ray production and neutron scattering cross sections.

to the incident neutron beam, was used to detect secondary gamma rays and scattered neutrons as a function of time, and hence incident neutron energy. Pulse-shape discrimination was used to separate neutron and gamma-ray counts.

Supplementary measurements include (1) measurement of the energy spectrum of source neutrons incident on the spherical samples, (2) background measurements made with no sample present, and (3) measurements made with an empty styrofoam container in position.

Three-parameter data acquisition and analysis[2,3] were used for these measurements. The first part of the data reduction included (1) correcting for dead time and pulse pileup rejection, (2) separating neutron and gamma-ray counts, (3) normalizing count rates to source monitors, (4) calculating standard deviations due to counting statistics, (5) subtracting time-dependent backgrounds measured with no sample present, (6) transforming from time-of-flight to incident neutron energy, and (7) dividing the resulting energy-dependent count rate (counts/MeV-source monitor) by the source spectrum (neutron/MeV-cm^2-source monitor) to obtain the ratio of count per incident neutron/cm^2. Results obtained for carbon and nitrogen at the forward 30° detector position are shown in Figs. B-2 and B-3 respectively. Additional data reduction involving the unfolding of pulse-height spectra measured in 8 to 12 time bins is in progress. This analysis will give the energy spectra of secondary gamma rays and scattered neutrons as a function of incident neutron energy.

Calculations of these measurements are in progress at several laboratories. Comparison of calculated gamma-ray and neutron count rates with those reported here will provide a direct and sensitive test of the accuracy of the total gamma-ray production and total neutron scattering cross sections at four key angles. Differences between measured and calculated results should be readily interpreted in terms of specific cross-section deficiencies at well-defined incident neutron energies in the 1.5- to 20-MeV energy range.

---

[3] H. Kendrick and L. Harris, Jr., "Numerical and Experimental Studies of Spectral Unfolding - Volume I," DASA 2720-1, Gulf Radiation Technology (1971).

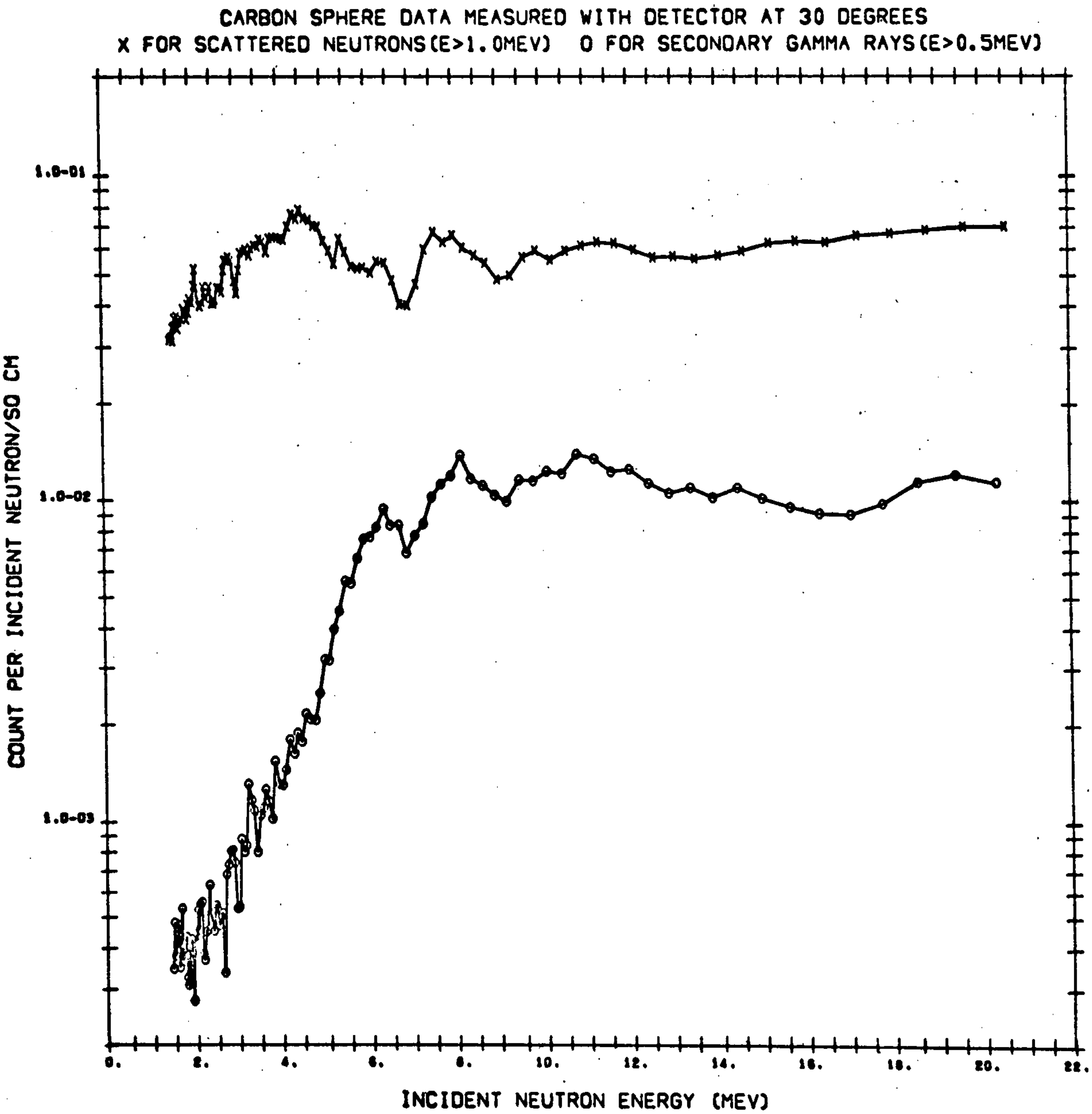

Fig. B-2. Carbon sphere data measured with detector at 90 degrees.

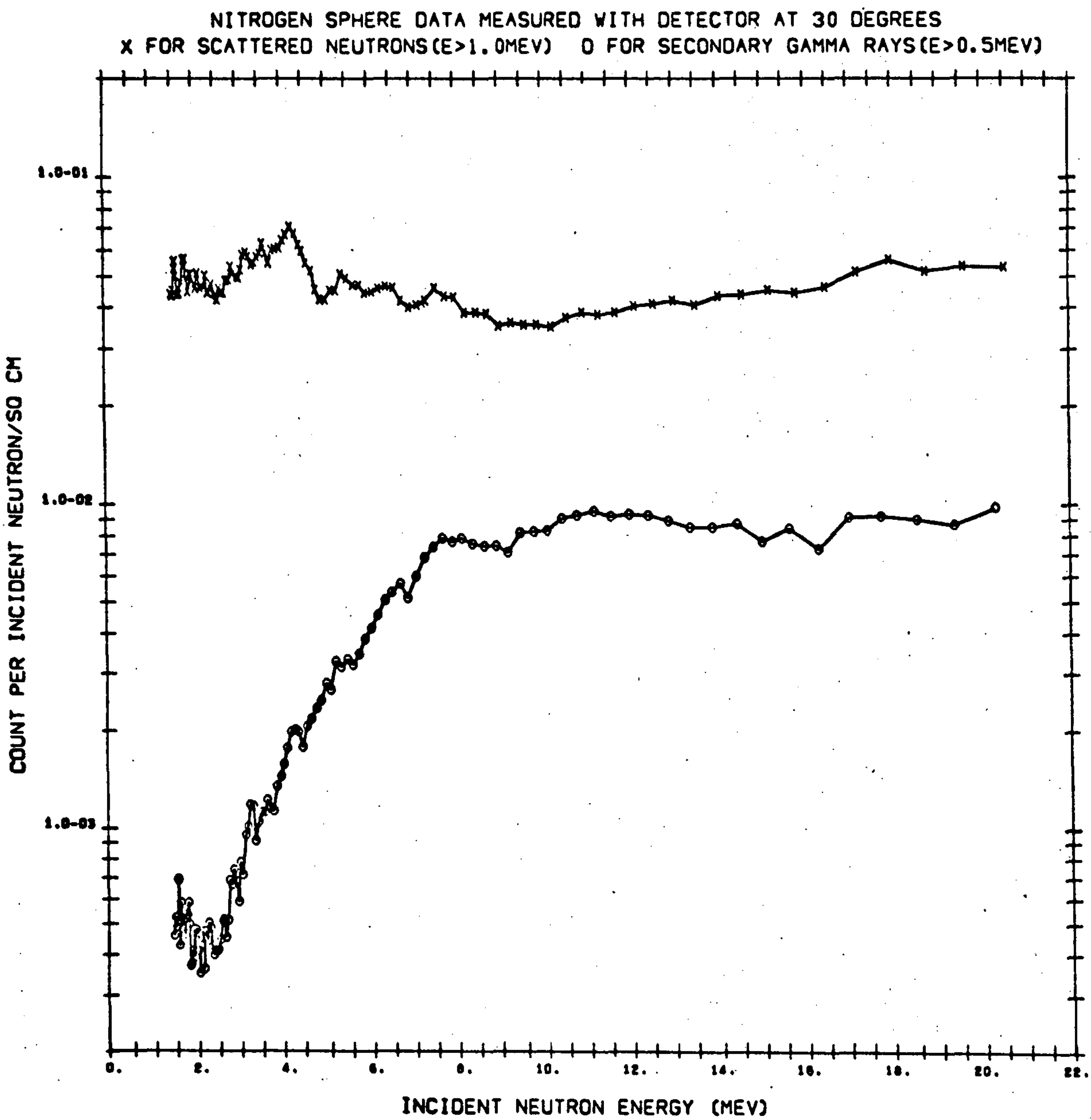

Fig. B-3. Nitrogen sphere data measured with detector at 30 degrees.

2. The (n, γn') Reaction in Fast-Spectrum Assemblies
(M. P. Fricke and J. M. Neill)

A short paper with the following abstract has been submitted for publication in Nuclear Science and Engineering.

The neutron spectrum and criticality of ZPR-3 Assembly 11 have been calculated using estimated cross sections for the $^{238}U(n, \gamma n')$ reaction. Inclusion of this reaction markedly improves agreement between the measured and calculated spectra and also produces a change in criticality. These and other ramifications of the (n, γn') reaction in fast-reactor assemblies are discussed.

C. CROSS SECTION EVALUATIONS

1. Evaluations of Magnesium and Copper Cross Sections
(M. K. Drake and M. P. Fricke)

The neutron and gamma-ray production cross sections for magnesium and copper are being evaluated. The recommended nuclear data for these elements will be sent to RSIC for incorporation into the DNA library, and they will also be submitted to the NNCSC to be considered for the ENDF/B-IV library. This evaluation task is expected to be completed by the end of 1972.

The evaluation of the angular distributions for elastic neutron scattering was done by utilizing interactive computer graphics techniques developed at Gulf Rad Tech. These techniques involved the use of a UNIVAC 1557/1558 Advanced Graphics Display System connected on-line to a UNIVAC 1108 central processor.

LAWRENCE LIVERMORE LABORATORY

A. NEUTRON PHYSICS

1. Fission $\bar{\nu}$ Measurements (R. E. Howe and C. D. Bowman*) Relevant to Requests 395 and 452.

We have performed measurements of $\bar{\nu}$ for ^{235}U neutron-induced fission in the energy range from 0.5 eV to 50 eV. Fast, spectrum-independent neutron detection was accomplished with the system previously described.**

Preliminary data analysis shows some indications of structure in $\bar{\nu}$ in this energy region. In particular, there is a definite rise of about 0.3% above the mean for neutron energies between 6.4 eV and 9.4 eV and a similar depression of about 0.5% below the mean between 11.6 eV and 40 eV. Elsewhere $\bar{\nu}$ is reasonably close to the mean value for all the data from 0.5 eV to 50 eV. These initial observations agree reasonably well, both quantitatively and qualitatively, with the RPI data.†

Future plans include completion of $\bar{\nu}$ measurements for ^{235}U from thermal energy up to 15 MeV. Preliminary experiments to evaluate $\bar{\nu}$ for ^{239}Pu neutron-induced fission over a similar energy range are also presently underway.

2. Investigation of γ-Ray Emission Preceding Isomeric Fission in ^{243}Pu (J. C. Browne and C. D. Bowman*) Relevant to Request 483.

Measurements were made to detect γ-ray emission preceding fission events corresponding to the subthreshold fission resonances in the ^{242}Pu (n,f) cross section. Subthreshold fission in ^{242}Pu exhibits weak coupling between the class I and class II states since one resonance in each subthreshold group carries the main fission strength. If the subthreshold fission resonances have a γ-decay branch (Γ_{γ_2}) to the isomeric ground state in the second well ($\tau_{1/2}$ = 30 nsec), it should be possible to observe γ-rays preceding fission events in these resonances.

---

* National Bureau of Standards, Washington D.C.

** NCSAC Report, dated 10 November 1971, UCID-15937

† S. Weinstein, R. Reed and R. C. Block, Physics and Chemistry of Fission, IAEA, Vienna (1969), p. 477.

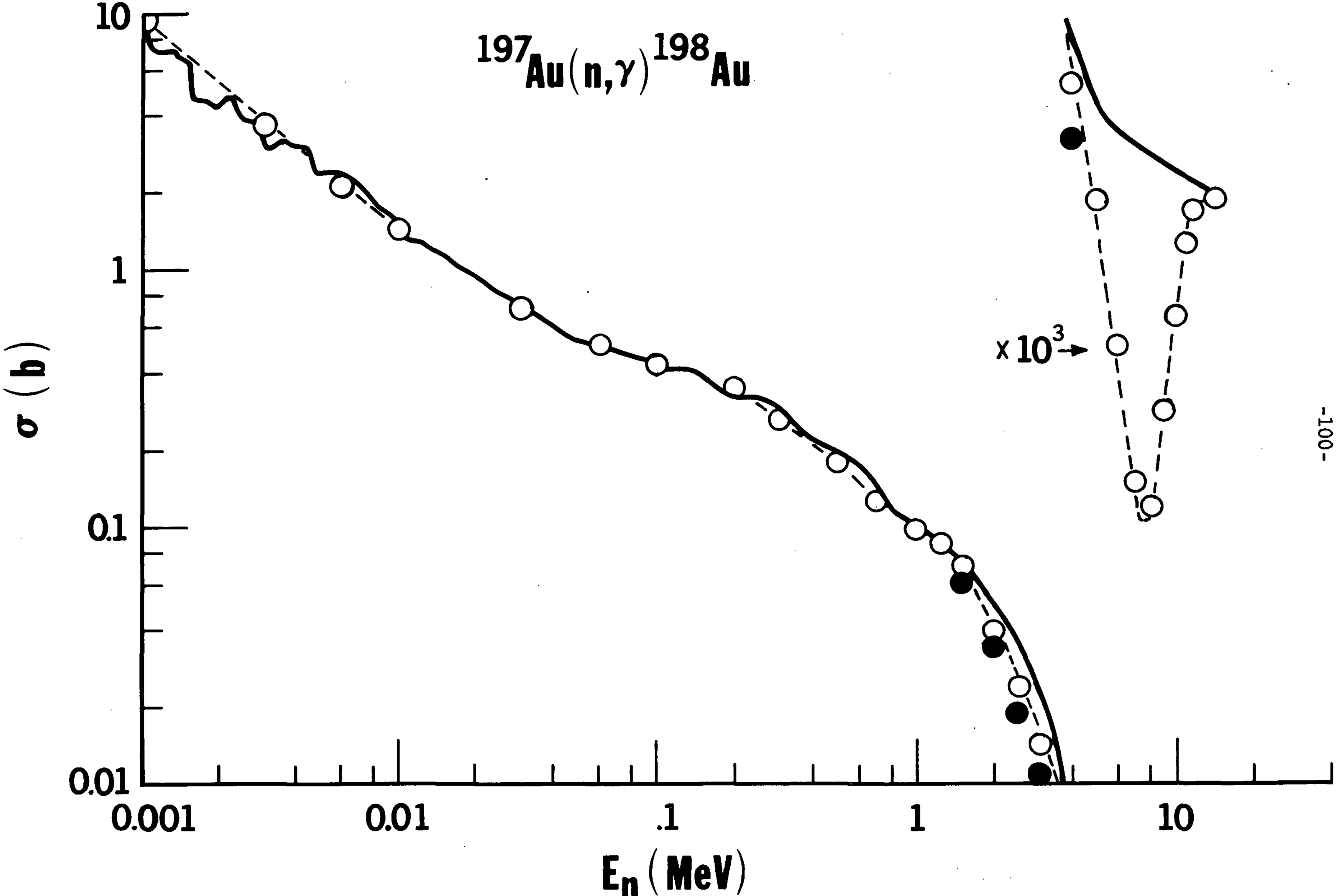

Figure A-1 Comparison of Two Calculations (O and ●) of the Excitation Function for the Reaction $^{197}Au(n,\gamma)^{198}Au$ with an Evaluation of Simons and McElroy(——).

A 10-g sample of ^{242}Pu was bombarded by neutrons from the pulsed neutron source of the Lawrence Livermore Laboratory 100-MeV Linac. A pair of C_6D_6 scintillators searched for both pre-fission γ-rays and fission events (prompt fission γ-rays). By storing both the time-of-flight of an event and the time relationship between γ-rays seen in the two scintillators in a two-dimensional matrix, it was possible to look at each subthreshold fission resonance for evidence of a γ-decay branch to the 30-nsec fission isomer.

The best cases examined involved the resonances at 763 eV and 1839 eV both of which have a very small neutron width* but also have a large fission cross section indicating that these states are mainly of class II nature. These resonances exhibited no γ-decay branch to the ground state in the second well within the limits of the sensitivity of the experiment. However, a limit on the ratio of the γ-decay width to the prompt fission width ($\Gamma_{\gamma 2}/\Gamma_{f2}$) can be obtained from our measurements. With a knowledge of Γ_{f2} from previous measurements* we can then obtain a limit for $\Gamma_{\gamma 2}$. For the 1839-eV resonance we obtain the result from our measurements that $\Gamma_{\gamma 2} < 1.75$ meV while for the 763-eV resonance we find $\Gamma_{\gamma 2} < 2.5$ meV. These values of $\Gamma_{\gamma 2}$ can be compared with a calculation of $\Gamma_{\gamma 2}$ using Lynn's prescription** which yields a result of 8 - 10 meV for ^{243}Pu. This calculation is sensitive to the excitation energy of the ground state in the second well (ε_0) relative to the equilibrium ground state which was estimated from the ^{242}Pu fission cross section to be $\varepsilon_0 = 1.86$ MeV.† However, our limit on $\Gamma_{\gamma 2}$ requires that ε_0 be on the order of 3 MeV. Further investigations of isomeric fission in ^{243}Pu are continuing.

3. <u>The ^{128}Te(n,γ) and ^{130}Te(n,γ) Cross Sections from 0.5 eV to 7 keV</u> (J. C. Browne and B. L. Berman)

Excess amounts of ^{129}Xe and ^{131}Xe have been found in various ores of tellurium from mines in Sweden, Colorado and Japan.‡ Attempts were made to explain the ratio of the amounts of ^{129}Xe to ^{131}Xe found in the ores by various nuclear reactions on the tellurium isotopes. It was shown that thermal neutron capture on ^{128}Te and ^{130}Te predicted a ratio of ^{129}Xe/^{131}Xe of 0.6 while experimentally this ratio was found to be 3.0.

---

* G. F. Auchampaugh and C. D. Bowman (to be published).

** J. E. Lynn, <u>Theory of Neutron Resonance Reactions</u>, Oxford (1968), pp. 459-469.

† G. F. Auchampaugh, T. A. Farrell and D. W. Bergen, Nucl. Phys. <u>A171</u>, 31 (1971).

‡ B. Srinivasan, E. C. Alexander, Jr. and O. K. Manuel, J. Inorg. Nucl. Chem. (to be published).

In order to determine whether neutron capture in the epithermal energy region could explain this "anomaly," we measured the neutron-capture cross section of ^{128}Te and ^{130}Te from 0.5 eV to 7 keV using the Lawrence Livermore Laboratory 100-MeV linac. Details of the experimental setup are discussed elsewhere.* Preliminary analysis shows 17 resonances in the ^{128}Te(n,γ) cross section in this energy region while the ^{130}Te(n,γ) cross section has only 6 resonances. Resonance parameters are being extracted to determine whether this difference in level density is sufficient to explain the ^{129}Xe/^{131}Xe ratio found in the tellurium ores.

4. Neutrons from Deuteron Bombardment of Li, C, and ^{2}H (K. A. Weaver**)

To investigate intense sources of fast neutrons we have measured spectra, yields, and average energies of neutrons from deuteron bombardment of thick Li and C targets. Deuteron energies ranged from 5 MeV to 19 MeV for Li measurements and 12 MeV to 18 MeV for C measurements. Neutrons were detected at lab angles from 3° to 32°. At 18 MeV and 3°, Li produced 5 x 10^{10} n/sr·μC with an average energy of 6.8 MeV, while C produced 3.5 x 10^{10} n/sr·μC with an average energy of 7 MeV.

We also measured relative spectra of neutrons from the D + D interaction of deuteron energies of 12.2 MeV, 14.3 MeV, and 16.4 MeV. Average neutron energies were calculated. The D(d,n)^{3}He cross section was used to normalize the spectra so that D(d,np)D cross sections could be calculated. At 16.4 MeV and 3° the average neutron energy was 10.7 MeV and the breakup cross section was 410 mb/sr.

Uncertainties in cross sections and yields were about 10%, and average-energy uncertainties were about 5%.

5. Nuclear Cross-Section Calculations (D. G. Gardner, J. L. Brownlee and A. Delucchi) Relevant to all Requests for Neutron Cross Sections

For the past year we have continued the development of the statistical-model codes COMNUC, CASCADE, and UHL. The coupled-channels optical-model program FOURPLUS was put into operation and tested. The principal modifications which have been introduced include: a) precompound evaporation, discrete final states in all available daughter nuclei, and the ability to use nuclei in isomeric states as target nuclei have been added to UHL; b) the optical model program written by

---

* J. C. Browne and B. L. Berman, USNDC Report, UCID-16037 dated 5 May 1972.

** Student Guest from the University of Wisconsin.

James Ferguson of Livermore has replaced the original optical-model subroutines in COMNUC and CASCADE.

Although there are still several important modifications and improvements yet to be made in the codes within their known limitations, the codes seem to be capable of calculating excitation functions in good agreement with experiments. Three examples will now be discussed.

a. (n, capture) Reactions

We have computed the $^{197}Au(n,\gamma)$ ^{198}Au excitation functions using various sets of neutron optical-model parameters. Fig. A-1 shows two sets of results compared with an evaluation by Simons and McElroy, of Hanford Engineering Development Laboratory. The original calculations were adjusted downward by 25% to force agreement with the evaluation. The neutron optical-model parameters were those of Holmquist and Wiedling of Studsvik. The empty circles were the result of the detailed calculation of the neutron and gamma-ray competition in ^{198}Au, whereas the filled circles resulted from the assumption that only the initial cascade gamma-rays that populated ^{198}Au below its neutron separation energy resulted in capture. The discrepancy above 1 MeV is not serious, because calculation in this region is quite sensitive to the choice of neutron optical-model parameters.

b. (n,n') Reactions

If one is interested in (n,n') reactions involving 14-MeV neutrons, then it is vitally important to consider precompound evaporation and, in some cases, direct reactions as well as compound nuclear reactions. Fig. A-2 shows a comparison of a recent calculation with experimental data for the $^{115}In(n,n')^{115m}In$ reaction. The precompound reaction produces the high-energy tail, whereas the compound nuclear reactions falls off rapidly above 9 MeV to only a few percent of the pre-compound cross section around 14 MeV. In the calculation it was assumed that the maximum precompound contribution was 3.5% of the total neutron emission cross section, and that the precompound fraction was zero below 8 MeV and grew to its maximum value around 14 MeV. No arbitrary assumptions were made concerning the compound nucleus part of the reaction, which indicates that the gamma-ray cascade populating the ^{115m}In isomer is handled well in the UHL code.

c. (n,α) Reactions

We have found that the original optical-model program in the COMNUC and CASCADE programs was not sufficiently accurate for charged particles, such as alpha particles, and so we have replaced it with the optical-model program of James Ferguson of Livermore. Our previous

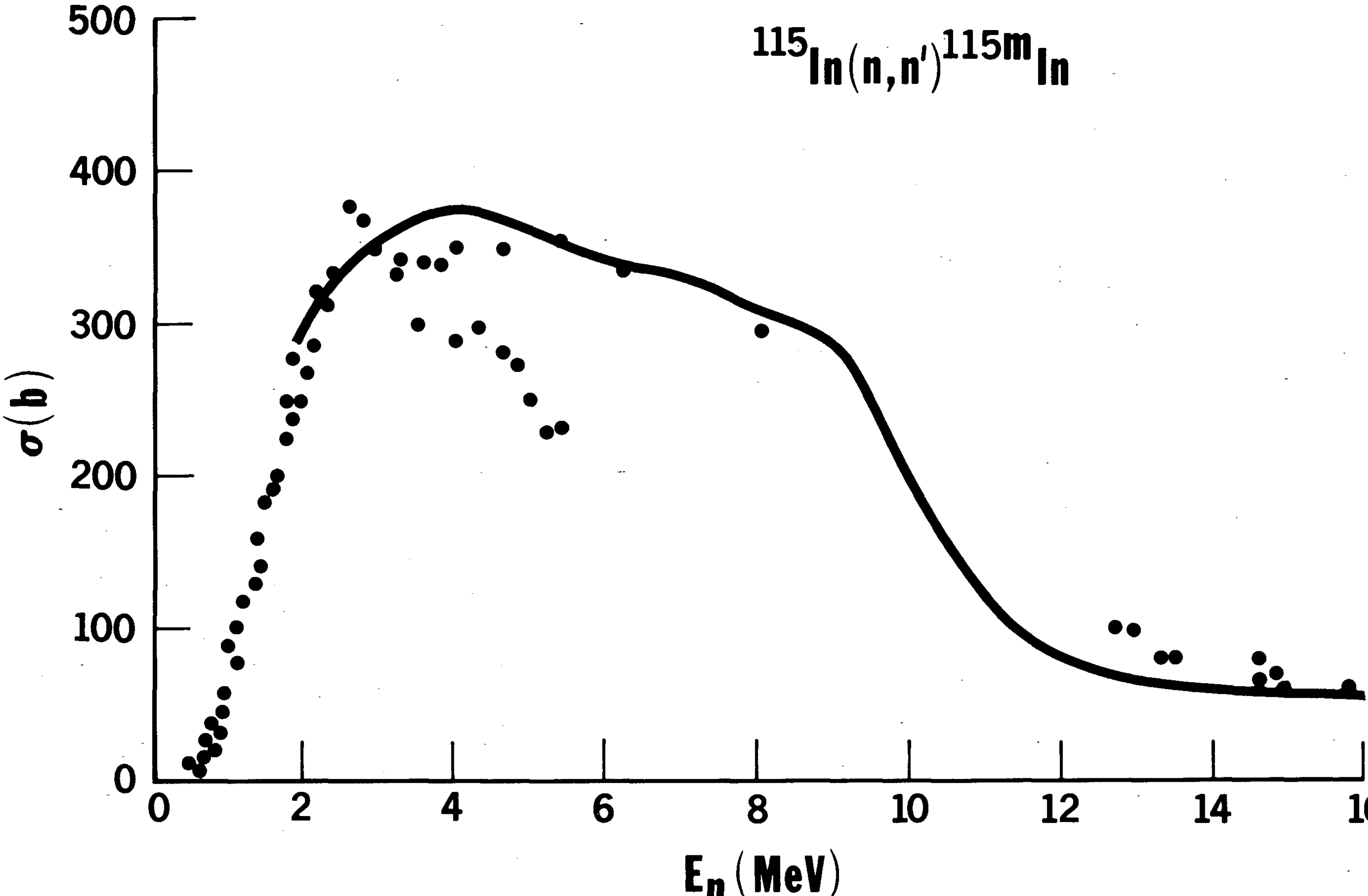

Figure A-2 Comparison of Calculated (-) and Experimental (●) Excitation Function for the Reaction $^{115}In(n,n')^{115m}In$.

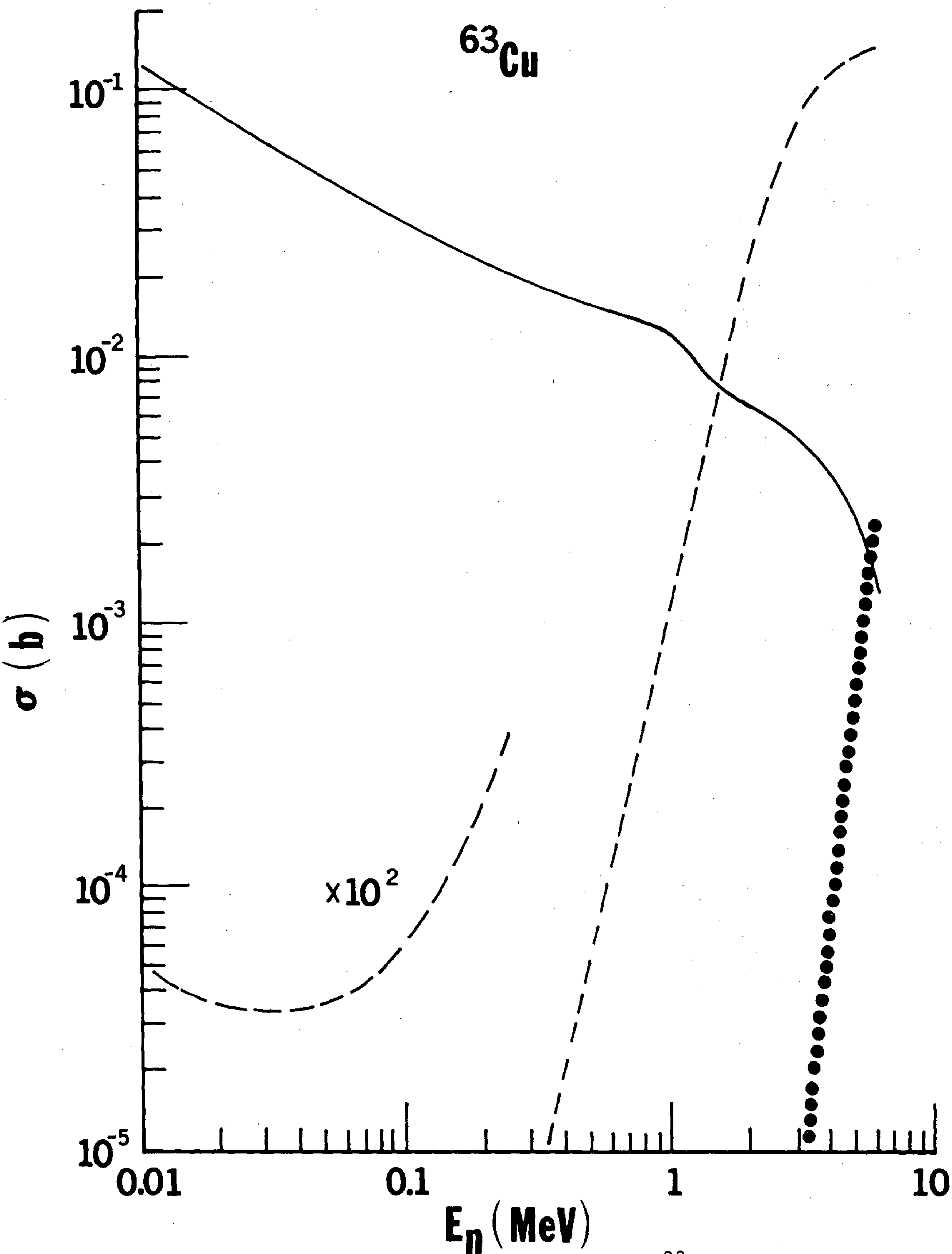

Figure A-3 Calculated Excitation Functions for ^{63}Cu.
___ (n,capture), --- (n,p), ... (n,α)

calculations for the $^{63}Cu(n,\alpha)^{60}Co$ reaction showed a very small, but finite, low-energy tail, that existed down to thermal energies. This appeared to be in agreement with some suggestions in the literature that such a low energy cross section was needed to produce the observed helium damage in copper components in reactors. Our latest results are shown in Fig. A-3. The calculated (n,capture) cross section is in good agreement with evaluations in the literature, and now the (n,α) cross section shows no low-energy tail such as the (n,p) reaction evidences. It would appear, therefore, that either the excess helium production in copper must be due to some source other than the $^{63}Cu(n,\alpha)^{60}Co$ reaction, or that the neutron energy spectrum assumed for certain reactors must be richer in high-energy neutrons than had previously been thought. In the former instance a possible candidate is the $^{64}Cu(n,\alpha)^{61}Co$ reaction, which does have a finite cross section for thermal neutrons. However, quite a bit of ^{64}Cu would have to be produced by the $^{63}Cu(n,\gamma)^{64}Cu$ reaction, in order for the helium production to arise from this source.

B. PHOTONUCLEAR PHYSICS

1. Photoneutron Cross Section of ^{55}Mn and ^{59}Co (R. A. Alvarez, B. L. Berman and P. Meyer)

We have measured the photoneutron cross sections of ^{55}Mn and ^{59}Co, using the monoenergetic photon beam at the Livermore Electron-Positron Linac. The measured cross sections, which extend from just below the peak of the giant resonance to 36.5 MeV, are shown in Figs. B-1 and B-2. The photon energy resolution was slightly greater than 1%.

In both isotopes there is a gross splitting of the main peak of the giant resonance into two major bumps which in turn show evidence of still finer structure; this is particularly evident in ^{55}Mn. Above the main peak of the giant resonance, both isotopes show additional structure in both the single-neutron and double-neutron cross sections. The triple-neutron cross sections are small in both cases, and are consistent with zero for several MeV above the $(\gamma,3n)$ threshold.

The splitting of the giant resonance in ^{59}Co is consistent with that determined in a previous experiment at this laboratory*; the maximum cross section in the present data is approximately 17% larger than that observed in the previous measurement.

The present results will be analyzed more completely after further data are obtained between threshold and the peak of the giant resonance.

---

* S. C. Fultz, R. L. Bramblett, J. T. Caldwell, N. E. Hansen and C. P. Jupiter, Phys. Rev. 128, 2345 (1962).

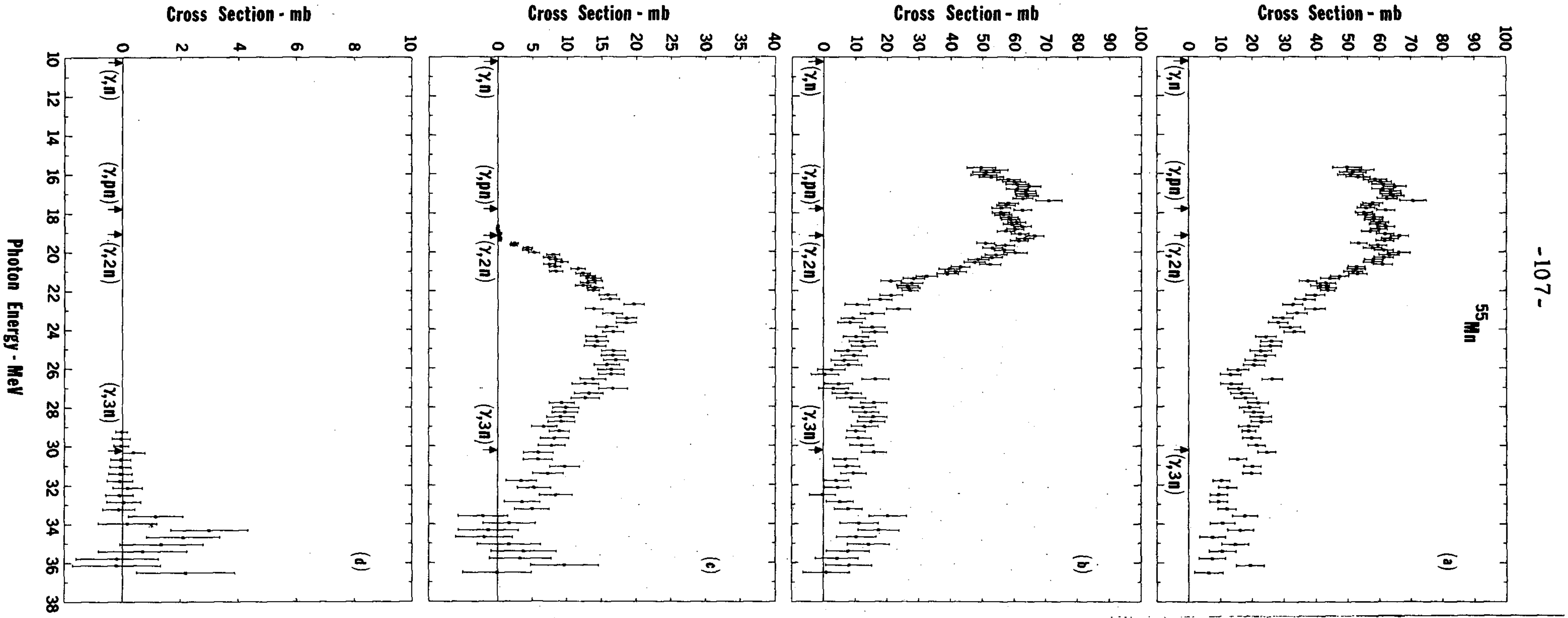

Figure B-1 (a) The ^{55}Mn total photoneutron cross section. (b) The ^{55}Mn(γ,n) cross section. (c) The ^{55}Mn(γ,2n) cross section. (d) The ^{55}Mn(γ,3n) cross section.

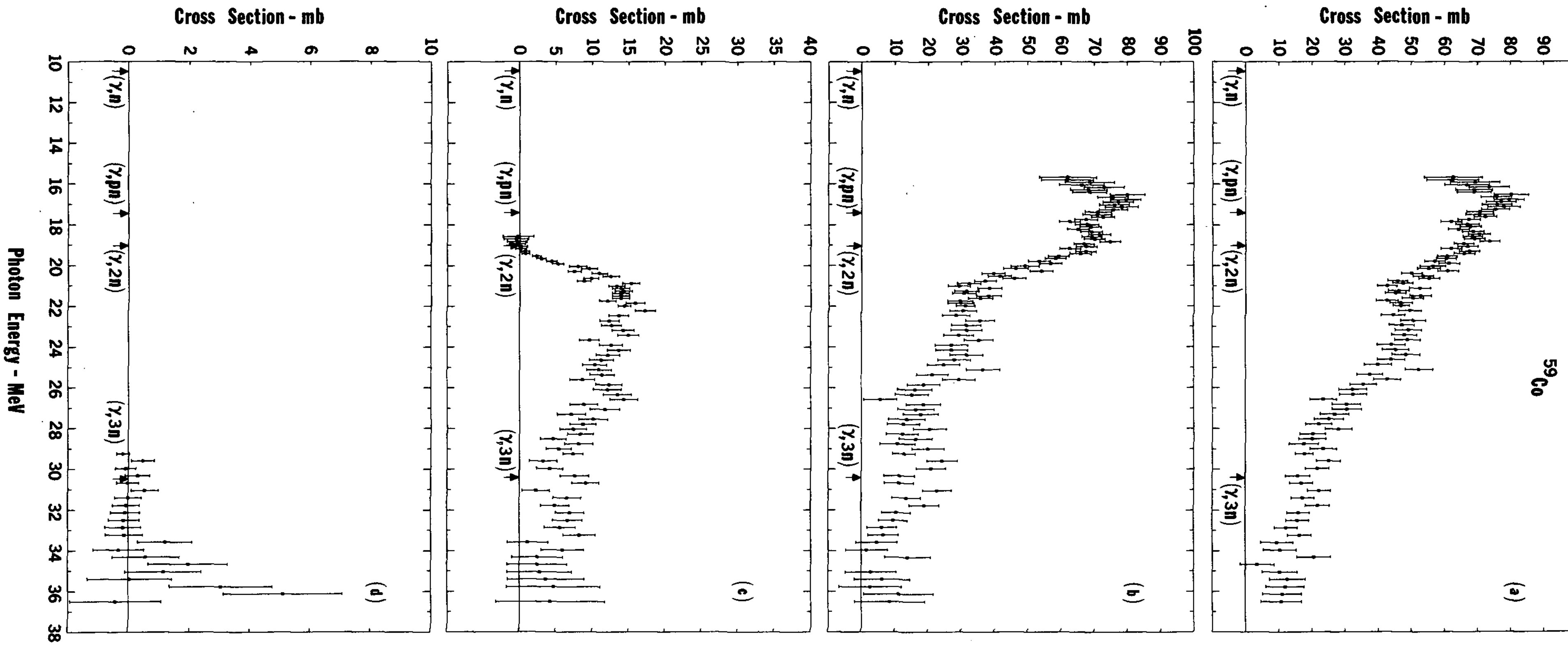

Figure B-2 (a) The ^{59}Co total photoneutron cross section. (b) The ^{59}Co(γ,n) cross section. (c) The ^{59}Co(γ,2n) cross section. (d) The ^{59}Co(γ,3n) cross section.

LOCKHEED PALO ALTO RESEARCH LABORATORY

A. NEUTRON PHYSICS

1. Gross-Fission-Product γ-Ray Spectroscopy (W. L. Imhof, L. F. Chase, R. A. Chalmers, F. J. Vaughn, and R. W. Nightingale)

Analysis of the fission-product γ-ray data is continuing. Recent emphasis has been placed on the data from the 5-h and 5-min neutron bombardments in order to study activities with half-lives both shorter and longer than those observed from the previously analysed 40-min irradiations.

2. Neutron Cross-Section Measurements with Polarized Targets (T. R. Fisher and B. A. Watson)

A ^{3}He - ^{4}He dilution-refrigerator system has been built which is suitable for polarizing large targets needed in fast-neutron cross-section measurements. Thus far, the system has been used to construct a polarized ^{59}Co target, namely, a Co single crystal 1 cm x 1 cm x 5 cm with the "C" axis in the direction of the long dimension. The crystal has been cooled to a temperature 0.035° K corresponding to a tensor polarization or alignment of 11%. Preliminary data have been taken on the "deformation effect" in the ^{59}Co+n total cross section. At a neutron energy of 1.7 MeV, a decrease of 15 ± 7 mb in the total cross was observed when the target was aligned. This change is related to the quadrupole moment of the ^{59}Co nucleus.

The addition of a magnetic field will produce an additional vector polarization of 40% in the target, which will be used in future experiments with polarized neutron beams to study spin-correlation effects.

B. CHARGED-PARTICLE REACTIONS

1. Profile Studies of ^{3}He Distributions (P. P. Pronko,* J. G. Pronko, and R. E. McDonald)

Studies were made regarding the feasability of using the ^{3}He $(d,p)^4$He reaction as a means of tracing depth distributions of implanted ^{3}He ions. It was found that at concentrations of 10^{14} ions/cm^2 the ^{3}He depth profile could be quite reliably traced using deuteron beam currents in the nA region. Further studies regarding the use of this method for locating substitutional and interstitial positions of the ^{3}He ions are being pursued as well as the use of this reaction in obtaining accurate dE/dx information for ^{3}He and d implants.

2. Beta Decay of ^{17}N (A. R. Poletti and J. G. Pronko)

The delayed neutron spectrum following the β decay of ^{17}N has been observed using the associated-particle time-of-flight method and neutron flight paths of up to 140 cm. The ^{17}N was formed by bombarding a gas cell containing $^{15}N_2$ gas with 2.9-MeV tritons. Three neutron groups were observed. Direct calibration of the time-to-amplitude converter in terms of a 50-MHz frequency enabled us to determine the mean energy of the three groups as 1.654 ± 0.024, 1.154 ± 0.014, and 0.385 ± 0.007 MeV. We can assign these groups unambiguously to the neutron decay of the established levels at 5.935, 5.377, and 4.554 MeV in ^{17}O. Further efforts are being made to accurately determine the β-decay branchings to both bound and unbound levels in ^{17}O.

3. Lifetime Measurements in ^{28}Mg (T. T. Bardin, J. A. Becker, L. F. Chase, T. R. Fisher, R. E. McDonald, A. R. Poletti, and J. G. Pronko)

Mean lifetimes have been measured for the excited states in ^{28}Mg using the Doppler-shift-attenuation technique. Gamma rays were detected at 0, 60, 90, and 120 deg by a Ge(Li) detector in coincidence with an annular particle detector using the ^{26}Mg$(t,p\gamma)^{28}$Mg reaction at $E_t = 2.9$ MeV. The nuclear properties of the excited states of ^{28}Mg deduced from this experiment together with previous (t,p) results[1,2]

---

*Argonne National Laboratory, Argonne, Illinois.

[1] R. Middleton and D. J. Pullen, Nucl. Phys. <u>51</u>, 77 (1964).

[2] L. F. Chase, J. A. Becker, D. A. Kohler, and R. E. McDonald, Bull. Am. Phys. Soc. <u>12</u>, 555 (1967).

are: [E_x (keV), J^π, τ_m(psec)] 1473.8 ± 0.4, 2^+, 1.45 ± 0.32; 3862.7 ± 0.7, 0^+, 0.70 ± 0.12; 4021.0 ± 1.6, 4^+, 0.20 ± 0.06; 4557.2 ± 0.8, 2^+, <0.04; 4877 ± 5, 2^+, 0.18 ± 0.15; 5171.3 ± 1.0, 3^-, 0.10± 0.03; and 5189.7 ± 3.0, 1^-, <0.03. Gamma-ray branching ratios have also been measured.

4. Lifetimes in ^{33}P by the Doppler-Shift-Attenuation Method (A. R. Poletti, T. T. Bardin, J. G. Pronko, and R. E. McDonald)

Lifetimes of low-lying states in the nucleus ^{33}P have been measured by the Doppler-shift-attenuation method. In addition to this, excitation energies of the excited states were measured using a Ge(Li) spectrometer.

5. Angular-Correlation Studies of Excited States of ^{33}P (A. R. Poletti, T. T. Bardin, R. E. Mcdonald, and J. G. Pronko)

The $^{31}P(t,p\gamma)^{33}P$ reaction has been used to investigate the spins and decay modes of many of the levels of ^{33}P below an excitation energy of 6.17 MeV, as well as the multipole-mixing ratios of the transitions between these levels. Gamma radiation was detected simultaneously in five NaI(Tℓ) detectors located at angles equivalent to 5, 35, 45, 60, and 90 deg, while outgoing protons were detected in an annular detector placed at 180 deg with respect to the beam direction. Multi-parameter techniques were used to measure the p-γ coincidence spectra. Spin assignments were made for 14 excited states.

6. Study of ^{52}Ti using the $^{50}Ti(t,p\gamma)^{52}Ti$ Reaction (J. G. Pronko, T. T. Bardin, A. R. Poletti, and R. E. McDonald)

The angular correlations of cascading γ rays observed in a collinear geometry with a 5-crystal array of NaI(Tℓ) detectors were measured. These studies provided information on the previously unobserved level scheme of ^{52}Ti including spin assignments and decay modes of the excited states. Further studies regarding the lifetimes of the excited states are still in progress.

7. Study of ^{56}Cr using the $^{54}Cr(t,p\gamma)^{56}Cr$ Reaction (T. T. Bardin, J. G. Pronko, A. R. Poletti, and R. E. McDonald)

The decay modes of the excited states of ^{56}Cr were studied using the technique whereby angular-correlation measurements are obtained in a collinear geometry. An array of 5 NaI(Tℓ) crystals was used in the collection of the correlation data. The analysis of the data has yielded information on spin assignments as well as branching and mixing ratios of the electromagnetic de-excitations. Further studies regarding the lifetimes of these excited states are still in progress.

8. Line-Shape Fitting of Doppler-Shifted γ-Ray Lines Excited by Coulomb Excitation (T. R. Fisher and P. D. Bond*)

Nuclear lifetimes have been extracted by fitting the line shapes of Doppler-shifted γ rays following Coulomb excitation. The lifetimes obtained are being compared with lifetimes measured by Coulomb excitation and resonance fluorescence to check the applicability of the Lindhard-Blaugrund energy-loss theory over a wide range of the periodic table. Thus far, transitions in the nuclei ^{24}Mg, ^{27}Al, ^{44}Ca, ^{48}Ti, ^{60}Ni, ^{63}Cu, ^{65}Zn, ^{93}Nb, ^{95}Mo, and ^{136}Ba have been investigated.

9. Investigation of Reactions Induced by ^{16}O Bombardment of Medium-Mass Nuclei (B. A. Watson, W. E. Meyerhof,* D. S. Slater,* J. R. Hall,* and J. Calarco*)

A 70-MeV ^{16}O beam has been employed to bombard a variety of targets between Ca and Ni. Of prime interest are the relative cross sections for the various possible cluster-transfer reactions as well as the production of exotic nuclei. Employing a system[1] for unique particle identification, a wide variety of particles between ^{4}He and ^{24}Mg have been observed. In the case of ^{40}Ca+^{16}O, the proton-rich nuclei ^{45}V and ^{47}Cr were produced. The study also indicates that multi-α-particle transfer reactions are quite strong for 4N nuclei.

10. Application of Superconductivity to the Detection of Nuclear Particles (B. A. Watson and T. R. Fisher)

It has been reported[2] that superconducting films have been successful in the detection of nuclear particles. We are in the process of further investigation of the properties of these detectors, primarily for their use in specific nuclear-physics experiments. Several detectors have been fabricated along with the facilities for the investigation of their characteristics.

---

*Stanford University, Stanford, California.

[1] B. A. Watson, C. C. Chang, and S. L. Tabor, Particles and Nuclei 2, 376 (1971).

[2] E. C. Crittenden, Jr. and E. Spiel, Jour. Appl. Phys. 42, 3182 (1971).

11. Radiation-Damage Effects on Superconducting Microwave Cavities (T. R. Fisher and I. Ben Zvi*)

An X-band Nb cavity having a Q of 2.0×10^9 and a breakdown field $H_{max} > 300$ Oe was irradiated by approximately 5×10^{16} deuterons of 2.5-MeV energy. The irradiation was confined to a spot size approximately 1.5 mm in diameter. No significant change in the Q of the cavity was observed, but a drastic reduction in the breakdown field ($H_{max} \approx 30$ Oe) occurred. Further measurements are in progress to study annealing and recovery rates. It appears desirable to increase the beam spot size in future measurements.

---

*Stanford University, Stanford, California.

LOS ALAMOS SCIENTIFIC LABORATORY, UNIVERSITY OF CALIFORNIA*

A. NEUTRON CROSS SECTIONS BY TIME OF FLIGHT

1. ^{238}Pu(n,γ); Resonance Parameters (Silbert; Berreth, ANC) (439, 440, 441, 443*)

A manuscript with the following abstract has been forwarded to the Physical Review for publication, together with the ^{238}Pu(n,f) paper that was submitted earlier:

"The radiative capture cross section of ^{238}Pu has been measured from 18-eV to 200-keV neutron energy. A time-of-flight experiment with a 300-m flight path was carried out in conjunction with the underground nuclear explosion Persimmon. Fission fragment detectors viewed a thin ^{238}Pu target to measure the fission cross section, while modified Moxon-Rae detectors viewed a second, thicker ^{238}Pu target to measure the gamma-ray emission. Subtraction of the fission gamma-ray contribution from the Moxon-Rae signal yielded the contribution due to radiative capture. The neutron flux was measured relative to the reactions ^{3}He(n,p), ^{6}Li(n,αt), and ^{235}U(n,f). Single-level area analysis of the measured fission and capture cross sections gave values for the neutron and fission widths of 49 resonances below 500 eV, under the assumption of a known, constant radiative capture width. The s-wave neutron strength function $\overline{\Gamma_n^0}/\overline{D}$ was determined to be (1.27 ± 0.25) x 10^{-4}. The derived fission widths exhibit a distinct maximum near 300 eV neutron energy. At higher energies, the fission-to-capture ratio shows pronounced intermediate-structure peaks attributed to second-well effects in the fission barrier."

2. ^{249}Cf(n,f) (Silbert) (528*)

A manuscript with the following abstract has been forwarded to the Physical Review:

"The neutron-induced fission cross section of ^{249}Cf was measured from 13 eV to 3 MeV. Neutrons from the Physics 8 underground nuclear explosion traversed a 240-m vertical evacuated flight path and interacted with a ^{249}Cf sample and with neutron flux monitors at ground level. Abundant fission was observed throughout the neutron energy region studied, although the several-MeV cross section was lower than expected on the basis of systematics. Forty-three resonances between 15 and 70 eV were parametrized using a multilevel R-matrix formalism. In this energy region, the average level

*Measurements, when appropriate, are identified as pertinent to requests in the U. S. Request Compilation, NCSAC-35.

spacing, corrected for five postulated unobserved levels, was 1.07 ± 0.14 eV, both spin states (4^-,5^-) of the compound nucleus being taken together. Assuming both spin states to have the same properties, the s-wave neutron strength function per spin state $\overline{\Gamma_n^0}/\overline{D}$ was (1.5 ± 0.3) x 10^{-4}. The average reduced neutron width $\overline{\Gamma_n^0}$ was (0.31 ± 0.08) MeV. For 35 well-defined resonances between 15 and 70 eV, the average fission width $\overline{\Gamma_f}$ was 180 meV."

2. ^{234}U(n,f) and ^{253}Es(n,f) (Silbert) (538*)

These remnants of the Physics 8 data are being studied. Each set of data, in its own way, is of marginal usefulness. For the ^{234}U, fission in the resonance region is small enough that the detector sensitivity to (n,γ) is an important interfering effect (analogous to the situation in ^{237}Np). Furthermore, the ^{235}U content of the sample, even though only 0.08%, produces prominent background. The contribution that our data would add to the literature is in doubt.

For ^{253}Es, this exotic, 20-d half-life sample has never before been measured. Unfortunately, our 3.3-microgram sample yields no resonance information. In the threshold and few-MeV region we see an effect above background, but its significance for a quantitative analysis is in doubt because of the widely differing cross sections derived from the two detectors.

3. Neutron Polarization Experiments (Keyworth, Seibel, Bautista; Dabbs, ORNL) (367, 400*)

The first attempt to polarize lanthanum magnesium nitrate (LMN) with a conventional NMR coil was highly successful. The LMN beam polarizing system was assembled in the final configuration to be used at Oak Ridge with six crystals totaling 18 cm^3. A maximum polarization of 75% ±10% was achieved. This figure compares well with the maximum polarization possible for large-volume cavities. The system was run for a period of two weeks to check the stability and to become familiar with the cryogenic characteristics of the system. The electronic stability is far better than expected, primarily due to a very stable type of klystron. High polarizations (>60%) appear to be reproducible and maintainable with only minor adjustments required on a daily basis. This system is now in operation at Oak Ridge.

The ^{3}He-^{4}He dilution refrigerator cryostat is now free of leaks. The new heat exchangers in the dilution refrigerator resulted in no improvement in refrigeration capacity, but resulted in a reduced ultimate low temperature of 8 m°K, measured on a simulated target. This temperature was reproduced and measured using a ^{54}Mn thermometer and represents as low a temperature as has been produced dynamically. A new, large mixing chamber has been tested and results in a slightly improved refrigeration rate, of primary interest when using targets with high natural radioactivity such as ^{237}Np and ^{233}U. An elevated ultimate low temperature of 16 m°K was realized due to viscous heating. However, these two mixing chambers permit maximum flexibility for the types of targets which are to be polarized. Preliminary measurements, using a target of ^{235}U monosulfide, are in progress on the ORELA.

4. Prompt Neutrons from Spontaneous Fission of ^{257}Fm (Veeser, Hemmendinger, Farrell, and the Los Alamos Radiochemistry Group)

About 6900 fission events from ^{257}Fm have been observed with a 75-cm-diam liquid scintillator tank. During the same period 46,000 fission events from ^{252}Cf were observed and the background rate was measured 60,000 times.

The ratio of the average number of prompt neutrons per fission from ^{257}Fm to that for ^{252}Cf is 1.014 ± 0.015, where the uncertainty is statistical. This is in agreement with a measurement of 1.067 ± 0.036 for the same quantity by Cheifetz.[1] If the number of prompt neutrons per fission for ^{252}Cf is assumed to be $\overline{\nu} = 3.771$, then for ^{257}Fm $\overline{\nu} = 3.83 \pm 0.06$.

The efficiency of the scintillator tank has been 0.66 during the runs. The background measurements are consistent with a Poisson distribution with about 0.13 counts per 40 μsec sampling. No high multiplicity background events, such as were seen by Cheifetz,[1] have been observed in this experiment, even though we have measured backgrounds three times as often. The lack of such high multiplicity backgrounds may be attributable to the thick concrete shielding of the counting room where the tank is located.

Table A-1 lists the results obtained to date for an assumed value of $\overline{\nu} = 3.771$ for ^{252}Cf. The uncertainties given are statistical and do not include the uncertainty in $\overline{\nu}$ for ^{252}Cf. The multiplicity probabilities for ^{257}Fm are given so that quantities such as the variance can be calculated.

5. n-^{4}He and n-^{3}He Total Cross Sections (Seagrave; Stoler, Block, Goulding, Clement, RPI) (6*)

Successful runs with ^{4}He, using cryopumping for filling and recovery operations as a dry run for the ^{3}He sample, established the technique of sample handling and confirmed the accuracy of the dead time

[1] E. Cheifetz, H. R. Bowman, J. B. Hunter, and S. G. Thompson, "Prompt Neutrons from Spontaneous Fission of ^{257}Fm," Phys. Rev. C3, 2017 (1971).

TABLE A-1

Summary of results: $\bar{\nu}$ is the average of the number of prompt neutrons per fission; P_0, P_1, P_2, ... are the respective probabilities of emission of 0, 1, 2, ... prompt neutrons per fission.

Nuclide	^{257}Fm	Background	^{252}Cf	$^{252}Cf^{b}$
Fissions Analyzed	6909	59,524	45,882	4545
$\bar{\nu}$	3.825 ± 0.057		3.771 ± 0.031[a]	3.869 ± 0.078
P_0	0.020 ± 0.006	0.879	0.006 ± 0.002	0.005 ± 0.002
P_1	0.085 ± 0.018	0.111	0.015 ± 0.009	0.004 ± 0.009
P_2	0.087 ± 0.043	0.008	0.134 ± 0.019	0.138 ± 0.032
P_3	0.217 ± 0.070	0.0004	0.253 ± 0.028	0.223 ± 0.032
P_4	0.189 ± 0.091		0.313 ± 0.030	0.356 ± 0.035
P_5	0.334 ± 0.098		0.223 ± 0.031	0.175 ± 0.034
P_6	-0.016 ± 0.078		0.039 ± 0.020	0.071 ± 0.028
P_7	0.102 ± 0.056		0.013 ± 0.010	0.022 ± 0.017
P_8	-0.028 ± 0.027		0.005 ± 0.003	0.006 ± 0.007
P_9	0.011 ± 0.007			

[a] J. C. Hopkins and B. C. Diven, "Prompt Neutrons from Fission," Nucl. Phys. 48, 433 (1963).

[b] B. C. Diven, H. C. Martin, R. F. Taschek, and J. Terrell, "Multiplicities of Fission Neutrons," Phys. Rev. 101, 1012 (1956).

corrections and the stability of the new electronic system using a Hewlett-Packard time-to-digital converter. Measurements extended from 0.7 to 30 MeV, and excellent agreement was observed between corrected sets of data taken with high and low counting rates. In the case of the ^3He sample, no anomaly outside of about 1% statistics was seen in the vicinity of 3.08 MeV which should correspond to the sharp anomaly in $D(d,n)^3He$ polarization reported by Hänsgen et al. [Nucl. Phys. 73, 417 (1965)]. The data were taken with a 250-m flight path and mostly with 20-nsec resolution. When sufficient data had accumulated for the higher cross-section portion of the data, the remaining accelerator time was devoted to higher counting-rate data at 50-nsec resolution to improve statistics at the higher energies. About 4% statistics in each channel should result near 24 MeV, so that a smooth fit should have an uncertainty approaching 1%. This should be more than sufficient to resolve the discrepancy between the elastic integral at 23.7 MeV and the extrapolation of old LASL total cross-section data extending to 21 MeV. The operations were so successful that serious consideration will be given to the possibility of similar measurements with tritium, in which both the sample and dummy cells would be enclosed in a sealed evacuated "dump" container while in use, and the whole system shipped in a heavy third shell for protection and containment.

B. FAST NEUTRON STUDIES

1. Fission Neutron Spectra of ^{238}U, ^{235}U, and ^{239}Pu at 1.85 MeV Excitation (Auchampaugh, Drake, Ragan) (396*)

The importance of the prompt fission neutron spectrum of ^{235}U, especially the high-energy region of this spectrum, to the U.S. applied fission programs has resulted in a series of measurements on the fission neutron spectrum of ^{238}U, ^{235}U, and ^{239}Pu at the LASL vertical Van de Graaff facility. Preliminary results of these measurements are plotted in the usual way $N(E)/\sqrt{E}$ in relative units vs E in Fig. B-1. These measurements were made over an 8-h period on the machine at a flight path of 2.04 m with 1.85-MeV neutrons. Pulse shape discrimination in a 1-in.-thick liquid scintillator was needed to extend the measurements to 13 MeV. The upper three curves represent the results on ^{238}U, ^{235}U, and ^{239}Pu with (n,γ) discrimination. The calculated efficiency for the detector did not take into account the loss of high-energy neutrons in the (n,γ) mode of operation. Therefore, the Maxwellian temperatures T_f measured are somewhat lower than those summarized by Barnard et al.[1] at comparable excitation energies. The bottom curve represents the results on ^{238}U without (n,γ) discrimination. The measured T_f of 1.30 ± 0.03 MeV for ^{238}U in this mode of operation agrees well with Barnard's value of 1.29 ± 0.03 MeV. Adjusting the detector efficiency for the loss of high-energy neutrons using the ^{238}U (n,γ) data results in a T_f = 1.38 ± 0.03 MeV for ^{235}U and a T_f = 1.44 ± 0.03 MeV for ^{239}Pu. These compare well with the reported values of 1.38 ± 0.04 MeV[2] and 1.42 ± 0.03[2,3] for ^{235}U and ^{239}Pu, respectively, for an excitation energy of 3.9 MeV. Further measurements are planned on ^{238}U to study the shape of the fission spectrum as a function of excitation from below the first fission barrier to above the second fission barrier.

---

[1] E. Barnard, A. T. G. Ferguson, W. R. McMurray, and I. J. Van Heerden, Nucl. Phys. 71, 238 (1965).

[2] I. I. Bondarenko et al., Proc. Sec. Int. Conf. on Peaceful Uses of Atomica Energy (Geneva) 15, 353 (1958).

[3] G. N. Smirenkin, JETP (USSR) 37, 1822 (1959).

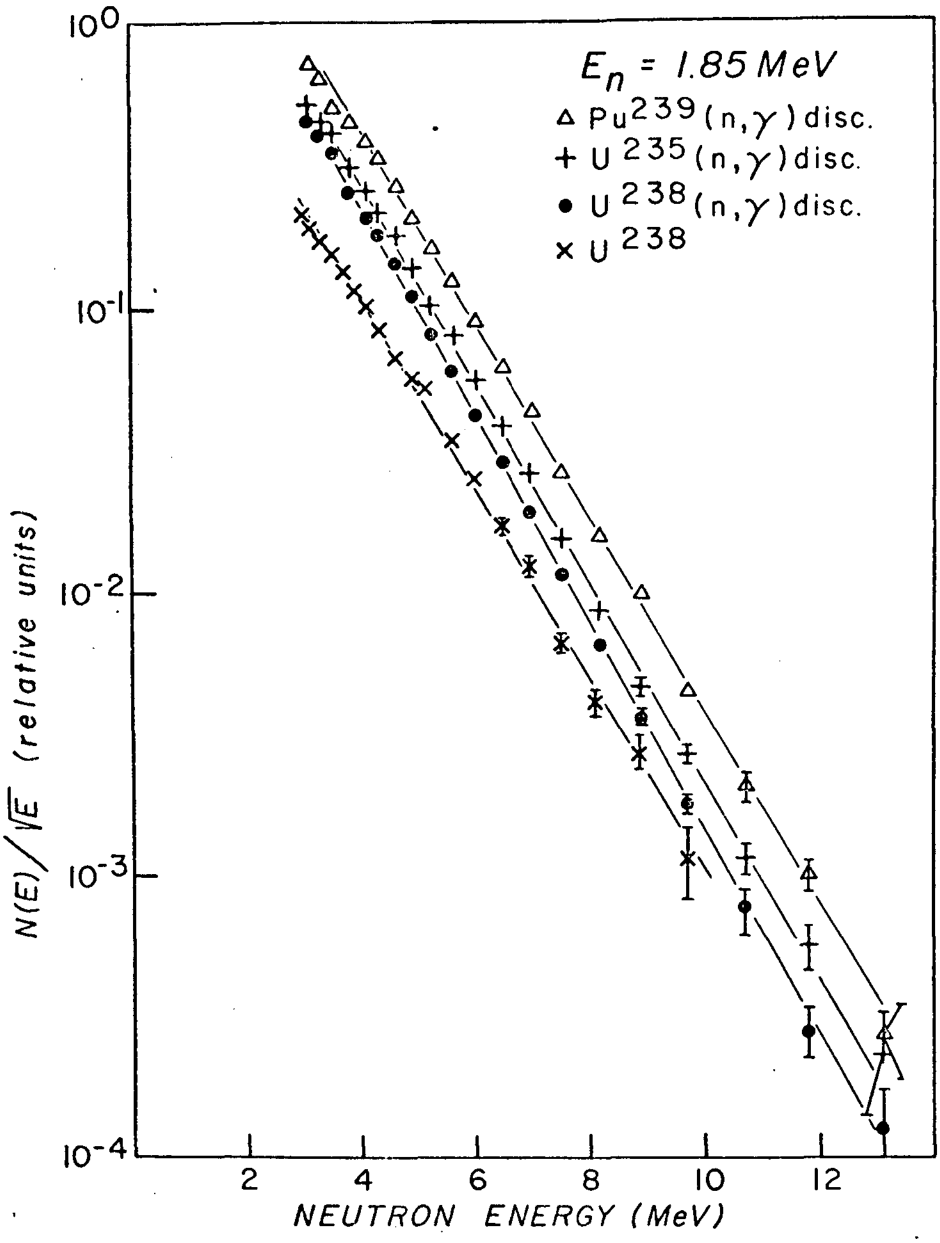

Fig. B-1. Neutron spectra for ^{239}Pu, ^{235}U, and ^{238}U for incident neutron energy of 1.85 MeV. Data labeled (n,γ) disc., imply the use of pulse-shape discrimination to eliminate gamma radiation in the detector.

2. Absolute Cross Sections for $^{235}U(n,f)$ (Barton, Jarvis, Smith) (389, 390, 391*)

Measurements have been essentially completed from 1-6 MeV. Further data reduction awaits results of ^{235}U fission foil assays from NBS and BCMN.

3. Gamma-Ray Production (Drake)

An LA report is being prepared which contains gamma-ray production cross sections measured for 1- and 2-MeV neutron interactions with ^{235}U and ^{239}Pu. A paper is being prepared which combines this report with the results of measurements of gamma-ray production cross sections of ^{235}U for neutron energies of 5 to 8 MeV in half-MeV steps. These higher energy measurements show good agreement in shape and magnitude when compared with the energy conservation relation given in the recent evaluation of Stewart and Hunter.[1]

4. Neutron Source Reaction: $^{3}T(p,n)^{3}He$ (Hopkins, Martin, Seagrave; McDaniels, U. of Oregon; Drosg, U. of Vienna)

A revised draft of the paper has been written, and Legendre polynominal fitting has been implemented. Final values should be available shortly. Revised zero-degree cross sections are given in Table B-2, which supersede those given on p. 113 of USNDC-1.

TABLE B-2

Zero-Degree Cross Sections for $^{3}T(p,n)^{3}He$

E_p (MeV)	$\sigma(0°)$ mb/sr
4.00	99.2 ± 2.3
5.00	71.6 ± 1.6
6.00	48.8 ± 1.1
7.00	36.3 ± 0.8
8.00	29.1 ± 0.7
9.00	27.2 ± 0.6
10.00	27.9 ± 0.6
11.00	30.8 ± 0.8
12.00	34.0 ± 0.8
13.00	36.8 ± 0.9
14.00	40.4 ± 0.9
15.00	43.5 ± 1.0
15.50	44.7 ± 1.0

[1] L. Stewart and R. E. Hunter, "Evaluated Neutron-Induced Gamma-Ray Production Cross Sections for ^{235}U and ^{238}U," LA-4918.

5. Neutron Source Reaction for Polarized Neutrons (Simmons, Broste, Martin; Donoghue, Ohio State University; Haight, LLL)

A paper entitled, "Sources of Polarized Neutrons from 2 to 33 MeV using Polarization Transfer Reactions at 0°," and with the following abstract has been submitted to Nuclear Instruments and Methods:

"In the recent polarization transfer measurements at 0° for the $T(\vec{p},\vec{n})^3He$, $D(\vec{d},\vec{n})^3He$, and $T(\vec{d},\vec{n})^4He$ reactions, large neutron polarizations were measured. Because the reaction cross sections are also large at this angle, the figures of merit for these reactions as sources of polarized neutrons are appreciably larger than for reactions initiated by unpolarized beams. Thus polarization transfer reactions are new and important sources of polarized neutrons over most of the 2 to 23 MeV energy interval. Other significant advantages of these reactions are discussed."

C. THERMAL NEUTRON CAPTURE GAMMA-RAY STUDIES

1. Study of the Levels in ^{151}Nd via the ^{150}Nd (n,γ) Reaction (Smith, Starner, Bunker)

We have continued our analysis and interpretation of the high- and low-energy ^{150}Nd neutron-capture γ-ray spectra. In addition to concluding that the ground-state assignment for ^{151}Nd is 3/2, $3/2^+[651]$, we have also identified the $1/2^-[530]$, $1/2^-[521]$, $3/2^-[521]$, and $3/2^-[532]$ Nilsson rotational bands. The $3/2^+[651]$ and $3/2^-[532]$ bands were not identified in the (d,p) work of Nealy and Sheline [C. L. Nealy and R. K. Sheline, Phys. Rev. 164, 1503 (1967)]. There are, however, some unanswered questions regarding the compatibility of the Nealy-Sheline (d,p) data and our (n,γ) data. It seems likely that there are a number of degenerate peaks in the existing (d,p) spectra, and we feel that a remeasurement of the $^{150}Nd(d,p)^{151}Nd$ spectrum (at the higher resolution now attainable) would be very helpful in clearing up the picture. Accordingly, D. G. Burke and J. C. Waddington (McMaster University) have consented to perform this measurement in the next few weeks. Further interpretation of the ^{151}Nd level scheme and final preparation of the manuscript describing our study of this nucleus will await their results.

2. $^{143}Nd(n,\gamma)^{144}Nd$ (Jurney; Raman, Slaughter, Harvey, ORNL; Wells, Lin, Tennessee Technological University; McClure, Georgia Inst. Tech.)

We have carried out extensive thermal neutron capture γ-ray measurements [singles and Ge(Li)-Ge(Li) coincidences] and resonance neutron capture γ-ray measurements leading to excited states in ^{114}Nd. The resulting level scheme is quite complex with ≈50 levels below 4.0 MeV. In

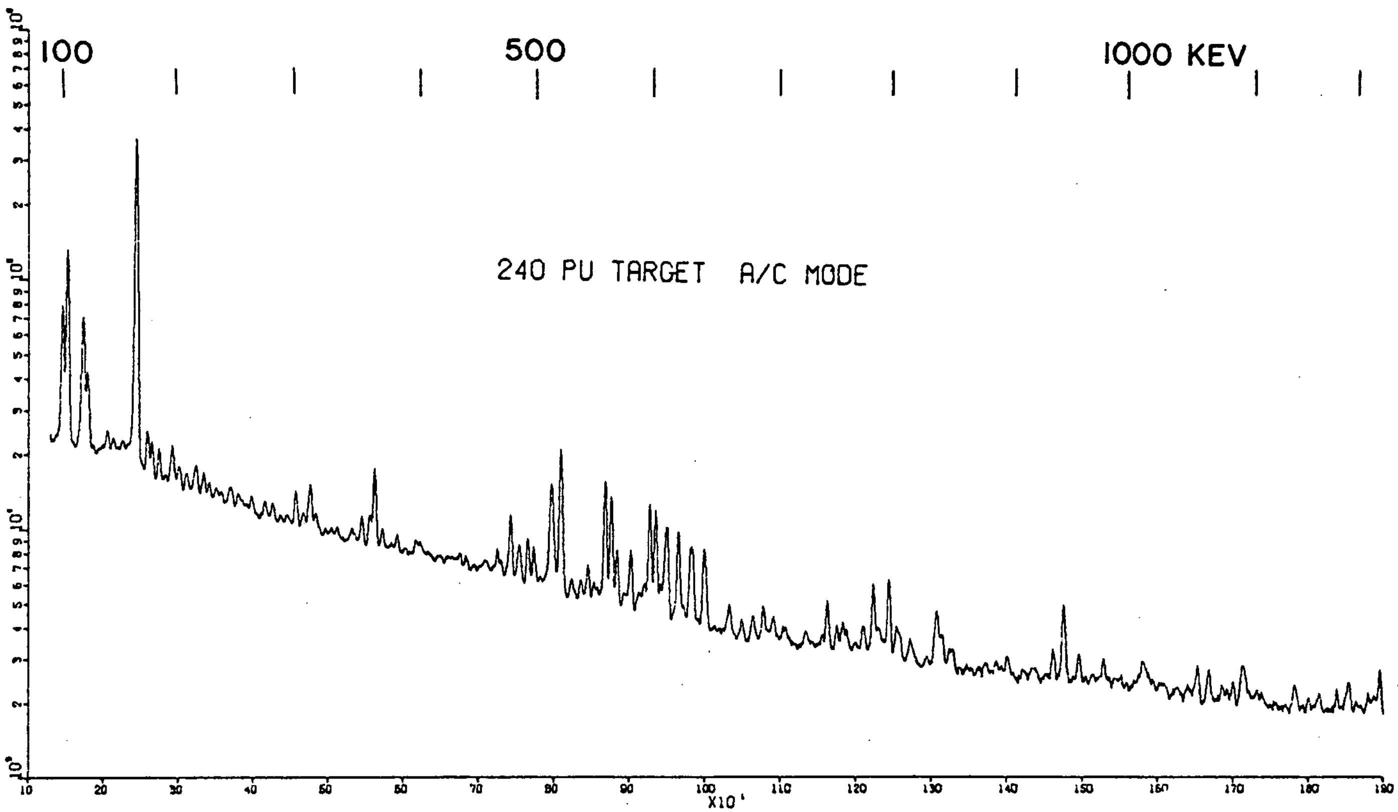

Fig. C-1. Gamma spectrum from $^{240}Pu(n,\gamma)$ observed with a Ge(Li) detector below 1.3 MeV.

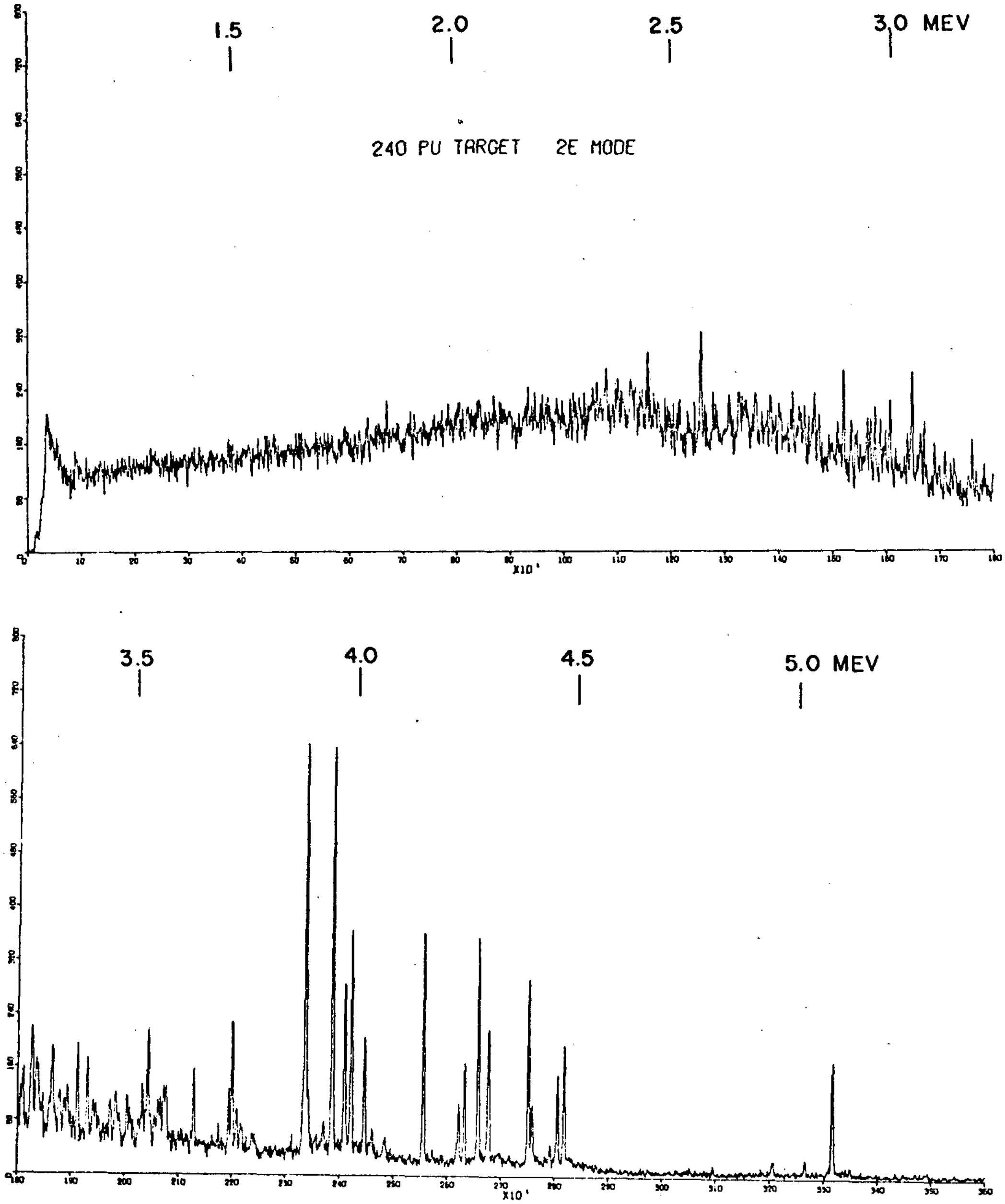

Fig. C-2. Gamma spectrum from ^{240}Pu(n,γ) observed with a Ge(Li) detector from 1.3 to 5 MeV.

thermal n-capture, we have observed for the first time the 7120-keV, primary E1 γ-ray from the 3^- capturing state to the 696-keV 2^+ first-excited state. The observed intensity is 0.0027 ± 0.0006 photons/100 n-captures. The 7120-keV γ-ray is also present in the γ-spectra from n-capture in all known 3^- resonances below 410 eV except the 350-eV resonance. A paper will be presented at the Seattle APS meeting describing this work.

3. $^{240}Pu(n,\gamma)^{241}Pu$ (Jurney)

The Ge(Li) data have been analyzed in those energy regions where it was possible to resolve individual transitions, up to 1.3 MeV and above 3.2 MeV. These regions yielded 182 and 62 lines, respectively. On an energy-weighted summation basis the fraction of the capture cross section thus resolved in the two regions is 8.0 and 8.4%. The strong line at 161.7 keV (Fig. C-1) is the deexcitation of the $1/2^+[631]$ band head to the ground state; its photon intensity is 24 γ/100 n, and, after correcting for internal conversion, the transition intensity corresponds to 188 b (70%) of capture cross section.

In the high-energy spectrum the strong transition at 5.08 MeV excites the $1/2^+$ member of the $1/2^+[631]$ band. Weak primary transitions are seen to the $3/2^+$ and $5/2^+$ members of this band. The absence of transitions between 4.5 and 5 MeV corresponds to the 126-neutron energy gap (Fig. C-2).

D. FISSION STUDIES

1. Fission Barriers Deduced from the Analysis of Fission Isomer Results (Britt, Bolsterli, Nix, Norton)

A paper with the above title and the following abstract will shortly be submitted to the Physical Review:

"Available experimental data on fission isomer excitation functions have been reanalyzed using an improved statistical model to determine values for the energies relative to the ground state of the secondary minimum and second maximum in the fission barrier for a series of plutonium, americium, and curium isotopes. The statistical model incorporates realistic decay width calculations for neutron emission, fission, and gamma-ray emission which are based on nuclear level densities derived from appropriate single particle level spectra. Values for the curvature $\hbar\omega_B$ of the second barrier are also estimated from the observed fission isomer half-lives. The fission barrier parameters determined from the analysis of experimental results are compared to theoretical calculations of barrier performed by several groups. The experimental barrier parameters agree with a variety of theoretical calculations to an accuracy of about 1 MeV. Systematic deviations between the experimental and theoretical results suggest that the surface asymmetry constant κ in the liquid drop mass surface should be substantially larger than the value of 1.7826 used in the second mass formula of Myers and Swiatecki."

2. Fission of Actinide Nuclei Induced by Direct Reactions (Back, Britt, Garrett, Lerous, Hansen, Kurjan)

The fission decay of a large number of isotopes in the actinide region has now been studied by means of the following reactions: (p,p'f) (d,pf), (t,pf), (t,df), (t,t'f), (t,αf), (^{3}He,df), (^{3}He,tf), and (^{3}He,αf). By these techniques we have obtained fission probabilities as a function of excitation energy in the fissioning nucleus for the following isotopes: ^{229,230,231,232,234}Th, ^{230,231,232,233}Pa, ^{231,232,236,238,240}U, ^{234,235,236,237,238,239}Np, ^{237,238,241,242,244}Pu, ^{239,240,241,243,245,247}Am, ^{243,244,248,249,250}Cm, and ^{249}Bk. With the last runs in September we have now finished the experimental program. The quality of the data is determined by the lowest fission probability $P_{f\ min}$ one can extract from the data and the energy resolution. This range is from ~50 keV resolution and $P_{f\ min}$ ~10^{-3} for the (t,pf) and (d,pf) reactions to ~150 keV resolution and $P_{f\ min}$ ~0.05 for some (^{3}He,αf), (t,αf), and (^{3}He,tf) reactions. The wide spread in quality is mainly caused by differences in cross sections and kinematics. Most of the high-quality data are for even-even nuclei. In the heavy Cm-isotopes the results show that the threshold in ^{250}Cm is ~1 MeV lower than in ^{248}Cm and ^{244}Cm. Such a large shift caused by adding on 2 neutrons has not been observed in other even actinide nuclei, and it is possibly connected with the N = 152 shell.

The analysis of data for even-even nuclei is almost finished, and barrier parameters are extracted for most of these nuclei. This was done in most cases by using a least-squares fitting program in connection with the analysis program, which calculates the fission probability using a double-humped fission barrier with damping in the second well.

E. EVALUATION

1. An R-Matrix Analysis of Reactions in the ^{17}O System (Hale, Young, Foster)

Data from the reactions ^{16}O(n,n), ^{16}O(n,α), and ^{13}C(α,α) corresponding to neutron energies below 4 MeV have been fit simultaneously, using the Energy Dependent Analysis code (EDA) at Los Alamos. EDA is a general multilevel, multichannel R-matrix fitting code that has the capability of calculating arbitrary observables for reactions involving two-body channels whose particles have arbitrary masses, spins, parities, and charges. The code incorporates an advanced variable-metric search algorithm. Included in the fit are: total and differential cross sections for $^{16}O(n,n)$; total cross sections, differential cross sections, and neutron analyzing powers for $^{16}O(n,\alpha)$; and differential cross sections for $^{13}C(\alpha,\alpha)$. The parameters found by Johnson[1] in a similar analysis were used as a guide to starting values for the search. Our parameters agree generally with those of Johnson, and the differences can be attributed to the somewhat different data selection and parameterization of the R-matrix used in the present analysis.

2. Test of Single-Channel Strength-Function Limit (Devaney)

A paper[2] describing our findings in testing the limitations of Γ/D, the strength function, has been accepted for publication by the Physical Review. We have shown rigorously for one simple potential (square well) that Γ/D is unbounded and, in particular, has the form $(2\pi\Gamma/D) = -\ln(1-T)$ suggested by Moldauer (T is transmission). Therefore, extrapolation of resonance parameters to higher energies, which is often the best way to estimate the higher energy cross sections, is a permissible procedure.

3. Absolute Yield and Neutron Spectrum from Thick Be and Li Targets (Foster, Auchampaugh, Drake)

Sharply renewed interest has developed recently in cheap, intense sources of polyenergetic neutrons produced by smaller and cheaper sources than the large linacs and cyclotrons. In particular, thick-target Li(d,n) may be a promising source of neutrons above 10 MeV for medical irradiations,[3] and both that and thick-target Be(d,n) offers promise for transmission measurements in the MeV range. Measurements of the absolute yield and neutron spectrum at 0° from thick targets of ^{6}Li, ^{7}Li, and ^{9}Be have been completed at the vertical Van de Graaff at selected energies related to proposed uses. The detector was placed at 3 m with a threshold of about 0.16 MeV. Tentatively, it was confirmed that much of the yield from natural lithium below 5 MeV comes from ^{6}Li, and therefore can be reduced by the use of enriched targets, but that an intense low-energy group from ^{7}Li appears for deuteron energies above 2 MeV. The yield of 3-MeV neutrons from ^{9}Be for 5.5-MeV deuterons at typical Van de Graaff currents competes favorably with the intensity of electron-linac sources.

---

[1] C. H. Johnson, submitted to Phys. Rev. (1972).

[2] J. J. Devaney, "Test of Single-Channel Strength-Function Limit," Phys. Rev. (to be published October 1972).

[3] L. Cranberg, "Reaction and Target Design Options for a Neutron Source for Neutron Teletherapy," Summer Meeting of the American Association of Physicists in Medicine, Philadelphia, PA (June 29, 1972).

F. NUCLEAR RESEARCH RELATED TO SAFEGUARDS: REVISED LASL DELAYED-NEUTRON YIELD DATA (Evans, Thorpe, Krick)

Delayed neutron yields measured by Krick and Evans[1] and by Masters et al.[2] have been reevaluated. The ^{238}Pu-Li calibration source used in both measurements was sent to the National Bureau of Standards, where a 1.3% calibration was performed. The source recalibration indicates that the yields reported by Masters et al. and by Krick and Evans are 4.6% high and should be reduced accordingly. Furthermore, the quantity of fissile material on ^{238}U and ^{239}Pu fission-chamber foils used for both experimental programs has been remeasured to ±2% using a low-geometry alpha-counting system of well determined accuracy. Since the prior ^{239}Pu foil value was within 1% of the remeasured value, the yield values were not adjusted for the new foil values. However, the ^{238}U foils were found to have 3.35% more uranium than was originally believed. The effect of this is to increase the measured value of the delayed neutron yield of ^{238}U proportionately, so that the combined effect of calibration-source and fission-foil renormalization of the delayed neutron yield of ^{238}U is to require multiplication of the values obtained by Masters et al. for this isotope by 0.988.

A technical note describing these results has been accepted by Nuclear Science and Engineering. On the basis of an error analysis, described in detail in this technical note, it is estimated that the revised Masters delayed-neutron yield values for 3.1-MeV fission are accurate to within ±7.4% for the ^{235}U, ^{238}U, and ^{239}Pu and 8.7% for ^{232}Th and ^{233}U. Uncertainties of the Krick-Evans values are of similar magnitude.

Data corrected in accordance with the above considerations are presented in Table F-1, together with the prior data of Keepin.[3] The probable errors quoted by Keepin have been multiplied by 1.49 in order to convert them into standard deviations for direct comparison with the new data. It is seen that adequate agreement exists among all of the LASL measurements of the delayed-neutron yield from fast fission of ^{233}U, ^{235}U, and ^{239}Pu. It is noted, however, that delayed-neutron yields from thermal fission appear to be systematically about 5% lower[3,4] than yields measured for fast fission, and this point will bear investigation, as will the 17.4% discrepancy in the measured delayed-neutron yield from fission of ^{238}U at fission-neutron energies.

[1]M. S. Krick and A. E. Evans, Nucl. Sci. and Eng. 47, 311 (1972).

[2]C. F. Masters, M. Thorpe, and D. Smith, Nucl. Sci. and Eng. 36, 202 (1969).

[3]C. R. Keepin, J. Nucl. Energy 7, Nos. 1 and 2, 13 (1958).

[4]J. F. Conant and P. F. Palmedo, Nucl. Sci. and Eng. 44, 173 (1971).

TABLE F-1

Comparison of Revised Delayed-Neutron Yield Data of Masters et al. (Ref. 2) and of Krick and Evans (Ref. 1) for fission induced by neutrons of various energies with Fast-Fission Yield Data of Keepin (Ref. 3)

	ABSOLUTE DELAYED NEUTRONS PER FISSION (AUTHOR, NEUTRON ENERGY)			
Element	Keepin et al. Fission Spectrum	Krick & Evans Averaged 0.1-1.8 MeV	Masters et al. 3.1-MeV Neutrons	Masters et al. 14.9-MeV Neutrons
^{232}Th	0.0496 ± 0.0035	---------------	0.057 ± 0.005	0.030 ± 0.0020
^{233}U	0.0070 ± 0.0006	0.0075 ± 0.0006	0.0074 ± 0.006	0.0041 ± 0.0003
^{235}U	0.0165 ± 0.0007	0.0163 ± 0.0013	0.0172 ± 0.0013	0.0091 ± 0.0004
^{238}U	0.0412 ± 0.0025	---------------	0.0484 ± 0.0036	0.0283 ± 0.0013
^{239}Pu	0.0063 ± 0.0005	0.0062 ± 0.0005	0.0066 ± 0.0005	0.0041 ± 0.0002
^{242}Pu	---------------	0.015 ± 0.005*	---------------	---------------

*Averaged 0.7 to 1.3 MeV

NATIONAL BUREAU OF STANDARDS

A. NEUTRON PHYSICS

1. MeV Neutron Total Cross Sections (R. B. Schwartz, R. A. Schrack, H. T. Heaton, II, and H. S. Camarda)

The total neutron cross sections of ^{235}U, ^{238}U, and ^{239}Pu were measured with high statistical precision over the range 0.5 to 15 MeV. The overall accuracy is estimated to be ~ 1%. Our ^{239}Pu data agree to within ~ 1-1/2% with the recent results of Smith, Guenther and Whalen, and our ^{238}U results are in equally good agreement with recent measurements of Hayes, et al at RPI. Our data are shown in Figures A-1, A-2, and A-3.

2. KeV Cross Sections (H. T. Heaton, II, J. Menke, R. A. Schrack, R. B. Schwartz, and H. S. Camarda)

A paper entitled "Use of a ^{10}B-NaI Neutron T-O-F Spectrometer" is to be presented at the Seattle Meeting of the American Physical Society. The abstract follows:

"We have developed a neutron detector for use with the NBS linac T-O-F facility to make neutron total cross section measurements from 1 keV to 1 MeV. A major feature of the detector system is the low and well behaved background characteristics. The detector consists of one kilogram of 92% ^{10}B contained in a 5" diam × 3" thick cylinder with the axis concentric to the incident beam. The 480 keV gamma rays produced by neutrons are viewed by four 3×3 NaI crystals. Extensive background investigations have been made from 1 keV to 250 keV. The crystal activation background is determined to high precision by counting during a 100 μs gate between each linac burst. An additional background has been determined by black resonance techniques and is analytically predictable for all experimental conditions. The efficiency of the detector could be increased by mixing vaseline with the ^{10}B but it was found that the background was thereby increased. Resolution measurements of the system have been made. Preliminary results of the carbon measurement will be presented.

3. Average Neutron Transmission Measurements from ~ 1 keV to ~ 700 keV (H. S. Camarda

The good stability of the NBS electron linac and the excellent signal to noise ratio of the underground T-O-F facility enable high precision neutron average transmission measurements to be made. By covering the energy range 1 keV to 700 keV it is possible to extract

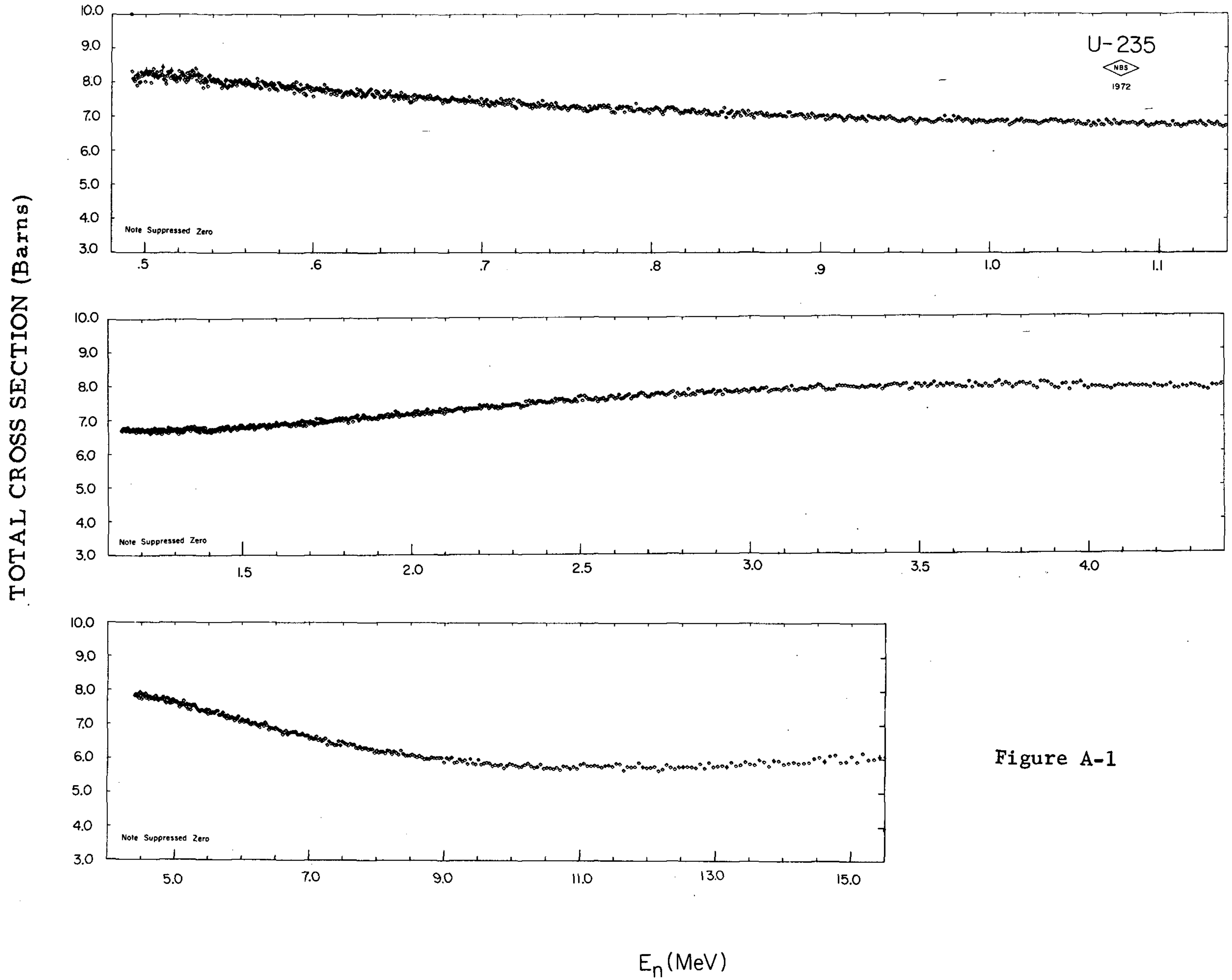
U-235
NBS
1972
TOTAL CROSS SECTION (Barns)
Note Suppressed Zero
10.0
9.0
8.0
7.0
6.0
5.0
4.0
3.0
.5
.6
.7
.8
.9
1.0
1.1
1.5
2.0
2.5
3.0
3.5
4.0
5.0
7.0
9.0
11.0
13.0
15.0
E_n (MeV)

Figure A-1

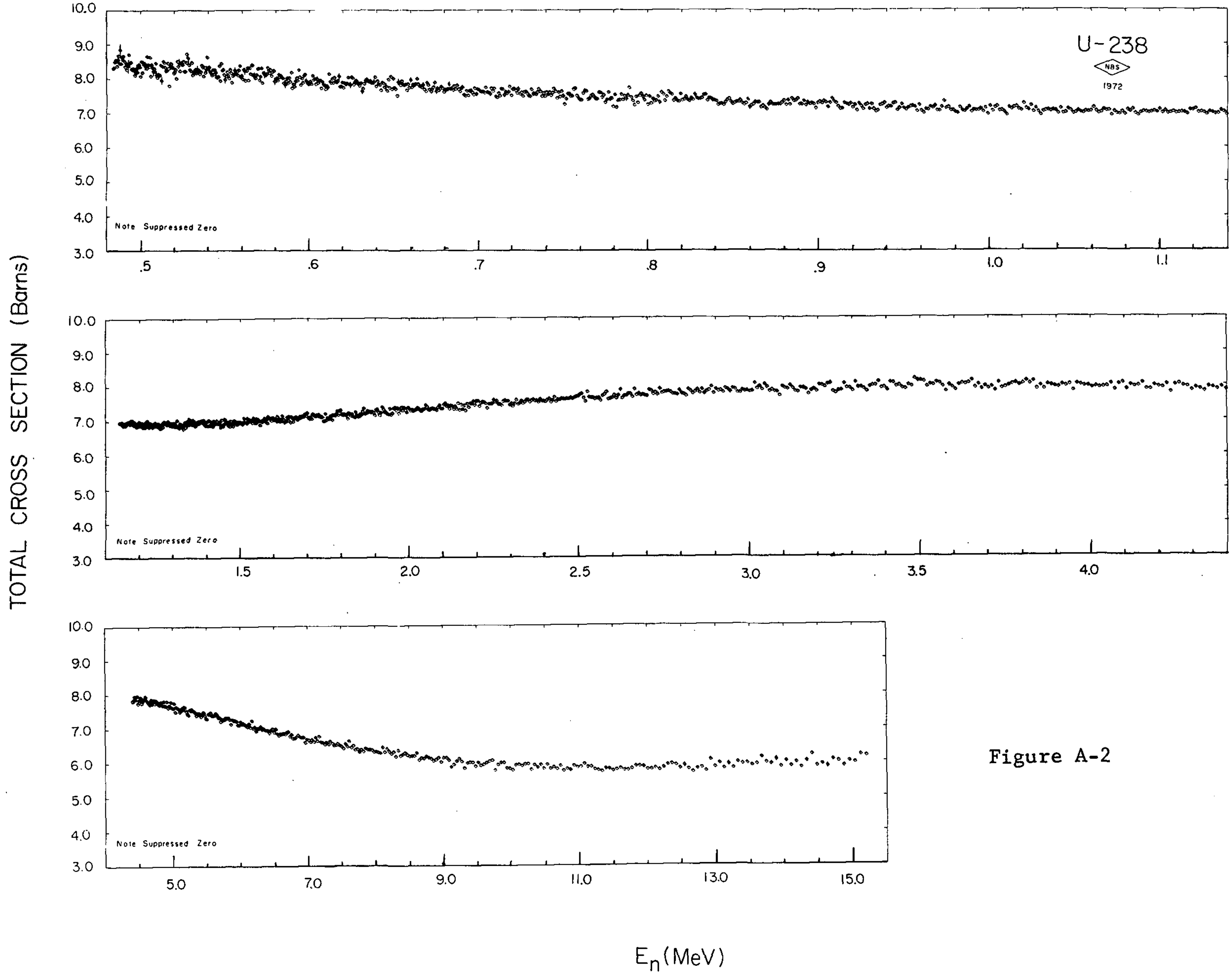
U-238
NBS
1972
TOTAL CROSS SECTION (Barns)
Note Suppressed Zero
E_n(MeV)

Figure A-2

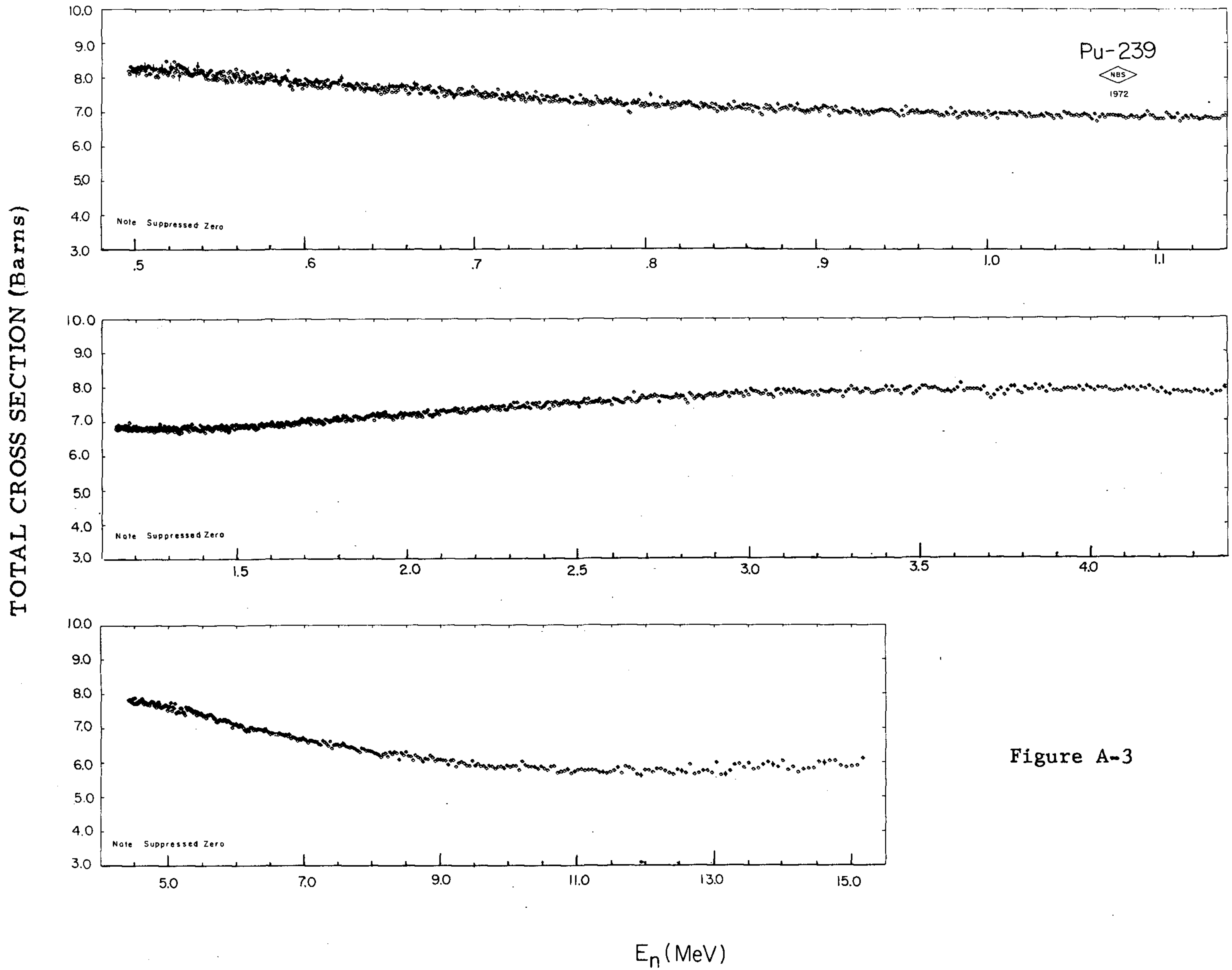
TOTAL CROSS SECTION (Barns)
Pu-239
NBS
1972
Note Suppressed Zero
10.0
9.0
8.0
7.0
6.0
5.0
4.0
3.0
.5
.6
.7
.8
.9
1.0
1.1
1.5
2.0
2.5
3.0
3.5
4.0
5.0
7.0
9.0
11.0
13.0
15.0
E_n (MeV)

Figure A-3

R_o^∞ (and hence R'), S_1 and R_1^∞ from the data. The s wave resonance contribution to the average transmission is determined by using published results obtained from the analysis of well resolved levels at low energies.

Generally, the very low energy average transmission data gives a value of R_o^∞, middle energies a determination of S_1, and higher energies R_1^∞.

The sample thicknesses used were "thick" in the sense that the s wave self-protection at low energies must be fully accounted for. However, the samples were still sufficiently thin that any errors introduced by neglecting p wave self-protection are negligible.

The initial measurements here concentrated on elements near $A \sim 100$. Preliminary results for some of the elements studied are given in the table below.

A	Sample	$S_1 \times 10^4$	R_o^∞	R_1^∞	R'(fermis)
93	N_b	5.83±.60	-.06±.02	.2±.1	6.69±.15
107.8	A_g	3.94±.50	+.03±.02	-.2±.1	6.43±.10
114.8	I_n	3.00±.50	+.085±.015	-.05±.10	6.20±.10

4. Age to Indium Resonance in Water for ^{252}Cf Neutrons (V. Spiegel)

Cadmium-covered indium foil irradiations have been made from 2.8 to 64 cm in water with 1, 3.23, and 4.47 cm diameter indium foils.

Preliminary normalization of activity as a function of distance has been done graphically. The distances were taken to be the root mean square distance between a point source and a disc detector. For about one half of the data the point source was located 0.05 cm from the geometrical axis of symmetry of the cylindrical source (0.76 cm diam × 0.76 cm height). The orientation of the source was lost when a crack developed in the aluminum tube, which supported the source. The center of the source must be redetermined for the orientation used in the latter half of the measurements. This redetermination is performed in air with a double fission ionization chamber.

Integration of the integrals

$$\tau = \int_0^\infty 4\pi r^2\ A(r) r^2\ dr \Big/ \left(6 \int_0^\infty 4\pi r^2\ A(r)\ dr\right)$$

gives an age of 28.8 cm^2, where A(r) is the indium resonance activity at the root mean square distance, r, from the source center, assumed to be 0.05 cm from the axis of symmetry in all the data.

A preliminary correction for the displacement of water by the source has been determined from the integrations of

$$\int_{r_o}^{\infty} 4\pi r^2 \, A(r)(r-r_o)^2 \, dr \Big/ \left(6 \int_{r_o}^{\infty} 4\pi r^2 \, A(r) \, dr \right)$$

where r_o (0.436 cm) is the radius of a sphere with volume equal to the cylindrical source. The corrected age is 27.3 cm^2. The correction is 5.5%, but a more exact method of calculation is being sought.

A second correction for the density of water at 20.5°C reduces the age an additional 0.4% to 27.2 cm^2.

This preliminary age, 27.2 cm^2, predicts an average energy for the ^{252}Cf neutron spectrum of 2.025 MeV from Goldstein's (1) relationship

$$\tau(\bar{E}) = 3.7 + 11\bar{E} + 0.3\,\bar{E}^2$$

whereas the uncorrected age, 28.8 cm^2, predicts 2.155 MeV.

(1) H. Goldstein et al, United Nations International Conference on the Peaceful Uses of Atomic Energy, Geneva, 1958, P/ 2375, Vol. 16, p. 385.

5. Measurement of ^{235}U and ^{238}U Fission Cross Sections for ^{252}Cf Spontaneous Fission Neutrons (J. A. Grundl, V. Spiegel, Jr., and C. M. Eisenhauer)

Absolute ^{235}U and ^{238}U fission cross sections have been measured with a small, low-mass ^{252}Cf spontaneous fission source and a lightweight, double fission ionization chamber. Main components of the measurement were (1) determination of the ^{252}Cf neutron source strength at the NBS manganous sulfate bath facility; (2) fission rate measurements in a low-scatter accelerator target room; (3) computation and experimental verification of corrections due to neutron scattering from proximate and remote structures; and (4) foil weight determinations by means of absolute alpha and thermal-neutron-induced fission counting.

The californium source is a single, cylindrical encapsulation of 0.51 mm thick stainless steel (7.6 mm long, 0.36 cc volume, and 1.5 grams total mass) enclosing a localized deposit of californium which emits 2×10^9 n/sec.* Approximately 0.5% of the spontaneous fission neutrons are absorbed or inelastically scattered by the capsule. The back-to-back

* Special fabrication of the source was carried out by personnel at the TRU Facility (ORNL).

fission chamber is of conventional design and resolves 99.4% of the fission fragments which emerge from a 0.2 mg/cm^2 fissile deposit.

Fission rate measurements were made with the source mounted at a distance of 5 cm from the fission chamber and 5 meters from the nearest section of the concrete foundation of the low-scatter room. Neutron return from the room foundations was ascertained by means of two supplementary fission rate measurements, one performed with the source at 10 cm from the fission chamber and the other with the source placed at the nearest section of the concrete foundation. Neutron return backgrounds derived from the two methods agree to better than ± 10% and give for the primary 5 cm position a background of 0.9% for ^{235}U and < 0.1% for ^{238}U. Corrections for neutron scattering in the Cf source, in individual chamber parts including the platinum-backed foils, and from nearby support structures have been estimated with the help of the NBS geometry code INTRAN which was developed for this experiment.

Fission-spectrum-averaged fission cross sections for ^{252}Cf spontaneous fission neutrons obtained from this experiment are as follows:

$$\bar{\sigma}_f\left(\chi_{Cf}, {}^{238}U\right) = 324 \pm 14 \text{ mb}$$

$$\bar{\sigma}_f\left(\chi_{Cf}, {}^{235}U\right) = 1207 \pm 52 \text{ mb}$$

$$\bar{\sigma}_f\left(\chi_{Cf}, {}^{235}U\right)/\bar{\sigma}_f\left(\chi_{Cf}, {}^{238}U\right) = 3.72_6 \pm 0.086.$$

These average cross section values provide a direct check of basic differential data. One pair of predicted values calculated with fission cross sections from ENDF/B, Version III, and a Maxwellian description of the Cf fission spectrum shape, $\chi(E) \sim \sqrt{E}\exp(-1.5E/2.13)$, is $\bar{\sigma}_f\left(\chi_{Cf}, {}^{238}U\right) = 314$ mb, $\bar{\sigma}_f\left(\chi_{Cf}, {}^{235}U\right) = 1241$ mb.

6. Cavity Fission Neutron Source (A. Fabry* and J. A. Grundl)

Extensive neutron transport computations of wall-return flux intensity and spectrum have been carried out. These computations, part of a joint effort with CEN-SCK to establish intense fluxes of pure fission neutrons, make it possible now to estimate reliably the wall-return background at the cavity Fission Neutron Source Facility. The following is an excerpt from the published summary of a paper presented at the Washington Meeting of the American Nuclear Society:

* CEN-SCK Laboratory, Mol, Belgium.

Wall-Return Neutron Fluxes for High- and Intermediate-Energy Cavity Neutron Sources. A. Fabry (CEN-SCK), D. J. Jenkins (ORNL). Spherical cavities in graphite thermal columns of nuclear reactors provide an ideal environment for the production of comparatively intense, energy distributed neutron fields, i.e., either intended pure fission neutron spectrum sources or intermediate-energy standard neutron spectra. Cavities of 50 cm diameter are used in various laboratories; a 30 cm diameter cavity is operated at NBS and a 1 meter diameter cavity has recently been implemented at CEN-SCK.

Numerical computations of graphite wall-return neutron spectra have been performed by means of the discrete ordinates multigroup method in one-dimensional spherical geometry. The evaluated nuclear data files KEDAK, ENDF/B Version 2, and ENDF/B Version 3 have been used and the convergence of the S_n multigroup multitable treatment has been established systematically.

Within the cavity, a good approximation of the wall-return is

$$\varphi_W(r,\mu,E;r_s) = \varphi_W(E) \ .$$

This relationship is correct to better than 2% for r, $r_s \leq R/2$ where R is the cavity radius and r_s the radius of a thin, fission spectrum source shell. This fundamental property has led to the development of an experimental method for determining wall-return backgrounds.

7. <u>Moments Method Calculations of Neutron and Gamma-Ray Penetration</u> (L. V. Spencer, C. Eisenhauer, and G. L. Simmons)

A report entitled "Moments Method Calculations of Neutron and Gamma-Ray Penetration in Bulk Media," describing several types of calculations performed with the NBS codes for computing distributions from moments, has been presented at the recent international shielding symposium held in Paris.1/ Included were slant penetration of fission neutrons in concrete, and description of preliminary calculations of the secondary gamma rays produced by the neutrons in concrete.

Comparison of the Snyder-Neufeld dose for normally incident neutrons is made with S_n calculations for concrete slabs, reported by F. R. Schmidt, 2/ using an ad hoc prescription that the slab boundaries

1/ Simmons, Eisenhauer, and Spencer, "Moments Method Calculations of Neutron and Gamma-Ray Penetration in Bulk Media," Fourth International Conference on Reactor Shielding, Paris, France, October 1972.

2/ F. A. R. Schmidt, "The Attenuation Properties of Concrete for Shielding of Neutrons of Energy Less than 15 MeV," ORNL-RSIC 26, Oak Ridge National Laboratory, Oak Ridge, Tennessee.

give a reduction factor in the flux which is independent of slab thickness. Agreement is within about 15% with the moments calculations slightly lower, except for large penetrations where the S_n calculations follow a systematically lower trend and the differences are much larger.

Comparisons with S_n calculations of n-γ dose by Schmidt are still too preliminary to say much about, and are more difficult because of the greater importance for γ-ray production of the low energy neutrons in slab versus infinite medium. It appears, however, that the gamma ray dose at deep penetrations is dependent mainly on the neutron flux at much lower penetration distances, so that realistic comparisons of the slab data can be made using infinite medium data adjusted to take account of an interface at the source plane. On this basis, agreement appears to be well within a factor of two, except for thin slabs which do not retain the neutrons very well. Different sets of gamma ray production cross sections are involved, and these and other differences are being investigated.

B. DATA COMPILATION

1. Photonuclear Data Center (E. G. Fuller, H. Gerstenberg, H. Vander Molen)

The Center prepared a draft supplement to NBS Special Publication 322 entitled "New Photonuclear Data" (January 1970 - July 1972) which was distributed to workers in the field at the time of the International Conference on Nuclear Structure Studies Using Electron Scattering on Photoreactions held in Sendai, Japan, September 12-15, 1972. In addition to being an annotated index to data entered in the Center's files in the period indicated, the report gives a listing of the approximately 500 curves that are now available in digital form in the Photonuclear Cross Section Library. At the time of the Asilomar Conference on Photonuclear Reactions and Applications (March 1973) the Center plans to publish a complete data index for the field covering information published in the period from 1955 through a cut-off date early in 1973.

2. Photon Cross Sections (J. H. Hubbell, G. L. Simmons)

As an NSRDS-NBS "X-ray Attenuation Coefficient Information Center" we are continuing to extract from the literature and systematize measured and theoretical photon cross section data over the energy range 10 eV to 100 GeV.

A compilation of x-ray cross section data at wavelengths used by crystallographers, produced in collaboration with LLL, is in galley proof stage.1/

Work continues on the DNA-sponsored intercomparison and evaluation of existing quasi-independent photon cross section compilations (NBS, LLL, LASL, Sandia, Kaman, and Gulf General Atomic). Results of the first phase of this intercomparison are available as a series of NBS reports. 2/

Through participation in the Shielding Subcommittee of CSEWG (Cross Section Evaluation Working Group, AEC) we are continuing to examine, update, and expand the ENDF/B photon cross section library tape. As part of this program, an evaluated set of coherent and incoherent scattering factors is in preparation, in collaboration with workers at LLL, LASL, EG&G, and Kaman, for publication in the new Journal of Physics and Chemistry Reference Data.

C. FACILITIES

1. Linac Above-Ground Neutron Facility (S. Penner)

Completion of the above-ground neutron facility for the NBS linac is behind schedule due to delays in construction of the building. We now expect to take occupancy of the building in December 1972. Construction of beam transport apparatus for this facility is essentially completed and large sections have been preassembled and aligned. Final installation will begin when we take occupancy. We will continue to use the existing time-of-flight system during installation with intermittent operation of the linac for this program and others. The above-ground facility should be ready for use in the spring of 1973.

2. 3-MeV Van de Graaff Facility (A. D. Carlson, M. Meier, and G. Lamaze)

The Van de Graaff accelerator and accompanying facility are now entirely operational. Auxiliary electronics which will allow variation of the pulsing repetition rate from 10 to 500 kHz with a variable pulse width are currently being tested. An associated particle system is being designed which will be used to produce absolutely calibrated

---

1/ J. Hubbell, W. McMaster, N. Del Grande and J. Mallett, X-Ray Cross Sections and Attenuation Coefficients, Sec. 1 of International Tables for X-Ray Crystallography, Vol. 4 (in press).

2/ G. L. Simmons and J. H. Hubbell, Comparison of Photon Interaction Cross Section Data Sets. I. Storm-Israel and ENDF/B, NBS 10668 (unpublished); II. Biggs-Lighthill and ENDF/B, NBS 10818 (unpublished); III. NSRDS-NBS 29 and ENDF/B, NBS 10842 (unpublished); IV. Kaman and ENDF/B, NBS 10847 (unpublished); and V. Photran and ENDF/B, NBS 10848 (unpublished).

neutron fluxes with the $T(p,n)^3He$ reaction. Electric and magnetic fields will be employed to analyze the outgoing ^3He particles. An on-line computer system to be used for acquisition and analysis of Van de-Graaff data is being purchased. This computer should be installed early next year. Experiments are currently being considered for the use of this facility in the measurement of standard neutron cross sections.

OAK RIDGE NATIONAL LABORATORY

A. NEUTRON PHYSICS

1. Secondary Gamma-Ray-Production Cross Sections of Several Materials*,** (G. L. Morgan, J. K. Dickens, T. A. Love and F. G. Perey)

Absolute gamma-ray-production cross sections have been measured as a function of both incident neutron and emitted gamma-ray energy for tantalum, iron, silicon, and carbon. The data include gamma-ray energies between 0.7 and 10.6 MeV for incident neutron energies up to 20 MeV. Measurements were made at angles of 90° and 125° for tantalum and carbon and at 125° for iron and silicon. Detailed tables of cross sections have been transmitted to the National Neutron Cross Section Center.

---

*Presented at the ANS Topical Meeting Kiamesha Lake, N. Y., September 12-15, 1972.

**Relevant to Request 35 for carbon, 103, 104, 105 for iron.

2. Compilation of Phenomenological Optical-Model Parameters* (C. M. Perey and F. G. Perey)

A pilot compilation, with bibliography, of optical-model parameters determined by fitting elastic-scattering angular distributions for various incident particles including heavy ions was made.

---

*To be published by Nuclear Data.

3. The ORNL Sodium Benchmark Experiment* (R. E. Maerker, F. J. Muckenthaler and C. E. Clifford)

The description of an experiment performed at the Tower Shielding Facility is presented which serves as a benchmark for deep neutron penetration through up to 15 ft of sodium. Results of calculations of the experiment are also described, using the MORSE multigroup Monte Carlo code and a preliminary version of the ENDF/B-III cross-section set for sodium. Comparison of the calculations with experiment indicate that the total neutron leakage above thermal energies penetrating 15 ft of sodium can be calculated to within ~30% and neutrons penetrating up to 10 ft of sodium to within ~10%.

---

*Presented at the ANS Topical Meeting Kiamesha Lake, N. Y. September 12-15, 1972.

4. Investigation of the Adequacy of Nitrogen Cross-Section Sets: Comparison of Neutron and Secondary Gamma-Ray Transport Calculations with Integral Experiments* (E. A. Straker,** ed)

Two sets of cross sections for neutron interactions and secondary gamma-ray production in nitrogen, one recently evaluated by P. G. Young and D. G. Foster and another assembled in 1968 by the author, have been tested in transport calculations corresponding to integral experiments. The experiments are Operation HENRE, during which measurements were made of the neutron and gamma-ray doses produced in the atmosphere by an accelerator emitting approximately 14-MeV neutrons, and two experiments in which liquid-nitrogen-filled dewars were pulsed with approximately 14-MeV neutrons. One of the nitrogen-dewar experiments, performed at Gulf Radiation Technology, yielded the energy spectra of fast and intermediate energy neutrons and secondary gamma rays within the nitrogen, and the other, performed at Lawrence Livermore Laboratory, gave time-dependent count rates due to neutrons leaking from the nitrogen. The comparisons of the calculated and measured results showed that for Operation HENRE both cross-section sets were adequate for calculating the neutron doses but that only the old set correctly predicted the gamma-ray doses, the new set giving results that are 30 to 50% lower than the data. Conversely, the comparisons for the GRT nitrogen-dewar experiment showed that the new set gives gamma-ray spectral data that are in reasonable agreement with the data, whereas the old set overpredicts by as much as a factor of 2. For both nitrogen-dewar experiments, the new cross sections give better predictions of the neutron spectra and time-dependent neutron count rates than the old cross sections. Additional calculations with both sets of cross sections for an infinite-air medium show that the two sets give identical neutron and secondary gamma-ray doses for a fission source; they also give very similar neutron doses for a 12.2- to 15-MeV neutron source, but the secondary gamma-ray doses are in disagreement, those obtained with the newer set being 30 to 50% lower. "Sensitivity" calculations indicate that for high-energy neutron sources most of the secondary gamma rays are produced by neutrons having energies greater than 10 MeV, and the greatest difference between the two cross-section sets is their gamma-ray production probabilities at high neutron energies. On the basis of the various comparisons, it appears that the new neutron cross sections give better predictions of neutron quantities, but that a choice between the gamma-ray production cross sections is not obvious since each set agrees with one of the two gamma-ray experiments.

---

*Paper presented by E. A. Straker at TTCP Working Panel N-6, London, England, September 21-24, 1971, and at RSIC Seminar-Workshop on Radiation Transport in Air, November 15-17, 1971; also ORNL-TM-3768.

**Present address: Science Applications, Inc., Huntsville, Alabama.

5. A General Formalism for Computing the Transition Matrix of Nuclear Reaction Theory, and Its Application to the Treatment of the Coupled Channel Equations* (R. B. Perez)

One develops a general integro-differential equation for the transition matrix of nuclear reaction theory in terms of the physical parameters of the nuclear reaction. On this basis, one arrives at a unified formalism which affords a great degree of flexibility regarding the boundary conditions of the basic set of eigenfunctions utilized to construct solutions of the radial Coupled Channel Equations.

One also develops, as a corrollary of the main result, a system of equations which describes the motion of the poles and residues of the collision matrix as a function of the parameters entering in the reaction formalism. Various applications are shown to illustrate the present technique.

---

*Abstract of ORNL-TM-3778.

6. A Test of Neutron Total Cross-Section Evaluations from 0.2 to 20 MeV for C, O, Al, Si, Ca, Fe and SiO_2*, (F. G. Perey, T. A. Love and W. E. Kinney)

Neutron transmission measurements, from 0.2 to 20.0 MeV, have been made for the shielding materials carbon, oxygen, aluminum, silicon, calcium, iron and the compound silicon dioxide. The measurements were performed at the ORELA Shield Test Station with a resolution of about 0.12 nsec/meter on sample thicknesses varying from 0.65 to 0.9 atoms/barn. The transmission measurements were compared with the predictions obtained from the Defense Nuclear Agency evaluated cross-section library. Since the total cross-section files for these elements are also the ones present in the ENDF/B-III library, we are also checking its total cross-section files for all of the elements with the exception of oxygen. There are serious discrepancies between our data and the predictions based on the evaluated files. These discrepancies are often large in the energy region from 0.2 to 0.6 MeV.

---

*Abstract of ORNL-4823.

7. Neutron-Induced Gamma-Ray Production in Iron for the Energy Range $0.8 \geq E_n \geq 20$ MeV*,** (J. K. Dickens, G. L. Morgan and F. G. Perey)

Cross sections for production of gamma rays due to neutron interactions with iron have been measured as a function of both neutron and gamma-ray energy. Two experimental configurations were used to obtain the data, and these were (a) a NaI-spectrometer system using the Oak Ridge Linear Accelerator as the neutron source, and (b) a Ge(Li)-spectrometer system using a pulsed Van de Graaff and the D(d,n) reaction as the neutron source. The NaI-spectrometer system is described completely in this report. It was used to acquire data for $0.8 \leq E_n \leq 20$ MeV and $\theta_\gamma = 125$ deg, which were unfolded to obtain $d^2\sigma/d\omega dE$ values for gamma-ray energies between 0.7 and 10 MeV. The Ge(Li) system was used to obtain high-resolution information on the production of discrete-line $d\sigma/d\omega$ values for $4.85 \leq E_n \leq 9.0$ MeV and θ_γ = 55, 75 and 90 deg. Our data are compared with previously reported experimental data and with the current ENDF/B evaluation. Although there is generally reasonable (20%) agreement, important differences among these data are discussed.

---

*Abstract of ORNL-TM-3850

**Relevant to Request Nos. 103, 104, 105.

8. Gamma-Ray Production Due to Neutron Interactions with Iron for Incident Neutron Energies Between 0.8 and 20 MeV: Tabulated Differential Cross Sections*,** (J. K. Dickens, G. L. Morgan and F. G. Perey)

Numerical values of differential cross sections for gamma rays produced by neutron reactions with iron have been obtained for neutron energies between 0.8 and 20 MeV. The data are primarily for $\theta_\gamma = 125$ deg with supporting data at θ_γ = 35, 75 and 90 deg. These data consist of (a) discrete-line values of $d\sigma/d\omega$ for 45 orbserved transitions due to neutron interactions with natural iron; and (b) neutron gamma-ray production group cross section values of $d^2\sigma/d\omega dE$ for $0.7 \geq E_\gamma \leq 10.5$ MeV, with gamma-ray group sizes ranging from 20 keV for $E_\gamma \leq 1$ MeV to 160 keV for $E_\gamma \leq 9$ MeV. The $d\sigma/d\omega$ values were obtained for $4.85 \leq E_n \leq 9.0$ MeV using a Ge(Li) spectrometer. Additional discrete-line $d\sigma/d\omega$ values for $4.85 \leq E_n \leq 6.45$ MeV at $\theta_\gamma = 125$ deg have been tabulated for 66 observed transitions due to neutron interactions with an iron sample enriched in the isotope ^{54}Fe. The $d^2\sigma/d\omega dE$ values were obtained for $0.8 \leq E_n \leq 20$ MeV using a NaI spectrometer.

---

*Abstract of ORNL-4798

**Relevant to Request Nos. 103, 104, 105.

9. Values of the Average Fission Cross Section of ^{235}U (R. Gwin, E. G. Silver and R. W. Ingle)

The energy dependence of the neutron fission cross section of ^{235}U has been measured relative to the $^{10}B(n,\alpha)$ cross sections. The normalization was made in the thermal energy region to values given in ENDF/B MAT 1157.

The following table shows average values of the ^{235}U fission cross sections for energy intervals which extend to 200 keV. There is both a normalization difference and a difference in energy dependence between the present work and the ENDF/B III values.

^{235}U (n,f) Average Cross Sections[a]

E1 → E2 (keV)	ORNL-RPI	LASL Lemley et al.	Gwin, Silver, Ingle,[b] 9-72	ENDF/B-III MAT 1157
0.1 - 0.2	21.03	20.90		21.42
0.2 - 0.3	20.86	20.15	19.80	20.30
0.3 - 1.0	11.58	11.09	11.07	11.77
1.0 - 2.0	7.51	6.74	7.06	7.68
2.0 - 3.0	5.60	5.06	5.16	5.70
3.0 - 4.0	5.09	4.51	4.55	5.05
4.0 - 5.0	4.56	4.01	4.11	4.52
5.0 - 10.0	3.46	3.11	3.14	3.50
10 - 20		2.34	2.42	2.80
20 - 30		2.10	2.04	2.37
30 - 40		1.90	1.88	2.20
40 - 50		1.81	1.72	2.03
50 - 60		1.77	1.76	1.98
60 - 70		1.71	1.70	1.88
70 - 80		1.62	1.66	1.81
80 - 90		1.59	1.55	1.74
90 - 100		1.55	1.52	1.68
100 - 200			1.44	1.50
10 - 100		1.82	1.81	
.1 - 100		2.12	2.11	

[a] $$\bar{\sigma}_f = \frac{\int_{E1}^{E2} \sigma_f(E)\,dE}{E2 - E1}$$

[b] Thermal normalization.

10. A Unified R-Matrix-plus-Potential Analysis for $^{16}O + n$ Cross Sections* (C. H. Johnson)

A multilevel two-channel R-matrix analysis is made for both the neutron total and angle-integrated (n,α) cross sections of ^{16}O for 0 - 5.8 MeV neutrons. Off-resonant phase shifts are described in terms of scattering in a real Saxon-Woods local potential with a Thomas-type spin-orbit term and with a parity dependence for the well depths. (An alternative energy-dependent potential is also chosen but not used.) The well parameters are chosen to bind the $1d_{5/2}$ and $2s_{1/2}$ levels at the energies of the ground and first excited states in ^{17}O and the quasibound $1d_{3/2}$ level at the centroid of five observed $3/2^+$ resonances. The $1d_{3/2}$ level is replaced in the analysis by five observed fragments which contain nearly 100% of the $1d_{3/2}$ strength and have their eigen-energy centroid at 5.74 MeV in ^{17}O. The well-known 5.08 MeV level in ^{17}O has 69% of the strength. The R-matrix boundary radius must be chosen rather carefully inside the tail of the potential in order to subtract the $1d_{3/2}$ state and in order to place the unbound 2p and 1f states at energies consistent with the observed p- and f-wave fragments. Thus, a composite model consisting of a potential well and a specific R-matrix boundary radius is used to describe the observed single-particle structure of ^{17}O in both the bound and the unbound regions. The resonance energies, neutron reduced widths and spectroscopic factors are deduced for 26 levels in ^{17}O between 4.5 and 9.5 MeV. The sums of the spectroscopic factors in this region are found to be 1% for $J^\pi = 1/2^+$; 5% for $1/2^-$; 12% for $3/2^-$; 99% for $3/2^+$; 0.1% for $5/2^+$; 1% for $5/2^-$ and 14% for $7/2^-$. Some J^π values are deduced and reported in a companion paper.

---

*Submitted to Phys. Rev. for publication.

11. Neutron Capture in Fluorine from 2.5 to 1500 keV* (R. L. Macklin and R. R. Winters**)

Neutron time-of-flight radiative capture data taken at the Oak Ridge Electron Linear Accelerator have been analyzed for single level resonance parameters. Ten resonances were found, with parameters as indicated, listing E_o (keV), J value assumed, and Γ_γ(eV) in order. 27.07 (2)1.4 $\pm$ .3, 48.7(1)1.73 $\pm$ .44, 97.0(1)6.0 $\pm$ 1.8, 269(1)4.2 $\pm$ 1.0, 386(1) 7 $\pm$ 2, 490.5(0)10 $\pm$ 3, 595(1)12.6 $\pm$ 2, 1460(1)11 $\pm$ 3. Values of total width were also found for these resonances. Two resonances are very narrow and their capture areas yield estimates of $g\Gamma_n$. At 43.5 keV $g\Gamma_n$ = .086 $\pm$ .02 eV if J $\geq$ 1 or Γ_n = .42 $\pm$ .1 eV if J=0, and at 173.5 keV $g\Gamma_n$ = .35 $\pm$ .10 eV. The increase of nearly an order of magnitude in radiative width with increasing energy is notable. Five large resonances between 1600 and 3000 keV were not analyzed because of detector sensitivity to the inelastic scattering channel which opens in that energy region and uncertainty of the flux normalization.

---

*To be presented at the Seattle, Washington APS Meeting, November 2-4, 1972.

**On sabbatical leave from Denison University.

12. keV Neutron Total Cross Section Measurements at ORELA* (J. A. Harvey)

Neutron total cross sections are measured at ORELA using samples as small as a few square millimeters, flight paths from 18 to 200 meters, with energy resolutions ($\Delta E/E$) from 1/300 for measurements below ~10 keV to ~1/2500 up to 200 keV and $\sqrt{E(\text{in MeV})}/1000$ above 1 MeV. A new efficient neutron detector using NE-110 has been developed for keV measurements whose efficiency is ~30% for 10 keV neutrons rising to 90% for 50 keV neutrons. Transmission measurements using iron-filtered neutron beams have been made upon thick samples of iron 4", 6", 12" and 20" to obtain accurate values of the cross-section minima. Enriched ^{54}Fe and ^{57}Fe samples have been measured to determine their contributions to the windows in natural iron.

*Presented at the ANS Topical Meeting Kiamesha Lake, N. Y. September 12-15, 1972

13. Valency Neutron Capture in ^{92}Mo(n,γ)^{93}Mo*† (O. A. Wasson** and G. G. Slaughter)

Capture γ ray spectra from the ^{92}Mo(n,γ)^{93}Mo reaction were measured at the Oak Ridge Electron Linear Accelerator. The partial radiation widths for 12 high energy γ ray transitions from 23 s- and p-wave resonances for E_n < 25 keV were deduced and compared with the predictions of the valency model of neutron capture. The spins and parities of the resonances were determined from γ ray angular distribution measurements and neutron transmission and total capture results. For E_γ < 6.5 MeV the average M1 partial width is about equal to the average E1 width. The reduced strengths are $\bar{k}(E1) = (1.2 \pm 0.2) \times 10^{-3}$ and $\bar{k}(M1) = (11.5 \pm 2.3) \times 10^{-3}$. For the 7129 keV transition to the s1/2 first excited state the reduced strength is larger by factors of 5 and 2 for E1 and M1 widths respectively. Nearly 30% of this enchancement for E1 multipoles is attributed to the valency model contribution while the remainder is assigned to other processes such as the giant dipole resonance and doorway state components. For the 8067 keV ground state γ ray $\{\Gamma(E2)\}$ ~0.10$\{\Gamma(E1)\}$.

*To be presented at the Seattle, Washington APS Meeting, November 2-4, 1972.
**Present address: Brookhaven National Laboratory, Upton, L. I., N. Y.
†Relevant to Request Nos. 222 and 223.

14. Neutron Capture Cross Section Measurements for ^{86}Sr, ^{87}Sr and ^{88}Sr* (G. J. Vanpraet,** R. L. Macklin, B. J. Allen,*** and R. R. Winters†)

Neutron capture cross sections for ^{86}Sr, ^{87}Sr and ^{88}Sr have been measured from 3 keV up to 600 keV with total energy detectors. Maxwellian averaged cross sections are calculated as a function of energy. The correlation between these values and the solar system isotopic abundances are discussed in terms of stellar nucleosynthesis by slow capture.

---

*Presented at the Nuclear Structure Study with Neutrons, Budapest, Hungary, July 31-August 5, 1972.

**Present address: State University Center of ANTWREP, Belgium.

***Present address: Australian Atomic Energy Commission, Lucas Heights.

†Present address: Denison University, Granville, Ohio

15. P-Wave Resonances in $^{111}Cd(n,\gamma)^{112}Cd$* (O. A. Wasson** and B. J. Allen***)

Gamma-ray spectra and total capture yields were measured for resonant neutron capture in an enriched ^{111}Cd sample for neutron energies less than 2.3 keV. The experiment utilized the 40 m flight path of the Oak Ridge Electron Linear Accelerator and a non-hydrogenous liquid scintillator γ ray detector. A total of 162 resonances were observed in this interval, and the resonance energies and neutron widths deduced. Approximately 14% of the resonances are assigned to p-wave capture on the basis of the γ-ray spectral measurements while an additional 23% are assigned to s-wave capture on the basis of their large neutron widths. The parity of the remainder is undetermined. A lower limit of 0.9×10^{-4} is observed for the p-wave neutron strength function $[\Sigma g\Gamma_n 1/(2\ell+1)\ \Delta E]$ while the s-wave neutron strength function $[\Sigma g\Gamma_n o/\Delta E]$ is 0.15×10^{-4}.

---

*Submitted for publication in Phys. Rev. C.

**Present address: Brookhaven National Laboratory, Upton, L. I. N. Y.

***Present address: Australian Atomic Energy Commission, Lucas Heights.

16. Doorway State in ^{206}Pb Revisited* (B. J. Allen,** R. L. Macklin, C. Y. Fu and R. R. Winters***)

The neutron capture cross section of $^{206}Pb(n,\gamma)$ has been measured with high resolution at the Oak Ridge Electron Linear Accelerator. The capture results show that the reported s1/2 doorway in ^{206}Pb is not observed in the photon channel.

---

*Submitted to Physical Review Letters for publication.

**Present address: Australian Atomic Energy Commission, Lucas Heights.

***Present address: Denison University, Granville, Ohio.

17. Neutron Resonance Parameters of ^{92}Mo*,** (O. A. Wasson,*** B. J. Allen,† R. W. Winters,†† R. L. Macklin and J. A. Harvey)

Neutron transmission and total neutron capture yields were measured using the time-of-flight technique at the Oak Ridge Electron Linear Accelerator facility using enriched samples of ^{92}Mo. A total of 42 resonances were observed for neutron energies less than 32 keV. Twelve are assigned to s-wave interactions while 23 are assigned to p-wave interactions. The resonant energies, neutron widths, radiation widths and spins are reduced. The average s- and p-wave radiation widths are equal to 0.178 $\pm$ 0.015 eV and 0.24 $\pm$ 0.03 eV respectively. The s-wave neutron strength function is (0.65 $\mp$ 0.26) x 10^{-4} while the p-wave strength function is (3.3 $\pm$ 1.1) x 10^{-4}.

*Submitted for publication in Phys. Rev. C.

**Relevant to Request No. 222.

***Present address: Brookhaven National Laboratory

†Present address: Australian Atomic Energy Commission, Lucas Heights.

††Present address: Denison University, Granville, Ohio.

18. Program for Measuring Radiative Capture Cross Sections* (R. L. Macklin, B. J. Allen,** R. W. Winters*** and J. Halperin)

The neutron capture cross section facility at ORELA has operated well during the year. Samples run from September 21, 1971 through September 20, 1972 (i.e. samples run since the last report) include: ^{19}F, ^{27}Al, ^{32}S, ^{43,44}Ca, ^{51}V, ^{55}Mn, ^{59}Co, ^{89}Y, ^{93}Nb, ^{106,108,112,113,114,116}Cd, ^{142,143,144,145,146,148}Nd, ^{196}Hg, and ^{209}Bi. Data reduction to cross sections has been completed for some of these but a comprehensive computer program is still under development. The energy range covered is generally from 3 keV to 500 keV or the first inelastic threshold if higher. In cases of particular interest for capture, the first few hundred keV above the inelastic threshold can be covered by raising the bias (from .15 MeV) or correcting for the inelastic gamma yield where the inelastic cross sections are known.

*Relevant to Request Nos. 95,113,207,242.

**Present address: Australian Atomic Energy Commission, Lucas Heights.

***Present address: Denison University, Granville, Ohio.

19. Neutron Fission and Absorption Cross-Section Measurements for ^{239}Pu and ^{241}Pu*,** (L. W. Weston and J. H. Todd)

The neutron fission and absorption cross sections for ^{239}Pu and ^{241}Pu were measured from thermal-neutron energies to 30 keV. Since the fission and absorption cross sections were measured simultaneously, the ratio of the capture and fission cross sections, $(\sigma_c)/(\sigma_f)$, could be derived up to a neutron energy of 250 keV. Although data analysis is in the preliminary stages, several conclusions can already be drawn.

The present data are normalized to the ENDF/B value at 0.025 eV. Above 30 keV the data show a more gentle decline than does ENDF/B. Below 2 keV the present data are appreciably higher than the ENDF values. The discrepancies between ENDF and the present data can be readily explained by the inadequacies of the experimental data on which the ENDF evaluation was based.

As a check on the method, and also because of its importance to the LMFBR program, the values of $(\sigma_c)/(\sigma_f)$ for ^{239}Pu were also measured. The results for ^{239}Pu were in excellent agreement with the measurements of Gwin et al.[1] This agreement is significant because of the very different techniques used. Since the more recent measurements of $(\sigma_c)/(\sigma_f)$ for ^{239}Pu by different experimenters using different techniques are now producing reasonably consistent agreement, much greater confidence can be placed in the knowledge of this parameter.

---

*Abstract of Paper 1.3 in ORNL-4800 (1972).

**Relevant to Request Nos. 450, 474.

[1] R. Gwin et al., Neutron Phys. Div. Annu. Progr. Rep., May 31, 1971, ORNL-4705, p. 4 (1971).

20. Measurement of Neutron Fission Cross Section for ^{239}Pu and ^{235}U from 0.02 eV to 200 keV*,** (R. Gwin, E. G. Silver and R. W. Ingle)

Experiments have been performed in which the neutron fission cross sections of ^{239}Pu and ^{235}U were measured over the energy region from 0.02 eV to 200 keV. The primary goal of these experiments was to provide neutron cross-section data over a neutron energy range of importance for the design of fast breeder reactors.

The experimental technique used was essentially the same as reported previously.[1] The neutron flux was based upon the $^{10}B(n,\alpha)$ cross section suggested by Sowerby et al.[2] Normalization of the data was made at thermal energy to values given in ENDF/B II.

The results on $\overline{\sigma}_f$ for ^{235}U and ^{239}Pu suggest that the ENDF/B II (March 1971) values for these isotopes are too large. Since the ENDF/B II data sets are reasonably consistent with integral experiments, the present results also suggest that other ENDF/B II neutron cross sections may be too large [$\overline{\sigma}_\gamma(^{238}U)$ for example].

---

*Abstract of Paper 1.4 in ORNL-4800 (1972).

**Relevant to Request Nos. 387-390,449,450.

[1] R. Gwin et al., Nucl. Sci. Eng. 45, 25 (1971).

[2] M. G. Sowerby et al., Proc. Conf. Nuclear Data for Reactors, Helsinki, Vol. I, p. 161, IAEA (1970).

21. Averaged ^{238}U Capture Cross Sections Between 100 and 1200 eV*
(E. G. Silver, G. de Saussure and R. B. Perez)

The capture cross section of ^{238}U, averaged in 100 eV intervals between 0.1 keV and 1.2 keV, has been obtained with samples of 3 mil and 25 mil thicknesses. For each of the two samples thicknesses, the resulting measured cross sections were corrected for the effects of multiple scattering and resonance self-shielding by calculating the cross sections, using the ENDF/B-III resonance parameter compilation, both for the zero-thickness case, where the corrections do not apply, and by the Monte-Carlo method for the thickness actually used. The ratio of the two calculated results, also averaged over the same energy intervals, was used to correct the experimental data. Although the corrections are very large in some energy regions (of the order of a factor of three in the largest case), the results for the two sample thicknesses agree to within better than one percent in all cases.

*Abstract of Paper 1.6 in ORNL-4800 (1972).

22. Preparations for Precision Measurements of Fission Cross Sections for ^{235}U and ^{239}Pu*,** (R. W. Peelle, R. W. Ingle, L. W. Weston, J. H. Todd and F. E. Gillespie)

Preparations for measurements of fission cross sections and their ratios using methods which sacrifice counting rate and perhaps resolution to obtain detector efficiencies which are stable and relate directly to the underlying energy-dependent cross sections have continued. The 20-m station at flight path 8 has been prepared for the experiment, the performance of a gridded ionization chamber containing boron has been evluated as a flux monitor, initial tests have been made on a double back-to-back fission chamber, and most of the required electronic gear has been assembled. Initial measurements are planned soon to search for any apparent energy dependence in the relative (2π) counting efficiency for foils with ^{235}U deposits of various thickness.

A series of high-isotopic-purity ^{235}U deposits of $\sim$0.04 and 0.1 mg/cm^2 on 0.5-mil Al foils were prepared by vacuum evaporation of UO_2 under direct heating by electron bombardment; a comparable set of $\sim$0.1 and $\sim$0.4-mg/cm^2 deposits were prepared by electrodeposition. For the thinner foils the evaporated deposits seem preferable. The deposits are being intercompared by gamma-ray, and in some cases alpha-particle, counting techniques. Efforts to obtain comparable deposits of ^{239}Pu ($\leq$0.1 mg/cm^2) are under way.

*Abstract of Paper 1.8 in ORNL-4800 (1972).

**Relevant to Request Nos. 387-391,450.

23. The Generation of Kapur-Peierls Parameters from R-Matrix Parameters by the Invariant Imbedding Techniques* (R. B. Perez and G. de Saussure)

The Kapur-Peierls[1] dispersion theory leads to a very convenient parameterization of the cross section. This is especially true for the fissile nuclei, where level interference and channel effects are of importance.[2] A drawback of these types of cross-section parameterizations is that very little is known about the statistical properties of the Kapur-Peierls-type parameters. However, from the existing relationships between these parameters and the R-matrix parameters, whose statistical properties are known, one can infer the statistical distribution of the former set by various techniques.

In this work we have developed equations that generate Kapur-Peierls parameters from R-matrix parameters by invariant imbedding techniques. These equations, together with the initial conditions $g_{\lambda c}(0) = \Gamma_{\lambda c}^{1/2}$ and $\varepsilon_{\lambda}(0) = E_{\lambda}$, form a Cauchy initial value problem, which lends itself easily to solution.

There are several advantages to our method. It applies to any value of the angular momentum and does not involve iterative techniques or the inversion of matrices.

To demonstrate the feasibility of this method, our equations have been coded for s-wave neutrons and the results compared with some POLLA[3] calculations.

---

*Abstract of Paper 1.11 in ORNL-4800 (1972)

[1]P. L. Kapur and R. E. Peierls, Proc. Roy. Soc. (London) 166,277 (1928).

[2]D. B. Adler and F. T. Adler, "Neutron Cross Sections in Fissile Elements," Proc. Conf. on Breeding, Economics, and Safety in Power Reactors, October, 1963, ANL-6792, p. 695 (1963).

[3]G. de Saussure and R. B. Perez, POLLA, a FORTRAN Program to Convert R-Matrix-Type Multi-level Resonance Parameters for Fissile Nuclei into Equivalent Kapur-Peierls-Type Parameters, ORNL-TM-3599 (1969).

B. CHARGED PARTICLES

1. The Calculation of Heavy-Ion Interactions* (H. W. Bertini, T. A. Gabriel, R. T. Santoro and J. D. Hunt**)

The interactions of energetic nucleons ($E \geq 100$ MeV) with complex nuclei have been shown to be reasonably well represented by the method of intranuclear cascades followed by evaporation.[1] In this method the life histories of each incident nucleon and all nucleons that interact with it are followed until they escape from the nucleus or are captured. Every interaction is assumed to be a free-particle-type interaction with the individual nucleons of the nucleus. These interactions are modified to include the effects of the Fermi motion of the bound nucleons, the changing nucleon density and changing nuclear potential with nuclear radius, and the exclusion principle. After the life histories of all of the particles involved in these collisions (for each incident particle) are followed, the remaining nucleus is made to lose its residual excitation energy by particle evaporation.[2]

This approach and the associated computer programs are being adapted to the calculation of heavy-ion interactions. The underlying assumption is that at sufficiently high interaction energies (MeV per nucleon >> binding energy per nucleon) the heavy-ion reaction can be represented in large part as the high-energy interaction of two Fermi gas clouds. As the clouds merge, cascades develop simultaneously in both, with nucleons being knocked out of both, until they separate. Each cloud (nucleus), now generally reduced in mass and in a highly excited state, moves away from the other, losing its excitation energy by the "boil off" of particles.

As a first step in these calculations, the simultaneous development of the cascade in each nucleus is approximated in the following manner: if the incident heavy ion consists of A_p nucleons ($p \equiv$ projectile), then $A_p - Z_p$ neutrons and Z_p protons are sent into a stationary target nucleus one at a time, and the cascades for each of these nucleons are allowed to develop in the target, independently of the other incident nucleons. The nucleons of the projectile that interact in the target are removed from the projectile leaving holes therein. The nucleons of the projectile that miss or simply pass through the target are considered to form a residual projectile (with the holes), and hence this fragment is in an excited state. The direction of the fragment is altered slightly from the initial projectile direction to account for the fact that the vector momentum of the particles (due to the Fermi motion) removed from the projectile does not, in general, add to zero. It is assumed that prior to the reaction the vector momenta of the Fermi motion of all of the particles within the projectile add to zero. When particles are removed, the vector momentum of the remaining particles is not zero, and hence the residual projectile is allowed recoil in the direction of the resultant momentum. Both the residual target and projectile are in excited states and they are made to lose this excitation energy by particle evaporation.[2]

For this first step in the calculation, the cascade is allowed to take place in the target only, but this accounts for only half of the reaction; i.e., the weight of this event is 1/2. The other half of the reaction is calculated by letting A_t ($t \equiv$ target) nucleons with appropriate energy strike the projectile (which is now assumed to be stationary) and by letting the cascade develop in the projectile. This calculation is carried out in the same manner described above, but at the end of the interacting process the results are transformed back to the laboratory frame. Each forward and corresponding "backward" calculation is repeated, using Monte Carlo techniques, until a sufficient number of samples representing the heavy-ion interactions has been taken.

It is acknowledged that there are many deficiencies in this approach; the most notable is probably the need to include the reduction in nuclear density as the cascade proceeds. However, the calculation of heavy-ion reactions is an extremely complicated problem that has heretofore defied formulation. The method being tried is our first attempt at penetrating the bulwarks of these reactions where existing programs need only be modified and not developed. Comparisons of the predicted results with experimental data will be made, but the supply of available data is extremely meager.

A somewhat similar approach was tried for alpha particles on complex nuclei, where the alpha particle was assumed to consist of four nucleons impinging on a target.[3] The "backward" calculation was not included. The agreement of the calculated results with experimental data was fair.

---

*To be presented at the ANS Meeting, Washington, D. C., November 12-17, 1972

**Present address: Sioux Falls College, Sioux Falls, South Dakota 57101.

[1]H. W. Bertini, M. P. Guthrie, and Arline H. Culkowski, ORNL-TM-3148 (1972) (to be published in Phys. Rev.); H. W. Bertini, Phys. Rev. 188, 1711 (1969); H. W. Bertini, Phys. Rev. 131, 1801 (1963), with erratum Phys. Rev. 138, AB2 (1965).

[2]M. P. Guthrie, ORNL-TM-3119 (1970).

[3]T. A. Gabriel, R. T. Santoro and R. G. Alsmiller, Jr., ORNL-TM-3153 (1970).

2. Elastic and Inelastic Scattering of 12-MeV Protons from ^{92}Mo, ^{94}Mo, ^{96}Mo, and ^{100}Mo: Tabulated Differential Cross Sections*

(J. K. Dickens, E. Eichler, R. J. Silva and I. R. Williams**)

Numerical values of differential cross sections for elastic and inelastic scattering of 12.0-MeV protons from ^{92}Mo, ^{94}Mo, ^{96}Mo, and ^{100}Mo are reported in tabular form. Cross sections were determined at 5-deg intervals between laboratory angles of 20 and 165 deg. Inelastic scattering data are reported for 23 excited states of ^{92}Mo, 14 excited states of ^{94}Mo, 2 excited states of ^{96}Mo, and 6 excited states of ^{100}Mo.

---

*Abstract of ORNL-TM-3913.

**Present address: Knoxville College, Knoxville, Tennessee.

OHIO UNIVERSITY ACCELERATOR LABORATORY

A. STRUCTURE OF ^{12}B BETWEEN E_x = 5.0 MeV AND E_x = 8.0 MeV. (C. E. Nelson, S. L. Hausladen, and R. O. Lane)

An R-matrix analysis has begun on ^{11}B + n neutron elastic differential cross section data taken at the Ohio University Tandem Accelerator Laboratory. Preliminary results support the J value assignments of Fossan* for the states at 5.610 MeV and 5.730 MeV excitation and indicate spins and parities of $J^{\pi} = 2^+$ and $J = 3^-$. There is also evidence for a new broad 1^- state near E_x = 5.90 MeV. In addition, the state or states near E_x = 6.6 MeV appear to have positive parity.

---

*D. B. Fossan *et al.*, Phys. Rev. **123**, 209(1961).

B. LEVEL STRUCTURE OF ^{11}B FROM FAST NEUTRON ELASTIC DIFFERENTIAL SCATTERING CROSS SECTIONS FOR ^{10}B. (S. L. Hausladen, C. E. Nelson, and R. O. Lane)

Differential scattering cross sections were measured for incident neutrons with energy between 1.4 and 4.5 MeV. Preliminary results show two overlapping states of opposite parity at E_n = 1.8 MeV. This agrees with a previous R-matrix analysis*. A state at E_n = 2.7 MeV shows strong d-wave formation. A weak d-wave state is also seen at 4.3 MeV. Analysis of this data via a 2 level-4 channel R-matrix formalism is currently in progress.

---

*Lane, Hausladen, Monahan, Mooring and Langsdorf, Jr., Phys. Rev. C**4**, 380(1971).

RENSSELAER POLYTECHNIC INSTITUTE

A. CROSS SECTION MEASUREMENTS

1. Neutron Capture and Total Cross Sections *

(R. W. Hockenbury, N. N. Kaushal, and R. C. Block)

Capture, transmission and neutron flux measurements have been completed on ^{54}Fe, ^{58}Ni and ^{64}Ni emphasizing the energy region from 100 eV to about 35 keV. Figures A1 and A2 show capture and transmission data for ^{61}Ni. Isotopic assignments of resonances have been made (see Tables A1 - A4). Tables A1 and A2 for ^{54}Fe and ^{58}Fe supercede those previously reported.[1] Note that the 11.2 keV resonance previously assigned to ^{56}Fe is now properly attributed to ^{54}Fe. Also two resonances previously assigned to ^{58}Fe have been deleted. The use of better samples and improved resolution also has caused some modification for ^{61}Ni and ^{64}Ni; the latest resonance listings are given in Tables A3 and A4.

A series of pulse-height vs. time-of-flight measurements were made in ^{54}Fe, ^{58}Fe, ^{61}Ni, and ^{64}Ni in order to determine the detector efficiency for neutron capture in these isotopes. The capture, transmission and pulse-height data are being analyzed in order to obtain resonance parameters and an estimate of p-wave strength functions below about 35 keV.

*Req. No. 102, 107, 111, 120, 126

2. Neutron Capture and Fission Cross Sections of ^{242}Pu*

(R. W. Hockenbury and R. C. Block)

The ^{242}Pu sample has been prepared for cross section measurements and canned in Al. New photomultiplier bases and a new preamplifier are being tested for these measurements since the ^{242}Pu is so radioactive. Foreground and background measurements have been made to determine the counting rates for various Linac operating conditions. Resonance structure and sub-threshold fission groups below 3 keV were observed in our preliminary measurements to be similar to that previously reported. The present measurements will concentrate on the region from 3 to 60 keV.

*Req. No. 489, 490

3. Total Neutron Cross Section of Deuterium From Approximately Zero to 1000 keV

(P. Stoler, N. N. Kaushal and F. Green)

Transmission measurements were carried out upon gaseous samples of deuterium over the energy range from ≈ 0 to 1000 eV. A combination of precise point cross section measurements, using an 8-in. iron filter

---

1. R. W. Hockenbury, Z. M. Bartolome, J. R. Tatarczuk, W. R. Moyer, and R. C. Block, Phys. Rev. 178, 1746 (1969)

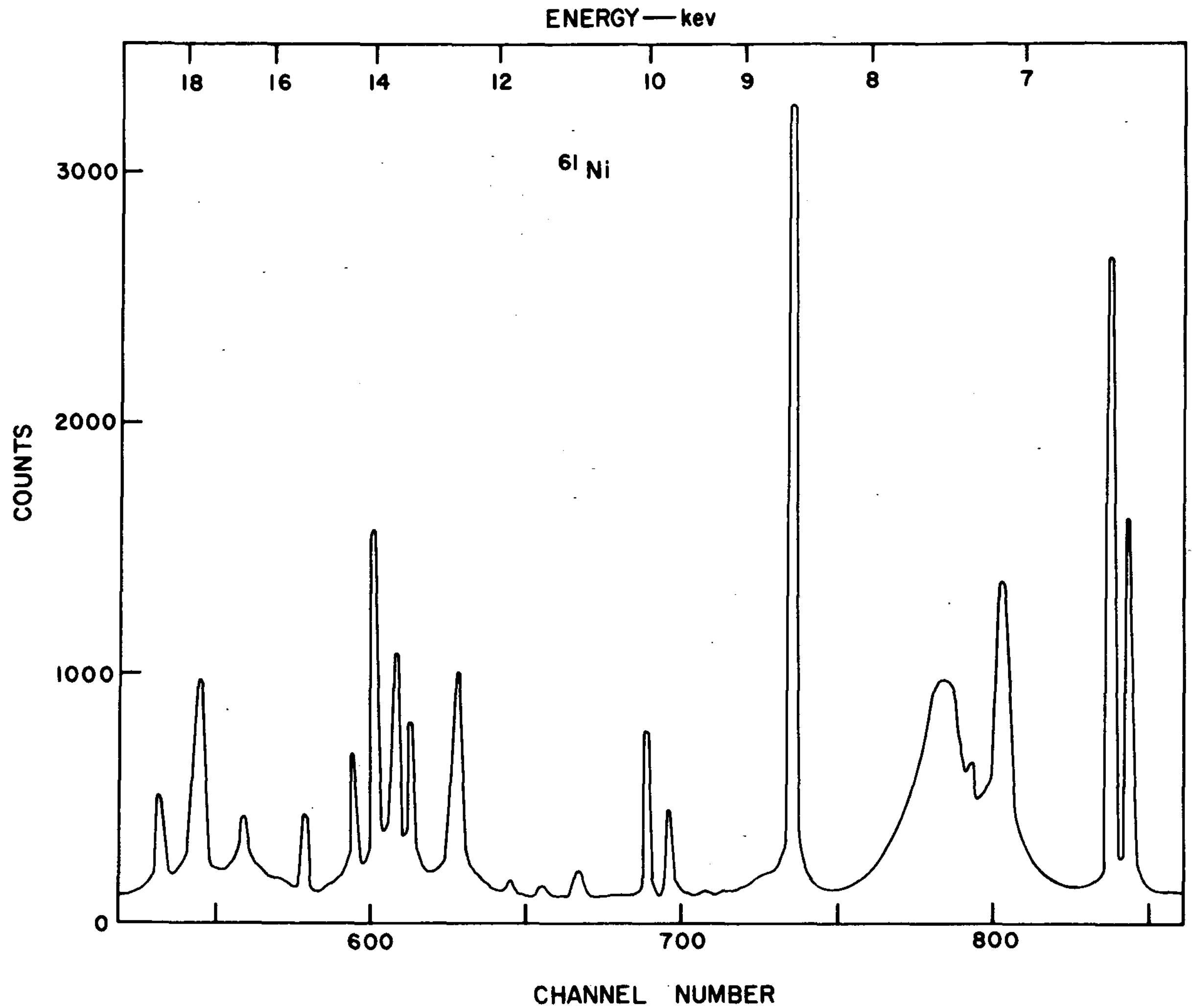
ENERGY — kev
18
16
14
12
10
9
8
7
61 Ni
3000
2000
1000
0
COUNTS
600
700
800
CHANNEL NUMBER

Figure A1

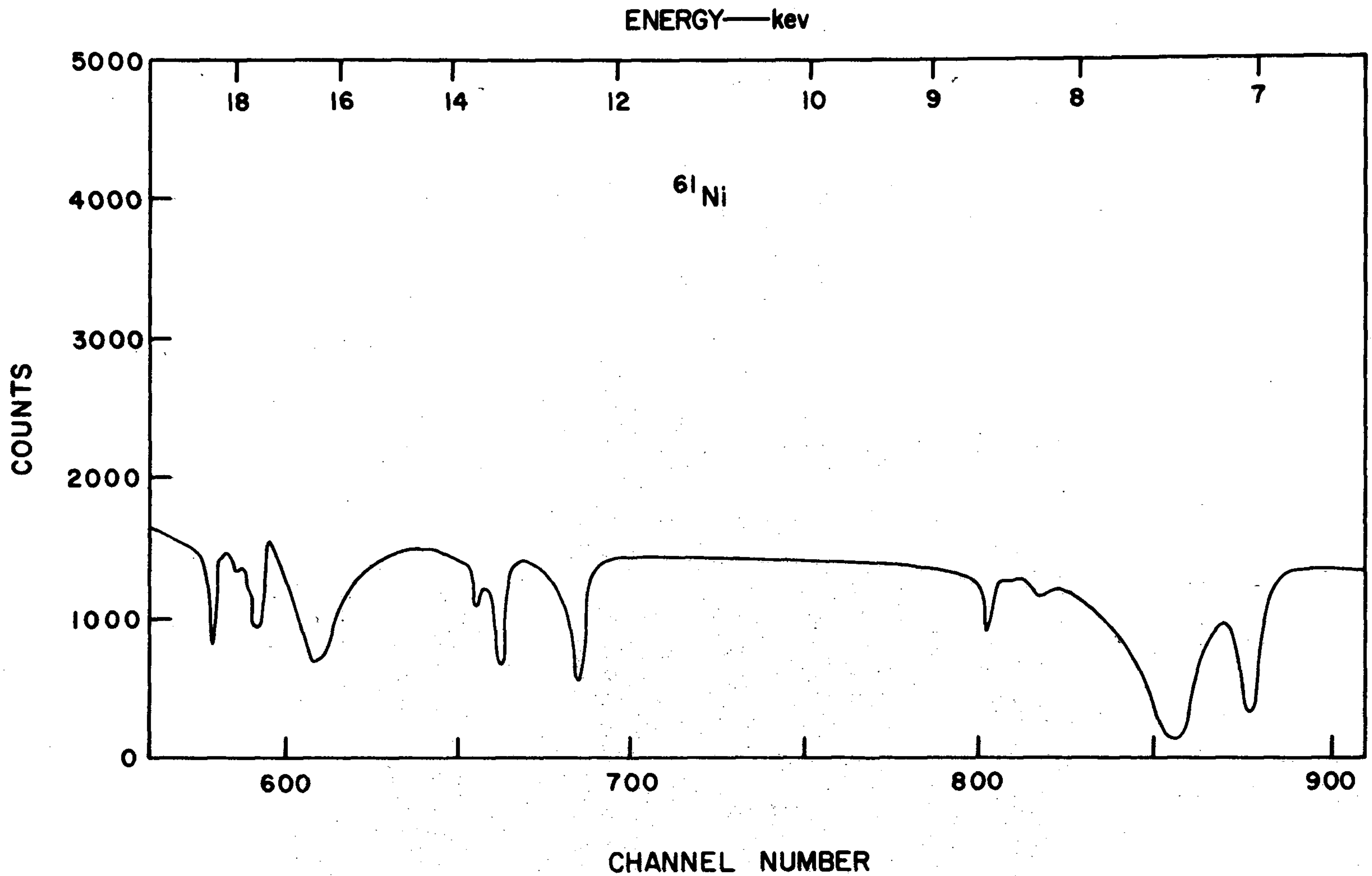
ENERGY——kev
18 16 14 12 10 9 8 7
^{61}Ni
5000
4000
3000
2000
1000
0
COUNTS
600 700 800 900
CHANNEL NUMBER

Figure A2

Table A1
^{54}Fe

E_o (keV)	E_o (keV)
3.10	23.0
8.10	28.2
9.48	30.6
11.2	35.1
13.5	38.3
14.4	39.1
19.2	

Table A2
^{58}Fe

E_o (keV)
0.230
0.359
6.20
10.5
19.2

Table A3
^{61}Ni

E_o (keV)	E_o (keV)
1.35	11.4
2.35	11.8
3.14	12.6
3.30	13.3
3.39*	13.5
4.59*	13.9
6.36	14.3
6.46	15.3
7.11	16.7
7.52	17.7
8.70	18.8
9.87	20.0
10.1	20.4
10.9	21.3

Table A4
^{64}Ni

E_o (keV)
14.3
25.8
31.8
32-35**
39.2**
45.8**
60.0**
62.4
82.8

*Assignment not definite probably ^{61}Ni

**Unresolved

in the beam, and a continous white source measurement was used to determine the cross section to the order of a few percent.

The final results are shown in Fig. A3. The solid curve is due to a three body theoretical calculation by Harms and Laroze[1] (private communication). The agreement appears to be quite good. The fairly rapid decrease in cross section from zero to about 200 keV energy is explained by the dominance of s-wave scattering in this region. The flattening out above 200 keV is explained by the early onset of higher scattering due to the large radius of the deuteron. This is in contrast to n-p cross sections, which are dominated by s-wave scattering to over 10 MeV. At lower energies, quartet scattering contributes nearly all of the n-d cross section.

Above 1 MeV, the present experimental cross sections join smoothly, and are consistent with the recent measurements of Clement et al.[2] and the evaluations by Seagrave,[3] and Horsely and Stewart[4]. At lower energies, the present measurements are consistent with the thermal measurements (σ_{free}) of Fermi and Marshall[5], and Dilg et al[6]. They do not agree with the evaluations of either Horsely and Stewart[4], or Seagrave[3]; both of which are basically extrapolations from higher energy[3] data, and appear to be significantly too low. The more recent Seagrave[3] evaluation which gives σ_{free} = 3.15 barns, is also based on an analysis by Van Oers and Seagrave[7], of spin coherent and spin incoherent cross section measurements by Gissler[8], and by Bartolini et al[9], respectively. This analsyis yields scattering lengths of $^2a=0.15\pm0.05$ fm and $^4a=6.13\pm0.03$ fm. The analysis also uses phase shifts from higher energy angular distribution data.

The present results, and the calculation by Harms and Laroze[1], tend to confirm the quarter scattering length, $^4a = 6.35 \pm 0.02$ fm which was obtained by Dilg et al[6], and are in basic agreement with theoretical expectations[1,10]. The present results do not specify ^2a because of its very small contribution to the cross section. However, the agreement with Dilg et al.[6] with respect to σ_{free} and ^4a lends confidence to their value of $^2a = 0.65 \pm 0.04$ fm, which is theoretically preferred over the smaller value.

1. E. Harms and L. Laroze (private communication)
2. J. M. Clement, P. Stoler, C. A. Goulding and R. W. Fairchild, Nucl. Phys. A183, (1972) 51.
3. J. D. Seagrave in The Three-Body Problem, Ed. J. S. C. McKee and R. M. Rolph (North-Holland, Amsterdam, 1970) p. 41
4. A. Horsely and L. Stewart, Evaluated Neutron Cross Sections for Deuterium, Los Alamos Scientific Report, LA-3271.
5. B. Fermi and L. Marshall, Phys, Rev. 75 (1949) 578.
6. W. Dilg , L. Koester and W. Nistler, Phys. Letters, 36B (1971) 208.
7. W. T. H. van Oers and J. D. Seagrave, Phys. Letters 24B (1967) 562.
8. W. Gissler, Z. Kristallographic 118 (1963) 149.
9. W. Bartolini, R. E. Donaldson and D. J. Groves, Phys. Rev. 174, (1968)
10. G. Barton and A. C. Phillips, Nucl. Phys. A132 (1969) 97.

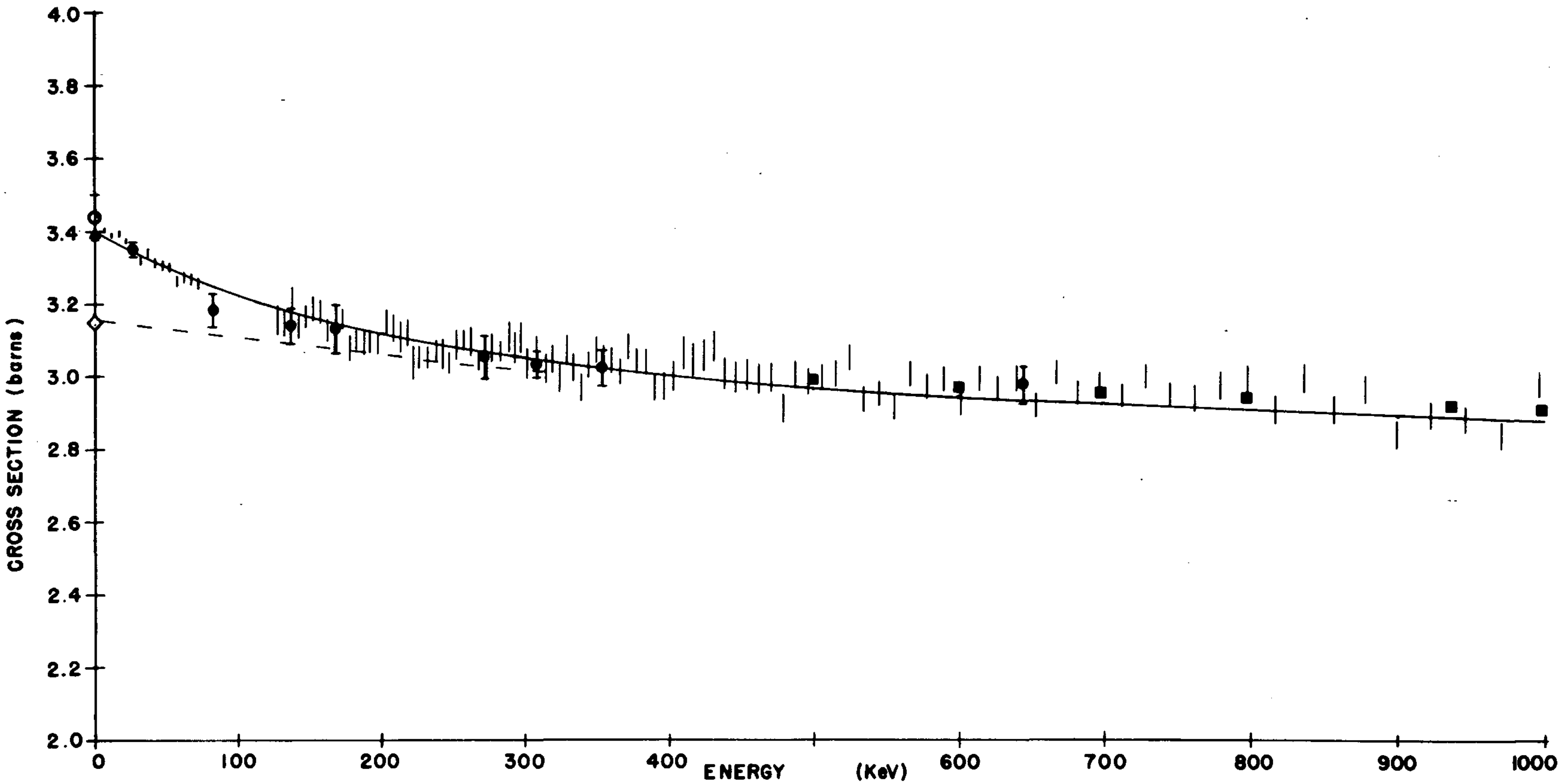

4.0
3.8
3.6
3.4
3.2
3.0
2.8
2.6
2.4
2.2
2.0
CROSS SECTION (barns)
0
100
200
300
400
ENERGY (KeV)
600
700
800
900
1000

Figure A3

Incidentally, the phase shift of van Oers and Seagrave[7] does not contradict the present results because of the large experimental errors in their quoted phase shifts. In fact, an extrapolation of their quartet values of k cot $^4\delta$ down to zero energy actually appears to prefer the Dilg et al.[6] value of $^4a = 6.36$ fm over the alternate value of 6.13 fm which they used. In addition, due to the large errors in the doublet phase shifts, their analysis appears to be as consistent with $^2a=0.65$fm as with the alternate value of $^2a = 0.15$ fm, which they used.

We conclude that the results of the present experiment are in basic agreement with the theoretical expectations, and tent to confirm the results of the thermal measurements of Dilg et al.

4. Total Neutron Cross Section of ^{4}He, ^{6}Li and ^{7}Li From 0.5 to 30 MeV*
(C. A. Goulding and P. Stoler)

The total cross section measurements of neutrons on ^{4}He have been completed. The data were taken at the 250 meter station in blocks of two separate runs. The first set of runs used a TAC-ADC timing system, moderate gas pressure (1700 psi) in the transmission sample cell and moderate neutron intensity (one count per machine burst). The latter run used an E. G. & G. TDC500 Time Digitizer with 4 ns channels, high pressure gas sample (2800 psi), and high neutron intensity (about 2 counts per machine burst). The transmission at the 1 MeV resonance was just a few percent.

Figure A4 shows a comparison of the results of the two runs. The excellent agreement at the 1 MeV peak is quite significant, considering the considerable difference in experimental conditions.

The ^{6}Li and ^{7}Li data have been reduced to total cross sections, and the results below 15 MeV are shown in Fig. A5.

*Req. No. 10, 17

5. Total Neutron Cross Rection of ^{3}He in the Energy Range 0.7 to 30 MeV.*
(C. A. Goulding, P. Stoler and J. D. Seagrave, LASL)

The total neutron cross section of ^{3}He was measured using a gaseous sample obtained from the Los Alamos Scientific Laboratory. The gas was contained in a stainless steel chamber with thin end windows.

Three seperate runs were taken with different neutron intensities and burst widths. This was done in order to insure maximum statistical accuracy and resolution over the entire energy range, since the cross section, and hence transmission, vary by almost an order of magnitude from 1 to 30 MeV. Agreement between the three runs was within 1% over most of the energy range covered, which lends confidence in the accuracy of the results. In addition, considering our experience in similar previous experiments, we feel that the cross section is now determined to within $\pm$ 1% over most of the energy range.

*Req. No. 6

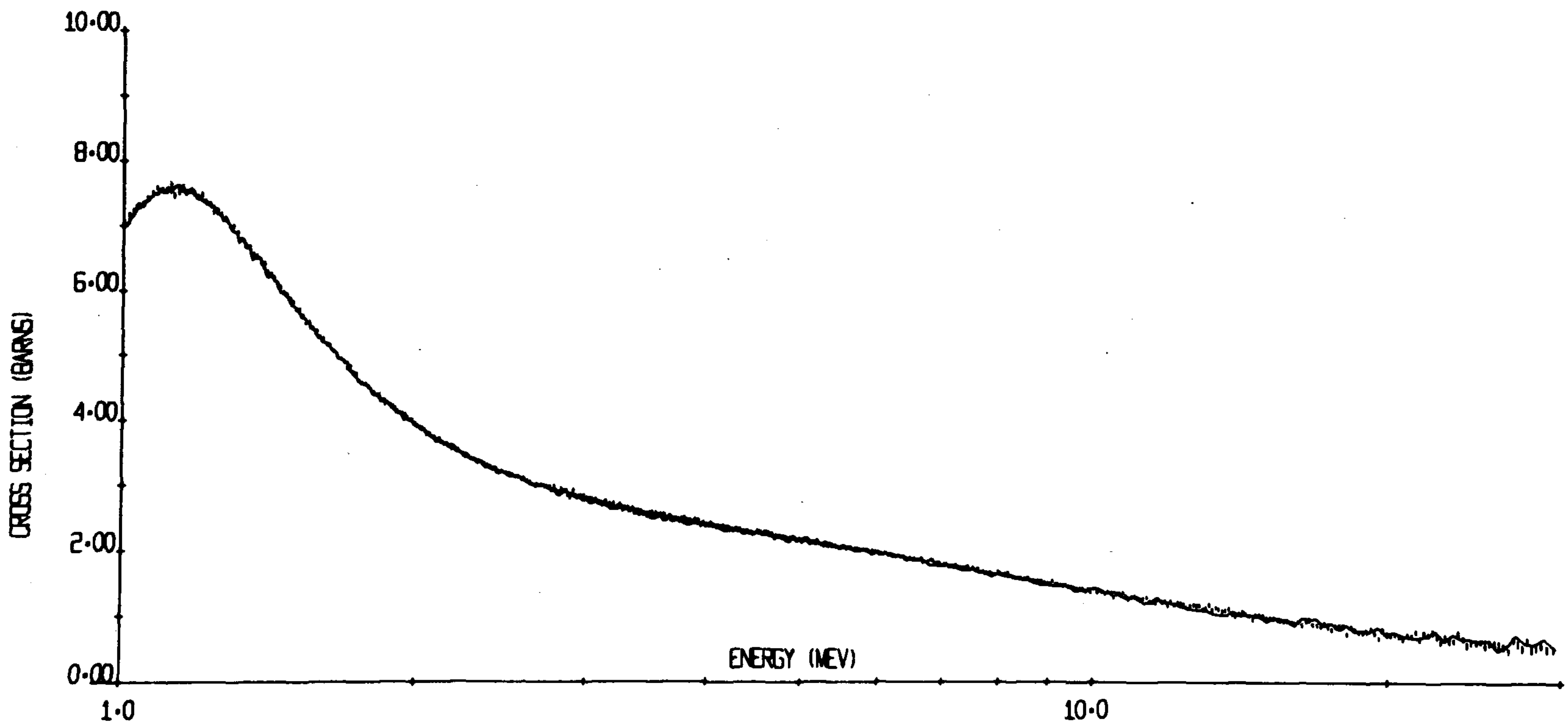
10·00
8·00
6·00
4·00
2·00
0·00
CROSS SECTION (BARNS)
ENERGY (MEV)
1·0
10·0

Figure A4

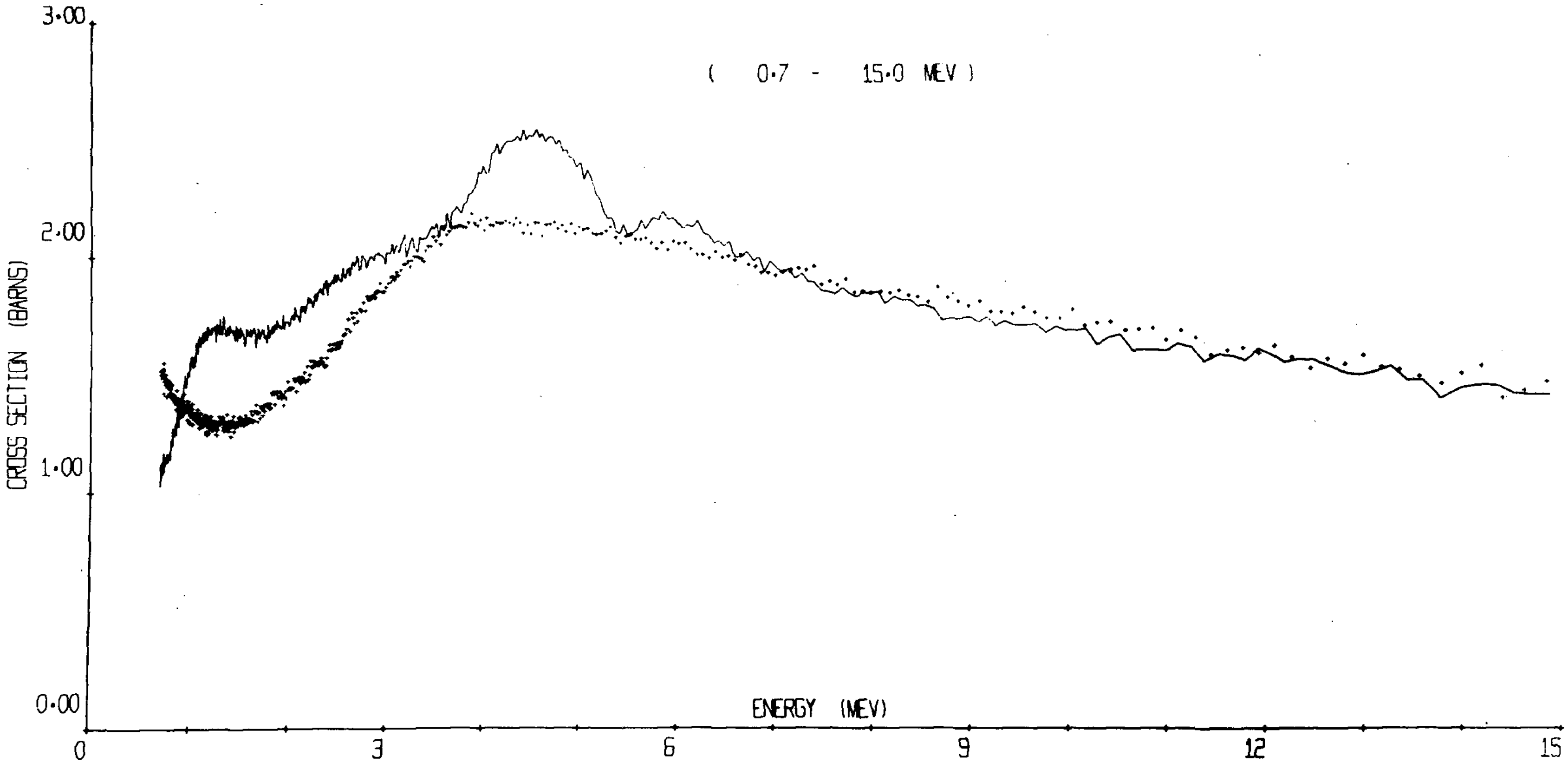
(0·7 - 15·0 MEV)
CROSS SECTION (BARNS)
3·00
2·00
1·00
0·00
ENERGY (MEV)
0
3
6
9
12
15

Figure A5

6. Capture Measurements Near 24 KeV with Iron-Filtered Beams*
(R. C. Block, N. N. Kaushal, and R. W. Hockenbury)

Neutron radioactive capture measurements have been completed on samples of Au, In, depleted U (99.8 % ^{238}U), and Ta. The preliminary results (reported in USNDC-1, pg. 176) have been corrected for multiple scattering and sample self-screening effects using the technique developed by H. Schmitt. In addition the neutron flux was determined for neutrons near the 24 keV minimum, and from this measurement we conclude that our effective capture cross sections should be compared to average capture cross sections at 23.5 keV.

The results are summarized in Table A5. In column (6) are listed the ratio relative to Au of the 23.5 keV effective capture cross section. In column (6) the Au capture cross sections at 23.5 keV was taken as 678 mb, as recommended by Poenitz. The results in columns (5) and (6) are considered accurate to 4 to 5 percent (one standard deviation).

*Req. No. 321, 336, 421, 422

7. Fission Neutron Multiplicity Measurements upon ^{233}U, ^{235}U and ^{239}Pu*
(R. L. Reed, R. W. Hockenbury and R. C. Block)

The nubar measurements for ^{233}U and ^{235}U have been finished. In using 60 hours and 72 hours of LINAC time for the thermal measurement on ^{235}U and ^{233}U, respectively, the results show that nubar remains constant over the thermal region to within a statistical accuracy (standard deviation) of $\pm$ 0.1% for both isotopes.

The resonance region results (5-40 eV for ^{235}U and 5-100 eV for ^{233}U) show that deviations of the resonance nubar values are less than 1% from the average of all values. The statistical error for the resonance measurements ranges from $\pm$0.1% to $\pm$1%, depending on the strength of the resonances. About 165 hours of LINAC time were used for the ^{235}U measurements and 240 hours for the ^{233}U measurement. Further analyses of the ^{233}U and ^{235}U results are being carried out, in particular, statistical distribution tests to determine if there are any correlations of the resonance nubar values with resonance parameters.

The 1.4 gram multiplate ^{239}Pu fission chamber has been borrowed from the Oak Ridge National Laboratory to carry out measurements in an attempt to resolve differences in results reported by several investigators. Using the improved detector system and a more efficient program in the data acquisition computer, the data are being accumulated at a rate four times that of the previous ^{239}Pu measurement carried out here.

*Req. No. 361, 395, 452

8. Neutron Capture Spectra for ^{60}Ni*
(P.H. Brown, S. Arendt, J. R. Tatarczuk, E. J. Winhold and W. R. Moyer)

Table A5

Capture near 24 keV

(1) SAMPLE	(2) THICKNESS (10^{-3} at/bn)	(3) NET CAPTURE COUNTS	(4) DETECTOR EFFICIENCY	(5) SAMPLE THICKNESS CORRECTION	(6) $\tilde{\sigma}_{\gamma,i} / \tilde{\sigma}_{\gamma,Au}$	(7) $\sigma^{*}_{\gamma,i}$ (barns)
Au	3.134	25,313(±0.7%)	0.694	3.6%	(1.00)	(0.68)
In	1.964	22,990(±0.8%)	0.777	2.2%	1.32	0.89
^{238}U(99.8%)	3.800	22,101(±0.8%)	0.680	6.8%	0.70+	0.47+
Ta	3.104	37,586(±0.6%)	0.714	4.9%	1.44	0.98

*Assuming $\tilde{\sigma}_{\gamma,Au}$ = 678 mb at 23.5 keV

+Corrected for ^{235}U contamination

Preliminary results (50 hours of LINAC time) of a neutron capture spectrum experiment in ^{60}Ni indicate the usefulness of the PDP-9/L TOF X PHA data acquisition system . The data were obtained in 22 regions of neutron energy, from 50 keV to 13 eV. The useful and interesting data are in the s-wave neutron resonance at 12 keV, and in the p-wave resonances at 2.3 and 24 keV. In the low energy regions and in the s-wave resonance the data yields the ratio of the GS (ground state) gamma ray (7.815 MeV) transition to the 2nd excited state gamma ray (7.534 MeV) transition. The data in the 2.2 keV p-wave resonance clearly show a transition to the 1st excited state (7.748 MeV) which is not seen in the s-wave neutron data.

*Req. No. 122, 123

9. Temperature-Dependent Transmission and Self-Indication Measurements Upon Depleted U in the Unresolved Region *
(T. Y. Byoun, R. C. Block and T. Semler, NASA)

Average transmission and self-indication ratio measurements upon depleted uranium (99.8% ^{238}U) up to 100 keV have been reported in the ANS National Topical Meeting at Kiamesha Lake (Sept. '72). The data were analyzed by averaging the resonance parameters over corresponding distribution functions, the Porter-Thomas width distribution and Wigner level spacing distribution.

The average resonance parameters that best fit the experimental data are listed in Table A6. The temperature dependence of the average transmission and self-indication ratio for a given sample thickness (0.03155 atom/barn) and for a given energy range (22.6 -25.0 keV) over a temperature range 77°K to 1000 °K are plotted in Fig. A6. Fig. A7 shows the sample thickness dependence of the data for the same energy range and for the room temperature.

*Req. No. 427

10. KeV Neuton Elastic Scattering Cross Section in Iron *
(R. Zuhr, Z. Bell, and K. Min)

The measurement of the neutron differential elastic scattering cross section of natural iron has continued. Forward scattering information has been improved by extending the data taking from 45 to 30 degrees. In order to improve the statistical accuracy of the cross sections reported previously, several changes have recently been made to the experimental apparatus. Two ^{6}Li glass detectors are now used, so that two angles can be measured simultaneously. Along with this, target geometry and beam collimation have been optimized, thereby increasing our overall data acquisition rate by an order of magnitude. Measurements on iron and nickel were made under these conditions, and the data are now being analyzed.

*Req. No. 97

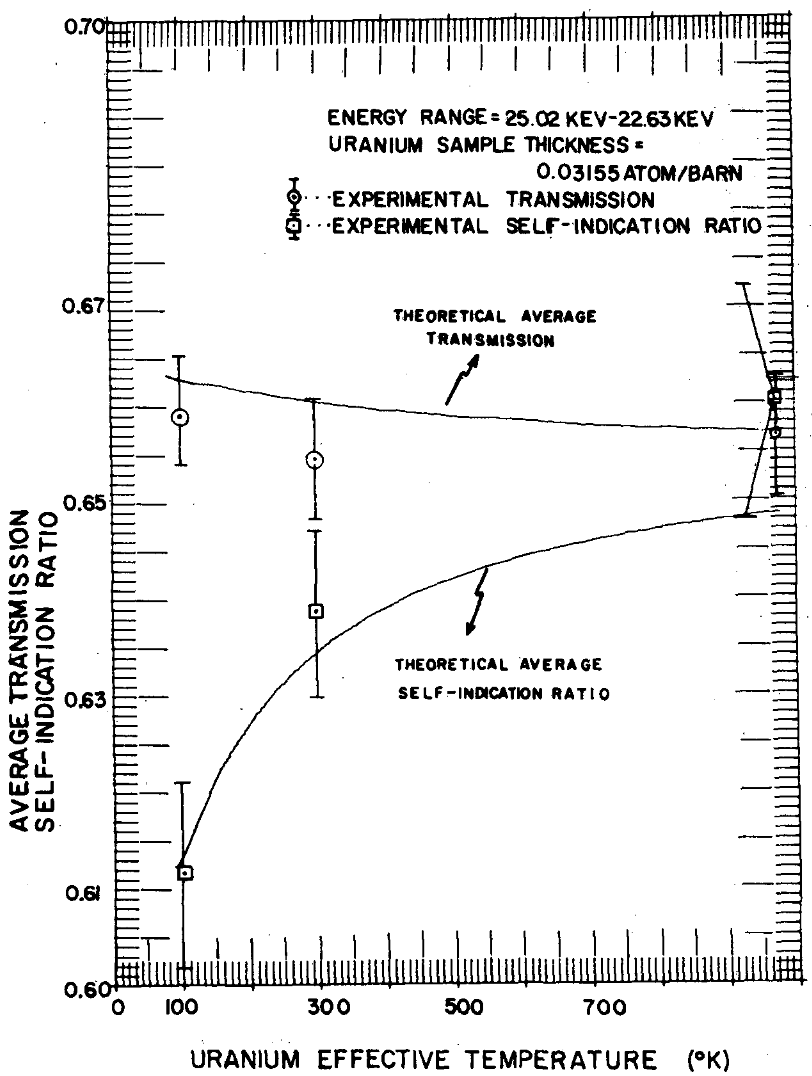
ENERGY RANGE = 25.02 KEV-22.63 KEV
URANIUM SAMPLE THICKNESS = 0.03155 ATOM/BARN
EXPERIMENTAL TRANSMISSION
EXPERIMENTAL SELF-INDICATION RATIO
THEORETICAL AVERAGE TRANSMISSION
THEORETICAL AVERAGE SELF-INDICATION RATIO
AVERAGE TRANSMISSION
SELF-INDICATION RATIO
0.70
0.67
0.65
0.63
0.61
0.60
0
100
300
500
700
URANIUM EFFECTIVE TEMPERATURE (°K)

Figure A6

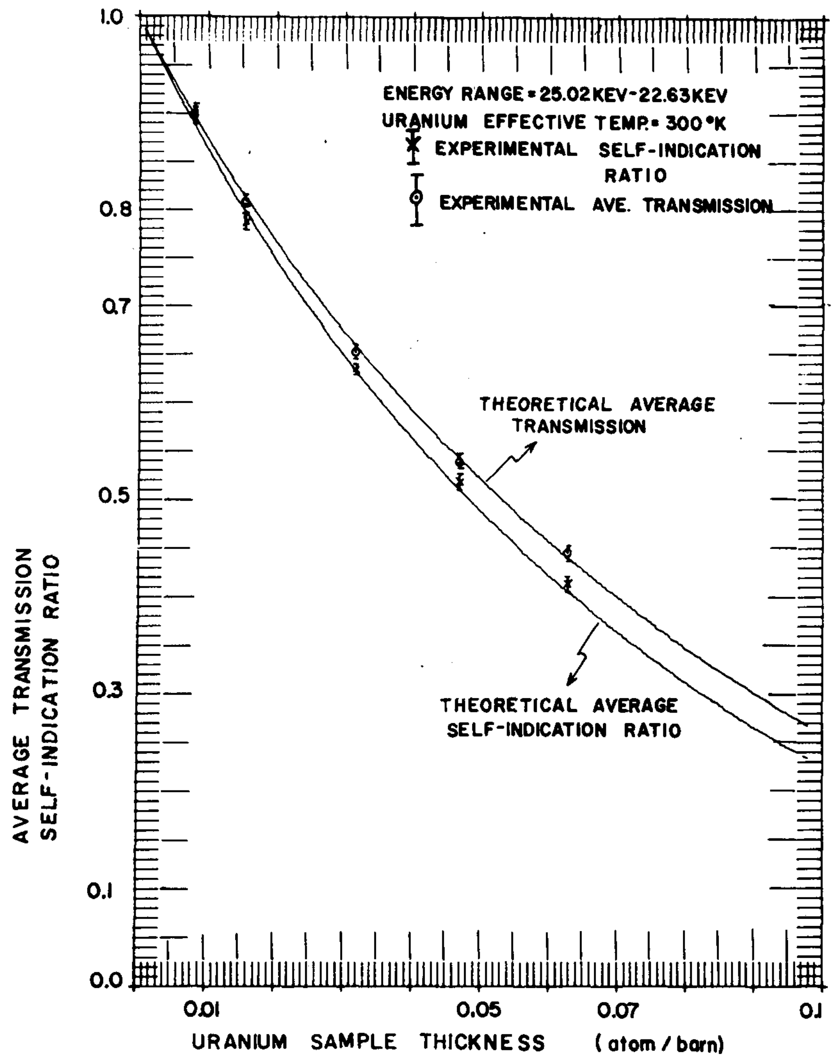
1.0
0.8
0.7
0.5
0.3
0.1
0.0
ENERGY RANGE = 25.02KEV-22.63KEV
URANIUM EFFECTIVE TEMP = 300°K
EXPERIMENTAL SELF-INDICATION RATIO
EXPERIMENTAL AVE. TRANSMISSION
THEORETICAL AVERAGE TRANSMISSION
THEORETICAL AVERAGE SELF-INDICATION RATIO
AVERAGE TRANSMISSION
SELF-INDICATION RATIO
0.01
0.05
0.07
0.1
URANIUM SAMPLE THICKNESS (atom / barn)

Figure A7

TABLE A6

"Best" ^{238}U Average Parameters

	S-Wave	P-Wave	
	J = 1/2	J = 1/2	J = 3/2
Strength Function	0.93×10^{-4}	2.3×10^{-4}	2.3×10^{-4}
Level Space	19.5 eV	19.5 eV	9.75 eV
Reduced Width	0.00181 eV	0.00487 eV	0.00243 eV
Radiation Width	0.0230 eV	0.0230 eV	0.0230 eV
Nuclear Radius		$R = 0.90 \times 10^{-12}$ cm	

B. NUCLEAR THEORY

1. P. J. Turinsky, K. Alfieri, J. Sierra and J. Biffer

Theoretical support of the neutron cross section program has centered on several projects. A satisfactory set of global optical model parameters has been found that simultaneously fit potential scattering radii, s-wave strength function and p-wave strength function for neutron interactions. To fit the deep minima observed in the p-wave strength function, a partial-wave-dependent imaginary shifted surface potential strength was found necessary, with all other optical potential parameters partial wave independent. In conjunction with our iron total cross section minima measurement by the TOF transmission method, both area and shape analysis capability to analyze the data have been developed. We conclude that with regard to predicting total neutron cross section minima in natural iron from 20 keV to 1 MeV, both the Penny-Kinney and Version 19 data files generally overestimate these minima with the Version 19 data file preferred. We quote $(\sigma_t)_{min} = 0.42 \pm 03$b at E=24.3 $\pm$0.1 keV. A statistical analysis computer code based on Monte Carlo techniques has been developed to quantify whether anomalously broad resonance structure observed in energy-averaged neutron scattering cross sections indicate intermediate structure, i.e. doorway states, or just semi-likely normal statistical behavior as contained in Porter-Thomas and Wigner distributions. Our analysis of neutron elastic s-wave scattering upon ^{40}Ca, leading to the $1/2^+$ interaction channel, indicated that the broad resonance structure in the average s-wave cross section experimentally observed to 1.3 MeV is not likely statistically. This indicated the likely existence of intermediate structure, which has hence been confirmed by coupled-channel calculations.

2. Correlations Between Neutron and Radiative Widths
(M. Lubert, N. C. Francis, and R. C. Block)

The cross section for the chromium isotopes measured at the RPI Linac indicate a positive correlation between the reduced neutron and radiative widths. In addition the experimental capture cross section for ^{60}Ni below the 12.4 keV resonance is roughly a constant 50mb. The correlation is not predicated for a compound nucleus process and the Breit Wigner Single Level formalism does not predict the large cross section below the resonance. Calculations have been performed in an attempt to understand these phenomena. The investigation examined the channel contribution to the (γ,n) cross section for the ^{57}Fe, ^{53}Cr, ^{61}Ni nuclei. The comparison of theory to experiment provides a measure of the reduced width factor, the channel and compound nucleus partial radiative widths, and the (γ,n) and (n,γ) cross sections.

The results to-date show: (1) the reduced width factors for these isotopes are $0.1 < \theta^2 < 0.5$; (2) the calculated channel contribution to the thermal (n,γ) cross section is significant for ^{57}Fe, ^{53}Cr and ^{61}Ni; (3) the computed compound nucleus partial radiative widths obey a Porter-Thomas distribution; (4) the radiative widths, including excited state contributions, are comparable to the experimental values; (5) correlations between Γ_γ and Γ_n^0 are seen; (6) the ^{60}Ni (n, γ) cross section below 12.4 keV has a substantial contribution.

C. INTEGRAL TESTS OF CROSS SECTION DATA

1. Fast Neutron Transport in Bulk Media

(M. Becker, E. R. Gaerttner, N. N. Kaushal, B. K. Malaviya A. Mallen, and R. Bandera)

The assessment of data files for iron and depleted uranium, based on the measurement and analysis of position-dependent fast neutron angular flux spectra in bulk assemblies, has continued. Some results of the tests of cross section data for iron, primarily relating to low and intermediate energy (below about 1MeV) spectra and based on P_o scattering matrix with the transport approximation, have been reported earlier[1]. The conclusions of such studies with respect to the minima in total cross section have prompted new measurements at RPI, Columbia and ORNL and these are expected to influence the new, revised data files. Further analysis[2] has incorporated anisotropic scattering (up to P_8) and extended the results to higher energies (about 10 MeV); a new recent data file, ORNL-1124 has also been included in the assessment. Preliminary results indicate that ENDF/B-I data for iron still are preferrable in terms of overall agreement with experiment at high energies (see Fig. C1), although lack of resolution in this file implies greater errors for very deep penetrations.

The analysis of fast neutron spectra in depleted uranium has included the assessment of several data files - ENDF/B-I, ENDF/B-II, KEDAK file and a multigroup set from the Argonne Cross Section library. A detailed report of this work will be published shortly[3]. It is concluded, for example, that for the low energy measured spectra to agree with the calculation, the effective self-shielded capture cross sections (as generated by MC^2) need to be lowered in ENDF/B-I and ENDF/B-II by about 10 per cent; this seems to support some recent experimental indications that the ^{235}U fission cross section may be lowered by 8 to 10 per cent (in the actual evaluation of absolute ^{238}U capture cross sections the data have been usually normalized to the fission cross sections of ^{235}U, which is adopted as a standard). Overall it is found that none of the above data files for uranium yields satisfactory agreement with experiment, although the ANL multigroup set gives reasonable results.

Current efforts in this program are primarily devoted to the study of fast neutron transport in bulk sodium. Detailed time-of-flight measurements of fast neutron angular flux spectra at different positions in a large assembly of metallic sodium at room temperature have been under way. The analysis of these spectra, principally with ENDF/B data as input, is also being initiated.

---

1. B. K. Malaviya, N. N. Kaushal, M. Becker, E. Burns, A. Ginsberg, and E. R. Gaerttner, Nucl. Sci. and Eng. 47, 329, (1972)
2. B. K. Malaviya, N. N. Kaushal, M. Becker, E. Burns, A. Ginsberg, E. R. Gaerttner, Proc. of Fourth International Conference on Reactor Shielding, Paris, October 9-13, 1972.
3. N. N. Kaushal, B. K. Malaviya, M. Becker, E. T. Burns, E. R. Gaerttner Nucl. Sci. Eng. (1972), to be published.

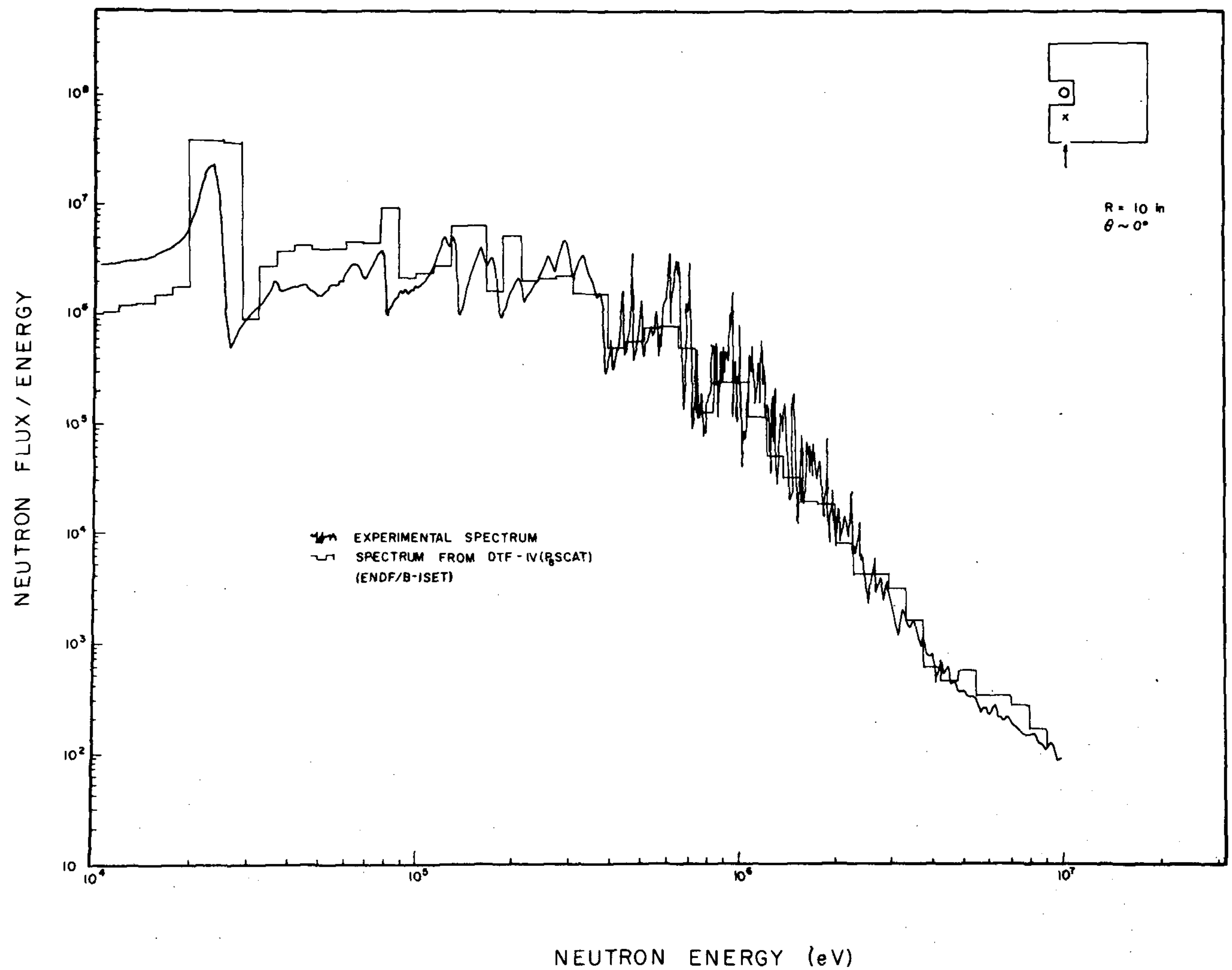
R = 10 in
θ ~ 0°
EXPERIMENTAL SPECTRUM
SPECTRUM FROM DTF-IV(P5SCAT)
(ENDF/B-I SET)
NEUTRON FLUX / ENERGY
NEUTRON ENERGY (eV)

Figure C-1

TRIANGLE UNIVERSITIES NUCLEAR LABORATORY

A. NEUTRON AND FISSION PHYSICS

1. Resonance Cross Section Measurements with Continuous Beam: Sr (J.G. Malan,* W. F. E. Pineo, E. G. Bilpuch, H. W. Newson)

   The analysis is being rechecked before preparation for publication.

2. Resolved Neutron Total Cross Sections and Intermediate Structure (J. Clement, B.-H. Choi, W. F. E. Pineo, M. Divadeenam, H. W. Newson)

Natural Si and S neutron cross section data have been analyzed with the help of our R-Matrix code. Strong s-, p- and f-wave doorways have been identified in Si data. However, Sulfur neutron cross section data do not exhibit noticeable doorway effects. Publication of the analyzed data is pending a more general theoretical doorway investigation.

Analysis of ^{209}Bi partially resolved data is almost complete. R-Matrix analysis reveals many s-wave resonances below 600 keV neutron energy. This is in agreement with the findings of the RPI group.[1] The observed intermediate structure is attributed to an s-wave doorway state similar in structure to the $1/2^+$ doorway in the Pb isotopes. See Section A-15(b).

An R-Matrix fit to the Rensselaer ^{60}Ni neutron cross sections is underway. The published Duke ^{60}Ni and the RPI data will be combined to look for doorway state effects.

3. Averaged Cross Sections, Strength Functions, and Intermediate Structure (W. F. E. Pineo, M. Divadeenam, E. G. Bilpuch, H. W. Newson)

The subject matter of the theses of M. Divadeenam and W. F. E. Pineo has been divided into two topics: one on average cross sections and potential scattering, the other on strength functions. A paper based on the former is almost ready for submission to Annals of Physics as Part II of our series on Neutron Strength Functions and Average Total Cross Sections. Cross Sections averaged over several hundred keV for nuclei ranging from A = 40-240 are compared with various optical model predictions. A discussion of potential scattering, the largest component in

---

* Now at the Atomic Energy Board of the Republic of South Africa

[1] R. C. Martin *et al.*, Physics Letters **24B**, 33, 1967

averaged cross section, is also included in this paper. Part III of the series is also in preparation; experimental strength functions estimated from averaged cross sections are compared to spherical and deformed optical model predictions.

4. Charged Particle Fission (F. O. Purser, J. R. Boyce, D. E. Epperson, E. G. Bilpuch, H. W. Newson, R. Bass,* H. W. Schmitt**)

a. Analysis of Fission Cross Section Measurements

A major computer program, PHROG, has been written to analyze the cross section data for the uranium isotopes. The program uses modified reaction cross sections calculated with the optical model and straightforward statistical model assumptions concerning the decay of the compound nucleus to calculate the measurable total fission probability resulting from the proton bombardment of a target. Comparison of calculated probabilities with experimental results for a series of neighboring nuclei such as the uranium isotopes allows determination of neutron to fission branching ratios for individual fissioning nuclei even in the presence of multiple chance fission events. A paper containing these ratios and several previously unreported fission threshold measurements for the neptunium compound nuclei is being prepared.

The program, PHROG, is being extended to include the effects of 4th chance fission, double peaked fission barriers and a more sophisticated treatment of saddle point level densities. The present version utilizes the Gilbert and Cameron level density formalism for ground state deformations and a modified Gilbert and Cameron version at the saddle point.

b. Mass and Kinetic Energy Distributions

With the completion of the uranium cross section work, this program has been reactivated. Accurate mass and kinetic energy distributions for $^{236}U + p$ have been measured at 1 MeV intervals from $E_p = 7.0 - 13.0$ MeV. These measurements will be extended and all the uranium isotopes included. Analysis of these data utilizing the information from PHROG should allow unambiguous determination of mass and K.E. information as a function of excitation energy of the fissioning nucleus. Presently available information of this nature for nuclei in the actinide region contains undifferentiated contributions from second and third chance fissions which can obscure the results when compared with theoretical predictions

* University of Frankfurt, Frankfurt, Germany

** Oak Ridge National Laboratory, Oak Ridge, Tennessee based on current models of the fission process.

c. Cross Section Measurements

This program will be continued with the next measurements scheduled to be cross sections for proton induced fission of thorium and radium.

5. A Fermi Gas Model for Fission (H. W. Newson)

The Fermi Gas Model (FGM) for fission products has been generalized by the inclusion of the oscillator shells at 40 nucleons in addition to Mayer-Jensen shells at 28, 50 and 82. The generalization adds little or nothing to our understanding of the asymmetric peaks in thermal and spontaneous fission yields of the actinides, but a strong effect of the Z = 40 shell on effective surface tension appears to be responsible both for the strong symmetric peak in the yield of ^{226}Ra(p,f) compared to the much weaker one observed in ^{232}Th(p,f), and the total (or nearly so) disappearance of asymmetric peaks in ^{209}Bi(p,f).

6. Cross-Section and Polarization in (^{3}He,n) Reactions from ^{12}C and ^{13}C from 8 to 22 MeV (T. C. Rhea, R. A. Hardekopf,* P. W. Lisowski, J. M. Joyce, R. Bass, R. L. Walter)

Relative cross-section measurements were obtained for ^{12}C(^{3}He,n) and ^{13}C(^{3}He,n) ground-state reactions were obtained between 8 and 22 MeV using a proton recoil scintillator (with γ-discrimination) and with the high pressure, high resolution ^{4}He gas scintillator. Excitation functions for ^{12}C(^{3}He,n_o), ^{13}C(^{3}He,n_o) and ^{13}C(^{3}He,p_o) were obtained at 0° from about 10 to 22 MeV. These data are to supplement the polarization data previously obtained for the (^{3}He,n) reactions. DWBA results are in agreement with the higher energy ^{12}C data but do not agree with the ^{13}C polarization data. A search for better optical model parameters for ^{13}C(^{3}He,^{3}He) is underway.

7. Neutron Polarization from (d,n) Reactions on ^{24}Mg, ^{28}Si and ^{40}Ca (J. Taylor,** Th. Stammbach,+ R. L. Walter)

This work (for $E_d < 4$ MeV) has been published in Nuclear Physics A186 (1972) 33.

---

* Now at Los Alamos Scientific Laboratory, Los Alamos, New Mexico

** Now at Armed Forces Institute of Pathology, Washington, D. C.

\+ Now at Schweiz. Inst. f. Nuklearphysik, Zurich, Switzerland

8. Polarization of Neutrons from ^{10}B, ^{11}B and $^{13}C(d,n)$ Reactions for $E_d < 4$ MeV (M. M. Meier,* R. L. Walter)

This work (for $E_d < 4$ MeV) has been published in Nuclear Physics A182 (1972) 468.

9. The j-dependence in the $^{11}B(d,\vec{n}_0)$ and $^{11}B(d,\vec{n}_1)$ Reactions (J. Taylor, G. Spalek,**, Th. Stammbach, R. A. Hardekopf, R. L. Walter)

A paper on the 7-12 MeV study is near completion.

10. The $^{9}Be(d,\vec{n})$ Reaction from 3 to 4 MeV (G. Spalek, J. Taylor, R. A. Hardekopf, Th. Stammbach, R. L. Walter)

The analysis of this study has been completed, and a report will be prepared for publication.

11. Polarization of Neutrons from the D(d,n) Reaction from 6 to 22 MeV (G. Spalek, R. A. Hardekopf, P. W. Lisowski, Th. Stammbach, J. M. Joyce, R. L. Walter)

The polarization of the neutrons from D(d,n) reactions has been measured from 6 to 14 MeV using the tandem beam and 14 to 22 MeV using the pulsed Cyclo-Graaff beam and time-of-flight techniques. The polarization at 45° c.m. was found to be larger than previously reported but still not equal to the proton polarization at the same deuteron energies. Two papers on this work are in press (Nuclear Physics).

12. Neutron Scattering Studies Utilizing Polarized Neutrons Produced with Polarized Deuteron Beams (P. W. Lisowski, T. C. Rhea, C. E. Busch, T. B. Clegg, R. L. Walter)

Neutron beams having a polarization of ~ 0.6 have been produced in the $D(\vec{d},\vec{n})^{3}He$ reaction with vector polarized deuteron beams. The following progress has been made:

a. $^{3}He(\vec{n},n)$ Reaction

Distributions were obtained at 8 and 12 MeV by scattering from a

---

* Now at National Bureau of Standards, Gaithersburg, Md.

** Now at the University of Wisconsin, Madison, Wisconsin

^{3}He gas scintillator. The statistical accuracy of the data is somewhat better than has previously obtained and significant differences to these data were noted. Closer similarity to the polarization in the mirror reaction T(p,p)T now exists. A preliminary report on the data will be given at the Seattle meeting of the APS.

b. ^{4}He($\vec{n}$,n) Reaction

Because accurate knowledge of the ^{4}He(n,n) reaction is crucial to many (past and present) neutron polarization measurements, another study of this reaction was initiated using 14- and 17-MeV polarized neutrons produced by the transfer polarization method. Data were obtained with better than ± 0.01 accuracy on the asymmetry in ^{4}He(n,n) scattering. Geometry corrections need to be calculated before valid comparisons can be made to predictions based on available phase shifts.

More work along these lines is planned but the technique for fast neutron scattering studies is limited to scatterers where the first-excited-state is well resolved from the ground state. Time-of-flight with pulsed polarized beams would be advantageous provided there is not much loss in average beam on target.

13. Transfer Polarization Studies in ($\vec{p}$,$\vec{n}$) Reactions (P. W. Lisowski, T. B. Clegg, R. L. Walter)

Attempts to measure the polarization transfer coefficient in (p,n) reaction on light nuclei have begun. The counting rates are low but perhaps sufficient information concerning the magnitude of the effect can be obtained to gain information on the reaction mechanism and, more importantly, on the spin dependence of the isospin interaction.

14. Survey of Neutron Polarization Phenomena in Nuclear Reactions (R. L. Walter)

A short version of a review paper on neutron polarization has been circulated among workers in the field for comments and for new information. A more lengthy manuscript (scheduled for publication in Reports on Progress in Physics) will follow.

15. Theoretical Investigation of Neutron Cross Section Measurements (M. Divadeenam, B.-H. Choi, W. P. Beres,* S. Ramavataram,** K. Ramavataram,+ H. W. Newson)

a. Shell Model

(1) Even-Odd Compound Nuclei

As reported earlier, good agreement is found between theory and experimentally observed doorway effects in $^{29}Si(^{28}Si + n)$. This was accomplished with drastic variation in one of the parameters that enters into the doorway state calculations. For internal consistency the effect of changing the neutron single particle state energies is being investigated. In addition the effect of including the deeper holes $1p_{3/2}$ and $1p_{1/2}$ in the 2p-1h state calculation will be studied.

The predicted s-wave doorway energies and widths for ^{41}Ca compare well with the observed resonance structure by Bowman et al.[1] and Nebe et al.[2] The 2p-1h doorway model does not predict any p-wave resonances. Experimental[3] p-wave strength function is certainly less than the black nucleus value in the s-d giant resonance region A = 40 - 65, and may be negligible. The reported weak p-wave structure might also be attributed either to 3p-2h states or to particle-vibration doorways.

Since the last report no progress has been made on Ni isotope calculations. The calculations for ^{92}Mo + n are complete and the doorway information will be used to explain qualitatively the possible observed intermediate structure (or fluctuations) in neutron total cross sections. Calculations for the case of ^{98}Mo + n are not complete yet.

(2) Odd-Odd Compound Nuclei

A generalized R-Matrix theory incorporating the Feshbach formalism of doorway states has been applied[4] to account for the neutron resonance

---

* Wayne State University, Detroit, Michigan

** Universite Laval, Quebec, Canada

\+ Universite Laval, Quebec, Canada

1 C. D. Bowman, E. G. Bilpuch and H. W. Newson, Annals of Physics 17 (1962) 319

2 J. Nebe and G. J. Kirouac, Nucl. Phys. A185 (1971) 113

3 H. W. Newson in Statistical Properties of Nuclei, Edited by J. B. Garg, Plenum Press, New York (1972) p. 309

4 S. Ramavataram, B. Goulard, J. Bergeron, to be published

structure observed in ^{89}Y + n scattering measurements.[1] The calculations were restricted to negative parity doorways corresponding to s-wave neutrons. However, recently we have alluded to the possible observation of strong p-wave doorway effects around 600 keV in the neutron cross section data. In addition Elwyn et al.[1] observed some p-wave resonance effects around 1 MeV. With the cooperation of two of the above authors (S.R. and R.R.) the calculations will be extended to p-wave doorways in the ^{90}Y compound nucleus. Application of the present model will be extended to suitable target nuclei which have one extra proton in the last unfilled subshell (eg., ^{209}Bi).

b. Particle-Vibration Model

(1) Even-Odd Compound Nuclei

Predicted widths for ^{41}Ca s-wave neutron doorways are in good agreement with experiment. See above. Calculations for the p-wave doorways are planned. For the cases of ^{28}Si + n and ^{32}S + n the predicted particle-vibration doorway widths are too large in comparison to the corresponding experimental results.

A short paper incorporating the spreading widths Γ for $1/2^+$ ^{207}Pb and ^{209}Pb doorways is in preparation.

A paper giving the predicted γ-ray widths for the ^{207}Pb $1/2^+$ doorway has been submitted to Physical Review Letters. The abstract follows:

> "Small admixtures of doorways d'> in with the dominant doorway d> are shown to account for the possibility of gamma decay from the neutron fine structure associated with the doorway d>. The example of low lying $1/2^+$ resonances in Pb^{207} is investigated via the particle-vibration model with the important doorway d'> for El γ decay found to be that based on the 1^- giant dipole resonance in Pb^{208}."

(2) Even Mass Compound Nuclei

Evan mass compound nuclei ^{208}Pb and ^{210}Bi have been con-

[1] A. J. Elwyn et al., private communication to S. Ramavataram

sidered as test cases for the application of the weak coupling particle-vibration model to explain the low-lying neutron resonances. The odd hole or particle in the target is treated as a passive spectator. The calculated resonance widths are in agreement with experiment. The s-wave resonances in Pb isotopes and ^{210}Bi are related to the same intrinsic doorway. A paper incorporating these findings is in the final stages of preparation for submission to Annals of Physics.

c. Particle-Rotation Model

Target nuclei with rotational properties are considered for the application of Feshbach's unified resonance reaction theory. Rotator-particle interaction is used to describe resonant states as odd neutron coupled to the excited states of the target nucleus. Coupled-channel Schrodinger equations with deformed Woods-Saxon well for the scattering are solved to predict potential scattering. A finite range multipole interaction between the open and closed channels is used to predict particle-Rotation doorway widths. Elastic and inelastic neutron scattering cross sections as a function of neutron energy are being calculated.

The above approach will be applied to light nuclei. ^{12}C and ^{28}Si are being considered as test cases. The formalism is general enough to apply to proton scattering also.

16. Computer Program MODSNOOP for Strength Functions And Single Particle Reduced Width (B.-H. Choi, M. Divadeenam)

The Modified SNOOPT2 (MODSNOOP) code which computes neutron strength functions $<\gamma^2>/D$, $\int_0^E n(\gamma^2)/D$ and reduced widths γ^2 will be extended to calculate similar quantities for incident protons on spherical nuclei.

17. Computer Program for Calculating Nucleon Resonance Scattering Cross Sections for Even-Even Deformed Nuclei within The Framework of Feshbach's Unified Reaction Theory (B.-H. Choi, M. Divadeenam)

A Fortran program to solve the Coupled Schrodinger equations to obtain potential scattering amplitude and cross sections has been written. The program generates bound and resonance states in the compound nucleus making use of the Nilsson model (Rotator-Particle coupling model). In addition it evaluates nucleon escape widths, elastic and inelastic cross sections as a function of incident nucleon energy within the framework of Feshbach's unified reaction theory.

B. CHARGED PARTICLE REACTIONS

1. Fine Structure of Isobaric Analogue States--Charged Particle Scattering (E. G. Bilpuch, T. Dittrich, J. D. Moses, D. Outlaw, N. H. Prochnow, W. M. Wilson, G. E. Mitchell, H. W. Newson)

a. The Chromium and Nickel Isotopes

The work on the Chromium and Nickel isotopes has been published. No further charged particle measurements are planned for the near future.

b. The Iron Isotopes

A second paper on the iron isotopes has been published: "Fine Structure of an Analogue State in ^{59}Co", Nuclear Physics A187 (1972) 481.

c. The Titanium Isotopes

A paper on $^{48}Ti(p,p)$ and (p,p') has been accepted for publication in Nuclear Physics. The following is the abstract of that paper:

> "Differential cross sections were measured for $^{48}Ti(p,p)$ and $^{48}Ti(p,p_1)$ at four angles between $E_p = 1.8$ and 3.1 MeV. The overall energy resolution was 250-350 eV. Spins, parities, total widths and partial widths were extracted for 301 resonances. Two analogue states were observed, and spectroscopic factors and Coulomb energies determined for these analogue states. A large, positive correlation was observed between the elastic and inelastic widths for one analogue; no correlation was observed away from the analogue. The spacing distributions of the $s_{1/2}$ and $p_{1/2}$ resonances (after correction for the energy dependence of the average spacing) are in reasonable agreement with the Wigner distribution. $s_{1/2}$, $p_{1/2}$ and $p_{3/2}$ proton strength functions were determined."

A paper on $^{46}Ti(p,p)$ and (p,p_1) has been submitted for publication. The following is the abstract of that paper:

> "Differential cross sections were measured for $^{46}Ti(p,p)$ and $^{46}Ti(p,p_1)$ at four angles between $E_p = 1.5$

and 3.1 MeV, with an overall energy resolution of about 300 eV. Spins, parities, total and partial widths were extracted for 144 resonances. Six analogue states were identified. The s-wave states have expected spacing and width distributions, while the $p_{1/2}$ states behave anomalously. $s_{1/2}$, $p_{1/2}$, and $p_{3/2}$ strength functions were determined."

The reaction $^{50}Ti(p,p)$ was studied and the analysis of these data is completed. Approximately 200 resonances were analyzed. A paper is being prepared for publication.

d. The Calcium Isotopes

Analysis of the resonances observed in $^{44}Ca(p,p)$ and (p,p_1) is completed. Over 400 resonances were analyzed. Three analogue states were observed. These data show promise for detailed statistical analyses which are now in progress.

The $^{42}Ca(p,p)$ excitation function was measured from Ep = 1.2-3.0 MeV. Analysis of these new data will be performed in the near future.

e. Silicon and Sulfur Isotopes

A technique was developed for making thin enriched silicon targets of a predetermined thickness using electron beam bombardment. These targets proved suitable for high resolution elastic scattering study of ^{30}Si. Differential cross sections have been measured at four angles (160, 135, 105 and 90 degrees) for the $^{30}Si(p,p)^{30}Si$ reaction over a proton range of 1.09-3.00 MeV. Overall energy resolution of 300-400 eV was obtained. Analysis of the data yielding spins, parities, and widths is now nearing completion. Preliminary analysis of these data indicates a total of 63 levels with J ranging from 1/2 to 7/2 was observed. Four analog states were observed. The overall average proton strength functions have been determined from the reduced widths of the $T_<$ levels. Preliminary results indicate that the $3/2^-$ strength function is approximately ten times the $1/2^-$ strength function. A similar study of the $^{34}S(p,p)^{34}S$ reaction is planned for the future.

f. Analysis of Fine Structure Distributions

The distributions of the fine structure reduced widths versus energy for analogue states measured in this laboratory over the past several years are being fit to the general form

$$S(E) = S_0 \frac{(E-E_\lambda-\Delta)^2 + \omega^2/4}{(E-E_\lambda)^2 + \Gamma^2/4}$$

Here S(E) is the local strength function $S = <\frac{\gamma^2}{D}>$ and S_0 is the background strength function, E_λ and Δ are the energy and displacement of the analogue state, Γ is the spreading width, and ω^2 is a parameter which indicates the effects of other open channels; it should vanish in the one-channel case. The fitting first averages both the data and the theoretical distribution using either a gaussian or a square weighing function, then is done by an automatic search code which varies any or all of the above parameters to minimize X^2. Studies are underway to determine the interdependence of the parameters and uniqueness of fit. This analysis is made difficult by the fact that the proton strength functions away from the analogue states are typically small and inaccurately measured, and that in most cases the analogue states have too few fine structure resonances for reliable fitting. Preliminary results on favorable cases indicate that the analogue state energy E_λ is well determined by this procedure, and that spreading widths can be extracted with approximately 25% accuracy. (The spreading widths in the mass region 50-65 are typically less than 10 keV.) The other parameters are less well determined, but approximate values should be obtainable. Most of the analogues are examples of weak mixing.

2. Fine Structure of Analogue States--The Capture Reaction (G. E. Mitchell, R. O. Nelson, W. C. Peters, J. F. Wimpey, E. G. Bilpuch)

a. ^{54}Fe and ^{58}Fe

The gamma decay of fragmented analogs in ^{55}Mn and ^{59}Co has been studied in detail. The following is the abstract of a dissertation by W. C. Peters:

> "The inelastic and gamma decay of the fragmented analogues of the ground states of ^{55}Cr and ^{59}Fe has been studied. Using the TUNL high resolution electrostatic analyzer-homogenizer system, the $^{54}Cr(p,\gamma)$ excitation function from 1.98 to 2.02 MeV and the $^{58}Fe(p,\gamma)$ excitation function from 2.15 to 2.30 MeV were measured with a 7.6 cm by 7.6 cm NaI(Tl) detector. The over-all proton energy resolution was ~350 eV. Using an 80 cm^3 Ge(Li) detector at 55° with respect to the incident beam, absolute inelastic proton and gamma decay widths were measured for 10 resonances in the vicinity of the ground state analogue in ^{55}Mn and for 22 resonances in the vicinity of the ground state analogue in ^{59}Co. The elastic

"proton widths and spins for these resonances has been previously determined in high resolution proton elastic scattering experiments.

Eight of the resonances in ^{55}Mn and ten of the resonances in ^{59}Co were identified as fragments of the respective ground state analogues. Absolute gamma decay widths for transitions from these fragments to the corresponding antianalogue states were found to be weak. The M1 strengths of both of these transitions, assuming no E2 admixtures, were 0.05 Weisskopf units, in agreement with results for non-fragmented analogue states in this mass region. Comparisons of the gamma decay of the ground state analogue with the beta decay of the ground states of ^{55}Cr and ^{59}Fe were made. In general, the widths corresponding to the beta decay were weaker than the experimentally determined gamma decay widths. The best agreement between the beta decay and gamma decay widths occurred for the transitions to the ground state of ^{55}Mn.

The inelastic proton and gamma decay widths were examined for possible correlations with the enhanced elastic channel widths. Positive correlations which were significant at a confidence level of greater than 95% were measured between the elastic and inelastic widths for both analogue states, between the elastic and ground state transition widths for the ground state analogue in ^{55}Mn, and between the elastic and total capture widths for the ground state analogue in ^{59}Co. The correlations of channel widths for resonances in ^{59}Co not associated with the ground state analogue were consistent with purely statistical behavior."

b. ^{62}Ni

The $p_{3/2}$ fragmented analogue state at $E_p \simeq 2.65$ has been studied in detail. The fourteen fragments of this analogue were studied by the (p,p), (p,pγ) and (p,γ) reactions. With improved experimental conditions four new elastic resonances were observed and one previous assignment was changed from p-wave to s-wave. The resolution obtained for the elastic studies was $\simeq$ 300 eV. The linear correlation coefficient (LCC) between the elastic and inelastic widths was 0.93, consistent with previous work on ^{55}Mn and ^{59}Co. The total gamma widths are correlated with the elastic widths--LCC = 0.69. Some of the other γ-transitions were correlated. The transitions to the G.S., 670.5 and 961.8 levels have LCC = 0.33, 0.76 and 0.60, respectively.

Also studied by the (p,pγ) and (p,γ) reactions were 21 s-wave resonances in the region E_p = 2.3 to 2.6 MeV. The elastic and inelastic correlation is 0.11, the correlations of elastic widths with $\Gamma_{\gamma\,\text{total}}$, and $\Gamma_{G.S.}$ are -0.06 and -0.21, respectively.

The resolution obtained for the (p,γ) work was ~350-450 eV.

c. ^{54}Fe

Decay of the $p_{3/2}$ analog at E_p = 2.242 MeV has been studied. This analog occurs as a single level. Since there has been some difficulty in interpreting the decay of this analogue, further studies are planned.

d. ^{44}Ca

Several fragmented analogues observed in ^{44}Ca(p,p) appear to be promising candidates for study. We plan to measure the gamma decay of some of these analogues.

3. Statistical Properties of Nuclei from Proton Resonance Reactions (E. G. Bilpuch, G. E. Mitchell, J. D. Moses, W. M. Wilson, H. W. Newson)

Statistical analysis of the high-resolution proton resonance data is in progress. Additional data have been obtained for the reactions ^{44}Ca(p,p), ^{46}Ti(p,p), ^{50}Ti(p,p) and ^{30}Si(p,p). New data on ^{42}Ca(p,p) await analysis.

Techniques for the analysis of level statistics of these data are being developed. As an example, we are exploring the feasibility of using the F-statistic of Dyson to expose missing or miss-assigned levels in resonance data of very high quality.

There is a preliminary result of interest in the behavior of the $1/2^-$ average strength function in the mass region A = 40 - 60. The strength function is much more sharply peaked as a function of A than standard optical model predictions. The effect is roughly reproduced by an optical model with a surface peaked absorption term with a smaller than usual diffuseness parameter. An apparent sharpening of the imaginary well has been previously reported by Moldauer[1] and by Johnson and Kernell.[2]

Even with the present high resolution, a rather large fraction of the levels are still being missed in many of the elastic scattering experiments. The level of observability in elastic scattering is a few eV. In experiments where gamma rays are observed, this level of observability has been reduced to $\sim$0.1 eV. Experiments designed to measure level densities by observation of gamma rays in the (p,γ) or (p,p'γ) reactions are in the planning stage.

4. Studies of The Gamma Decay of Excited Levels of ^{51}Ti (G. P. Lamaze*, C. R. Gould, N. R. Roberson, D. R. Tilley)

Preparation of a paper on this subject, based on the Ph.D. dissertation of G. P. Lamaze, is in progress.

5. Gamma Decay of Excited Levels of ^{38}Ca (E. C. Hagen, N. R. Roberson, C. R. Gould, D. R. Tilley)

The reaction ^{36}Ar(τ,nγ)^{38}Ca has been used to populate excited states in ^{38}Ca. Neutron gamma ray coincidence measurements have been performed at 9 and 10 MeV beam energy.

A target was prepared by implanting ^{36}Ar in a thick Ta foil. The implantation was performed with a ^{36}Ar$^+$ beam of 500 keV to 2500 keV from the TUNL 4 MV single-ended Van de Graaff accelerator. A gas cell has also been used, and measurements at pressures between 1 and 6 atm. are being performed. The high stopping power of the Ta allows lifetimes as short as 10^{-14}f sec to be measured, using the Doppler shift attenuation method and the lower stopping power of the gas will allow measurements of lifetimes as short as 5×10^{-11} and as long as 10^{-9} seconds.

6. Lifetime Measurements of Excited Levels in ^{39}Ca (W. Kessel, E. C. Hagen, N. R. Roberson, R. Bass, C. R. Gould, D. R. Tilley)

With the reaction ^{36}Ar(α,nγ)^{39}Ca levels in ^{39}Ca were excited up to about 4 MeV using beam energies of 15.8 and 17.0 MeV. In a gas cell, the ^{36}Ar gas (enriched to 99.5%) served both as target and as stopping medium for the

---

* Now at the National Bureau of Standards, Washington, D. C.

1 P. A. Moldauer, Nucl. Phys. 47, 65 (1963)

2 C. H. Johnson and R. L. Kernell, Phys. Rev. C2, 639 (1970)

Doppler-state-attenuation method. Taking the data in γ-n coincidence, the background from competing reactions (e.g., ((α,p)) was avoided. With gas pressures of 1 atm. and 6 atm. lifetimes in the range of 10^{-11} - 10^{-9} sec can be measured. The mean lives of the levels at 2.468 MeV ($7/2^-$) and 3.642 MeV ($9/2^-$) are supposed to be well within this range.

In analyzing the data with respect to γ-γ coincidences, the lines from the reaction ^{36}Ar(α,pp)^{39}K show up and can be used for calibration purposes. In addition, further information on long living levels in ^{39}K could be gained.

7. Lifetime Measurements in ^{42}Sc (C. R. Gould, J. D. Hutton, N. R. Roberson, D. R. Tilley)

This work has been submitted for publication in Nuclear Physics.

8. Lifetimes of Levels in ^{26}Al (C. R. Gould, D. R. Tilley, J. D. Hutton, N. R. Roberson)

This work is being readied for publication in The Physical Review.

9. A Study of Low-Lying Levels in ^{59}Ni (J. D. Hutton, N. R. Roberson, C. R. Gould, D. R. Tilley)

The properties of excited states of ^{59}Ni up to 2 MeV excitation energy have been studied using the ^{56}Fe(α,n)^{59}Ni reaction. Angular correlation, Doppler-Shift attenuation, and recoil-distance method techniques were used to assign spins, mixing and branching ratios, and lifetimes. The excited states at 340, 465, 878, 1189, 1302, 1680, 1735 and 1948 keV were found to have lifetimes of 120, 29, 0.62, 0.44, 0.18, 0.5, 0.18 and 0.2 picoseconds, respectively. The observation of two gamma rays of 1430 and 430 keV suggest the possibility of a new high spin state at 1770 keV. This work was reported at the Washington meeting of the American Physical Society, 24-27 April 1972 (Bull. Am. Phys. Soc. 2, No. 4, Abs. No. KE9).

10. The Decay Properties of Low Lying Levels of ^{53}Fe (R. O. Nelson, N. R. Roberson, C. R. Gould, D. R. Tilley)

The low lying levels of ^{53}Fe have been studied using the ^{50}Cr(α,nγ)^{53}Fe reaction. Gamma ray angular distributions were measured for the 1328-, 1423- and 1696-keV levels in order to measure their spin and decay properties. The levels were populated near threshold with an α-particle beam of 7.45 MeV, and the gamma rays were detected in singles at nine angles between 0° and 90° to the beam with a 30 cc Ge(Li) detector. The doppler shift attenuation method was used to study the lifetimes of these levels at bombarding energies of 8.7- and 10.5-MeV. Gamma rays were detected in coincidence with neutrons detected at 0° in a 4" x 5" NE213 liquid scintillator. A spectrum was also obtained with a natural Cr target in an effort to identify contaminent γ-rays. Preliminary results are summarized in Table B-1.

11. Study of The γ-decay of ^{23}Mg Excited by The ^{12}C(^{12}C,n)^{23}Mg Reaction (R. O. Nelson, J. D. Hutton, N. R. Roberson, C. R. Gould, D. R. Tilley)

High spin states of ^{23}Mg are currently being studied through γ-decay measurements of states excited by the ^{12}C(^{12}C,n)^{23}Mg reaction. Preliminary work with 22 MeV ^{12}C beams indicated these levels were populated with considerable strength. Angular correlation and lifetime measurements are planned.

12. ^{3}He Reactions and Scattering on Light Nuclei (E. J. Ludwig, T. B. Clegg, R. L. Walter)

a. The Polarization of ^{3}He Particles from ^{27}Al and ^{28}Si

The polarization of ^{3}He particles scattered at a mean energy of 21 MeV from targets of ^{27}Al and ^{28}Si has been studied over an angular range of $25° \leq \theta_{LAB} \leq 56°$. The polarization distributions from the two nuclei are similar with polarizations in both cases failing to exceed 0.15. The results have been analyzed and a paper prepared for submission to Physics Letters.

b. The ^{28}Si(^{3}He,α)^{27}Si Reaction at 21 MeV

These results are being prepared for submission to Nuclear Physics.

13. Deuteron Induced Reactions and Scattering on Light Nuclei (S. Datta, C. Busch, T. B. Clegg, E. J. Ludwig, W. Thompson)

a. Elastic Deuteron Scattering from ^{14}N, ^{13}C and ^{10}B

Cross section and vector analyzing power angular distributions have been measured using a beam of 15 MeV vector polarized deuterons from the TUNL Lamb-Shift polarized source. These distributions have been analyzed with an optical model search code SNOOPY in order to obtain an optical model description of the deuteron-nucleus interaction for these nuclei. A set of parameters could be obtained which varied smoothly with A and fit the cross section data quite well. The shapes of the analyzing power distributions were also in rough

TABLE B-1

Transition Properties for Levels of ^{53}Fe

E_x (keV)	E_γ (keV)	J_i^π	J_f^π	τ (fsec)	δ	Multipole	M^2 (w.u.)
741	741	$3/2^-$	$7/2^-$	92 ± 2 ns[a]	0.0[b]	E2	3.4×10^{-3}
1328	1328	$9/2^-$	$7/2^-$	25 ± 10	0.15 ± 0.03	M1	0.53
1423	682	$5/2$	$3/2^-$	$1_{ps} < \tau < 3ns$	-0.34 ± 0.03 or $< -10.$		
		$3/2$	$3/2^-$		-3.50 ± 1.70		
1696	955	$7/2$	$3/2^-$	$1_{ps} < \tau < 3ns$	0.07 ± 0.07		
2043	2043	$3/2^-$	$7/2^-$	345 ± 75	0.0[b]	E2	5.6
2339	1011	$11/2^-$	$9/2^-$	76 ± 17	0.04[c]	M1	0.32
2967	2226	$1/2^+$	$3/2^-$	112 ± 22		E1	5.6×10^{-4}

[a] S. Cochavi *et al.*

[b] Assumed to be zero.

[c] Z. P. Sawa *et al.*

agreement with theory when this smoothly varying set of potentials was used.

b. (d,t) and (d,^{3}He) Reactions on 1-p Shell Nuclei

Vector analyzing powers have been measured for $\ell = 1$ transfers (J^π = 3/2$^-$ or 1/2$^-$) occuring with targets of ^{10}B, ^{13}C, ^{14}N and ^{16}O are bombarded by 15 MeV vector polarized deuterons. The analyzing power distributions for J^π = 1/2$^-$ transfers were inverted from those for J^π = 3/2$^-$ transfers over the forward angular region when the Q-values for the reactions were similar. Calculations made with DWBA code DWUCK could predict the shift in angle between the distributions when the Q values were markedly different. A J-dependence for $\ell = 1$ transfers can therefore be inferred from our analyses of pickup reactions on 1-p shell nuclei. Comparisons of (d,t) and (d,^{3}He) cross sections distributions and vector analyzing power distributions show nearly identical shapes for the two indicating that the charge symmetry of nuclear forces has been maintained.

c. The Comparison of Vector Analyzing Powers for (d,d) Scattering with (d,t) or (d,^{3}He) Analyzing Powers Using Targets of ^{14}N and ^{32}S

A polarized beam of 15 MeV deuterons was used to study certain states populated in the reactions ^{32}S(d,^{3}He)^{31}P and ^{14}N(d,t)^{13}N. The vector analyzing powers were measured in the angular range $30° \leq \theta_{LAB} \leq 80°$. The states studied were populated by an ℓ_n = 0 transfer. Vector analyzing powers for the corresponding elastic deuteron scattering were also measured in the same angular range. A comparison of the analyzing power distribution with that of the corresponding elastic scattering showed a strong similarity. This similarity is even more evident when the analyzing power times the cross section is plotted versus angle or momentum transfer.

The close comparison of the distributions is not a direct consequence of a DWBA analysis. The Weakly Bound Projectile model (WBP) however may be extended to predict the results of this experiment.

14. Polarization Transfer in The D($\vec{d}$,$\vec{p}$)T at $\theta = 0°$ (T. B. Clegg, with R. A. Hardekopf, P. W. Keaton and D. D. Armstrong, Los Alamos Scientific Laboratory)

Measurements have been made of the polarization of the protons emerg-at $\theta = 0°$ from the D(d,p)T reaction when the reaction is initiated by polarized deuterons. These have resulted in an excitation function from 6 to 15 MeV of the polarization transfer coefficients $K_y^{y'}$ and $K_{yz}^{x'}$ in approximately 2 MeV steps.

Where comparison can be made with other $D(\vec{d},\vec{p})T$ and $D(\vec{d},\vec{n})^3He$ results for these same transfer coefficients. The results are the same showing that these mirror reactions are identical insofar as these coefficients are concerned. The outgoing proton polarization is reduced by about 10% from the value one would expect from the assumption of simple stripping of the proton from the incident deuteron. This means there is some spin-dependent interaction causing the small depolarization.

A report of this work is being given at the Seattle APS meeting in November 1972 and a paper is being prepared for publication in Physical Review.

15. Elastic Deuteron Scattering at 15 MeV (C. E. Busch, T. B. Clegg, S. Datta, E. J. Ludwig)

Cross section angular distributions and asymmetry distributions for vector polarized deuterons have been obtained for elastic scattering from ^{10}B, ^{13}C, and ^{14}N. An optical model analysis using the on line program OPTICS and the search program SNOOPY was undertaken. Systematic trends in the optical-model parameters are noted for the above nuclei. This work is being prepared for publication.

16. The $^{54}Fe(p,t)^{52}Fe$ Reaction (R. O. Nelson, N. R. Roberson, C. R. Gould)

This work is being prepared for publication.

17. The $^{54}Fe(p,d)^{53}Fe$ Reaction (R. O. Nelson, N. R. Roberson, C. R. Gould, D. R. Tilley)

Low-lying levels of ^{53}Fe have been investigated with the $^{54}Fe(p,d)^{53}Fe$ reaction with a bombarding energy of 30 MeV. A DWBA analysis of the angular distributions measured for the 0.0-, 0.74- and 2.04-MeV states have established ℓ-values assignments for these states of 3, 1 and 1, respectively.

In conjunction with recent lifetime measurements made in this laboratory, these assignments allow unique spin and parity assignments of $3/2^-$ for both the 0.74 and 2.04 MeV states.

18. Inelastic Effects in The Study of ^{23}Na and ^{23}Mg (R. O. Nelson, N. R. Roberson)

A paper entitled Inelastic Effects in The Study of ^{23}Na and ^{23}Mg has been accepted for publication in The Physical Review. The abstract is given below:

"Fourteen states of ^{23}Na with excitation energies <5.6 MeV and their mirror states in ^{23}Mg have been studied with the ^{24}Mg(d,^{3}He)^{23}Na and ^{24}Mg(d,t)^{23}Mg reactions with a bombarding energy of 21.1 MeV. Differential cross section measurements indicated significant differences between established $\ell = 2$ transitions and large cross sections for "j-forbidden" $7/2^+$ and $9/2^+$ states. Failure of a distorted-wave analysis to predict these anomalies suggested that inelastic effects should not be neglected. Calculations with the coupled-channel Born approximation (CCBA) have produced agreement with experiment and have shown that multiple-step processes not only dominate the transitions to the "j-forbidden" states, but have large effects upon allowed transitions as well. From the CCBA predictions it was possible to identify mirror states of the nuclei and to establish J^π assignments of $9/2^+$, $3/2^+$ $(5/2^+)$, $(5/2^-)$, $(7/2^+)$, $(5/2^+)$ and $(11/2^+)$ for the states in ^{23}Mg at 2.71, 2.90, 3.86, 3.97, 4.68, 5.29 and 5.45 MeV, respectively."

19. Inelastic Deuteron Scattering from ^{24}Mg, ^{28}Si, ^{208,206}Pb (R. A. Hilko, R. O. Nelson, T. G. Dzubay, N. R. Roberson)

Coupled-channel analysis of ^{24}Mg has yielded a good fit to the first four levels assuming an asymmetric rotor picture with $\beta_2 = 0.47$ and $\gamma = 20°$. (See above abstract.) As of now, ^{28}Si has been harder to fit, but a coupled-channel search favors an oblate shape rather than prolate.

20. The (d,t) and (d,^{3}He) Reaction on ^{28}Si (R. A. Hilko, R. O. Nelson, N. R. Roberson, C. R. Gould)

Triton and helion spectra were taken from 25° to 70° in the laboratory with a 23.0 MeV deuteron beam from the TUNL Cyclo-Graaff. Two solid-state $\Delta E - E$ telescopes were used to collect the data from an enriched ^{28}Si target of silicon monoxide approximately $\mu g/cm^2$ thick. Data will be analyzed with the coupled-channel Born approximation.

21. Search for The Lowest $T = 3/2$ Level in ^{41}Sc (T. A. Trainor, T. B. Clegg, E. J. Ludwig, W. J. Thompson)

Further efforts have been made to locate the $T = 3/2$, $J^\pi = 3/2^+$ analogue of the ^{41}K ground state as a resonance in ^{40}Ca(p,p)^{40}Ca elastic scattering. Previous attempts have been hampered by the presence of several overlapping levels in the immediate vicinity of the level tentatively assigned as the analogue resonance. In addition, an isolated $\ell = 2$ resonance in the vicinity of this group possesses the correct ℓ value to be included as a candidate for the analogue. In order to unravel the group of overlapping resonances data have been taken in the energy range 4.880–4.920 MeV with improved energy resolution. Both cross section and polarization data have been obtained with a resolution of 2 keV. Work is underway to obtain fits to the data which will yield resonance parameters for the obscured $\ell = 2$ resonance. It is then necessary to identify one of the two $\ell = 2$ candidates as the T = 3/2 analogue.

22. ^{208}Pb(p,p'), ^{208}Pb(p,d) and ^{208}Pb(p,t) Reactions from 16.7 to 27.3 MeV (E. J. Ludwig, P. Nettles, C. Busch, E. Klema)

Excitation curve data have been taken with the Cyclo-Graaff for ^{208}Pb + p in an energy range from 16.7 to 27.3 MeV at θ_{LAB} = 90° and 150°. The excitation curves for tritons from the (p,t) reaction show little structure over the entire energy range while those for deuterons from the (p,d) reaction show strong resonances for several groups at energies below 20 MeV. The elastically scattered protons and low-lying inelastically scattered protons show resonance structure at energies below 22.5 MeV. The resonances seen in inelastic scattering occur at energies where excited core plus single particle state in the compound nucleus might be expected to occur. The excitation curves have now all been obtained and an analysis of the resonances will now be attempted using a weak-coupling model.

23. Isobaric Analog Resonances in ^{71}Ge (P. G. Ikossi, C. E. Busch, T. B. Clegg, E. J. Ludwig, W. J. Thompson)

Isobaric analog resonances in ^{71}Ge have been investigated by the reaction ^{70}Zn(p,p)^{70}Zn. Cross section excitation functions at Lab. angles 90° and 155° have been measured between 3.66 and 5.34 MeV. Polarization excitation functions were taken at Lab angles 115° and 155° over an energy range of 3.68 MeV to 4.89 MeV. Two differential cross section angular distributions were measured at energies 3.58 MeV and 3.96 MeV between 40° and 160°. The data have been analyzed using the computer code ANSPEC. Resonance parameters and spectroscopic factors were extracted for resonances up to .86 MeV excitation energies in ^{71}Ga and compared to the results of (d,p) reactions. Difficulties due to impurities in the target were encountered in the analysis of the resonance corresponding to the ground state of ^{71}Zn.

24. Capture Gamma Ray Studies (S. M. Shafroth, P. H. Nettles, T. A. White)

The plastic anticoincidence annulus for the 9"x9" NaI crystal has been painted with white paint as recommended by Nuclear Enterprises Corporation. This has improved the signal to noise ratio but not enough. The next step is to substitute premium photomultipliers such as RCA 8575 tubes. This should give several orders of magnitude better performance.

25. X-Ray Studies (A. B. Baskin, G. A. Bissinger, C. E. Busch, P. H. Nettles, J. T. May, A. W. Waltner, S. M. Shafroth, T. A. White)

a. Ag K and L and Au L X-rays Produced by 12-50 MeV ^{16}O Ion Bombardment

This work is being prepared for journal publication. It has been presented at the International Conference on Inner Shell Ionization Phenomena, Atlanta, April 17-21, 1972 and will be published in the Conference Proceedings. Since that time the Ag K shell ionization cross section data have been compared with the PWBA calculation corrected to order $(Z_1/Z_2)^3$ for Coulomb and binding energy effects and gives very good agreement with experiment.

b. Yields of K and L x-rays Produced by 2-30 MeV Proton Bombardment of Ag

This work has been presented at the International Conference on Inner Shell Ionization Phenomena, Atlanta, April 17-21, 1972 and will be published in the Conference Proceedings.

It is also published in Phys. Rev. A5, 2046 (1972).

c. Relativistic Effects in Au L x-ray Production by 0.5-3.0 MeV Protons

This work has been presented at the International Conference on Inner Shell Ionization Phenomena, Atlanta, April 17-21, 1972. It is published in Physical Review A6, 545 (1972).

d. Au L x-ray Production by 0.5-30 MeV Protons

This work has been accepted for publication in Phys. Rev. A.

e. Yields and Ratios of Au K x-rays, $E_p = 2\text{-}14$, $E_{^{16}O}$ 18-42 MeV

This work is being prepared for journal publication and has been presented at Atlanta. Since TUNL VIII, a companion study of Au K x-ray yields and ratios has been made using up to 1/2 amp beams of ^{16}O ions from the newly installed direct extraction negative ion source. Effects of nuclear Coulomb excitation of the first excited level of ^{197}Au at 77 keV which could give rise to a γ-ray peak in the K_{β_1} peak are being investigated. This work will be reported on at the S. E. section meeting of the APS at Birmingham, November 1972.

f. M X-Rays

Pb. M X-rays arising from 0.5-14 MeV proton bombardment have been observed. The M shell ionization cross section is compared with B.E.A. calculations. The trend of σ_m vs. E_p is well described by B.E.A. theory but at higher proton energies the experimental values are well above theory.

g. Pb L X-Rays

A study of Pb L X-rays over the energy range from 0.5-14 MeV has been made and comparison of α/β, α/γ and L_ℓ/L_α ratios as well as the total L shell ionization cross section with theory has been made. The L_α/L_β ratio changes from 2.1 at $E_p = 0.5$ MeV to 1.55 at $E_p = 14$ MeV. The L_α/L_γ ratio changes from 20 at $E_p = 0.5$ MeV to 10 at $E_p = 14$ MeV. These large changes may be useful in trace element analysis.

The L_α/L_ℓ ratio should be independent of E_p if the incident proton interacts with only one L_{III} $(2p_{3/2})$ electron at a time. However we find a 5% dip in this ratio at $E_p = 1.3$ MeV. This effect is being searched for in neighboring atoms such as Au and Bi, and we are trying to understand it with the help of our theorists. The work on the Pb L x-rays is being prepared for journal publication.

h. Ratios of L Subshell Cross Sections

We have gone over the region from $E_p = 0.5 - 3$ MeV for Pb with a KeVex (SiLi) detector whose resolution is 190 eV at 5.9 keV using the 4 MeV Van de Graaff to obtain better statistics. This has permitted us to attempt to decompose L_γ into 4 components, L_β into several components and to extract areas for the weak L_n peak. Thus ratios of L subshell cross sections can be extracted. This work will constitute the M.S. thesis of Mr. A. B. Baskin. He has extended the GAUSSN program so that it can now fit 4 Gaussian curves to an unresolved structure.

26. (p,n) Experiments with Chopped Beam (S. M. Shafroth, A. A. Jaffe,* G. A. Bissinger,** T. G. Dzubay,+ F. Everling,‡ D. W. Miller,‡+ D. A. Outlaw, E. J. Ludwig, P. Nettles‡‡)

The $^{36}Ar(p,n)^{36}K \rightarrow \beta^{+} + {}^{36}Ar^{*}/\gamma)$ reaction work is published in Physical Review 6, 869 (1972).

27. Channeling Studies (R. Haglund, B. Doyle, T. B. Clegg, E. J. Ludwig) A system was constructed and installed on the 4 MeV accelerator to measure the channeling of ions in single crystals in order to evaluate nickel foil which might be used to produce polarized beams of deuterons and ^{3}He via channeling. The foils which were produced in the laboratory of E. N. Mitchell of UNC proved to be unsuitable for channeling and will be made again using modified techniques.

28. Tests of The Suitability of a 3 MeV Proton Beam for Trace Element Studies (R. L. Walter, R. D. Willis, J. M. Joyce,‡‡+ A. Larkins‡‡‡)

Stimulated by numerous people and reasons, a study of the sensitivity of the method of using characteristic X-rays emitted from a thin sample under 3 MeV proton bombardment was initiated. Using available beam time on the 4 MeV Van de Graaff and borrowed Si detectors from the Environmental Protection Agency and AEC more than 400 irradiations of targets supplied by the EPA and several of the science and medical departments have been made. As is widely known, the method is sensitive to small amounts of elements (parts per billion) in some selected samples under special conditions. As there are other ways of measuring concentrations at this level, the true value of using 3 MeV accelerators is not clear. A proposal (1) to evaluate the method, (2) to compare explicitly results for the same samples with those obtained using the best available X-ray induced fluorescence system and (3) to compare with results for the same samples from analytical chemistry methods such as atomic absorption is being prepared for submission to the EPA. With this full co-

---
* Now at Hebrew University, Jerusalem, Israel

** Now at Rutgers University, New Brunswick, N. J.

\+ Environmental Protection Agency, Research Triangle Park, N. C.

‡ 2104 Hamberg 92, Wiedenthaler Bogen 61, West Germany

‡+ Memorial Hospital for Cancer and Allied Diseases, New York, N. Y.

‡‡ Scientific Atlanta, Atlanta, Georgia

‡‡+ East Carolina University, Greenville, N. C.

‡‡‡ East Carolina University, Greenville, N. C.

operation on the latter two aims and continued cooperation of the local medical and science departments and the EPA to provide samples of current importance, the proposed program should be extremely significant for research planning and funding and for 3 MeV accelerator owners. Beam time for this work will also be available at the 4 MeV Nuclear Research Laboratory at ECU. A paper on one small aspect, trace elements in clean water obtained by irradiating selected ion-exchange membranes, has been submitted to the Birmingham meeting of the ACS.

C. DEVELOPMENT

1. Accelerator Improvements (F. O. Purser, J. R. Boyce, Jr., H. W. Newson, M. T. Smith, E. G. Bilpuch, R. L. Rummel, J. D. Moses, D. E. Epperson, G. E. Mitchell)

a. Tandem Accelerator

The previously reported increase in terminal ripple associated with installation of a new type of charging belt has gradually lessened as the belt has aged. Present ripple figures are marginally higher than those experienced with the former belts, and voltage holding and dust characteristics remain superior.

The direct extraction source has been installed on the tandem and is in successful routine operation. Beam currents of 27 μA of H^-, 20 μA of D^-, 2.5 μA of O^-, 0.9 μA of C^-, and 1.5 μA of S^- have been measured in the low energy Faraday cup. The source runs very stably and thus far has experienced no difficulties with arc down. With the source voltage of -45 kV, beam transmissions from low energy to high energy cup of as much as 90% have been measured with protons and transmissions of 70% with protons are routine. It has been a very successful addition to our capabilities.

In preparation for expected extensive heavy ion work (O^-, C^-, S^-) a set of beam defining slits has been installed in the low energy extension. These ions are customarily accompanied by radical beams OH^-, CH^- which unless intercepted can cause extensive damage to the low energy accelerating tubes of the tandem.

The ^3He recovery system is nearing completion and will be placed in use in the coming report period.

b. Injector Cyclotron

This accelerator has run routinely during this report period.

c. Improved Beam Energy Resolution for The Tandem Accelerator

This program has been dormant pending installation of the direct extraction source. Now that this source is in routine operation, work will begin again during the coming report period.

2. Pulsed Beams (F. O. Purser, D. E. Elliott, H. W. Newson, R. O. Nelson, R. A. Hilko, N. R. Roberson)

a. Mass Identification of Charged Particles by Time of Flight

By using the pulsed deuteron beam from the TUNL Cyclo-Graaff, we were able to identify by kinematics of angular distribution mass groups 1, 2, 4, 6, 10, and 12 from targets of ^{28}Si, ^{24}Mg, ^{16}O, and ^{12}C. A computer on-line analysis program forms the product of pulse height from detector (E) and square of time-of-flight (T^2) which is found to be roughly proportional to mass. Time resolution of 550 picoseconds has been measured. Incorporated in the on-line computer program is a time monitor which checks for drifts in the beam burst relative to the rf frequency. The data is corrected for drifts during a run and the time structure of a selected energy peak is displayed. Data can also be stored on magnetic tape for subsequent reanalysis.

3. Polarized Ion Source Improvements (T. B. Clegg, C. E. Busch, P. W. Lisowski, T. A. Trainor, R. T. Hawkins, Jr.)

The last six months have provided the most reliable and stable operation of any comparable period of time since the ion source was first installed. Typical accelerated beams have ranged between 10 and 50 nA for both proton and deuteron operation. Typical beam polarizations have ranged between 0.70 and 0.88 for protons and 65% to 80% of the theoretical maximum values for deuterons.

The ion source is beginning to be used extensively by experimental groups of widely varying interests. As an indication, during the last scheduling period approximately 60% of the total time was requested by groups using the polarized source for experiments on polarized neutron elastic scattering, analog state studies with polarized protons, transfer reaction studies using polarized deuterons, and gamma ray angular correlation studies following reactions induced by polarized deuterons.

The major effort toward polarized source operation in this period has been:

1. Complete realignment of the entire low energy ion transport system for the tandem accelerator and polarized ion source components. This was required because the floor in the ion source area continues to settle by approximately 3 mm in the last two years.

2. Modification of the second electrostatic mirror to allow installation of the direct extraction source on the left 20° port of the standard tandem ion source box.

3. Repair of small oil leaks inside the source so the base vaccua in the actual ion source are all in the range 1-3 x 10^{-6} mm Hg.

4. Ion optics calculations for all the focussing elements between the polarized source and the low energy end of the tandem accelerator. A computer program has been written to facilitate the calculations. Preliminary conclusions are: (a) that the beam is diverging enough inside the quadrupole triplet lens for the accelerator so it is partially lost from striking the inside of the beam tube; (b) the beam entering the low energy acceleration tube does not have an emittance which matches the phase space acceptance of the tube. In particular a much more highly divergent beam could be used than can be produced with the present lens system. Further calculations will be made to determine if the present lenses should be moved or new lenses should be added.

5. Designing and ordering parts for an interlock system for the source to protect against power failures and failures of the oil or water cooling system. The system has been partially assembled and should be completed within the next few months.

6. Making measurements to determine the reliability of the "quench ratio" for determining the beam polarization. The "quench ratio" is the ratio of (total plus quenched beam) / (quenched beam) measured on a Faraday cup at the scattering chamber. Our measured values thus far indicate that we can determine the proton polarization to ±0.5% and deuteron polarization to ±1.0% by this method if the measurements are made carefully and the ion source is operating stably.

7. Programs and hardware for remote computer control of the polarized source. It is now becoming possible (a) to have the computer flip the spin direction by reversing the polarity of all magnetic fields in the "spin filter" and

argon regions of the source; (b) to quench the polarized beam by computer control applying either a large d.c. electric field on the deflection plates, a large r.f. electric field to the "spin filter" cavity, or by changing slightly the magnetic field in the spin filter region; (c) to have the computer select either the $m_I = +1/2$ or $m_I = -1/2$ magnetic substate for proton beams, and either the $m_I = +1, 0,$ or -1 magnetic substate for deuteron beams. This is done by remote control of the magnetic field in the "spin filter" region.

4. Chamber Rotation Control System (R. F. Haglund, Jr., T. B. Clegg)

Measurement of tensor analyzing powers in nuclear reactions requires counters both in and out of the scattering plane. A system is being developed to permit computer-controlled rotation of the scattering chamber about the beam axis. Using photodiodes as position sensors, the chamber can be set to any of four different positions. Switching logic (to be mounted in a control panel at the chamber) has already been designed which will ensure the proper sequence of rotations. In addition, the control circuit will signal the chamber position to the computer, so that data can be stored and processed automatically. A micro-switch-controlled relay--separate from the logic circuitry--will provide a fail-safe mechanism to cut off power to the chamber drive motor should the chamber fail to return to the initial position after reaching the final stop.

5. High Intensity Duoplasmatron for Polarized Ion Source (T. A. Trainor, T. B. Clegg)

Further testing and development of a high intensity duoplasmatron for the TUNL Lamb-shift source is in progress. Lifetime problems due to sputtering of the multi-aperture accel-decel electrodes by the low energy ion beam have been considerably reduced. The multi-aperture decel electrode has been replaced by a thoriated tungsten grid used both as an electrode and as an electron emitter to space charge neutralize the intense ion beam.

The source has been operated with 20A arc current and 50 mA total extracted beam. Test bench measurements with a 1.1 kV deuteron beam indicate a total beam current of 21 μA in a 1.25 cm diameter Faraday cup 160 cm from the source expansion cup. This beam is composed of 83% D^+ when a magnetic lens is used and 53% D^+ with no magnetic lens, as determined by momentum analysis in a deflection magnet.

The duoplasmatron was installed briefly on the Lamb-shift source. The source arc current was limited to 13A. Total positive beam through the Argon charge exchange canal was 150 μA. Negative deuterium ion beams up to 2 μA were observed after acceleration to 50 kV. However, beam polarization was low due to a large unpolarized background component.

6. Pre-Bunching in A Lamb-Shift Polarized Ion Source (T. B. Clegg with G. P. Lawrence, J. L. McKibben, and A. R. Koelle, Los Alamos Scientific Laboratory, and with G. Roy, University of Alberta)

A circuit has been built and tested on the Los Alamos Lamb-shift polarized ion source which generates a pulsed polarized beam by bunching the d.c. beam. The circuit makes a high frequency voltage vamp signal. The frequency is variable between 1 and $5 \times 10^{+6}$ Hertz. The peak ramp voltage is variable between about 40 and 160 volts. This ramp voltage is applied to the duoplasmatron anode plate of the polarized source and causes the actual energy of the beam extracted from the duoplasmatron to vary linearly with time as the voltage increases along the ramp. This linear change in beam energy with time becomes a modulation of the beam intensity in time after the beam has drifted through the 1.6 in. path through the rest of the ion source.

Initial tests showed that beam pulses of minimum time widths of 40-70 nsec could be obtained. When used with a subsequent Klystron buncher before injection into the tandem accelerator, increases of the average beam on target of a factor of 4 or 5 are probably possible over operation of the Klystron buncher alone without the prebuncher ramp circuit.

This work has been reported at the International Conference on Ion Sources and The Formulation of Ion Beams held in Vienna, Austria in September 1972. Also a report is available from Los Alamos (LA-DC-72-1019) and an article is being prepared for publication in Nuclear Instruments and Methods.

7. Design of a Lamb-Shift Polarized Source for Tritons (T. B. Clegg with J. L. McKibben, R. A. Hardekopf, P. W. Keaton, D. D. Armstrong, and G. P. Lawrence, Los Alamos Scientific Laboratory)

Preliminary design studies have been made for a Lamb-Shift polarized ion source for tritons for the Los Alamos tandem accelerator. The source will be installed in a vertical-configuration close to the base of the tandem accelerator tank with the polarized beam reflected onto the tandem axis by an electrostatic mirror. The basic ion source components are similar to the present source operating at Los Alamos and the triton source will be operated using the present polarized source electronics.

Basic problems which must be overcome for successful triton operation are: (a) a recirculating system for the large tritium gas flow required by the duoplasmatron; (b) a cesium oven design which requires very little maintenance and will operate in a vertical orientation; (c) cryogenic pumping of the argon to avoid tritium contamination of oils used in other types of possible vacuum pumps.

Design drawings are completed well enough that some components can be ordered and shop work can begin.

8. A Two-Crystal NaI Polarimeter for Gamma Rays (J. R. Williams, C. R. Gould, R. Bass, D. R. Tilley, N. R. Roberson)

This project is awaiting delivery of some new detectors.

9. Development of a High Resolution System for The 4 MeV Van de Graaff Accelerator (D. Flynn, F. O. Purser, E. G. Bilpuch, H. W. Newson, G. E. Mitchell, L. W. Seagondollar)

The high resolution system has been tested by measuring known resonances in ^{30}Si at approximately 1.2 MeV proton energy. The data as fitted indicate a beam energy resolution of about 500 eV or less.

Following the above tests, the system was used to measure elastic scattering differential cross sections at 90° and 150° for ^{54}Fe for proton energies from 3.3 to 4.0 MeV. Preliminary analysis of these data indicates a beam energy resolution between 400 and 700 eV. For the higher energies involved this compares reasonably well with the resolution attainable on the 3 MeV machine (~ 300 eV).

D. THEORY

1. $^9Be(p,p_0)$ and $^9Be(p,p_2)^9Be$ and Deformed Optical Model Potentials (H. J. Votava, W. J. Thompson)

Analyses of TUNL cross section and polarization data for 13- to 30-MeV protons has been completed and an abstract submitted to the Birmingham APS meeting. A paper is in final preparation summarizing the results from Votava's Ph.D. thesis. The thesis abstract follows:

"Differential cross-section excitation functions at lab scattering angles 86.9°, 120.0°, 140.0°, and 160.0° were measured for $^9Be(p,p_0)^9Be$, $^9Be(p,p_2)^9Be$, and $^9Be(p,d_0)^8Be$

from 6 to 15 MeV proton lab energy in 100 keV steps. An anomaly near 6.7 MeV, corresponding to 12.6 MeV excitation in the compound nucleus ^{10}B, was observed in the $^{9}Be(p,p_0)^{9}Be$ excitation curves and was analyzed along with a neutron threshold in $^{9}Be(p,n_4)^{9}B$ at 6.55 MeV with an excited-state-threshold resonance theory using energy dependent Breit-Wigner resonance parameters $\Gamma(E)$ and $E_0(E)$. Non-optical-model off-resonance cross sections were needed to fit the resonant cross-section shapes and magnitudes. A probable spin-parity assignment of (2^+) for the 12.6 MeV level in ^{10}B and probable spin-parity assignments $(3/2^+, 5/2^+)$ for the 4.05 MeV level in ^{9}B were made. The 6.7 MeV resonance suggests that the optical-model is inapplicable to $^{9}Be(p,p_0)^{9}Be$ below 10 MeV. Differential cross-section angular distributions were measured for $^{9}Be(p,p_0)^{9}Be$ and $^{9}Be(p,p_2)^{9}Be$ at proton lab energies of 13.0, 14.0, 15.0, 21.35, and 30.3 MeV and for $^{9}Be(p,d_0)^{8}Be$ at 13.0, 14.0, 15.0, and 21.35 MeV. Angular distributions of polarizations for $^{9}Be(\vec{p},p_0)^{9}Be$ and of analyzing powers for $^{9}Be(\vec{p},p_2)^{9}Be$ and $^{9}Be(\vec{p},d_0)^{8}Be$ were also measured at 13.0 and 15.0 MeV. A spherical optical-model (SOM) analysis of $^{9}Be(p,p_0)^{9}Be$ angular distributions from 13.0 to 30.3 MeV showed that allowing only an energy dependence in the parameters V_R and W_S, the volume real and surface imaginary potential depths, respectively, reproduced the measurements. Elastic-scattering SOM wavefunctions for $^{9}Be(p,p_0)^{9}Be$ were used to calculate probability densities and flux divergences displayed in three-dimensional computer-generated plots revealing the McCarthy focus and were used to predict large local polarizations within the nuclear surface. A non-adiabatic coupled-channels (NACC) analysis was made assuming a quadrupole deformed optical-model potential and assuming that the $3/2^-$, $5/2^-$, and $7/2^-$ levels of the $K=3/2$ ground-state rotational band of ^{9}Be were strongly coupled. The $^{9}Be(p,p_0)^{9}Be$ and $^{9}Be(p,p_2)^{9}Be$ measurements from 13.0 to 30.3 MeV were simultaneously reproduced at each energy for a nuclear deformation of $\beta = 1.1$. The NACC fits were obtained as in the SOM case by varying only V_R and W_S with energy. Comparisons between the DWBA and NACC indicated that the former is inadequate for large deformations. Both SOM and NACC analyses in this work indicated the same energy dependence in V_R while the NACC analysis indicated W_S was 4 MeV lower than the SOM W_S

at each energy of the analysis. Both SOM and NACC analyses ignored the 3/2 spin of ^{9}Be and measured polarizations were reproduced using only the standard undeformed spin-orbit potential. Comparable SOM and NACC fits indicated that the SOM parameterization was able to compensate for the highly deformed surface of ^{9}Be. The SOM and NACC energy dependence in V_R and W_S in this work was consistent with other parameterizations describing elastic nucleon scattering from other nuclei."

2. Excited-State-Threshold Resonance Effects in ^{9}Be(p,p$_0$)^{9}Be and ^{9}Be(p,n)^{9}B (H. J. Votava, W. J. Thompson)

The first reported observation of excited-state-threshold resonance effects (from the ^{9}Be(p,n$_4$)^{9}B near 7 MeV) has been described in a paper to be published in Physics Letters. A detailed description has been made using an R-matrix analysis.

3. Proton Optical-Model Potential Near the Coulomb Barrier (J. S. Eck (Kansas State University), W. J. Thompson)

Final analysis of these data has shown that the traditional optical model potential varies too slowly with energy near the Coulomb barrier. This is related to the non-locality of the optical model potential. A surface-peaked real potential improves the fits without altering the above conclusions. All calculations were made using OPTICS on the TUNL DDP-224. A paper describing the results has been submitted to Physical Review.

4. Compound Elastic Scattering and Tensor Polarizations (R. J. Eastgate, W. J. Thompson)

Simplified formulas for compound elastic tensor polarizations have been programmed for the DDP-224 as an extra Link in OPTICS. Compound elastic effects in T_{20} at backward angles are predicted to be especially large.

5. Binding Energies, Two-Body Correlations and The Energy and Symmetry Dependence of Nucleon-Nucleus Potentials (W. J. Thompson)

A Fermi-gas treatment of nuclear matter including two-body density correlations has been used to calculate the energy and isospin symmetry dependence of nucleon-nucleus potentials for heavy nuclei. A more-rapid energy dependence and a much weaker symmetry dependence than used in phenomenological analyses are suggested. A description of the results has been submitted to Physics Letters.

6. Formalism and Calculation of Generalized DWBA (S. Edwards, D. Robson, T. L. Talley, M. F. Werby ((Florida State University)), W. J. Thompson)

A paper on finite-range, multi-mode, direct and exchange, transfer reactions, together with calculations for several light nuclei made using the code FANLU2, has been submitted to Physical Review.

7. Scattering Wave Functions and Spin Precession in Nuclear Potentials (H. J. Votava, W. J. Thompson)

Computer graphics for perspective and stereoscopic view of flux densities and scattering probabilities in nuclear potentials, including spin-orbit coupling, have been completed. Further work will improve the presentation of spin vectors and will be used to help understand spin dependence in scattering.

8. Reaction Mechanism Studies in $(\alpha,\alpha'\gamma)$ Reactions (C. E. Ahlfeld, G. E. Assousa, R. A. LaSalle, H. A. Van Rinsvelt, G. S. McNeilly, W. I. van Rij, N. P. Heydenberg ((Florida State University)), W. J. Thompson)

Reports of this work have been prepared for publication in Nuclear Physics. The paper on $^{28}Si(\alpha,\alpha'\gamma)^{28}Si$ at 18.0 MeV has been published, while that on $^{24}Mg(\alpha,\alpha'\gamma)^{24}Mg$ at 16.25 MeV is in final preparation.

9. Cluster Effects in Elastic α Scattering Using a New α-α Interaction (W. J. Thompson)

An attractive, L-independent optical potential recently shown to describe α-α phase shifts was used to recalculate α-cluster effects in $^{40}Ca(\alpha,\alpha)^{40}Ca$ at 29 MeV. The effects are even smaller than those previously obtained with repulsive-core, L-dependent α-α potentials. An account of these results is to be published in Particles and Nuclei.

10. O-L-O γ-γ and α-γ Angular Correlations (W. J. Thompson)

A simple derivation of these angular correlations has been made in order to clarify the mechanisms of angular correlations for beginners in the field. A paper on this has been submitted to the Birmingham APS meeting.

11. Nuclear Theory Computer Programs (S. K. Datta, R. J. Eastgate, W. J. Thompson)

Computer programs for theoretical analysis of nuclear data, with particular emphasis on the use of the DDP-224 display facilities at TUNL, are continually being written.

The optical model analysis program OPTICS has been extended to include compound elastic tensor polarizations. (See Section 4.)

Subroutines for accurate evaluation of angular momentum coupling coefficients even for large angular momenta (up to 30) have been debugged for the TUNL and TUCC computers. The Regge symmetries have been used to provide an increase in accuracy of several orders of magnitude over values obtained using the Racah expressions directly, without significant increase in computation times or in core storage requirements.

Outlines for a DWBA code for the DDP-224 have been completed and the subroutines of the scattering and bound state wave functions completed. Use of the DDP-224 will require extensive utilization of the disk storage.

An off-line disk pack has been rented from Memorex Corp. for use at TUCC. Frequently-used programs such as SNOOPT2 (optical model search) and ANSPEC2 (optical model plus resonance and isobaric analog spectroscopic factors) have been stored on the disk. Data storage charges and program initialization time have thus been drastically reduced.

12. Computer Codes for Analysis of Fission Data (J. R. Boyce, R. Bass, F. O. Purser)

Two computer codes have been written to analyze fission data taken at TUNL. The first, MERLIN, is a modification of the optical model program OPTIC.[1] By utilizing mass and energy dependent optical model parameters MERLIN calculates reaction cross sections for incident neutrons or protons over an energy range 0.125 MeV $\leq E_{LAB} \leq$ 40.0 MeV. Preliminary results indicate that conventional optical model parameters overestimate proton reaction cross sections for proton energies below the Coulomb barrier.

---

[1] R. J. Eastgate and R. A. Hardekopf, Bull. Am. Phys. Soc. 16, 517 (1971)

The second code, PHROG, calculates fission probabilities for an excited compound nucleus. The code is based on a statistical model which assumes either fission or neutron emission as primary decay channels. Input data consists of reaction cross sections calculated by MERLIN, experimental total fission cross sections, ground state deformation level density parameters, and fission barrier parameters. Multiple applications of a nine point Gaussian quadrature is used to insure convergence of the integrations over energy distributions and level density expressions of the model. Tables are calculated and interpolation is used whenever possible to reduce computer time. Extensive tests have been performed to insure calculational accuracy especially in the double and triple integral routines. In its present form PHROG calculates the contributions to the total fission probability from first, second, and third chance fission. The results are then compared to the fission data to obtain a self consistent set of fission thresholds and Γ_n/Γ_f curves for the isotopes studied and over the energy range $0 \leq E \leq 30$ MeV.

13. New Methods for High Accuracy Calculations of Shell Model States (R. Y. Cusson, H. W. Meldmer (Univ. of California, San Diego), M. S. Weiss (Livermore), H. P. Trivedi)

Following the 1969 pioneering work of Meldmer (Phys. Rev. 178 (1969) 1815), we have obtained, starting from Brueckner theory, some very accurate models for the single particle shell model Hamiltonian which can reproduce binding energies to 1% accuracy or better, radii to 0.1 F or better, electron scattering cross-section fits as good as those obtained using empirical density distributions and single particle energy predictions for levels both above and below threshold for single nucleon emission. An article describing these results is in preparation.

14. Computer Codes for High Accuracy Single Particle States (R. Y. Cusson, H. P. Trivedi, D. Kolb)

Starting from unpublished notes from B. Buck, a fast and accurate method has been devised[1] to find the self consistent eigenvalues and eigenfunctions of the realistic, non-local, density dependent, single particle Meldmer reaction matrix. This code is now being used in Livermore, Berkeley and Los Alamos to obtain single particle states of spherical nuclei. It is presently being modified, by adding a pairing interaction term, to include nuclei near closed shells. In particular the resonances near threshold of the region $28 \leq A \leq 60$ are expected to be readily obtained.[2]

---

[1] "Fast and Accurate Solutions for Meldmer's Realistic Single-Particle Hamiltonian", by R. Y. Cusson, H. Trivedi and D. Kolb, Phys. Rev. C5 (1972) 2120

[2] H. Trivedi, Ph.D. thesis topic

15. Single Particle Wavefunctions for Stripping and Pickup Reactions (R. Y. Cusson)

In view of the excellent agreement between theory and experiment which is found when using the realistic Duke-Meldmer code for electron scattering, it is of interest to test the wavefunction for unoccupied states also. Thus the Duke-Meldmer code is being set up at Oak Ridge where Dr. Ray Satchler has agreed to test the unoccupied orbits of ^{208}Pb by comparing the results with (d,p) experiments, using the computed single particle wavefunctions. The results of this comparison are expected to provide a test of our understanding of the stripping processes.

16. Realistic Single Particle Hamiltonian for Fission Calculations (R. Y. Cusson, D. Kolb, H. W. Schmitt (Oak Ridge), H. W. Newson, M. Harvey (Chalk River))

It is easily seen that Meldmer's realistic single-particle K-matrix can be used to perform calculations for deformed nuclei. We have set up a new basis, consisting of two overlapping deformed oscillators, in which the asymptotic limit of binary fission clusters can be reached. This basis allows the calculation of the fission potential energy without the use of the Strutinsky prescription. Preliminary results for ^{8}Be, ^{20}Ne, ^{235}U show that this method can yield realistic fission barrier estimates, especially if one performs a careful calculation of the Coulomb energy (Zeitschriff für Fysik, in press). This work is in progress.

17. Light Nuclei Systematics in The Projected Hartree-Fock Scheme (R. Y. Cusson, H. C. Lee (Chalk River))

Following an extensive study by the authors (Annals of Physics 72 (1972) 353) of the deformed intrinsic states of some 56 light nuclei in the p- and s-d shell, a detailed article is under preparation (Nuclear Physics, to be published), where rotational excitations and transitions (M1, E2, M3, E4, E0) are being systematically compared with experiment. In particular, excellent agreement with experiment has been found for ^{20}Ne, ^{22}Na, ^{24}Mg, as reported in an invited paper at the Gordon Conference on Nuclear Structure, 1972, by one of us (R.Y.C.).

18. Coriolis Anti-Stretching in ^{20}Ne and α Widths (H. C. Lee and R. Y. Cusson)

An interesting correlation between the decrease in B(E2) values as one goes up the ^{20}Ne ground state band, and the decrease in α emission width has been found (submitted to Physics Letters). Both the B(E2) and the α-width are found to decrease for the same reason, namely: the radius of ^{20}Ne is calculated to decrease as J increases, due mainly to the s-d to p-f shell gap. This effect has been confirmed by Dr. J. McGrory (private communication) in the Oak Ridge shell model calculation.

19. Applications of Group Theory to Rotational Bands in Nuclei (L. C. Biedenharn, R. Y. Cusson, O. L. Weaver ((Kansas State University)))

A contracted version of the SL(3,R) algebra proposed by Dothan Gell-Mann and Neiman, namely $T_5 \circledast SU(2)$ has been used to classify all the nuclear rotational bands (Annsls of Physics, in press), including those with half-integral spin, without having recourse to the ad hoc assumption of recoupling of an odd nucleon. The full algebra of SL(3,R) has been found to yield parameter free predictions for ratios of cross-band E2 transitions (Nuclear Physics, 1972) and has recently been found to yield a generalization of rotational-vibrational motion in which the presence of the odd particle is accounted for by introducing quantized amount of vorticity (in preparation).

20. Do Protons and Neutrons Have Internal Rotational Vibrational Excitations? (L. C. Biedenharn, R. Y. Cusson, O. L. Staunton)

For completeness in any theoretical program of nuclear studies it would not be wise to neglect the possible influence of nucleon structure on nuclear structure. The expertise required in dealing with the group theoretical foundations of nuclear collective motion is of use in discussing the possibility of such internal structure for the nucleons themselves. Thus a model involving the algebra of SL(3,R) and a "deformable" nucleon has been put forward (Physics Letters, to be published) and studies have shown that rotational excitations of the nucleon are quite consistent with the requirement of relativity (in preparation).

US ARMY BALLISTIC RESEARCH LABORATORIES
RADIATION LABORATORY

SMALL-ANGLE ELASTIC SCATTERING OF FAST NEUTRONS.

1. Small-angle Scattering Cross Sections for C, N, and O.
(W. P. Bucher, C. E. Hollandsworth, and A. Niiler) Relevant to NCSAC-35, Requests 31, 33, 38, 39, and 43.

Elastic scattering measurements for C, N, and O in the angular range 2.5° to 15° will be made for neutron energies between 10 MeV and 14 MeV in the next reporting period. To obtain increased sensitivity for these measurements the collimator, described in previous reports, has been rebuilt. The new collimator will be slightly larger. Modifications also include a more flexible shielding arrangement in the critical region near the entrance to the collimating channels. The construction of all parts has been completed, but final assembly has not been made.

2. Small-angle Elastic Scattering of 7.55 MeV neutrons: A Survey
(W. P. Bucher, C. E. Hollandsworth, D. McNatt, and A. Niiler) Relevant to NCSAC-35, Requests 22, 31, 33, 60, and 98.

Measurements of the forward-angle scattering of 7.55 MeV neutrons from Be, C, Al, Fe, Cu, Sn, and W have been made for six angles between 2.5° and 15°. Preliminary results for Sn, Fe, and Al are shown in Figure 1. Included in this figure are previous results for Pb and O.

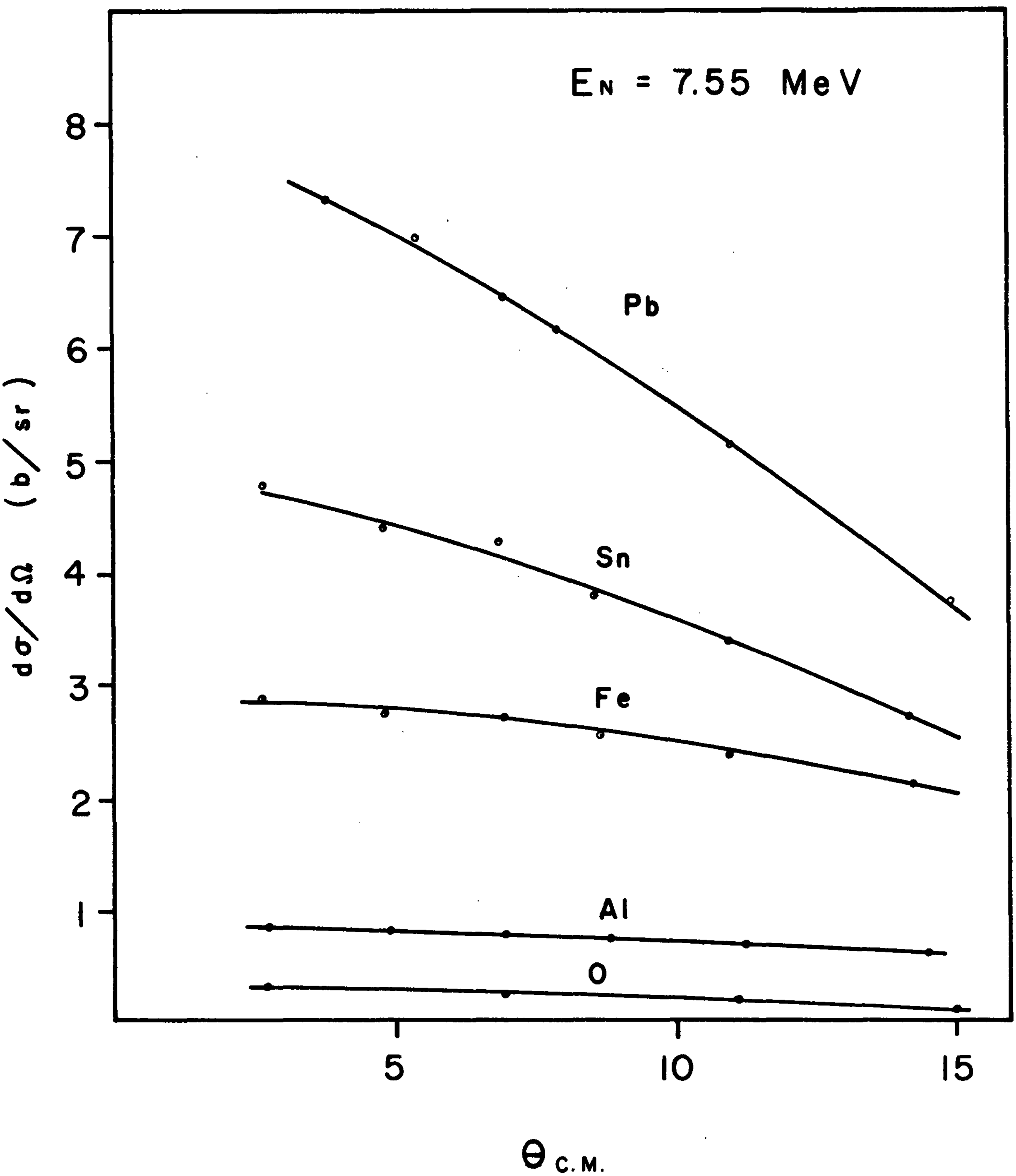
E_N = 7.55 MeV
Pb
Sn
Fe
Al
O
$d\sigma/d\Omega$ (b/sr)
8
7
6
5
4
3
2
1
5
10
15
$\Theta_{C.M.}$

Figure 1.

YALE UNIVERSITY

FAST NEUTRON POLARIZATION STUDIES (F. W. K. Firk, R. Nath, R. J. Holt and H. L. Schultz)

A. Differential Polarization of Neutrons in $n-^{12}C$ Scattering

The absolute polarization of neutrons elastically scattered from ^{12}C has been measured at eight angles between 20° and 150° at energies from 2 to 5 MeV.[1] The differential polarizations have been analyzed using a multi-level R-function analysis. The effects of distant levels have been estimated using a model in which these effects have a smooth linear-dependence on energy throughout the energy range of its measurement. Examples of the fitted polarizations are shown in Figure A-1 at four energies. Predicted angular distributions are shown in Figure A-2 where they are compared with published results and the predicted total cross section is shown in Figure A-3. For completeness, we have computed the total cross section at all energies from 0 to 5 MeV: the R-function prediction, based for the most part, upon our polarization results is compared with the measurements of the Karsruhe group and with the JAERI compilation of work below 2 MeV.

We have also carried out a phase-shift analysis and the results are shown in Figure A-4.

The R-function parameters deduced from the analysis are listed in Table A-1.

B. Polarization of Photoneutrons

The polarization of photoneutrons from the reaction $^{16}O(\gamma,n)^{15}O$ is being measured at a reaction angle of

[1] R.J. Holt, F. W. K. Firk., N. Nath and H. L. Schultz Phys. Rev. Letters, 28, 114 (1972)

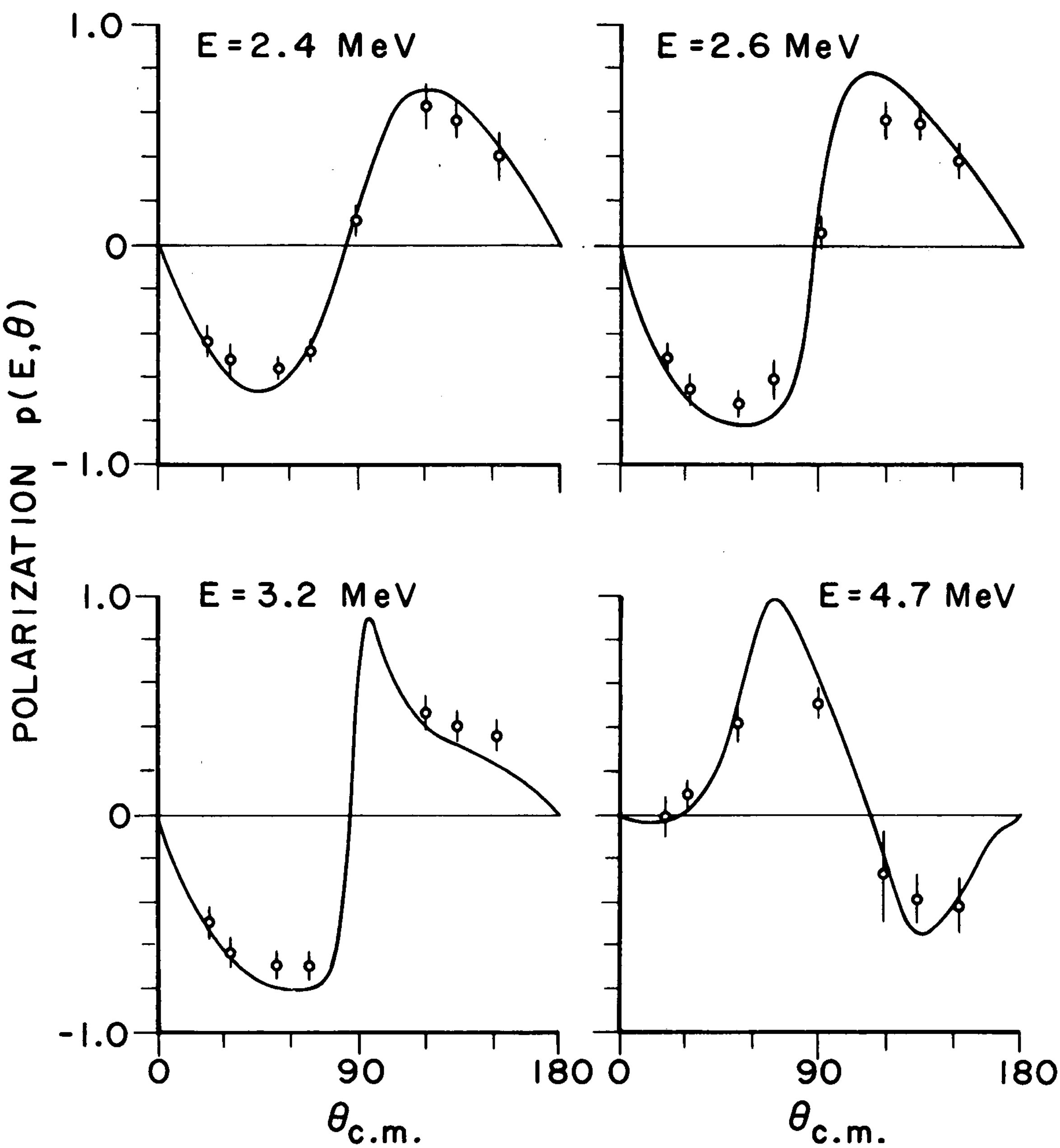
E=2.4 MeV
E=2.6 MeV
E=3.2 MeV
E=4.7 MeV
POLARIZATION p(E,θ)
1.0
0
-1.0
0
90
180
θc.m.

Figure A-1.

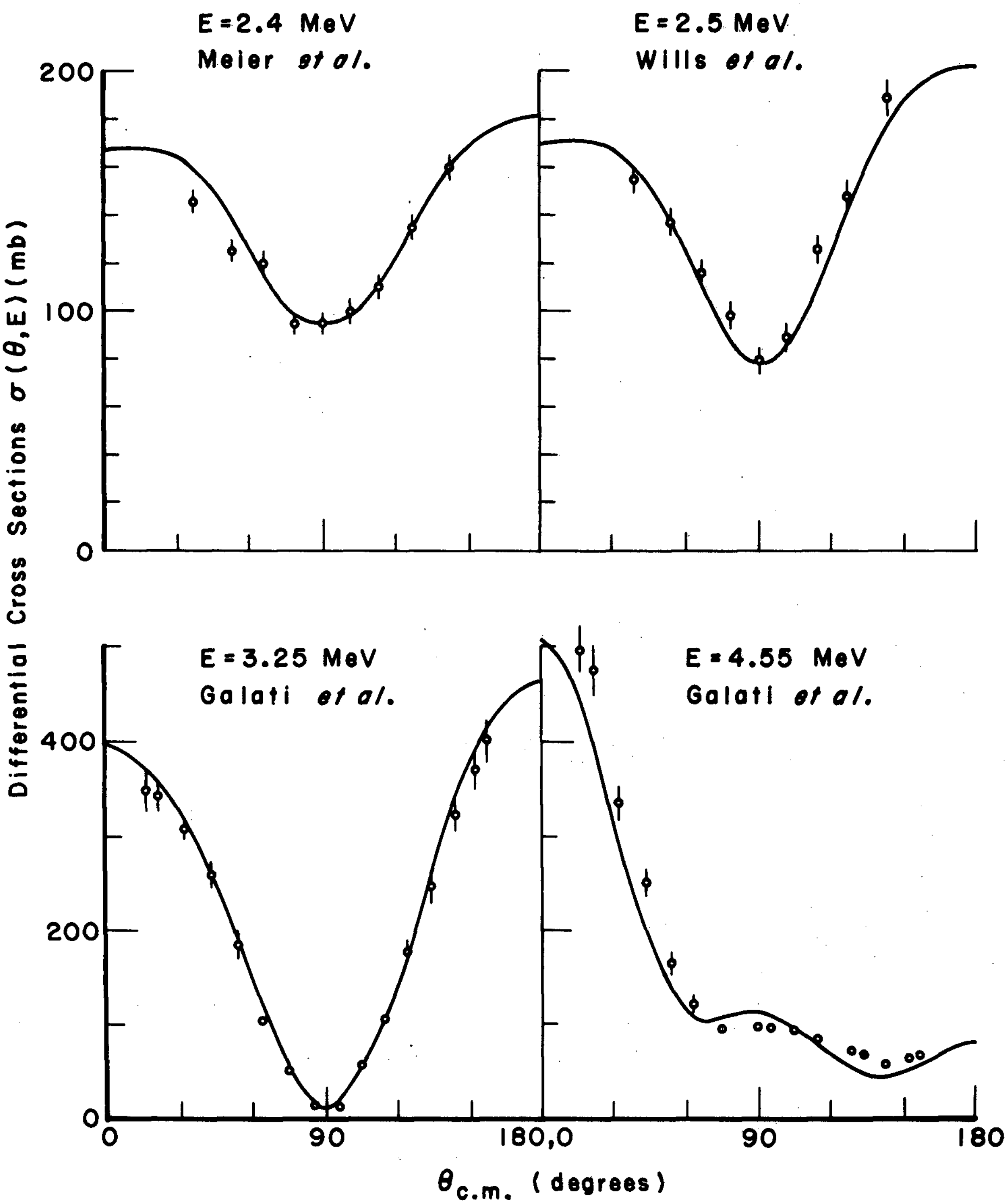
E=2.4 MeV
Meier et al.
E=2.5 MeV
Wills et al.
E=3.25 MeV
Galati et al.
E=4.55 MeV
Galati et al.
200
100
0
400
200
0
0
90
180,0
90
180
Differential Cross Sections σ(θ,E)(mb)
θc.m. (degrees)

Figure A-2.

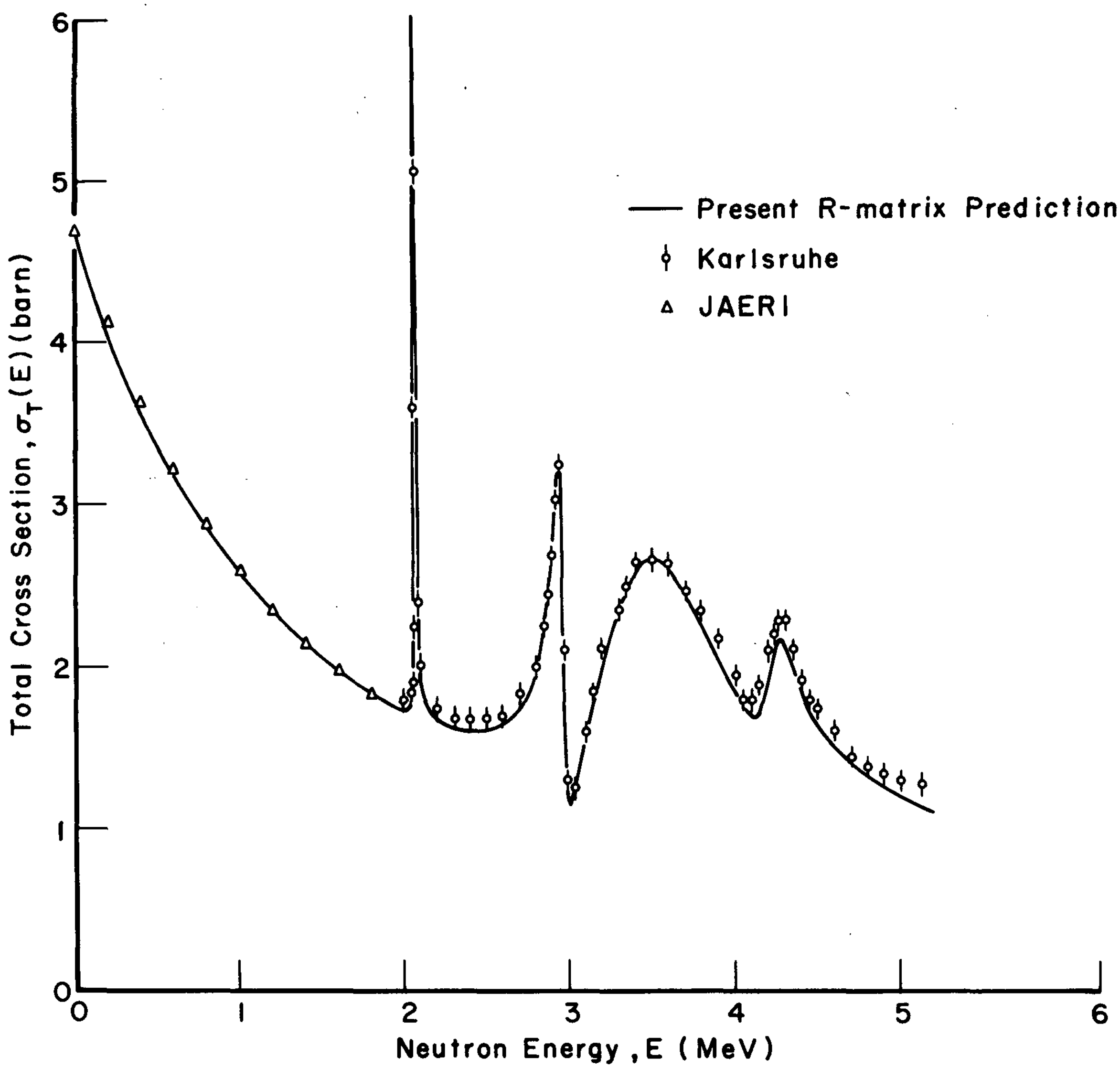

Total Cross Section, $\sigma_T(E)$ (barn)
0
1
2
3
4
5
6
Neutron Energy, E (MeV)
Present R-matrix Prediction
Karlsruhe
JAERI

Figure A-3.

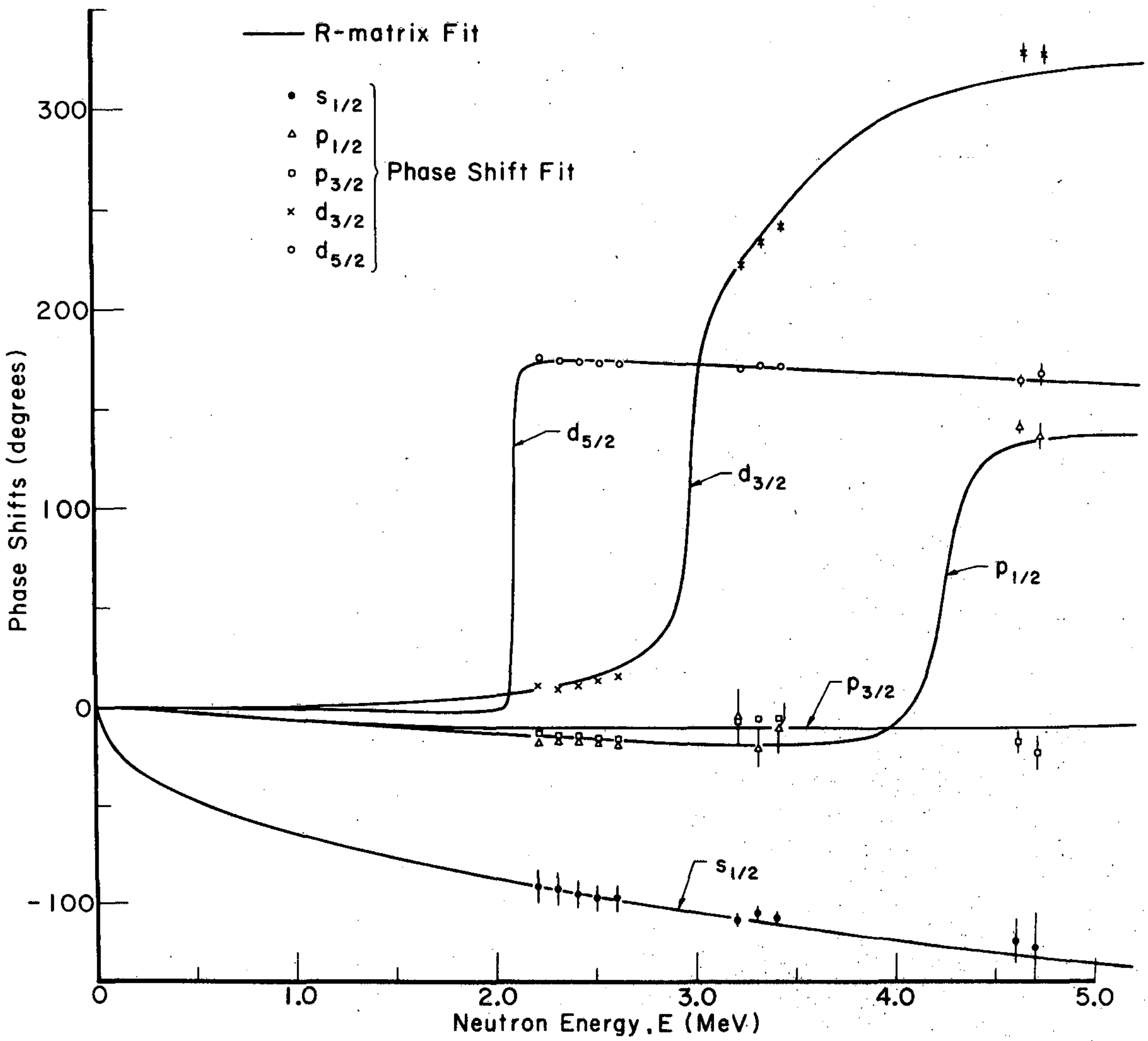

R-matrix Fit
$s_{1/2}$
$p_{1/2}$
$p_{3/2}$
$d_{3/2}$
$d_{5/2}$
Phase Shift Fit
300
200
100
0
-100
Phase Shifts (degrees)
$d_{5/2}$
$d_{3/2}$
$p_{1/2}$
$p_{3/2}$
$s_{1/2}$
0
1.0
2.0
3.0
4.0
5.0
Neutron Energy, E (MeV)

Figure A-4.

Table A-1. R-matrix parameters with a = 4.61 fermis.

ℓJ	$\lambda = 1$: $E_{\ell J}$ (MeV)	$\lambda = 1$: $\gamma^2_{\ell J}$ (MeV)	$\lambda = 1$: $\Gamma_{\ell J}$ (MeV)	$\lambda = 2$: $E_{\ell J}$ (MeV)	$\lambda = 2$: $\gamma^2_{\ell J}$ (MeV)	$\lambda = 2$: $\Gamma_{\ell J}$ (MeV)	$R_0^{\ell J}$ (MeV^{-1})	$R_1^{\ell J}$ (MeV^{-1})	$B_{\ell J}$
$s_{1/2}$	-1.86	.61	0	...	...	...	0	0	0
$p_{1/2}$	...	...	...	4.2	.0654	.2	.17	.012	-.211
$p_{3/2}$	...	...	...	...	...	...	.28	.08	-.176
$d_{3/2}$	2.92	.16	.15	3.5	.93	1.1	.18	.025	-1.00
$d_{5/2}$	...	...	...	2.076	.014	.007	.04	0	-1.32

45° relative to the absolute analyzing power of ^{12}C at 65°, measured in this laboratory. In particular, the effects of non-ground state photoneutrons on our earlier measurements (made with a bremsstrahlung end-point-energy of 50 MeV) are being investigated. These measurements are nearing completion.

C. A paper on the polarization of photoneutrons from deuterium is in press in Nuclear Physics.